

UNITUE-THEP-00/09, FAU-TP3-00/8
<http://xxx.lanl.gov/abs/hep-ph/0007355>

The Infrared Behavior of QCD Green's Functions

Confinement, Dynamical Symmetry Breaking, and Hadrons as Relativistic Bound States [★]

Reinhard Alkofer ¹

*Institut für Theoretische Physik, Universität Tübingen, Auf der Morgenstelle 14,
72076 Tübingen, Germany*

and

Lorenz von Smekal ²

*Institut für Theoretische Physik III, Universität Erlangen-Nürnberg, Staudtstr. 7,
91058 Erlangen, Germany*

[★] Supported in part by DFG (Al 279/3-3) and COSY (contract no. 41376610).

¹ E-Mail: reinhard.alkofer@uni-tuebingen.de

² E-Mail:smekal@theorie3.physik.uni-erlangen.de

Abstract

Recent studies of QCD Green's functions and their applications in hadronic physics are reviewed. We discuss the definition of the generating functional in gauge theories, in particular, the rôle of redundant degrees of freedom, possibilities of a complete gauge fixing versus gauge fixing in presence of Gribov copies, BRS invariance and positivity. The apparent contradiction between positivity and color antiscreening in combination with BRS invariance in QCD is considered. Evidence for the violation of positivity by quarks and transverse gluons in the covariant gauge is collected, and it is argued that this is one manifestation of confinement.

We summarize the derivation of the Dyson–Schwinger equations (DSEs) of QED and QCD. For the latter, the implications of BRS invariance on the Green's functions are explored. The possible influence of instantons on DSEs is discussed in a two-dimensional model. In QED in 2+1 and 3+1 dimensions, the solutions for Green's functions provide tests of truncation schemes which can under certain circumstances be extended to the DSEs of QCD. We discuss some limitations of such extensions and assess the validity of assumptions for QCD as motivated from studies in QED. Truncation schemes for DSEs are discussed in axial and related gauges, as well as in the Landau gauge. Furthermore, we review the available results from a systematic non-perturbative expansion scheme established for Landau gauge QCD. Comparisons to related lattice results, where available, are presented.

The applications of QCD Green's functions to hadron physics are summarized. Properties of ground state mesons are discussed on the basis of the ladder Bethe–Salpeter equation for quarks and antiquarks. The Goldstone nature of pseudoscalar mesons and a mechanism for diquark confinement beyond the ladder approximation are reviewed. We discuss some properties of ground state baryons based on their description as Bethe–Salpeter/Faddeev bound states of quark–diquark correlations in the quantum field theory of confined quarks and gluons.

Key words: Strong QCD, Green's functions, Confinement, Chiral symmetry breaking, Dyson–Schwinger equations, Bethe–Salpeter equation.

PACS numbers: 02.30.Rz 11.10.Gh 11.10.Hi 11.10.St 11.15.Tk 12.20.Ds 12.38.Aw 12.38.Lg 14.20.Dh 14.20.Jn 14.40.Aq 14.65.Bt 14.70.Dj

Contents

1	Introduction	5
2	Basic Concepts in Quantum Field Theory	9
2.1	Generating Functional of QED and QCD	11
2.2	Gribov Copies, Monopoles and Gauge Fixing	15
2.3	Positivity versus Color Antiscreening	22
2.4	Description of Confinement in the Linear Covariant Gauge	28
2.5	Alternative singularity structures of Green's functions	36
3	The Dyson–Schwinger Formalism	40
3.1	Dyson–Schwinger Equations for QED and QCD Propagators	40
3.2	BRS Invariance of Green's Functions	49
3.3	The Structure of Vertex Functions	53
4	Green's Functions of QED	57
4.1	1+1 Dimensional QED (Schwinger model): Dyson–Schwinger Equations in a Model with Instantons	57
4.2	Confinement in 2+1 Dimensional QED	58
4.3	Dynamical Chiral Symmetry Breaking in 3+1 Dimensional QED	64
5	The Infrared Behavior of QCD Green's Functions	70
5.1	“Confined” or “Confining” Gluons?	70
5.2	The Gluon Propagator in Axial Gauge	73
5.3	Truncation Schemes for Propagators in Landau Gauge	78
5.4	A Non-Perturbative Expansion Scheme in Landau Gauge QCD	109
5.5	Lattice Results	112
6	Mesons as Quark–Antiquark Bound States	120
6.1	Bethe–Salpeter Equation for Mesons	120
6.2	Ground State Mesons	128
7	Baryons as Diquark–Quark Bound States	147
7.1	Goldstone Theorem and Diquark Confinement	148
7.2	Modelling of Diquarks	155
7.3	Quark–Diquark Bethe–Salpeter Equations	160
7.4	Electromagnetic Form Factors	168
7.5	Strong and Weak Form Factors	173
7.6	Hadronic Reactions	176
8	Concluding Remarks	180
A	Real vs. Complex Ghost Fields: Ghost-Antighost Symmetry and $SL(2, \mathbb{R})$	182
B	Conventions for Fourier Transformations	189

C	Dyson–Schwinger Equation for the Gluon Propagator	190
D	3–Gluon Vertex in Axial Gauge	193
	References	194
	List of Figures	209
	List of Tables	212

1 Introduction

Looking at the plethora of different hadrons it is evident that baryons and mesons are not elementary particles in the naive sense of the word “elementary”. Experimental hadron physics has determined the partonic substructure of the nucleon to an enormous precision leaving no doubt that the parton picture emerges from quarks and gluons, the elementary fields of Quantum Chromodynamics (QCD). On the other hand, it is a well-known fact that these quarks and gluons have not been detected outside hadrons. This puzzle was given a name: confinement. Despite the fact that the confinement hypothesis was formulated several decades ago our understanding of the confinement mechanism(s) is still not satisfactory. And, in contrast to other non-perturbative phenomena of interest in QCD (*e.g.*, dynamical breaking of chiral symmetry, $U_A(1)$ anomaly, and formation of relativistic bound states) the phenomenon of confinement might to some extend be in conflict with nowadays widely accepted foundations of quantum field theory.

Quantum field theory provides the basis for our current understanding of particle physics. The quantum field theoretical description of elementary particles has been impressively successful since it was first developed in the quantization of electrodynamics in the late 20ties. After its first applications to elementary processes like the spontaneous decays of exited atoms, the photo and the Compton effect, electron-electron scattering, pair creation and Bremsstrahlung, the next major step was accomplished in the late 40ties. The anomalous magnetic moment of the free electron from the Dirac theory of relativistic quantum mechanics was observed experimentally. The development of the covariant perturbation expansion by Tomonaga, Schwinger and Feynman together with the concept of renormalization allowed to calculate higher order corrections to the elementary processes of electrons and photons. Its application to the Lamb shift explained the experimental observations, and higher order corrections subsequently agreed with the results of refined experiments.

Since these developments of Quantum Electrodynamics (QED), local quantum field theory has further been developed and applied to the descriptions of elementary particles. Their processes are accounted for by the collision theory developed by Lehmann, Symanzik and Zimmermann, the so-called LSZ formalism [1] (for a description of its role in modern quantum field theory see *e.g.* refs. [2] or [3]). Together with perturbation theory it describes the processes of elementary particles at high energies based on asymptotically free gauge theories. In particular, in the weak coupling regime of QCD, *i.e.*, at high energies, the agreement of perturbative calculations with the huge number of measurements available is impressive (see *e.g.* fig. 14 in sec. 5.3).

The perturbative description of elementary particles is essentially based on the field-particle duality which means that each field in a quantum field theory is associated with a physical particle. A simple example for this being the Fermi theory of the β -decay where a field is associated to all particles involved, the proton, the neutron, as well as the electron and the neutrino. This is of course not what one has in mind in describing hadrons as composite states with quark and gluonic substructure in hadronic processes. On the one hand, scattering theory can be extended to include processes of composite particles described by “almost local” fields leading to a generalized LSZ formalism for bound states [4–6] (described also in the book of ref. [3]). On the other hand, the situation in QCD is more complicated, however. Not only

does the asymptotic state space contain composite states, but the physical Hilbert space of the asymptotic hadron states does not contain any states corresponding to particles associated with the elementary fields in QCD, the quarks and gluons. For a description of confinement of quarks and gluons within the framework of local quantum field theory, the elementary fields have to be divorced completely from a particle interpretation. A quote from Haag's book [3] expresses this in a clear way as follows:

“The rôle of fields is to implement the principle of locality. The number and the nature of different basic fields needed in the theory is related to the charge structure, not to the empirical spectrum of particles.”

The description of hadronic states and processes based on the dynamics of the confined correlations of quark and glue is the outstanding challenge in the formulation of QCD as a local quantum field theory. In particular, assuming that only hadrons are produced from processes involving hadronic initial states, one has to explain that the only thresholds in hadronic amplitudes are due to the productions of other hadronic states, and that possible structure singularities occur in composite states which are due to their hadronic substructure only.

Some theoretical insight into the mechanism(s) for confinement into colorless hadrons could be obtained from disproving the cluster decomposition property for color–nonsinglet gauge–covariant operators. One idea in this direction is based on the possible existence of severe infrared divergences, *i.e.* divergences which cannot be removed from physical cross sections by a suitable summation over degenerate states by virtue of the Kinoshita–Lee–Nauenberg theorem [7].³ Such severe infrared divergences could provide damping factors for the emission of colored states from color–singlet states (see [9]). However, the Kinoshita–Lee–Nauenberg theorem applies to non-Abelian gauge theories in four dimensions order by order in perturbation theory [10,11]. Therefore, such a description of confinement in terms of perturbation theory is impossible. In fact, extended to Green's functions, the absence of unphysical infrared divergences implies that the spectrum of QCD necessarily includes colored quark and gluon states to every order in perturbation theory [12].

An alternative way to understand the insufficiency of perturbation theory to account for confinement in four–dimensional field theories is that confinement requires the dynamical generation of a physical mass scale. In presence of such a mass scale, however, the renormalization group (RG) equations imply the existence of essential singularities in physical quantities, such as the S –matrix, as functions of the coupling at $g = 0$. This is because the dependence of the RG invariant confinement scale on the coupling and the renormalization scale μ near the ultraviolet fixed point is determined by [13]

$$\Lambda = \mu \exp \left(- \int^g \frac{dg'}{\beta(g')} \right) \xrightarrow{g \rightarrow 0} \mu \exp \left(- \frac{1}{2\beta_0 g^2} \right), \quad \beta_0 > 0. \quad (1)$$

Since all RG invariant masses in massless QCD will exhibit the behavior (1) up to a multiplicative constant the ratios of all bound state masses are, at least in the chiral limit, determined independent of all parameters.

³ Also referred to as the non-Abelian Bloch-Nordsieck prescription, *c.f.*, ref. [8].

Therefore, to study the infrared behavior of QCD amplitudes non-perturbative methods are required. In addition, as singularities are anticipated, a formulation in the continuum is desirable. One promising approach to non-perturbative phenomena in QCD is provided by studies of truncated systems of its Dyson–Schwinger equations (DSEs) [14,15], the equations of motion for QCD Green’s functions. Typical truncation schemes resort to additional sources of information like the Slavnov–Taylor identities [16,17], as entailed by gauge invariance, to express vertex functions and higher n -point functions in terms of the elementary two-point functions, *i.e.*, the quark, ghost and gluon propagators. In principle, these propagators can then be obtained as self-consistent solutions to the non-linear integral equations representing the closed set of truncated DSEs.

The underlying conjecture to justify such a truncation of the originally infinite set of DSEs is that a successive inclusion of higher n -point functions in selfconsistent calculations will not result in dramatic changes to previously obtained lower n -point functions. To achieve this it is important to incorporate as much independent information as possible in constructing those n -point functions which close the system. Such information, *e.g.*, from implications of gauge invariance or symmetry properties, can be relied on if they are reproduced from solutions to subsequent truncation schemes.

Until recently, available solutions to truncated DSEs of QCD did not even fully include all contributions of the propagators itself. In particular, even in absence of quarks, solutions for the gluon propagator in Landau gauge used to rely on neglecting ghost contributions [18–21] which, though numerically small in perturbation theory, are unavoidable in this gauge. While this particular problem can be avoided by ghost free gauges such as the axial gauge, in studies of the gluon DSE in the axial gauge [22–26], the possible occurrence of an independent second term in the tensor structure of the gluon propagator has been disregarded [27]. In fact, if the complete tensor structure of the gluon propagator in axial gauge is taken into account properly, one arrives at a coupled system of equations which is of similar complexity as the ghost–gluon system in the Landau gauge and which is yet to be solved.

In addition to providing a better understanding of confinement based on studies of the behavior of QCD Green’s functions in the infrared, DSEs have proven successful in developing a hadron phenomenology which interpolates smoothly between the infrared (non-perturbative) and the ultraviolet (perturbative) regime, for recent reviews see, *e.g.*, [28,29]. In particular, a dynamical description of the spontaneous breaking of chiral symmetry from studies of the DSE for the quark propagator is well established in a variety of models for the gluonic interactions of quarks [30]. For a sufficiently large low-energy quark–quark interaction quark masses are generated dynamically in the quark DSE in some analogy to the gap equation in superconductivity. This in turn leads naturally to the Goldstone nature of the pion and explains the smallness of its mass as compared to all other hadrons. In this framework a description of the different types of mesons is obtained from Bethe–Salpeter equations (BSEs) for quark–antiquark bound states. Recent progress towards a solution of a fully relativistic three–body equation extends this consistent framework to baryonic bound states.

Investigations of QCD Green’s functions have been extended sucessfully to finite temperatures and densities during the last few years. As this is a subject of its own, and with regard to the length of the present review we have refrained from reviewing this topic. Instead we refer the

interested reader to the excellent recent review provided by ref. [31].

This review is organized as follows: Chapter 2 introduces reviews some basic concepts of quantum field theory and especially QCD, some derivations and the notations to provide the necessary background for the later chapters. In Chapter 3 the Dyson–Schwinger formalism is presented. Chapter 4 provides a short summary of QED Green’s functions in 1+1, 2+1 and 3+1 dimensions. These results are helpful to put the corresponding results for QCD into perspective. Chapter 5 is the central part of this review: The infrared behaviour of QCD Green’s function and its implications for confinement, for dynamical breaking of chiral symmetry and the structure of hadrons in general are discussed. Phenomenological studies of mesons which are based on the results for the propagators are summarized in Chapter 6. On the way towards a description of baryons as bound states in color singlet 3–quark channels a detailed understanding of diquark correlations is necessary. In Chapter 7 the corresponding framework is provided, and baryonic bound states of quarks and diquarks are described in reduced Bethe–Salpeter/Faddeev equations obtained for separable diquark correlations. A few concluding remarks are given in the last chapter. Some more technical issues are presented in several appendices.

We wish to emphasize that this review is a status report on an on-going effort. The long way from the dynamics of quark and glue to hadrons in one coherent description is far from paved. Considerable segments are, however, increasingly well understood, some on a fairly fundamental level, others from temporarily used model assumptions. Connections between the various pieces are made in form of justifications and improvements of the respective model assumptions. The present review describes some of these segments along the way.

2 Basic Concepts in Quantum Field Theory

In this chapter, some underlying concepts of the subsequent chapters are briefly reviewed, mainly to introduce definitions and conventions for later use. In addition, and maybe more importantly, we discuss some of the fundamental issues in this chapter which might in future lead to advances in the understanding of hadronic physics based on the dynamics of quark and glue.

Since a comprehensive and final quantum field theoretic description of a confining theory is not established yet, it is necessary to cover various descriptions in this review. However, even the most widely adopted ones possess some quite complementary aspects. A rough classification may be possible in realizing that the least modifications, necessary to accommodate confinement in quantum field theory, seem to be given by the choice of either relaxing the principle of locality or abandoning the positivity of the representation space.⁴ We will discuss some of the implications of both these possibilities in this chapter. Since abandoning locality has much further reaching consequences, the latter choice, the description of QCD based on local quantum field theory with indefinite metric spaces, might be the more viable possibility of the two, if the cluster decomposition property of local fields can be circumvented.

As was originally suggested for QED by Gupta [32] and Bleuler [33], the starting point for a covariant description of gauge theories is an indefinite metric space. In particular, this implies that, besides positivity, most other properties of local quantum field theory, and hereby most importantly the analyticity properties of Green's functions and amplitudes, remain to be valid in such a formulation. In QCD, colored states are supposed to exist in the indefinite metric space of asymptotic states. A semidefinite subspace is obtained as the kernel of an operator. Just as in QED, where the Gupta-Bleuler condition is to enforce the Lorentz condition on physical states, this subspace, called the *physical subspace*, has a partition in equivalence classes of states which differ by zero norm components.

A first impression of such a description of confinement can be obtained from the analogy with QED. Quantizing the electromagnetic field in a linear covariant gauge, besides transverse photons one also obtains longitudinal and scalar (time-like) photons. The latter two are unobservable because one eliminates indefinite metric states by requiring the Lorentz condition on all physical states. The *S*-Matrix of QED scatters physical states into physical ones only, because it commutes with the Lorentz condition. The scalar photons are “eaten up” by the longitudinal ones with which they form metric partners. Color confinement in QCD can be described by an analogous mechanism: No colored states should be present in the positive definite space of physical states defined by some suitable condition which has to commute with the *S*-Matrix of QCD to ensure scattering of physical states into physical ones. The dynamical aspect of such a formulation resides in the cluster decomposition property of local field theory. The proof of which, absolutely general otherwise [34], does not include the indefinite metric spaces of covariant gauge theory. In fact, there is quite convincing evidence for the contrary, namely that the cluster decomposition property does not hold for colored correlations of QCD in such a description [35]. This would thus eliminate the possibility of scattering a physical

⁴ As a third alternative both might eventually turn out to be necessary, of course.

state into color singlet states consisting of widely separated colored clusters (the “behind-the-moon” problem, see also Ref. [36] and references therein). We will return in some more detail in Sec. 2.4 to the foundations of this description which is based on the representations of a particular symmetry of covariant gauge theories found by Becchi, Rouet and Stora, the BRS symmetry [37].

The dynamics of the elementary degrees of freedom of QCD is encoded in its n -point correlation functions, *i.e.*, the hierarchy of the (time-ordered) Green’s functions $G^{(n)}(x_1, \dots x_n)$. Owing to the axioms of local quantum field theory, in Minkowski space-time these are defined to be boundary values (by $\eta_k \rightarrow 0$ from below) of analytic functions of $n - 1$ complex 4-vectors $z_k^\mu = \xi_k^\mu + i\eta_k^\mu$ which are complex extensions of the relative coordinates $\xi_k \equiv x_k - x_{k+1}$ (with $k = 1, \dots, n - 1$). The complicated domain of holomorphy of the correlation functions is then established in several steps, see Refs. [38,3] for more details. First, one observes that it contains the *primitive domain* which is defined by the requirement that the negative imaginary parts of all z_k lie in the forward cone, $-\eta_k \in V_+$. Then, all “points” are included which can be reached from the primitive domain by *complex* Lorentz transformations, *i.e.*, by extending $SL(2, \mathbb{C})$, the double cover of the proper orthochronous Lorentz group, to $SL(2, \mathbb{C}) \times SL(2, \mathbb{C})$. Permutations of the $n - 1$ variables z_k and the theory of functions of several complex variables then lead to the so-called envelope of holomorphy of *permuted extended tubes*. This connects the primitive domain with the non-coincident Euclidean region, $\{(x_1, \dots x_n) \in \mathbb{R}^{4n} : x_k \neq x_l \forall k \neq l \in \{1, \dots, n\}\}$. Or *vice versa*, with the Euclidean $SU(2) \times SU(2)$ symmetry as subgroup of $SL(2, \mathbb{C}) \times SL(2, \mathbb{C})$, the domain of holomorphy allows a complex extension of the Euclidean space. This apparently technical issue is quite important to realize, however, since it justifies the incorporation of time-like vectors (*e.g.*, the total momenta of bound states) as complex 4-vectors in an analytically continued Euclidean formulation.

We will adopt such a Euclidean formulation throughout the following chapters with few exceptions which will be mentioned explicitly where they occur.

The first of the alternatives mentioned in the beginning of this section is based on describing confinement by an absence of colored states from the asymptotic state-space altogether. In particular, for a formulation in terms of some elementary quark and gluon fields this requires a relaxation of the principle of locality in order to admit singularity structures of their Green’s functions that cannot occur in a local quantum field theory. We will discuss some consequences of this in Sec. 2.5.

One way to implement confinement in such a description might be provided by assuming that the elementary correlations are given by entire functions in momentum space, *e.g.*, that no singularities are present at all in any finite region of the complex p^2 -plane of the 2-point correlations reflecting their confined character. While (finite) time-like momenta are readily incorporated in such a description, singularities for $p^2 \rightarrow \infty$ are indispensable for non-trivial entire functions. Asymptotic freedom, however, entails that analytic 2-point functions need to vanish in this limit for all directions of the complex p^2 -plane [39,40], see also Sec. 2.3 below. Perturbation theory, yielding the perturbative logarithms for large p^2 , thus seems hard to be reconciled with the idea of entire 2-point functions. A singularity structure which generates the perturbative logarithms and complies at the same time with the analyticity considerations above entails that singularities occur on the time-like real p^2 -axis only. The 2-point correlations

of quarks and transverse gluons are then analytic functions in the cut complex p^2 -plane. While the phenomenologically appealing models employing entire 2-point functions can therefore be motivated only as approximations for not too large $|p^2|$, the required analyticity structure is evident in the local description of covariant gauge theories based on indefinite metric spaces. Confinement of quarks and transverse gluons is hereby attributed to violations of positivity which should result in indefinite spectral densities for their respective correlations, see, *e.g.*, Ref. [40]. It has in fact been argued that such a violation of positivity can already be inferred from asymptotic freedom in combination with the unbroken BRS invariance in QCD [40,41]. The subtleties in this argument which might be regarded as not absolutely conclusive are discussed further in Sec. 2.3. Independent of this perturbative argument, however, such violations of positivity are observed in the presently available solutions to Dyson–Schwinger equations as well as in lattice results for the transverse gluon propagator, see Chapter 5. Since these results together seem to provide quite convincing evidence for such violations of positivity of the elementary correlations of QCD in the covariant formulation, we will return to this issue repeatedly in the following chapters.

2.1 Generating Functional of QED and QCD

The Feynman–Schwinger functional integral representation of the generating functional for a gauge theory coupled to fermions is in the Euclidean domain formally given by,

$$Z[j, \bar{\eta}, \eta] = \int \mathcal{D}[A, q, \bar{q}] \Delta[A] \delta(f^a(A)) \exp \left\{ - \int d^4x \left(\frac{1}{4} F_{\mu\nu}^a F_{\mu\nu}^a + \bar{q}(-\not{D} + m)q \right) + \int d^4x \left(A_\mu^a j_\mu^a + \bar{\eta}q + \bar{q}\eta \right) \right\}. \quad (2)$$

Hereby sources j_μ^a for the gauge fields A_μ^a , and Grassmannian sources $\bar{\eta}$ and η for the fermion fields q and \bar{q} , have been introduced. In the case of QED, an Abelian gauge theory with gauge coupling e , the field strengths are given by

$$F_{\mu\nu} = \partial_\mu A_\nu - \partial_\nu A_\mu, \quad \text{and} \quad D_\mu = \partial_\mu + ieA_\mu, \quad (3)$$

is the covariant derivative. The other case of interest is QCD, *i.e.* the gauge group $SU(3)$. As for several reasons the number of colours, N_c , will be considered as a variable we will present the following discussions in a way that everything is applicable to gauge groups $SU(N_c)$. Then the field strengths are given by

$$F_{\mu\nu}^a = \partial_\mu A_\nu^a - \partial_\nu A_\mu^a - g f^{abc} A_\mu^b A_\nu^c, \quad \text{and} \quad D_\mu^{ab} = \delta^{ab} \partial_\mu + g f^{abc} A_\mu^c, \quad (4)$$

is the covariant derivative in the adjoint representation of $SU(N_c)$ with f^{abc} being the corresponding structure constants, and g is the coupling constant. Denoting the generators of $SU(N_c)$ as t^a we can rewrite the covariant derivative in the fundamental representation:

$$A_\mu = t^a A_\mu^a, \quad \text{and} \quad D_\mu = \partial_\mu + ig A_\mu, \quad \text{with} \quad [t^a, t^b] = if^{abc}t^c. \quad (5)$$

The functional integration of the gauge fields over the hypersurface $f^a(A) = 0$ involves the measure $\Delta[A]$, called the Faddeev–Popov determinant [42]. In linear covariant gauges one uses $f^a(A) = \partial_\mu A_\mu^a$. In the case of QED the corresponding condition $f(A) = \partial_\mu A_\mu$ leads to a field-independent Faddeev–Popov determinant, *i.e.* a pure number, and Faddeev–Popov ghosts do not couple to physical fields. The situation is very different in non-Abelian gauge theories despite the fact that the underlying idea is very similar. To obtain the physical configuration space it is necessary to divide the set of all gauge potentials by the set of all gauge transformations including the homotopically non-trivial one [43,44]. A local gauge fixing condition is introduced to select a particular gauge field configuration A^{U_0} by $f^a(A^{U_0}) = 0$ from the equivalence class of gauge fields belonging to the same orbit,

$$[A^U] := \{A^U = UAU^\dagger + UdU^\dagger : U(x) \in SU(N_c)\} . \quad (6)$$

This procedure is locally unique if for infinitesimally neighboring configurations along the orbit, $A^U = A^{U_0} + \delta A^\theta$ with $\delta A_\mu^{a\theta} = -D_\mu^{ab}\delta\theta^b$, one has:

$$\Delta[A] = \text{Det} \left(\frac{\delta f^a(A^U(x))}{\delta\theta^b(y)} \right) \Big|_{\theta=0} \neq 0 . \quad (7)$$

In linear covariant gauges the Faddeev–Popov determinant reads explicitly:

$$\Delta[A] = \text{Det} \left(-\partial_\mu D_\mu^{ab} \right) . \quad (8)$$

Perturbatively this Jacobian factor is taken care of by introducing ghost fields, *i.e.*, scalar Grassmann fields \bar{c}^a and c^a in the adjoint representation, such that the Faddeev–Popov determinant is written as a Gaussian integral of these ghost fields.

The scalar ghost fields belong to the trivial representation of $SL(2, \mathbb{C})$, the cover of the connected part of the Lorentz group. As local fields with spacelike anti-commutativity, they violate the spin-statistics theorem and are thus necessarily unphysical. The domain of holomorphy of the vacuum expectation value of any product of local fields together with the positive definiteness of the scalar product entails that anti-commutativity is tied to fields belonging to half-odd integer spin representations of $SL(2, \mathbb{C})$, see, *e.g.*, [3]. This is not necessarily so in the indefinite-metric spaces of covariant gauge theories, however, in which the scalar product is replaced by an indefinite sesquilinear form. It implies of course that Faddeev–Popov ghosts are unobservable, see also [45].

As we shall describe in a little more detail in the context of BRS invariance in Sec. 2.4, in the covariant operator formulation of gauge theories ghosts and antighosts together with longitudinal and timelike gluons form quartets of metric partners, see, *e.g.*, [36]. With the exception that ghosts decouple in QED this is no different from the case of longitudinal and timelike photons [32,33]. In contrast to QED, however, in QCD positivity is violated for transverse gluon states too. This can be inferred already in perturbation theory from asymptotic freedom (and unbroken global gauge invariance) for less than 10 quark flavors [46,47], see the discussion at the end of Sec. 2.3. It implies that the massless transverse asymptotic gluon

states of perturbation theory belong to unphysical quartets also.⁵ This alone is *not* sufficient for a realization of confinement, however, for which it is absolutely crucial that nonperturbatively no such *massless* transverse gluon states exist, regardless of the fact that possible asymptotic single particle states in transverse gluon correlations generally form quartets. We will come back to this point in Sec. 2.4. The results presented in Chap. 5 for the Landau gauge gluon propagator from both, solutions to Dyson-Schwinger equations [48,49] and lattice simulations [50,51] demonstrate the violation of positivity for transverse gluons nonperturbatively and,⁶ in addition, agree in confirming the absence of massless asymptotic transverse single gluon states.

The gauge condition $f^a(A) = 0$, formally represented by a delta functional, is usually relaxed into $f^a(A) = i\xi B^a$ with a Gaussian distribution of width ξ . In the linear covariant gauges this amounts to the replacement,

$$\delta(f^a(A)) \rightarrow \exp -\frac{1}{2\xi} \int d^4x (\partial_\mu A_\mu^a)^2 = \int \mathcal{D}B \exp -\int d^4x \left(iB^a \partial_\mu A_\mu^a + \frac{\xi}{2} B^a B^a \right), \quad (9)$$

which may or may not be represented by a Gaussian integration of the (Euclidean) Nakanishi-Lautrup auxiliary field B^a . The Lorentz condition $\partial_\mu A_\mu^a = 0$ is strictly implemented only in the limit $\xi \rightarrow 0$ which defines the Landau gauge.

Perturbation theory can then be defined by choosing the Gaussian measure of free quark, gluon and ghost fields as a starting point for a power series expansion of the non-Gaussian interaction terms in the effective Lagrangean \mathcal{L}_{eff} of covariant perturbation theory,

$$Z[j, \bar{\eta}, \eta, \bar{\sigma}, \sigma] = \int \mathcal{D}[A, q, \bar{q}, \bar{c}, c] \exp \left\{ - \int d^4x \mathcal{L}_{\text{eff}} + \int d^4x (A^a j^a + \bar{\eta} q + \bar{q} \eta + \bar{\sigma} c + \bar{c} \sigma) \right\}, \quad (10)$$

$$\text{with } \mathcal{L}_{\text{eff}} = \frac{1}{2} A_\mu^a (-\partial^2 \delta_{\mu\nu} - \left(\frac{1}{\xi} - 1\right) \partial_\mu \partial_\nu) A_\nu^a + \bar{c}^a \partial^2 c^a + g f^{abc} \bar{c}^a \partial_\mu (A_\mu^c c^b) - g f^{abc} (\partial_\mu A_\nu^a) A_\mu^b A_\nu^c + \frac{1}{4} g^2 f^{abe} f^{cde} A_\mu^a A_\nu^b A_\mu^c A_\nu^d + \bar{q}(-\partial^2 + m) q - i g \bar{q} \gamma_\mu t^a q A_\mu^a. \quad (11)$$

Here, sources σ and $\bar{\sigma}$ have been introduced for the (anti)ghost fields $(\bar{c})c$, in exactly the same way as the sources for the quark fields. The sign convention adopted for Grassmann fields is that derivatives generically denote,

$$\frac{\delta}{\delta(\bar{\eta}, \bar{\sigma})} := \text{left derivative}, \quad \frac{\delta}{\delta(\eta, \sigma)} := \text{right derivative}. \quad (12)$$

Despite the gauge invariance of the generating functional the Green's functions, obtained as the moments of this functional by taking derivatives with respect to the sources, are of

⁵ Together with massless states in certain ghost-gluon composite operators, see Sec. 4.4.3 in [36].

⁶ Positivity violation was already observed in the lattice studies of refs. [52,53].

course gauge dependent. The underlying gauge invariance, however, leads to relations between different Green's functions: the Ward–Takahashi identities in QED [54,55] and the Slavnov–Taylor identities in QCD [16,17]. The most convenient device to derive the Slavnov–Taylor identities is to exploit the Becchi–Rouet–Stora (BRS) symmetry [37] of Green's functions [56]. This will be discussed in detail in section 3.2. Here, for completeness, we give the (on-shell) nilpotent BRS transformations for linear covariant gauges:

$$\begin{aligned}\delta A_\mu^a &= D_\mu^{ab} c^b \lambda, & \delta q &= -ig t^a c^a q \lambda, \\ \delta c^a &= -\frac{g}{2} f^{abc} c^b c^c \lambda, & \delta \bar{c}^a &= \frac{1}{\xi} \partial_\mu A_\mu^a \lambda,\end{aligned}\tag{13}$$

with the global parameter λ belonging to the Grassmann algebra of the ghost fields. This parameter thus (anti)commutes with monomials in the fields that contain (odd)even powers of ghost or antighost fields. Here it commutes with the quark fields since we assumed commutativity of ghosts with quark fields (without loss of generality, because of ghost number conservation, either commutativity or anticommutativity can be assumed, see Ref. [36]). Therefore, one can assign λ the ghost number $N_{\text{FP}} = -1$ reflecting the fact that the BRS charge has ghost number $N_{\text{FP}} = 1$. The BRS invariance of the total Lagrangian in Eq. (11) follows from the gauge invariance of the classical action and the fact that gauge fixing and ghost terms can be expressed as a BRS variation themselves (*i.e.*, they are BRS-exact).

We use complex ghost fields with $\bar{c} \equiv c^\dagger$. With this hermiticity assignment the Lagrangian of Eq. (11) is not strictly hermitean and, furthermore, the BRS transformation given in Eq. (13) is not compatible with this assignment, as discussed, *e.g.*, in [36]. To avoid this, independent (here Euclidean) real Grassmann fields u, v should be introduced by substituting $c \rightarrow u$ and $\bar{c} \rightarrow iv$ in Eqs. (11) and (13) above. In Landau gauge ($\xi = 0$) we can make use of the additional ghost-antighost symmetry, however, to maintain the hermiticity of the Lagrangian and compatibility with the larger *double* BRS symmetry also for the assignment $\bar{c} = c^\dagger$. For $\xi \neq 0$, in the more general covariant gauge, this assignment is possible only at the expense of a quartic ghost interaction (which vanishes for $\xi \rightarrow 0$). Since we are mainly interested in the Landau gauge, we can disregard this subtlety and employ the naive BRS transformations together with the apparently *wrong* hermiticity assignment for the ghost fields in the derivations of Slavnov–Taylor identities. The results obtained in this way will be correct as long as we let $\xi \rightarrow 0$ eventually in these derivations. The explicit connection between independent real and complex ghost fields is provided by realizing that, in Landau gauge, the ghost number Q_c and the ghost-antighost symmetry of the real formulation are actually both part of a larger global $SL(2, \mathbb{R})$ symmetry (which can be maintained for $\xi \neq 0$ by introducing the quartic ghost self-interactions). The connection with the complex formulation is provided by the Cayley map and $SL(2, \mathbb{R}) \simeq SU(1, 1)$. Some details of this connection are provided in App. A.

Noether's theorem implies that there is a conserved anti-commuting charge. The existence of this non-trivial nilpotent and Hermitean charge is only possible because the state space has indefinite metric. From Noether's theorem one deduces furthermore that the BRS charge is the generator of BRS transformations: The BRS transform of an operator is given by the (anti-)commutator of it with the BRS charge. An operator which is the BRS transform of an other operator is called exact. From the nilpotency of the BRS charge one immediately concludes that the BRS transform of an exact operator vanishes. Taking furthermore into

account that the BRS charge commutes with the S -matrix this has lead to the conjecture that physical states are the ones which are annihilated by the BRS charge [57,41]. Furthermore, we note here that $\delta\lambda$ need not be infinitesimal nor need it be field-independent for (13) to be a symmetry of the Faddeev–Popov gauge fixed action [58]. However, the use of a field-dependent BRS transformation is complicated by the fact that the functional measure is in general not invariant under this non-local transformation.

Within linear covariant gauges the Green’s functions also depend on the gauge parameter ξ . Using BRS symmetry one can also derive the Nielsen identities [59] which control the gauge parameter dependence of Green’s functions. These identities can be used to prove the gauge independence of particle poles in the standard model to all orders in perturbation theory, for recent applications see ref. [60] and references therein.

Concluding this section we would like to add a remark regarding the non-perturbative use of the generating functional. In perturbation theory, the Gaussian measure over the free fields can formally be defined as a probability measure with support over the space of tempered distributions, see refs. [61,38]. For ghosts and longitudinal gluons this measure is not positive. The products of free fields occurring in the interactions, the composite fields, may also be well defined as tempered distributions. Ambiguities arise for products of these composite fields at coinciding Euclidean points. This is the origin for the need of renormalization. In a renormalizable theory there exists a finite set of composite fields such that the product of any of them at coinciding points contains composite fields within the same set multiplied by (formally infinite) renormalization constants. This is usually proven at all orders in perturbation theory. Multiplicative renormalizability beyond perturbation theory has the status of a conjecture.

Beyond perturbation theory, the only safe way to define the measure in the Euclidean generating functional, and thus the Euclidean Green’s functions as its moments, is given by the continuum limit of the lattice formulation of quantum field theory. The need for gauge fixing, the presence of long-range correlations such as the infrared divergences caused by the soft photons in QED,⁷ the possibility of infrared slavery in QCD, and triviality are some obstacles in a proper definition of the generating functional beyond perturbation theory. Some of these can be taken care of, others are less understood. In order to proceed, the existence of the generating functional has to some extend still be postulated for many realistic theories. This will be also the point of view in the following chapters. Before we move on, however, we briefly discuss the issue of the incompleteness of the gauge fixing procedure and some related issues in the next section.

2.2 *Gribov Copies, Monopoles and Gauge Fixing*

It is a well known problem that the Lorentz gauge condition $\partial A^a = 0$ is not complete [64]. On compact space-time manifolds it has been proven that solutions to local gauge conditions of the form $f(A) = 0$ are generally unable to uniquely specify the connection, *i.e.*, the gauge potentials A . The problem is generic and due to the topological structure of the non-Abelian gauge group [65], for a pedagogical discussion see chapter 8 of [66].

⁷ For two recent reviews on the treatment of soft and collinear infrared divergencies see, *e.g.*, [62,63].

Gribov's observation from the Coulomb, or analogously, from the Lorentz gauge condition $\partial A = 0$ is intuitively easy to understand. Consider the set of connections $\Gamma := \{A : \partial A = 0\}$ with the further constraint that all A connected by global transformations $SU(N_c)_{\text{global}}$ have to be identified in addition. For sufficiently strong $A(x)$ the Faddeev–Popov operator $-\partial D(A)$ can be shown not to be positive. Very much like bound states in quantum mechanics arise for sufficiently strong potentials, there is a critical A_c for which the lowest eigenvalue λ_0 of the Faddeev–Popov operator is zero. A normalizable zero-mode always arises from the analog of the bound state wave-function in the limit $A \rightarrow A_c$ from that side for which $\lambda_0 \rightarrow 0^-$.

Field configurations for which such zero modes occur in the Faddeev–Popov operator $-\partial D(A)$ constitute the Gribov horizons. In particular, the configurations A_c where this happens for the lowest eigenvalue are said to lie on the first Gribov horizon $\partial\Omega$, *i.e.*, the set of field configurations for which the lowest eigenvalue of the Faddeev–Popov operator vanishes. It can be shown that any point on $\partial\Omega$ has a finite distance to the origin in field space [44]. Furthermore, in Coulomb gauge (for any compact three-manifold) every Gribov copy obtained by a homotopically non-trivial gauge transformation of the trivial gauge field $A = 0$ has a vanishing Faddeev–Popov determinant. An example of this has already been given in the appendix of Gribov's original paper [64]. He considered a pure gauge potential $A^\mu = (0, \vec{A}^{pg}) = (0, -iU^\dagger \vec{\nabla} U)$ in Coulomb gauge $\vec{\nabla} \vec{A}^{pg} = 0$. If the gauge condition was unique the only solution should be $\vec{A}^{pg} = 0$. However, choosing an hedgehog configuration in an $SU(2)$ subgroup parametrized by the generators $\vec{\tau}$

$$U(\vec{r}) = \cos \frac{\theta(r)}{2} + i\vec{\tau} \hat{r} \sin \frac{\theta(r)}{2}, \quad \hat{r} = \frac{\vec{r}}{|\vec{r}|} \quad (14)$$

the gauge condition becomes

$$\frac{d^2\tilde{\theta}}{dt^2} + \frac{d\tilde{\theta}}{dt} - 2 \sin \tilde{\theta} = 0, \quad \text{with} \quad t = \ln \mu r \quad \text{and} \quad \tilde{\theta}(t) = \theta(r). \quad (15)$$

This is the classical equation of motion of a damped pendulum corresponding to the motion of a particle in the potential $V(\tilde{\theta}) = 2 \cos \tilde{\theta}$ with friction $d\tilde{\theta}/dt$ of unit strength. The static solutions $d\tilde{\theta}/dt = 0$ are given by $\tilde{\theta} = \theta = l\pi$ which decomposes into two sequences, the even and the odd multiples of π for $l = 2n$ and $l = 2n + 1$ with $n \in \mathbb{Z}$, respectively. For all pure gauge field configurations that approach these solutions at spatial infinity,

$$\vec{A}^{pg} \xrightarrow{r \rightarrow \infty} -iU^\dagger \vec{\nabla} U = -i \exp(-i\frac{\theta}{2}\vec{\tau} \hat{r}) \vec{\nabla} \exp(i\frac{\theta}{2}\vec{\tau} \hat{r}), \quad (16)$$

the Pontryagin index (winding number) is found to be half integer,

$$\nu = \frac{-i}{24\pi^2} \int d^3x \epsilon_{ijk} \text{tr}(A_i^{pg} A_j^{pg} A_k^{pg}) = \frac{l}{2} \quad \text{with} \quad l \in \mathbb{Z}. \quad (17)$$

Note that even though

$$\vec{A}^{pg} = 0, \quad \text{and} \quad \vec{A}^{pg} = \left(\frac{\vec{\tau}}{2} \times \hat{r}\right) \frac{2}{r}, \quad \text{at } r \neq 0 \quad (18)$$

for the even $\theta = 2n\pi$ and the odd $\theta = (2n+1)\pi$ static solutions, respectively, neither of these need to be entirely trivial. They can carry winding number concentrated at $\vec{r} = 0$ (for $l \neq 0$). For regularized $\theta_\epsilon^l(r) = l\pi r/\sqrt{r^2 + \epsilon^2}$ one verifies,

$$-\frac{1}{24\pi^2} \epsilon_{ijk} \text{tr} \left[(U_\epsilon^\dagger \nabla_i U_\epsilon) (U_\epsilon^\dagger \nabla_j U_\epsilon) (U_\epsilon^\dagger \nabla_k U_\epsilon) \right] \xrightarrow{\epsilon \rightarrow 0} \frac{l}{2} \delta^3(\vec{x}), \quad \text{for } U_\epsilon = \exp\left(i \frac{\theta_\epsilon^l(r)}{2} \vec{\tau} \hat{r}\right). \quad (19)$$

The even sequence $l = 2n$ yields infinitesimal (and thus singular) n -vacua obtained from the regular ones, $\theta_\epsilon^{2n}(r) = 2\pi n r/\sqrt{r^2 + \epsilon^2} \rightarrow 2n\pi$, for $\epsilon \rightarrow 0$. These, of course, correspond to the classification of configurations according to $\pi_3[SU(N)] = \mathbb{Z}$, *i.e.*, of configurations with the boundary condition that $U \rightarrow U_0$ for a unique $U_0 \in SU(2)$ in all directions at spatial infinity. The odd sequence on the other hand, corresponds to configurations for which two group elements at spatial infinity in opposite directions differ by a non-trivial central element (here by $-\mathbb{1} \in Z_2 = \{\pm\mathbb{1}\}$ for $SU(2)$) which does not affect adjoint fields such as the gauge potentials.⁸ This additional classification into even and odd sequences generalizes for the $SU(N)$ pure gauge theory according to $\pi_1[SU(N)/Z_N] = Z_N$ corresponding to fractional topological indices k/N with $k = 0, \dots, N-1$, see [67]. Instantons change the index ν by one unit. Those of infinitesimal size $\rho = \epsilon \rightarrow 0$ connect the vacua from the even sequence with the adjacent even ones and those of the odd sequence with adjacent odd ones.

Instantons at finite temperature $T = 1/\beta$ are the Harrington-Shepard calorons [68]. Calorons of formally infinite size $\rho \gg \beta$ (for $T \rightarrow 0$ it suffices to require $\rho \sim \beta$ in the following argument), on the other hand, can be obtained from (anti-periodic) gauge transformations of special types of the static, (anti)selfdual Bogomolnyi-Prasad-Sommerfield (BPS) monopoles, those with topological charge $Q = \beta\mu/2\pi = 1$, where μ is the scale of the BPS monopole, see [69,70]. The Polyakov-loop of these special BPS monopoles passes through the center of $SU(2)$ at the position of the monopole, and it approaches the center at spatial infinity. They thus correspond to two axial-gauge monopoles, the ramifications of the Gribov problem in the axial gauge (one at the position of the BPS monopole and the other one at infinity with zero total magnetic charge). This is a special case of the general relation between instantons and axial-gauge monopoles which was clarified in refs. [71,72]. Instantons corresponding to two axial-gauge monopoles at a finite distance of each other, called the non-trivial holonomy instantons because the Polyakov-loop does not approach the center at spatial infinity for these instantons, were found in refs. [73,74]. For the relation between instantons and the magnetic monopoles of general Abelian gauges, see ref. [75]. For gauge fixing and instantons in a field strength formulation, see ref. [76]. A relation to monopoles might be provided by a field strength formulation in the maximal Abelian gauge [77].

In the present context, however, we would like to point out that another special case of BPS monopoles might be of interest also: Consider BPS monopoles with topological charge

⁸ For the pure gauge theory these boundary conditions are equivalent and combined in $U \rightarrow Z_N U_0$.

$Q = \beta\mu/2\pi = 1/2$ for which the Polyakov-loop passes through the center only once, at the position of the monopole, and which thus correspond to one single axial-gauge monopole (these have non-trivial holonomy). The same gauge transformation, that of ref. [69] which provides the connection of the $Q = 1$ BPS monopoles with the calorons, can then be shown to lead to (anti)selfdual (finite-temperature) configurations (with $Q = 1/2$) which connect vacua from the even sequence (at $t = 0$, say) with neighboring ones of the odd sequence (for $t = \beta$).⁹ These might thus be of interest in connection with the realization of the center symmetry for spatial Polyakov loops, the Wilson lines discussed below. Unfortunately, as temperature approaches zero, the scale of the BPS monopole μ (for fixed $Q = \beta\mu/2\pi$) necessarily also vanishes with the effect that the transition from the (even) n -vacuum to its odd neighbor can be shown to occur infinitely close to the end-point of the time interval at the odd state with $\theta = (2n + 1)\pi$. So that this naive argument alone would leave one with the n -vacua as the only configurations stable for $T \rightarrow 0$.

Another possibility to connect vacua of the even sequence with neighboring odd ones is provided by merons which are singular, non-selfdual and thus of infinite action, classical solutions of the $SU(N)$ pure gauge theory [78,79]. Explicitly, an Euclidean one-meron solution in Coulomb gauge, see the review in ref. [80], is for an arbitrary $SU(2)$ subgroup given by

$$\vec{A}^{\text{mn}}(\vec{r}, t) = \left(\frac{\vec{\tau}}{2} \times \hat{r} \right) \frac{1}{r} \left(1 - \frac{t}{\sqrt{t^2 + r^2}} \right). \quad (20)$$

Clearly, for $t \rightarrow \infty$ (and $r \neq 0$) the meron configuration vanishes. More carefully, including the singularity at $r = 0$, one finds that it approaches a vacuum of the even sequence, corresponding to the $\epsilon \rightarrow 0$ limit of $\theta_\epsilon^{2n}(r) \rightarrow 2n\pi$. On the other hand, for $t \rightarrow -\infty$, $\vec{A}^{\text{mn}} \rightarrow \vec{A}^{\text{pg}} = (\vec{\tau} \times \hat{r})/r$ corresponds to $\theta_\epsilon^{2n+1}(r) \rightarrow (2n+1)\pi$ of the odd sequence. The connection to monopoles is quite obvious, the meron passes through a chromomagnetic monopole at $t = 0$ (with $B_i^a = -r_i r_a / r^4$ and $E_i^a = 0$ which was first reported as a static solution to the classical Yang-Mills equations in ref. [81]). Furthermore, it is also well known that the gauge potential of a meron is exactly half that of an infinitesimally small instanton (with size $\rho = \epsilon \rightarrow 0$), see refs. [79,80], just as expected for a configuration that connects the even with the odd vacua. The infinitesimal instanton corresponds to an analytically known solution for two merons at distance zero. The hypothesis that exact two-meron solutions with finite distance [78] might provide a more general connection between instantons and monopoles, in particular also for Coulomb and Landau gauges, is a long-standing conjecture, see refs. [82,83]. For a recent lattice study of meron-pairs, see ref. [84].

In addition to the (even and odd) static solutions with $\theta = l\pi$ discussed so far, there are of course also solutions to the equation (15) for $\tilde{\theta}(t)$ which start at one of the maxima of the potential $V(\tilde{\theta}) = 2 \cos \tilde{\theta}$ at $\tilde{\theta} = 2n\pi$ (with infinitesimal velocity) for $t \rightarrow -\infty$, and which approach one of the two neighboring minima at $\tilde{\theta} = (2n \pm 1)\pi$ for $t \rightarrow \infty$ (where they come to rest due to the friction term). For $n = 0$ these correspond to everywhere regular pure gauge field configurations, *i.e.*, Gribov copies of the vacuum, with $U(\vec{r}) \rightarrow \pm \mathbb{1}$ for $r \rightarrow 0$ and $U(\vec{r}) \rightarrow \pm i \vec{\tau} \hat{r}$ for $r \rightarrow \infty$, and with topological index $\nu = \pm 1/2$. The property of these

⁹ It is straightforward to obtain these configurations in the Landau gauge approaching the Coulomb gauge at the end-points of the (finite) time interval.

regular solutions to reach the odd sequence asymptotically (at $r \rightarrow \infty$) suffices to show that any Wilson line-integral along a curve γ starting from spatial infinity in some direction and leading to spatial infinity in the opposite direction is $-\mathbb{1}$, see ref. [67],

$$W_{\text{fd}}(\vec{A}^{pg}) = P \exp \left\{ i \int_{\gamma} \vec{A}^{pg} d\vec{s} \right\} = -\mathbb{1}, \quad \text{for } \vec{A}^{pg} = -i \exp(-i \frac{\theta(r)}{2} \vec{\tau} \hat{r}) \vec{\nabla} \exp(i \frac{\theta(r)}{2} \vec{\tau} \hat{r}) \quad (21)$$

in the fundamental representation for these configurations. (n -vacua yield $+\mathbb{1}$ just as the trivial vacuum, and adjoint Wilson lines yield $+\mathbb{1}$ in either case, of course).

For reasons that will become clear shortly, consider now the square norm of the various pure gauge configurations obtained from eq. (14). It is straightforward to see that

$$\|A^{pg}\|^2 = \int d^3x \text{tr} A_i^{pg} A_i^{pg} = 2\pi \int_0^\infty r^2 dr \left((\theta'(r))^2 + \frac{4}{r^2} (1 - \cos \theta(r)) \right) \quad (22)$$

which vanishes for $\vec{A} = 0$ and for all static $\theta = 2n\pi$ copies thereof. (The fact that these are singular at $\vec{r} = 0$ is irrelevant here, one readily verifies that the norm of the regular n -vacuum configurations $\theta_\epsilon(r) = 2\pi nr/\sqrt{r^2 + \epsilon^2}$ is of order ϵ and thus vanishes for $\epsilon \rightarrow 0$). From eq. (22) it is clear that $\theta(r) \rightarrow 2n\pi$ for $r \rightarrow \infty$, corresponding to the maxima of the potential $V(\tilde{\theta})$ in order for the square norm of such a pure gauge configuration to be finite. This is the case only for those configurations that approach n -vacua at large r . In particular, it is not the case for the regular Gribov copies discussed in the preceding paragraph (nor for regularized odd vacua). In addition, from the first term in the norm integral one then finds,

$$\int_0^\infty r^2 dr (\theta'(r))^2 = \int_{-\infty}^\infty dt' \left(\frac{d\tilde{\theta}(t')}{dt'} \right)^2 \quad (23)$$

which corresponds to the total dissipated energy (for $t \rightarrow \infty$) of the particle $\tilde{\theta}(t)$ in the potential $V(\tilde{\theta}) = 2 \cos \tilde{\theta}$. This implies that, due to the friction $d\tilde{\theta}(t)/dt$ in its equation of motion (15), any particle that comes to rest at one of the maxima $\tilde{\theta} = 2\pi l$ for $t \rightarrow \infty$ must have come from infinity with infinite initial energy (from either side for $t \rightarrow -\infty$). Therefore, the dissipated energy of this particle is also infinite except for $\tilde{\theta}(t) \equiv 2n\pi$ for all t . The only configurations with finite square norm are thus the singular n -vacua of the even sequence, for which $\|A^{pg}\|^2 = 0$ degenerate with the trivial configuration $\vec{A} = 0$. The even sequence $\theta = 2n\pi$ with $n \in \mathbb{Z}$ provides a set of degenerate absolute minima of the square norm.

Generally, the Gribov region Ω is defined as the set of connections within the Gribov horizon, *i.e.*, as the set of fields for which the Faddeev–Popov operator is positive. In the linear covariant gauges it explicitly reads $\Omega := \{A : \partial A = 0, -\partial D(A) \geq 0\}$. This convex Gribov region Ω is the set of the *local* minima of the functional

$$E_A[U] \equiv \|A^U\|^2 := \frac{1}{2} \int d^4x A_\mu^{aU}(x) A_\mu^{aU}(x) \quad (24)$$

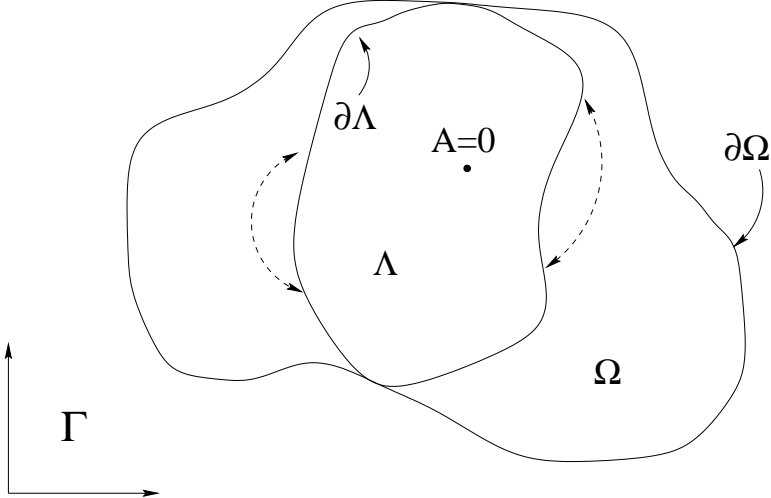


Fig. 1. Sketch of the hypersurface $\Gamma = \{A : \partial A = 0\}$, the Gribov and the fundamental modular region, Ω and Λ , respectively. The necessity of identifications on the boundary of Λ is indicated by dashed arrows.

with the equivalence class of gauge fields $[A^U]$ given in eq. (6). There are in general many local minima, and the Gribov region still contains gauge copies. As a further restriction, the fundamental modular region Λ is defined as the set of absolute minima of the functional (24). Each orbit (6) intersects Λ exactly once [85]. The fundamental modular region is contained within the Gribov region. In the interior of Λ the absolute minima are non-degenerate. Degenerate minima exist, however, on the boundary $\partial\Lambda$. These minima have to be identified [43,44]. The Gribov horizon, *i.e.*, the boundary of the Gribov region Ω , touches $\partial\Lambda$ at the so-called singular boundary points. The situation is sketched in Fig. 1. Note that the relevant configuration space is $\Lambda/SU(N_c)$, since the origin of the fundamental modular region, $A = 0$, is invariant under global gauge transformations [43,44].

In a continuum formulation of QCD it seems unlikely that a systematic elimination of gauge copies is possible at all.¹⁰ Their presence may or may not be a serious problem. On the other hand, there has been recently some progress treating the Gribov problem in lattice calculations. The lattice analog of restricting to the absolute minima of E_A is called minimal Landau gauge [92,93]. Various algorithms are used in gauge fixed Lattice calculations to minimize this functional, *e.g.*, in refs. [94,95,53,96]. Methods to find the absolute minima and the influence of Gribov copies are assessed in ref. [97]. Therefore a solution of the Gribov problem might in principle be feasible on the lattice. However, the question of existence and uniqueness of the continuum limit for corresponding quantities still remains an open question.

On compact manifolds, gauge fixing without the necessity of elimination of Gribov copies can

¹⁰ For completeness we mention that using Stochastic Quantization there is no need for a gauge fixing term and the Gribov problem is thus avoided, see ref. [86] for a pedagogical treatment of this topic. A related continuum formulation [87,88] considers QCD from a five-dimensional point of view, the fifth dimension playing the role of the “stochastic time”. This leads to parabolic equation for the propagators of the various ghost fields in the five-dimensional bulk and thus yields a trivial Faddeev–Popov determinant. There are also recent numerical investigations on the lattice based on Stochastic Quantization, see *e.g.* [89–91].

be formulated systematically in terms of a (Witten type) topological quantum field theory on the gauge group \mathcal{G} (see refs. [98,66]). In such a formulation, the standard Faddeev-Popov procedure of inserting unity into the unfixed generating functional which generalizes to a weighted average over all U with $A^U \in \Gamma = \{A : \partial A = 0\}$ in presence of Gribov copies [99,100] or, equivalently, the perturbative BRS quantization, essentially correspond to constructing a topological quantum field theory whose partition function computes the generalized Euler characteristic $\chi(\mathcal{G})$ of the gauge group [101]. This can vanish, however, just as the Witten index vanishes in theories with spontaneously broken supersymmetry. For the $SU(2)$ lattice gauge theory the vanishing of the Euler character follows quite trivially from $\chi(\otimes_{\text{sites}} SU(2)) = \chi(S^3)^{\#\text{sites}} = 0$, see also ref. [102]. In the continuum this remains to be the case due to the global gauge transformations which provide one vanishing factor $\chi(S^3)$ that survives the continuum limit. One way to cure this problem is to remove the global ghost zero modes by constructing a topological quantum field theory that computes the Euler character of the coset space $\otimes_x SU(N_c)/SU(N_c)_{\text{global}}$ which was shown not to vanish for $SU(2)$ in ref. [101]. Within the framework of BRS quantization this procedure has been worked out for QCD in the covariant gauge on the 4-torus in refs. [103,104].

An alternative way to avoid a vanishing Euler character proposed in ref. [105] is to fix the $SU(N)$ gauge symmetry only partially to the maximal Abelian subgroup $U(1)^{N-1}$. For the $SU(2)$ lattice gauge theory the BRS construction to compute $\chi(\otimes_{\text{sites}} SU(2)/U(1)) = \chi(S^2)^{\#\text{sites}} = 2^{\#\text{sites}}$ can then be used to obtain a reduced $U(1)$ lattice gauge theory [105]. Within covariant Abelian gauges in the continuum this kind of BRS quantization by ghost-antighost condensation can lead to mass generation for off-diagonal gauge bosons and thus to finite propagators at all Euclidean momenta except for the the diagonal “Abelian” gauge boson which remains massless [106,107]. The most important difference between this scheme and the standard Faddeev-Popov gauge fixing adopted for the maximal Abelian gauge, *e.g.*, in ref. [77], is that the maximal Abelian gauge condition is not implemented exactly in the former but softened by a Gaussian weight of width ξ analogous to the Lorentz condition in the linear covariant gauge. This leads to the occurrence of quartic ghost self-interactions (which formally vanish for $\xi = 0$) together with a global $SL(2, \mathbb{R})$ symmetry in the BRS construction of refs. [106,107]. The global $SL(2, \mathbb{R})$ can dynamically break down to the usual ghost number symmetry in the phase with ghost-antighost condensation (with the condensate as the order parameter). Besides being responsible for the ghost-antighost condensation and mass generation in some analogy to the BCS theory of superconductivity (with Higgs mechanism for the plasmon excitation), technically, the quartic ghost-selfinteractions eliminate the global gauge zero modes due to the constant (in this case the off-diagonal) ghosts. In this description, screening masses for the off-diagonal gauge bosons thus emerge naturally which persist in the high temperature phase [106]. This last conclusion is due to the relation of the ghost condensate with the scale anomaly which at the same time seems to show that it cannot provide an order parameter for the chiral symmetry breaking and/or confinement transition. It rather suggests that the global $SL(2, \mathbb{R})$ is broken in both, the high *and* the low temperature phases. In order to understand the possible origin of confinement in such a formulation, which in the usual BRS framework is related to the realization of the global gauge symmetry (on unphysical states), an application to the Higgs mechanism in the $SU(2) \times U(1)$ electroweak interactions would seem to be a natural next step.¹¹

¹¹In particular, the question might arise why the massive gauge boson belongs to an unphysical

It might be interesting for our present purposes, however, to note that a global $SL(2, \mathbb{R})$ symmetry containing ghost number and ghost-antighost symmetry emerges also in the Landau gauge (the special case of the linear covariant gauge with $\xi = 0$ in which the Lorentz condition is implemented “exactly”). Maintaining this symmetry in covariant gauges for gauge parameters $\xi \neq 0$ leads to the (massless) Curci-Ferrari gauges discussed in Appendix A. The significance of this symmetry seems not entirely clear at present. The differences between these Curci-Ferrari gauges and the standard linear covariant gauge seems, however, quite analogous to the situation in the maximal Abelian gauge discussed above.

While the presence of the quartic ghost self-interactions might at first not seem to be a very appealing feature of the Curci-Ferrari generalization of the Landau gauge (apart from maintaining its special symmetry), they do have one possibly quite interesting effect: The quartic ghost-selfinteractions are effective to eliminate all constant ghost (and antighost) zero modes for the gauge group $SU(3)$ of QCD.¹² This might therefore provide for a BRS formulation by a topological quantum field theory with non-vanishing partition function without need to eliminate the global gauge invariance. As we shall discuss in Section 2.4 the realization of the global gauge symmetry is of particular importance in the BRS formulation of the linear covariant gauge. The Kugo-Ojima criterion is based on the necessity of this global symmetry to be unbroken for a realization of confinement. Its breaking, on the other hand, leads via the *converse of the Higgs mechanism* to massive physical (BRS singlet) states in transverse gauge boson channels. In light of this, a formulation that allows both these possibilities by leaving the global gauge invariance untouched clearly seems desirable.

Among the $SL(2, \mathbb{R})$ -symmetric covariant gauges Landau gauge is special in that the quartic ghost interactions disappear for $\xi = 0$ with the effect that constant ghost zero modes arise. These are certainly problematic for a proper formulation of the gauge fixed theory at a finite volume as discussed above. It is not inconceivable, however, that it might suffice to deform the Landau gauge just slightly into an $SL(2, \mathbb{R})$ -symmetric covariant gauge without such zero modes at large but finite volume without modifying the naive Landau gauge results presented in later chapters of this review in the infinite volume limit (in which $\xi \rightarrow 0$ might be retained). This is certainly a quite optimistic assessment of the current situation about gauge fixing in presence of Gribov copies, and considerable further studies will be necessary to clarify this issue. Apart from some evidence in favor of the naive procedure, by comparing the results from Dyson-Schwinger equations to the conjectures of Gribov [64] and Zwanziger [92] and to lattice results, we will not have much more to say about this problem in the following chapters.

2.3 Positivity versus Color Antiscreening

In this section we briefly review and discuss a quite long known contradiction between asymptotic freedom, implying antiscreening of the color charge in the sense of Källén, and the posi-

quartet (see below) in one case while it definitely is a BRS singlet in any of the known Higgs models.

¹² For $SU(3)$ there are 16 constant (anti)ghost modes, and the expansion of the exponential of their quartic interaction to fourth order yields exactly one non-vanishing term that contains each of them exactly once. The same is not possible for $SU(2)$ with 6 constant modes, since no 6-(anti)ghost term arises in this expansion.

tivity of the spectral density for gluons in the covariant gauge [39]. While the apparent paradox was argued to be resolved for the (spacelike) axial gauge by West [108], as will be discussed in Sec. 5.2.3, present knowledge of the axial gauge suggests that this resolution is itself likely to be an artifact of a violation of positivity introduced by the axial-gauge singularity of the gluon propagator.¹³ The root of the contradiction thus seems to be more generic and not special to the covariant gauge. As will become clear in subsequent chapters, combined evidence from different non-perturbative calculations indicates quite convincingly that gluonic correlations do indeed violate positivity. As mentioned in the beginning of this chapter, and discussed in more detail in the next section, this can be interpreted as a manifestation of confinement. In the present section, we describe the original argument that this might be inferred already from asymptotic freedom and BRS invariance [46,109,41].

To understand the origin of the problem some basic properties of interacting fields are briefly recalled. For the moment a one-to-one correspondence between basic fields and stable particles is assumed which is of course not the case in QCD. Assuming field-particle duality and asymptotic completeness, the Lehmann-Symanzik-Zimmermann asymptotic condition for $t \rightarrow -\infty$ on an interacting field $\Phi(\varphi; t)$ states that it converges weakly on a dense domain \mathcal{D} to the creation operator $a_{in}^\dagger(\varphi)$ of a single particle state with wave function $\varphi(x)$:

$$\langle \alpha | \Phi(\varphi; t) | \beta \rangle \xrightarrow{t \rightarrow -\infty} Z^{1/2} \langle \alpha | a_{in}^\dagger(\varphi) | \beta \rangle , \quad (25)$$

i.e., the matrix elements of all states $|\alpha\rangle$, $|\beta\rangle$ in \mathcal{D} converge to those of the asymptotic field involving a normalization constant Z for the overlap with the corresponding single particle state of mass m_φ . This constant appears, of course, in the Lehmann representation of the propagator of the Φ -field ($m > m_\varphi$),¹⁴

$$D_\Phi(k) = \frac{Z}{k^2 + m_\varphi^2} + \int_{m^2}^{\infty} d\kappa^2 \frac{\tilde{\rho}(\kappa^2)}{k^2 + \kappa^2} . \quad (26)$$

The single particle contribution is explicitly separated here, *i.e.*, a full spectral function can be defined as $\rho(k^2) := Z \delta(k^2 - m_\varphi^2) + \tilde{\rho}(k^2)$. If one insisted on equal-time commutation relations for the interacting fields (*e.g.*, as in [2]), the following spectral sum rule would be obtained,

$$1 = Z + \int_{m^2}^{\infty} d\kappa^2 \tilde{\rho}(\kappa^2) , \quad (27)$$

¹³ In fact, recent studies of the axial gauge and, in particular, of the singularities in the corresponding tree-level gluon propagator, start from linear covariant gauges in defining the axial gauge, see Ref. [58] and the references therein.

¹⁴ The difficulties encountered in presence of massless particles are ignored here. Loosing the correspondence between single particle states and the discrete eigenvalues of the mass operator one has to account for the infrared divergences caused by, *e.g.*, the soft photons in QED. These can be dealt with by introducing coherent states. Thus, this complication is of no further significance for the arguments sketched in the following.

which would thus imply $1 \geq Z \geq 0$ for positive $\tilde{\rho}$. In general however, the second term on the r.h.s. of Eq. (27) is a divergent quantity associated with the field renormalization necessary in a renormalizable theory. This reflects the fact that, in contrast to free fields which are as operator valued distributions defined at fixed times, the interacting fields in a renormalizable theory are more singular objects. In particular, smearing over both the space *and* time variables is necessary in their definition. Their equal time commutation relations are no longer well-defined. Heuristically, they involve the divergent field renormalization constants. In the case of the gluon field being primarily under consideration here this constant is usually called Z_3 , and the resulting spectral sum rule reads,

$$Z_3^{-1} = Z + \int_{m^2}^{\infty} d\kappa^2 \tilde{\rho}(\kappa^2). \quad (28)$$

Turning the above argument around, the necessity of renormalization can be understood as follows: If the canonical equal-time commutation relations of the free theory ($g = 0$) are retained in the interacting theory ($g \neq 0$), the constant Z has to acquire a divergence so as to cancel the one on the r.h.s. of Eq. (27). This would imply that the asymptotic condition, Eq. (25), is lost. The representation of the interacting fields and the Fock space representation of the free canonical fields are inequivalent which is referred to as Haag's theorem. It is an example of the general representation problem in quantum field theory, the existence of inequivalent representations of the canonical commutation relations being the rule rather than the exception. Of course, in constructive field theory the equal-time canonical commutation relations are replaced by spacelike commutativity as the more general implementation of locality for interacting fields, see Haag's book for a thorough presentation and an account of the mathematical background [3].

The renormalized version of the spectral sum rule for the interacting theory given in Eq. (28) is in conflict with positivity of the spectral density of the (transverse) gluon propagator in Landau gauge QCD as was first observed in Ref. [39].

To see this, we note that Eq. (28) implies $Z_3^{-1} \leq Z$ for a positive spectral function, $\tilde{\rho}(\kappa^2) \geq 0$. Near the renormalization fixed point, however, one has in linear covariant gauges,

$$Z_3 = \left(\frac{g^2}{g_0^2} \right)^\gamma = \frac{\xi_0}{\xi} \quad (29)$$

with the renormalized gauge parameter ξ , the bare one ξ_0 , and γ being the leading coefficient of the anomalous dimension of the gauge field. The second equality is meaningful only, of course, if one is not considering the Landau gauge $\xi = \xi_0 = 0$. The first equality, however, holds for general covariant gauges including $\xi = 0$.

In QED the spectral density $\rho(k^2)$ of the photon propagator in the covariant gauge is identical to its axial gauge counterpart $\rho_g(k^2)$, *c.f.*, Sec. 5.2.2, which is a consequence of the gauge invariance of the Coulomb potential. In QED one furthermore has $\gamma = 1$, and from the gauge invariance of ρ it was argued that for the bare gauge parameter only the choices $\xi_0 = 0$ and $\xi_0 = \infty$ exist, implying the possible values of the bare coupling to be $e_0^2 \in \{\infty, 0\}$ [110].

The second choice corresponding to asymptotic freedom, in QED one might thus expect that the bare coupling diverges, *i.e.*, that the running coupling behaves as $\bar{e}^2(\mu) \rightarrow \infty$ for $\mu \rightarrow \infty$ (beyond one-loop). Here, a possible problem might rather be triviality of QED in the absence of an ultraviolet fixed point (for a pedagogical discussion see, *e.g.*, Huang's text book on quantum field theory [111]). In fact, recent evidence in favor of triviality is obtained for instance in the lattice simulation of Ref. [112]. Without a further fixed point, it follows that $Z_3 \rightarrow 0$. Due to the infrared fixed point at $e^2 = 0$, however, it is sufficient to note that the positive β -function near this fixed point generally implies a renormalized charge which is smaller than the bare charge. This is referred to as Källén screening. Therefore, in QED one has $Z_3 < 1 \leq Z^{-1}$ as one should.

In contrast, asymptotic freedom corresponds to the scaling limit $g_0 \rightarrow 0$. Therefore, for $\gamma > 0$ one has $Z_3 \rightarrow \infty$, and from Eq. (28) one thus concludes that the spectral density cannot be positive. In perturbative QCD in Landau gauge one has $1 > \gamma > 0$ for $N_f < 10$ quark flavors. Then, $Z_3^{-1} \rightarrow 0$ leads to the Oehme-Zimmermann superconvergence relation [39]. Its generalization to the complete class of linear covariant gauges leads to the following form of the spectral sum rule for the transverse gluon propagator [46,47,109],

$$Z + \int_{m^2}^{\infty} d\kappa^2 \tilde{\rho}(\kappa^2) = \begin{cases} 0, & \text{for } \xi \leq 0 \\ \xi/\xi_0, & \text{for } \xi > 0 \end{cases}. \quad (30)$$

Positivity of the gluon spectral density in Landau gauge is thus apparently in contradiction with antiscreening. As a result of this, it was concluded that positivity for gauge-boson fields is indeed violated in gauge theories with $Z_3^{-1} \rightarrow 0$ [109].

This has been interpreted as a manifestation of confinement from asymptotic freedom and unbroken BRS invariance, since the existence of a semi-definite *physical* space of transverse gluon states obtained after projecting out longitudinal gluon and ghost degrees of freedom would imply that $\rho(\kappa^2) \geq 0$ [46,40,41]. The significance of the global BRS charge structure here, to describe confinement in QCD on one hand versus the Higgs mechanism in the standard model of electroweak interactions on the other, will be discussed in the next section.

In order to look into the origin of the superconvergence relation, we recall that the renormalized gluon propagator in linear covariant gauges (explicitly including the dependence on the renormalization scale μ for the moment) has the general structure,

$$D_{\mu\nu}(k, \mu) = \left(\delta_{\mu\nu} - \frac{k_\mu k_\nu}{k^2} \right) \frac{Z(k^2, \mu^2)}{k^2} + \xi \frac{k_\mu k_\nu}{k^4}. \quad (31)$$

The subtlety of the argument can be made a little more explicit by considering the gluon renormalization function $Z(k^2, \mu^2)$ which depends on the invariant momentum k^2 , the scale μ and the gauge parameter ξ . In a perturbative momentum subtraction scheme in Landau gauge (*i.e.*, $\xi = 0$) one obtains for sufficiently large μ its leading logarithmic behavior to be

(also compare Sec. 5.3.3),

$$Z(k^2, \mu^2) = \left(\frac{\bar{g}^2(t_k, g)}{g^2} \right)^\gamma = Z_3^{-1}(\mu^2, k^2) \rightarrow 0, \quad \text{for } k^2 \rightarrow \infty, \quad (32)$$

with a positive anomalous dimension γ (for $N_f < 10$). Here, $\bar{g}^2(t_k, g)$ is the one-loop running coupling with $t_k = \frac{1}{2} \ln(k^2/\mu^2)$ and $\bar{g}^2(0, g) = g^2$. $Z_3(\mu^2, \mu'^2)$ is the multiplicative constant of finite renormalization group transformations. Depending on the details of the regularization scheme it is related to the gluon field renormalization constant essentially by $Z_3(\mu^2, \Lambda^2) \rightarrow Z_3$ for $\Lambda \rightarrow \infty$. The spectral representation of the gluon propagator, on the other hand, leads to

$$Z(k^2, \mu^2) = \int_0^\infty dm^2 \frac{k^2}{k^2 + m^2} \rho(m^2, \mu^2, g), \quad (33)$$

where the dependence of the spectral function ρ on μ^2 and g was made explicit again (the pair (g, μ) really represents only one parameter, of course). The renormalization condition of the momentum subtraction scheme fixes the gluon propagator to the tree-level one at a sufficiently large spacelike renormalization point $k^2 = \mu^2$,

$$\begin{aligned} Z(\mu^2, \mu^2) &= 1 \\ &= \int_0^\infty dm^2 \frac{\mu^2}{\mu^2 + m^2} \rho(m^2, \mu^2, g) \rightarrow \int_0^\infty dm^2 \rho(m^2), \quad \text{for } \mu^2 \rightarrow \infty. \end{aligned} \quad (34)$$

Comparing Eq. (34) to the limit in (32) one thus realizes that

$$\int_0^\infty dm^2 \rho(m^2, \infty, 0) = 1, \quad (35)$$

as expected for the free theory, whereas from Eq. (33) for $k^2 \rightarrow \infty$ one obtains,

$$\int_0^\infty dm^2 \rho(m^2, \mu^2 < \infty, g > 0) = 0. \quad (36)$$

Note that this last limit results by choosing a strictly finite renormalization point μ^2 and employing the limit $k^2/\mu^2 \rightarrow \infty$. This thus demonstrates explicitly that it is not possible to renormalize the interacting theory at a strictly finite scale, and a small but finite coupling g , to the free theory (corresponding to $g \equiv 0$). The superconvergence relation might therefore be interpreted as a reincarnation of Haag's theorem. The free theory and the interacting theory are inequivalent no matter how small the coupling is. The contradiction with positivity from the superconvergence relation could be avoided at this stage by supplying the definition of the asymptotic subtraction scheme with an implicit limit $\mu \rightarrow \infty$,

$$\lim_{\mu^2 \rightarrow \infty} D(k)|_{k^2=\mu^2} = D(k)_{\text{tree-level}} \quad (37)$$

In practical applications of the renormalization group this means that momenta larger than the renormalization point can be considered, their rough order of magnitude, however, is bound by that of the renormalization scale (with the momentum dependence for $k^2 \sim \mu^2$ governed by the scaling fixed point). Ambiguities in the non-commuting limits $k^2 \rightarrow \infty$ and $\mu^2 \rightarrow \infty$ as those leading to Eqs. (35) versus (36) arise, if momenta are taken to infinity relative to the subtraction point.

This same spirit of renormalizing the interacting theory to the free one *asymptotically* was actually adopted previously also for the quark propagator [113]. In that context it turned out to be necessary in order to implement the quark-confinement mechanism of infrared slavery into the asymptotically free theory.

The alert reader will have noticed that the Landau gauge considered so far is exceptional ($\xi = 0$), and that for other possible choices of the gauge parameter ξ in Eq. (30) the superconvergence relation might not rule out positivity anyway. The generalization of the Oehme-Zimmermann argument to the whole family of linear covariant gauges is less obvious. It is, in fact, long known that QCD in the covariant gauge has an ultraviolet fixed point in the (g^2, ξ) plane at a finite positive value of the gauge parameter $(0, \xi_0)$ with $\xi_0 = 13/3 - 4N_f/9$, see, *e.g.*, ref. [9]. Therefore, naively one might think that with $\xi \rightarrow \xi_0$ the spectral sum rule of the free theory (27) is recovered. A more detailed analysis shows, however, that the gluon spectral function $\rho(k^2)$ is negative for sufficiently large k^2 also in this case. Assuming that the only singularities of the gluon propagator lie on the timelike real axis in the complex k^2 -plane, one can still show that the discontinuity at the cut behaves asymptotically [46,47],

$$\rho(k^2) \equiv \rho(k^2, g^2, \mu^2, \xi) \rightarrow -\gamma C_R(g^2, \xi) \frac{1}{k^2} \left(\ln \frac{k^2}{\mu^2} \right)^{-\gamma-1}, \quad \text{for } k^2 \rightarrow \infty. \quad (38)$$

Here, γ is the same positive (for $N_f < 10$) anomalous dimension of the gluon field and $C_R(g^2, \xi)$ some positive constant. Therefore, $\rho(k^2)$ is shown not to be positive also in the general, linear covariant gauges. Analogous results from the renormalization group analysis employing analyticity in the cut complex k^2 -plane exist also for the ghost and the quark propagator for asymptotically large but complex k^2 , see Ref. [114]. While this demonstrates the violation of positivity of transverse gluons independent of the spectral sum rule in eq. (30), and already at the level of perturbation theory, by itself it is of course not sufficient to yield confinement. It can serve to demonstrate that the massless transverse gluon states of perturbation theory have to belong to unphysical BRS quartets (see the next section). For the realization of confinement it is necessary in addition that there is a mass gap in the transverse gluon correlations, *i.e.*, that the massless one-gluon pole of perturbation theory is screened non-perturbatively. Only then the Kugo-Ojima confinement criterion can establish the equivalence of BRS singlets with color singlets by requiring the global color symmetry to be unbroken. This will be discussed next. Note, however, that the requirement of an unbroken global gauge symmetry, the absence of both, physical as well as unphysical massless states from the spectrum of the global gauge current, is a necessary condition in the derivation of the superconvergence relations discussed in this section [41]. This condition is violated in models with Higgs mechanism which prevents one from concluding a positivity violation of the massive physical vector-states in the transverse gauge-boson correlations in that case.

The non-positivity of the gluon spectral density will be discussed in Sec. 5.3.4 again. There we collect the present evidence for its violation from two sources of non-perturbative results, from lattice simulations of the gluon propagator in the Landau gauge, and from the solutions to truncated Dyson-Schwinger equations. These two kinds of non-perturbative results furthermore both agree in indicating that no massless one-particle pole exists in the transverse gluon correlations.

2.4 Description of Confinement in the Linear Covariant Gauge

Covariant quantum theories of gauge fields require indefinite metric spaces. This implies some modifications to the standard (axiomatic) framework of quantum field theory. Modifications are also necessary to accommodate confinement in QCD. These seem to be given by the choice of either relaxing the principle of locality or abandoning the positivity of the representation space. The much stronger of the two principles being locality, non-local descriptions (see Sec. 2.5) have received far less attention than local ones. Great emphasis has therefore been put on the idea of relating confinement to the violation of positivity in QCD. Just as in QED, where the Gupta-Bleuler prescription is to enforce the Lorentz condition on physical states, a semi-definite *physical subspace* can be defined as the kernel of an operator. The physical states then correspond to equivalence classes of states in this subspace differing by zero norm components. Besides transverse photons covariance implies the existence of longitudinal and scalar photons in QED. The latter two form metric partners in the indefinite space. The Lorentz condition eliminates half of these leaving unpaired states of zero norm which do not contribute to observables. Since the Lorentz condition commutes with the *S*-Matrix, physical states scatter into physical ones exclusively. Color confinement in QCD is ascribed to an analogous mechanism: No colored states should be present in the positive definite space of physical states defined by some suitable condition maintaining physical *S*-matrix unitarity. A comprehensive and detailed account of most of the material summarized in this section can be found in the textbook by Nakanishi and Ojima [36]. Here, we briefly recall those of the general concepts that relate to some of the results presented in Chapter 5. In particular, we would like to emphasize the following three aspects: positivity violations of transverse gluon and quark states, the Kugo-Ojima confinement criterion, and the conditions necessary for a failure of the cluster decomposition. We describe each of these in the next three subsections, and we will find that the results of Chapter 5 nicely fit into these general considerations which thus together lead to a quite coherent, though certainly still somewhat incomplete picture.

2.4.1 Representations of the BRS Algebra and Positivity

Within the framework of BRS algebra, in the simplest version for the BRS-charge Q_B and the ghost number Q_c (both hermitean with respect to an indefinite inner product) given by,

$$Q_B^2 = 0 , \quad [iQ_c, Q_B] = Q_B , \quad (39)$$

completeness of the nilpotent BRS-charge Q_B in a state space \mathcal{V} of indefinite metric is assumed. This charge generates the BRS transformations ($\delta\Phi \equiv \lambda\delta_B\Phi$ with Grassmann parameter λ)

of a generic field Φ by the ghost number graded commutator,

$$\delta_B \Phi = \{iQ_B, \Phi\} \quad (40)$$

i.e., by a commutator or anticommutator for fields Φ with even or odd ghost number Q_c , respectively. In presence of ghost-antighost symmetry by Faddeev-Popov conjugation, this structure generalizes to that for the semi-direct product of the global $SL(2, \mathbf{R})$ with the double BRS invariance,¹⁵ see App. A. The semi-definite *physical* subspace $\mathcal{V}_{\text{phys}} = \text{Ker } Q_B$ is defined on the basis of this algebra by those states which are annihilated by the BRS charge Q_B ,

$$\mathcal{V}_{\text{phys}} = \{|\psi\rangle \in \mathcal{V} : Q_B|\psi\rangle = 0\} = \text{Ker } Q_B. \quad (41)$$

Since $Q_B^2 = 0$ this subspace contains the space of so-called daughter states which are images of others, their parent states in \mathcal{V} ,

$$\text{Im } Q_B = \{|\psi\rangle \in \mathcal{V} : |\psi\rangle = Q_B|\phi\rangle, |\phi\rangle \in \mathcal{V}\} \subset \mathcal{V}_{\text{phys}}. \quad (42)$$

A physical Hilbert space is then obtained as (the completion of) the covariant space of equivalence classes, the BRS-cohomology of states in the kernel modulo those in the image of Q_B ,

$$\mathcal{H}(Q_B, \mathcal{V}) = \text{Ker } Q_B / \text{Im } Q_B \simeq \mathcal{V}_s, \quad (43)$$

which is isomorphic to the space \mathcal{V}_s of BRS singlets. It is easy to see that the image is furthermore contained in the orthogonal complement of the kernel. Given completeness they are identical, $\text{Im } Q_B = (\text{Ker } Q_B)^\perp = \text{Ker } Q_B \cap (\text{Ker } Q_B)^\perp$ which is the isotropic subspace of $\mathcal{V}_{\text{phys}}$. It follows that states in $\text{Im } Q_B$, in the language of de Rham cohomology called BRS-coboundaries, do not contribute to the inner product in $\mathcal{V}_{\text{phys}}$. Completeness is thereby important in the proof of positivity for physical states [57,116,36], because it assures the absence of metric partners of BRS-singlets, so-called “singlet pairs” which would otherwise jeopardize the proof.

With completeness all states in \mathcal{V} can be shown to be either BRS singlets in \mathcal{V}_s or belong to so-called quartets which are metric-partner pairs of BRS-doublets (of parent with daughter states), and that this exhausts all possibilities. The generalization of the Gupta-Bleuler condition on physical states, $Q_B|\psi\rangle = 0$ in $\mathcal{V}_{\text{phys}}$, eliminates half of these metric partners leaving unpaired states of zero norm (in the isotropic subspace of $\mathcal{V}_{\text{phys}}$) which do not contribute to any observable. This essentially is the quartet mechanism:

Just as in QED, one such quartet, the elementary quartet, is formed by the massless asymptotic states of longitudinal and timelike gluons together with ghosts and antighosts which are thus all unobservable.

In contrast to QED, however, one expects the quartet mechanism also to apply to transverse gluon and quark states, as far as they exist asymptotically. A violation of positivity for such states then entails that they have to be unobservable also.

¹⁵ Corresponding to a Inonu-Wigner contraction of a $OSp(1, 2)$ superalgebra, see refs. [115,36].

The combined evidence for this, as collected in our present review, provides strong indication in favor of such a violation for possible transverse gluon states.

The members of quartets are frequently said to be confined kinematically. This is no comprehensive explanation of confinement, of course, but one aspect (among others as we shall describe below) of its description within the covariant operator formulation [36]. In particular, asymptotic transverse gluon and quark states may or may not exist in the indefinite metric space \mathcal{V} . If either of them do exist and the Kugo-Ojima criterion is realized (see below), they belong to unobservable quartets. In that case, the BRS-transformations of their asymptotic fields entail that they form these quartets together with ghost-gluon and/or ghost-quark bound states, respectively, see Sec. 4.4.3 in [36]. We reiterate that it is furthermore crucial for confinement, however, to have a mass gap in transverse gluon correlations, *i.e.*, the massless transverse gluon states of perturbation theory have to disappear (even though they should belong to quartets due to superconvergence in asymptotically free (and local) theories, see the discussion at the end of Sec. 2.3).

Before we continue we add two brief remarks. The BRS construction of the physical state space sketched above is endowed with a quantum mechanical interpretation in terms of transition probabilities and measurements as expectation values of observables. A necessary *and* sufficient condition on a (smeared local) operator¹⁶ A is that the isotropic subspace of zero norm states does not affect its expectation values in $\mathcal{V}_{\text{phys}}$ [117,36], *i.e.*

$$\delta_B A = \{iQ_B, A\} = 0 . \quad (44)$$

A is then called a (smeared local) observable in the present context thereby slightly generalizing the usual notion of an observable (by self-adjointness). It then follows that for all states generated from the vacuum $|\Omega\rangle$ by any such observable, *i.e.* a BRS-closed operator, one has

$$\langle \Omega | A^\dagger A | \Omega \rangle \geq 0 . \quad (45)$$

The interesting ones among the BRS-closed operators here are those, of course, which are not BRS-exact, *i.e.*, which are not BRS variations of others. On the other hand, the vacuum should be a BRS-invariant physical state, and thus for any BRS-exact operator $A = \delta_B B$,

$$\langle \Omega | \delta_B B | \Omega \rangle = \langle \Omega | \{iQ_B, B\} | \Omega \rangle = 0 , \quad (46)$$

from which all the famous Slavnov-Taylor identities can be derived by BRS transformations with choosing some suitable product of fields for B .

If this construction is shown to apply to a QCD description of hadrons as the genuine physical particles of \mathcal{H} , it is intuitively quite clear, and it can be established rigorously from physical S -matrix unitarity (with respect to the indefinite inner product), that absorptive thresholds in hadronic amplitudes can only be due to intermediate hadronic states. The S -matrix commutes with the BRS-charge, it is an observable in the above sense, and it thus transforms physical

¹⁶ One in the polynomial algebra of fields on a bounded open set of space-time, see, *e.g.*, ref. [3].

sates into physical ones exclusively and without leading to measurable effects of possible zero norm components [36]. Anomalous thresholds, the singularities related to the substructure of hadrons, can in this description also arise only from substructure of a given hadron as a composite state of other hadrons. The argument to establish this employs standard analyticity properties for hadronic amplitudes and crossing to relate them to absorptive singularities of other hadronic amplitudes which by the first argument above can only be due to intermediate hadronic states [40].

2.4.2 The Kugo-Ojima confinement criterion

In the BRS formulation of gauge theories, the realization of confinement by the quartet mechanism explained above depends on the realization of the unfixed global gauge symmetries. In particular, the identification of the BRS singlet states in the physical Hilbert space \mathcal{H} with color singlets is possible only if the charge of global gauge transformations is BRS-exact *and* unbroken, *i.e.*, well-defined in the whole of the indefinite metric space \mathcal{V} . The sufficient conditions for this are provided by the Kugo-Ojima criterion.

The starting point for this discussion, for the details of which we again refer to ref. [36] and the references therein, is the globally conserved current J_μ^a , *i.e.*, with $\partial_\mu J_\mu^a = 0$, given by

$$J_\mu^a = \partial_\nu F_{\mu\nu}^a + \{Q_B, D_\mu^{ab} \bar{c}^b\} . \quad (47)$$

It consists of two terms, the first one corresponding to a coboundary term with respect to the space-time exterior derivative and the other to a BRS-coboundary term. The spatial integrations of the zeroth components give their corresponding charges G^a and N^a , respectively, and the charge of the global gauge symmetry as the sum of the two,

$$Q^a = \int d^3x \partial_i F_{0i}^a + \int d^3x \{Q_B, D_0^{ab} \bar{c}^b\} = G^a + N^a . \quad (48)$$

For the first term herein there are only two options, it is either ill-defined due to massless states in the spectrum of $\partial_\nu F_{\mu\nu}^a$, or else it vanishes (as a total derivative).

Without going into detail, due to the masslessness of photons in QED, massless states contribute to both currents in (47), and both charges in (48) are separately ill-defined (the second term is given by the Nakanishi-Lautrup B -field as $N = \int d^3x \partial_0 B$ in this case). One can, however, employ an arbitrariness in the definition of the generator of the global gauge transformations (48) to multiply the first term by a constant suitably chosen so that the massless contributions cancel, and one arrives at a well defined and unbroken global gauge charge to replace the naive definition in (48) above, see also [118]. Roughly speaking, there are two independent structures in the globally conserved gauge currents in QED which both contain massless photon contributions. These can be combined to yield one well-defined charge as the generator of global gauge transformations leaving any other combination as a spontaneously broken global symmetry. One such combination generates the displacement symmetry, and the photon has conversely been interpreted as the massless Goldstone boson of its spontaneous breaking [119–121].

If on the other hand, $\partial_\nu F_{\mu\nu}^a$ contains no massless discrete spectrum (*i.e.*, if there is no massless particle pole in the Fourier transform of transverse gluon correlations), then $G^a \equiv 0$ [57]. In particular, this is the case for channels with massive vector fields in theories with Higgs mechanism, and it is expected to be also the case in any color channel for QCD with confinement for which it actually represents one of the two conditions formulated by Kugo and Ojima. In both these situations one first has, however,

$$Q^a = N^a = \left\{ Q_B, \int d^3x D_0^{ab} \bar{c}^b \right\}, \quad (49)$$

which is BRS-exact. The second of the two conditions for confinement which together are sufficient to establish that all BRS-singlet physical states in \mathcal{H} are also color singlets, and that, the other way around, all colored states are subject to the quartet mechanism, is to guarantee that the BRS-exact charge of global gauge transformations above be well-defined in the whole of the indefinite metric space \mathcal{V} .

This second condition obviously provides the essential difference between Higgs mechanism and confinement at the present stage. The operator $D_\mu^{ab} \bar{c}^b$ determining the charge N^a usually contains a contribution from the *massless* asymptotic field $\bar{\gamma}^a(x)$ of the elementary quartet contained in the asymptotic antighost field, $\bar{c}^a \xrightarrow{x_0 \rightarrow \pm\infty} \bar{\gamma}^a + \dots$,¹⁷

$$D_\mu^{ab} \bar{c}^b \xrightarrow{x_0 \rightarrow \pm\infty} (\delta^{ab} + u^{ab}) \partial_\mu \bar{\gamma}^b(x) + \dots \quad (50)$$

Here, the u^{ab} are dynamical parameters which determine the contribution of the massless asymptotic state to the composite field, $g f^{abc} A_\mu^c \bar{c}^b \xrightarrow{x_0 \rightarrow \pm\infty} u^{ab} \partial_\mu \bar{\gamma}^b + \dots$. These parameters can be obtained in the limit $p^2 \rightarrow 0$ from (here Euclidean) correlation functions of this composite field, *e.g.*,

$$\int d^4x e^{ip(x-y)} \langle D_\mu^{ae} c^e(x) g f^{bcd} A_\nu^d(y) \bar{c}^c(y) \rangle =: \left(\delta_{\mu\nu} - \frac{p_\mu p_\nu}{p^2} \right) u^{ab}(p^2). \quad (51)$$

The theorem by Kugo and Ojima [57] asserts that all $Q^a = N^a$ are well-defined in the whole of \mathcal{V} (and do not suffer from spontaneous breakdown), if and only if

$$u^{ab} \equiv u^{ab}(0) \stackrel{!}{=} -\delta^{ab}. \quad (52)$$

Then the massless states from the elementary quartet do not contribute to the spectrum of the current in N^a , and the equivalence between physical states as BRS-singlets and color singlets can be established, details and proofs are provided in refs. [57,36,118].

For a discussion of the fate of the non-Abelian version of the displacement symmetry, the vector symmetry cooresponding to gauge transformations $\theta^a(x) = a_\mu^a x^\mu$ with global parameters a_μ^a , see refs. [118,122]. Essentially, one finds that the Kugo-Ojima criterion $\mathbf{1} + u \equiv 0$, also removes the massless states from the correlation functions of its corresponding current.

¹⁷ These are understood as weak limits in the sense of LSZ, see also sec. 2.3.

If, however, as the other extreme, no eigenvalue of $\mathbb{1} + u$ vanishes, *i.e.*, for $\det(\mathbb{1} + u) \neq 0$, then the so-called *converse of the Higgs theorem* asserts that the global gauge symmetry generated by the charges Q^a in eq. (48) is spontaneously broken in each channel in which the gauge potential A_μ^a contains an asymptotic massive vector field (leading to a mass gap in $\partial_\nu F_{\mu\nu}^a$ and thus $G^a = 0$ for that channel), see refs. [57,36].

Spontaneous breakdown of any (combination) of the charges Q^a really is in one-to-one correspondence with the occurrence of a massive gauge boson in this framework. And as a consequence of this breaking, the massive vector asymptotic field contained in the gauge potential results to be a BRS-singlet and thus physical. Whereas the massless Goldstone boson states usually occurring in some components of a Higgs field, belong to the elementary quartet and are thus unphysical. Therein they take the place of one of the components of the gauge field which in turn becomes a BRS-singlet to yield the third component of the massive physical vector field. This is explicitly worked out in detail for the Abelian Higgs and the Higgs-Kibble models also in ref. [36].

Since the Goldstone bosons are altogether unphysical and the broken charges BRS-exact in this case, called *hidden* spontaneous symmetry breaking, nothing of this breaking is observed in the Hilbert space of physical states \mathcal{H} , and no conflict with Elitzur's theorem [123] arises which asserts that local gauge symmetries should not be spontaneously broken for reasons similar to ordinary quantum mechanics where spontaneous symmetry breaking is precluded by von Neumann's uniqueness theorem for the representations of the canonical commutation relations.¹⁸ The same can be understood from an alternative description. Eliminating the redundant variables of gauge theories in a non-covariant canonical formulation explicitly, the Higgs mechanism can be shown to generate the masses of physical vector bosons without breaking of the gauge symmetry [125,126]. Mass generation without symmetry breaking is in fact a well known mechanism. It occurs in the large N limit of the $O(N)$ -vector model [127–130] of N selfinteracting scalar fields in four dimensions,¹⁹ as well as in the $O(N)$ -symmetric Gross–Neveu or $SU(N)$ Thirring model [13,132] of selfinteracting fermions in two dimensions.²⁰ It usually requires breaking of scale invariance only, which is an anomaly rather than a broken symmetry [134,135].

Nevertheless, it is instructive to classify the different scenarios by considering the realization of the global gauge symmetry on the whole of the indefinite metric space \mathcal{V} of covariant gauge theories. In this formulation, however, as long as the global gauge symmetry is unbroken, *i.e.*, for QED and QCD, the first of the two conditions becomes the relevant one. Namely, it is then necessary for confinement to have a mass gap in transverse gluon correlations (*i.e.*, in $\partial_\nu F_{\mu\nu}^a$), since otherwise one could in principle have *non-local* physical (BRS-singlet and thus gauge invariant) states which are no color singlets, however, just as one has non-local gauge invariant charged states in QED, *e.g.*, the state of one electron alone in the world with its

¹⁸ Some spin transformation symmetries can also be spontaneously broken even in quantum mechanics. This is important in systems with spontaneously broken supersymmetry for instance [124].

¹⁹ Scalar ϕ^4 -theory likely is trivial [38] but it can be analytically continued in the complex coupling to yield a stable Euclidean field theory, in general, on the cost of reflection positivity [131].

²⁰ In two dimensions there cannot be a chiral phase transition due to the Coleman–Mermin–Wagner theorem. The large N results can, however, be interpreted as a Kosterlitz–Thouless transition. What occurs is a mass gap for the fermions but no Goldstone bosons [133].

long-range Coulomb tail. Indeed, with unbroken global gauge invariance QED and QCD have in common that any gauge invariant localized state must be chargeless/colorless, see Sec 4.3.3 in [36]. The question is the extension to non-local states as approximated by local ones. In QED this leads to the so-called charge superselection sectors, see [3], and non-local charged physical states arise. In QCD, with mass gap *and* unbroken global gauge symmetry, the representations of (the net of) algebras of local observables will be irreducible in \mathcal{H} and every gauge-invariant state can therefore be approximated by gauge-invariant localized ones (which are colorless), thus *every* gauge invariant (BRS-singlet) state in \mathcal{H} will be a color singlet.

We close this subsection with one more comment relevant to the results presented in Chap. 5: It concerns the observation pointed out by Kugo in ref. [118] that the (2nd condition in the) Kugo-Ojima confinement criterion, $u = -1$, in Landau gauge is equivalent to an infrared enhanced ghost propagator. In particular, based on standard arguments employing Dyson-Schwinger equations and Slavnov-Taylor identities, one can show that the nonperturbative ghost propagator of Landau gauge QCD in momentum space is related to the form factor occurring in the corelations of eq. (51) as follows,

$$D_G(p) = \frac{-1}{p^2} \frac{1}{1 + u(p^2)}, \quad \text{with } u^{ab}(p^2) = \delta^{ab}u(p^2). \quad (53)$$

The Kugo-Ojima criterion, $u(0) = -1$, thus entails that the Landau gauge ghost propagator should be more singular than a massless particle pole in the infrared.

Indeed, we will present quite compelling evidence (from DSEs and lattice simulations) for this exact infrared enhancement of ghosts in Landau gauge necessary for a realization of the Kugo-Ojima confinement criterion. It is furthermore interesting to note that there are recent lattice simulations also testing this criterion directly [136,137]: Instead of $-\delta_b^a$ they obtain numerical values of around $u = -0.7$ for the unrenormalized diagonal parts and zero (within statistical errors) for the off-diagonal parts. After renormalization, diagonal parts very close to -1 result. Taking into account the finite size effects on the lattices employed in the simulations, these preliminary results might be perfectly reconciled with the Kugo-Ojima confinement criterion (52). Certainly, they serve to demonstrate the utility of such an independent test.

2.4.3 Cluster decomposition property and observables

The remaining dynamical aspect of confinement in this formulation resides in the cluster decomposition property of local quantum field theory. Its proof [138,139], which is absolutely general otherwise, does not include the indefinite metric spaces of covariant gauge theories [34,140]. The situation in local quantum field theory including indefinite metric spaces can roughly be summarized as follows, see refs. [36,3]: For the vacuum expectation values of two (smeared local) operators A and B , translated to a large spacelike separation R of each other one obtains the following bounds depending on the existence of a finite gap M in the spectrum of the mass operator in \mathcal{V} ,

$$\begin{aligned}
& \left| \langle \Omega | A(x) B(0) | \Omega \rangle - \langle \Omega | A(x) | \Omega \rangle \langle \Omega | B(0) | \Omega \rangle \right| \\
& \leq \begin{cases} \text{Const.} \times R^{-3/2+2N} e^{-MR}, & \text{mass gap } M, \\ \text{Const.} \times R^{-2+2N}, & \text{no mass gap,} \end{cases} \tag{54}
\end{aligned}$$

for $R^2 = -x^2 \rightarrow \infty$. Herein, positivity entails that $N = 0$, but a positive integer N is possible for the indefinite inner product structure in \mathcal{V} . Therefore, in order to avoid the decomposition property for products of unobservable A, B which together with the Kugo-Ojima criterion is equivalent to avoiding the decomposition property for colored clusters, there should be no mass gap in the indefinite space \mathcal{V} . Of course, this implies nothing on the physical spectrum of the mass operator in \mathcal{H} which certainly should have a mass gap. In fact, it was shown within the covariant BRS formulation of gauge theories that if the cluster decomposition property holds for a product $A(x)B(0)$ which together forms a (smeared local) observable in the sense of condition 44, that both, A and B also satisfy this condition separately and are thus observables themselves [35]. This would then eliminate the possibility of scattering a physical state into color singlet states consisting of widely separated colored clusters (the “behind-the-moon” problem, see also Ref. [36] and references therein).²¹

The necessity for the absence of the massless particle pole in $\partial_\nu F_{\mu\nu}^a$ in the Kugo-Ojima criterion shows that the (unphysical) massless correlations to avoid the cluster decomposition property are *not* the transverse gluon correlations. In that sense, an infrared suppressed propagator for the transverse gluons in Landau gauge confirms this condition. This holds equally well for the infrared vanishing propagator obtained from DSEs and conjectured in refs. [64,92] studying the implications of the Gribov horizon, as for the suppressed but possibly infrared finite ones extracted from improved lattice actions for quite large volumes [51]. At the same time, however, it shows that transverse gluons are not responsible for a failure of the cluster decomposition property. The infrared enhanced correlations responsible for this in Landau gauge can be identified with the ghost correlations which at the same time provide for the realization of the Kugo-Ojima criterion.

Then, the question for massless unphysical single particle states remains. Here, for the Landau gauge results the infrared fixed point obtained in the nonperturbative running coupling as defined in chapter 5, if it will be confirmed, implies the existence of unphysical massless bound states, *i.e.*, massless single particle poles corresponding to asymptotic states in colored composite operators which by virtue of the Kugo-Ojima criterion belong to unobservable quartets. This should be further studied, in particular, with emphasis on the relation of these massless states to a hidden spontaneous breakdown of some symmetry. As a candidate for this symmetry breaking, the global $SL(2, \mathbb{R}) \rightarrow \mathbb{R}$ (ghost number) common to the Landau (the Curci-Ferrari) and the BRS formulation of covariant Abelian gauges was suggested in refs. [106,107]. This certainly offers an interesting possibility for further studies extending the Landau gauge results to the more general, $SL(2, \mathbb{R})$ symmetric gauges discussed in appendix A.

We close this section with an interesting technical side remark on implications of the results from the Landau gauge DSEs presented in Chapter 5. This DSE solution entails an infrared

²¹ It is always an alternative possibility, of course, that spacelike commutativity does not hold for unphysical fields, see the discussion in the next section.

vanishing gluon propagator together with an infrared fixed point for the coupling. The latter arises from the infrared finiteness of the product of $G^2(k^2)Z(k^2)$, where $Z(k^2)$ is the infrared vanishing gluon renormalization function and $G(k^2) = 1/(1 + u(k^2))$ is the infrared singular ghost renormalization function. This scenario corresponds to the third of three different possibilities discussed by Kugo in ref. [118] for the realization of the Kugo-Ojima criterion in Landau gauge. This third possibility, the one favored by Kugo from plausibility arguments, in addition to a vanishing gluon propagator also leads to an infrared vanishing renormalization function for the 3-gluon vertex at symmetric momenta, see also secs. 5.3.2 and 5.3.3.

2.5 Alternative singularity structures of Green's functions

As stated above, possibilities other than the description of confinement in QCD in terms of local quark and gluon fields are also viable. Since spacelike commutativity of local fields is such a strong principle, and any relaxation of this has quite severe consequences, non-local descriptions have received far less attention than local ones. The most elementary examples to discuss differences between local and non-local descriptions are provided by 2-point correlation functions. While any 2-point correlation, *i.e.*, the quark and gluon propagators in QCD, in a local field theory is an analytic function in the cut complex p^2 -plane with singularities along the time-like real axis only, for any other singularity structure the two fields in the correlation function have a commutator with non-vanishing support into a region of spacelike separations.

Nevertheless, complex singularities with time-like real part might be considered as acceptable for the propagators of unphysical (colored) fields. Such singularities might then conspire to cancel with singularities or zeros in other unphysical correlation functions so as to be absent from physical amplitudes. This will give rise to an infinite hierarchy of constraints on such unphysical singularities in arbitrarily high n -point functions. An example of such compensating singularities are those inherent in the non-perturbative expansion scheme of refs. [141,142] which we describe briefly in sec. 2.5.2, and later in sec. 5.4.

Another phenomenologically appealing model of confinement is based on entire 2-point correlation functions. Asymptotic freedom entails, however, that these functions would have to vanish for $p^2 \rightarrow \infty$ in all directions of the complex p^2 -plane [39,40]. Non-trivial entire functions with that property do not exist. The use of entire functions with an essential singularity at infinity might still be interesting as a phenomenological concept, the difficulty will then in general be, however, to prevent the resulting “signals” from such unphysical correlations which will grow exponentially in time to lead to measurable effects.

2.5.1 Entire correlation functions

Entire correlation functions occur *e.g.* in constant background fields. Historically the Euler-Heisenberg Lagrangean (see *e.g.* sec. 4.3 of ref. [2]) provided the first example. The constant electric and magnetic background field introduces a non-local interaction. Correspondingly, the correlation functions for charged particles, usually expressed as proper time integrals, display a non-standard singularity structure, see *e.g.* Chapter 2 of ref. [143] and references therein. Note

that a constant field in an infinite volume is an infinitely large energy reservoir. This underlines the impossibility of such a background field in QED: Pair creation would immediately set in. Therefore it is safe to conclude that the appearance of such effects in certain treatments of QED in strong fields is due to the employed approximations.²² As for QCD one might take a different point of view and consider entire correlation functions as physical accepting hereby the existence of non-local interactions.

Causality might be kept in a non-local quantum field theory if one requires that only exponentially localized sources are allowed. Of course, as the aim is to describe confinement such a restriction seems to be quite natural: Confinement implies that colored sources are strongly localized. Despite the non-local interaction, and the resulting non-vanishing commutators of operators over spacelike distances, physical amplitudes possess then a causal behavior. For the purpose of this review it is instructive to turn the argument around. Suppose the propagator of a field is, apart from the tensorial structure related to the spin of the field, given by

$$D(p^2) = b \int_0^1 ds e^{-sb(p^2+m^2)} = \frac{e^{-b(p^2+m^2)}}{p^2 + m^2}. \quad (55)$$

For spacelike (Euclidean) momenta $p^2 > 0$ it differs from the propagator of a free field with mass m only by an exponentially small number, for timelike momenta, however, the pole at $p^2 = -m^2$ is removed at the expense of an essential singularity at $-p^2 \rightarrow \infty$. Note that this qualitative type of behavior occurs in some terms of the propagator of charged particles in constant background fields. Obviously, with the usual constraints to sources, such a propagator would violate causality. On the other hand, if the Fourier transforms of all sources, $\tilde{J}(p)$, are restricted such that

$$|\tilde{J}(p)| < e^{-|p^2|+\epsilon} \quad \text{with } \epsilon > 0, \quad (56)$$

causality is restored. This implies that

$$|J(x_0, \vec{x})| < e^{-|x_0|+\delta} \quad \text{with } \delta > 0. \quad (57)$$

Thus, in turn, can be interpreted as confinement [144]: All charged, *i.e.*, colored, sources are exponentially localized in time. The disadvantage has been turned into a virtue: Claiming the realization of confinement via entire correlation functions one has to require localized sources for consistency.

Ansätze for propagators which consist of sums and/or products of the form (55) have been widely used in models for meson and baryon physics, see refs. [31,144] and references therein as well as Chapters 6 and 7 of this review. These propagators are entire functions in the whole complex p^2 plane and are non-trivial only due to the essential singularity at infinite timelike momentum. Of course, these parametrizations contain a number of parameters which

²²This remark does not apply to the time evolution in a plasma based on a kinetic description, see Chapter 5 of ref. [31] and references therein.

are fitted to observables, *e.g.*, in ref. [145] the quark propagator being an entire function with six parameters has been fixed in a least-squares fit to light meson observables. It should be noted, however, that such propagators have zeros in the complex p^2 -plane. As we will see in the course of this review Ward identities require that vertex functions are proportional to inverse propagators. Obviously, these vertex functions then possess singularities at finite (complex) values of p^2 . Of course, these singularities are highly problematic when calculating hadronic reactions with timelike momentum transfers.

In ref. [113] the quark DSE in Landau gauge has been solved using a regularized $1/k^4$ interaction in the infrared ($k^2 \rightarrow 0$). This has resulted in a quark propagator which is only non-vanishing as long as the regularization is kept. With finite regularization the propagator possesses a pole for timelike momenta but removing the regularization the quark propagator vanishes for all momenta. Nevertheless, a finite pion mass and decay constant results by employing the propagator of the regularized interaction and extrapolating to zero regularization parameter at the end of the calculation.

There are also a number of models where a momentum dependent quark mass is tuned such that the quark cannot go on-shell, see *e.g.* refs. [146,147]. Nevertheless, the quark propagator possesses singularities in the complex p^2 plane. These singularities are again highly problematic if such a propagator is used to calculate hadronic processes.

Summarizing this subsection it is probably fair to say that the idea to realize confinement via the use of entire correlation functions is neither understood on a fundamental level nor it is without technical problems.

2.5.2 Compensating singularities

Apparently unphysical singularities in proper vertex functions induced by the zeros of the propagators are inherent in the scheme of refs. [141,142]. In this approach rational Ansätze are employed in DSEs to account for the essential singularities that occur in the Green's functions as functions of the coupling due to the dynamical generation of a nonperturbative mass scale, see Sec. 5.4. As we will see there, the hierarchical coupling of the different vertex functions implies common poles in external momenta.

In particular, poles in the 2-point vertices, *i.e.* the zeros of the propagators, reappear in all higher vertex functions. For scattering amplitudes, the poles in the external lines are compensated by the corresponding zeros of the propagators attached to these lines. Thus, these artifacts of the approximation will not give rise to unphysical asymptotic particle states.

The situation is more complicated, however. It can be inferred from the hierarchy of DSEs, together with the exchange symmetries, that the presence of poles in the external momenta of lower n -point ($n = 2, 3$) vertex functions furthermore implies poles in the Mandelstam variables of successively higher n -point vertices (s, t, u, \dots , for $n \geq 4$). These pole contributions cannot be represented by one-particle reducible contributions and thus in no way contradict the 1-PI property of these vertex functions (just as bound state poles do not). However, analogous poles occur also in 1-particle reducible contributions to scattering amplitudes: In such contributions, an internal propagator having say one simple zero is connected to two vertex functions each

contributing a simple pole at the momentum of the zero in the propagator. One simple pole remains in this exchange. The important but non-trivial observation is now that these poles exactly cancel those appearing in the Mandelstam variables of the 1-PI contributions to the scattering amplitudes in the scheme of Refs. [148,149]. The respective contributions to scattering amplitudes that remain after this cancellation can be classified according to an extended notion of irreducibility. It involves subtracted, softened one-particle reducible exchanges and equally subtracted 1-PI contributions. As a result, no unphysical particle productions according to Cutkosky's rule will occur in the scattering amplitudes due to these compensating poles. In the integration kernels of the DSEs for arbitrary 1-PI n -point functions, on the other hand, this cancellation is incomplete. The necessary pole contributions reproduce themselves in the hierarchy [148,149].

The first studies within this approach, restricted to the lowest non-trivial order in the rational approximation scheme for pure QCD, and furthermore assuming a perturbative ghost propagator in Landau gauge, suggested an infrared vanishing gluon propagator $\sim k^2$ for small spacelike momenta [141,142]. Extended to include the DSE for the 3-gluon vertex it was later concluded that the pure gauge theory no longer allows for a physically acceptable solution with infrared vanishing gluon propagator. Solutions were instead obtained for an infrared finite gluon propagator [148]. This statement is, of course, strictly restricted to the lowest order of the rational approximation, and without radiative corrections to this approximation, as employed in these studies. Furthermore, the inclusion of two flavors of dynamical quarks changed this same conclusion and a sign change was observed in the gluon propagator in this case. This latter result might seem questionable as it implies tachyonic poles in the vertex functions. While the mechanism of pole compensation does not make a formal difference between unphysical non-tachyonic and tachyonic compensating poles, the presence of the latter is usually a sure sign of a vacuum instability. Nevertheless this shows that the infrared vanishing scenario of a gluon propagator cannot be ruled out from the present stage of these studies.

The ghost propagator and the ghost-gluon vertex were in all presently available solutions to this scheme taken to be the tree-level ones. While in the first studies [141,142] this was still an additional assumption, the more complete solutions seemed to verify this assumption at a more complete approximation level recently [148,149]. This together with an infrared finite or vanishing gluon propagator contradicts the masslessness condition which was obtained by Mandelstam for the gluon propagator in Landau gauge when a trivial ghost sector is assumed [18]. A non-trivial ghost self-energy which affects the masslessness condition becomes unavoidable also in this approach, however, when perturbative corrections are taken into account via the operator product expansion [150].

3 The Dyson–Schwinger Formalism

Being the vacuum expectation values of fields the Green's functions are constrained by the classical action principle and the equal-time commutation relations. Thus, at least formally, their equations of motion, the Dyson–Schwinger equations (DSEs) [14,15], and the existence of a generating functional are tied together. Based on purely combinatorical arguments, DSEs can be established from the way how particles interact based on canonical quantization. The generating functional can in simple cases be constructed from these equations. On the other hand, a proper definition of the generating functional for the Green's functions, together with a linked cluster theorem to classify the (dis)connected contributions, allows to derive the corresponding DSEs.

Practically, such definitions are full of mathematical difficulties. In neither direction, from the combinatorics of interactions to the generating functional nor the other way round, from the generating functional to DSEs, can the derivation of both as yet be fully divorced from perturbation theory. Just as multiplicative renormalizability, proven at every order in perturbation theory, is assumed to hold non-perturbatively, the DSEs are nevertheless considered to reflect the full non-perturbative dynamics of the quantum field theory they describe.

Since lattice formulations seem to provide non-perturbative constructions of quantum field theory of unprecedented rigor, a corresponding formulation of DSEs might in principle be considered a promising approach to their non-perturbative definition also (see, *e.g.*, ref. [151] and the references therein). In such an approach the problem arises, however, that lattice regularized DSEs do in general not possess unique solutions. This has been traced to ambiguities in the selection of boundary conditions [152]. The search for the correct ones is aggravated by the fact that there are so many of them. In the continuum limit, however, many of the solutions associated with different boundary conditions coalesce while solutions for others disappear. In matrix models countable sets of solutions are obtained in some instances, and continua of distinct solutions somewhat analogous to the occurrence of θ -vacua in others [152]. It was furthermore observed that the set of boundary conditions for which the “thermodynamic limit” exists can vary along certain paths in the space of coupling constants thus leading to discontinuous changes in the solutions as such “phase boundaries” are crossed. The phase structures of quantum field theories might therefore have one explanation in terms of the boundary conditions on the solutions to their DSEs. These studies provide some indication towards the considerable power and flexibility of DSEs in describing non-perturbative physics, at least in principle, which to a large extend is yet to be explored.

3.1 Dyson–Schwinger Equations for QED and QCD Propagators

Assuming the existence of a well-defined measure in a functional integral representation of the generating functional for QED or QCD, here we briefly present the derivation of the corresponding DSEs describing the non-perturbative dynamics of electrons and photons or quarks and gluons, respectively. To avoid unnecessary confusion, we will adopt somewhat symbolic and simplified notations to outline the basic steps in this derivation first.

Corresponding to the classification of full, connected and proper (*i.e.*, one-particle irreducible) Green's functions various kinds of different generating functionals are introduced. First, the generating functional of section 2.1,

$$Z[j] = \int \mathcal{D}\phi \exp \{-S[\phi] + j_i \phi_i\} = \langle e^{j_i \phi_i} \rangle = \sum_{n=0}^{\infty} G_{i_1 \dots i_n} j_{i_1} \dots j_{i_n}, \quad (58)$$

generates the full Green's functions abbreviated here as $G_{i_1 \dots i_n}$. The symbolic notation adopted herein is such that the indices include the (Euclidean) space-time variables the summations of which represent 4-dimensional integrations, $j_i \phi_i := \int d^4x j_a(x) \phi_a(x)$ with a denoting the totality of additionally possible discrete (Lorentz, Dirac, color, flavor ...) indices. The irreducible (connected) contributions to the full n -point Green's functions can be extracted recursively by subtracting all possible partitionings of the n points that lead to disconnected contributions described by products of lower m -point functions ($m < n$). The combinatorics in the relation between the full Green's functions and their connected contributions is combined in the linked cluster theorem: With the generating functional for the full Green's functions $Z[j]$ the connected ones are obtained from the Taylor expansion of the functional

$$W[j] := \ln Z[j], \quad \text{with normalizations } Z[0] = 1, \quad W[0] = 0, \quad (59)$$

which are assumed implicitly from now on. A functional Legendre transform then leads to the generating functional Γ for the one-particle irreducible (1-PI) vertex functions called the effective action,

$$\Gamma[\phi^c] := -\ln Z[j] + \phi_i^c j_i, \quad \text{with } \phi_i^c = \frac{\delta W[j]}{\delta j_i} = \langle \phi_i \rangle_{[j]}. \quad (60)$$

Its leading term in a derivative expansion, formally obtained by inserting constant fields $\phi_i^c \equiv \phi^c$, with $\Gamma[\phi^c = \text{const}] = \int d^4x V(\phi_c)$, yields the effective potential $V(\phi^c)$ which gives the energy density as a function of the expectation values of the fields in states $|\psi\rangle$ with $\langle \psi | \phi(x) | \psi \rangle = \phi_c$. The identification $\Gamma[\phi^c] = S[\phi^c]$ is useful to derive the explicit forms of the tree-level vertices (*e.g.*, that of the tree-level ghost-gluon vertex in the ghost DSE (84)).

Given the functional integral representation (58) of the generating functional is well-defined, DSEs follow from the observation that the integral of a total derivative vanishes,

$$0 = \int \mathcal{D}\phi \exp \{-S[\phi] + j_i \phi_i\} \left(\frac{\delta}{\delta \phi_k} S[\phi] - j_k \right) =: \left\langle \left(\frac{\delta}{\delta \phi_k} S[\phi] - j_k \right) \right\rangle_{[j]}, \quad (61)$$

provided the measure herein, $\mathcal{D}\Phi \exp -S[\phi]$, is invariant under field translations, $\Phi(x) \rightarrow \Phi(x) + \Lambda(x)$, for arbitrary $\Lambda(x)$, see, *e.g.*, refs. [153,86].

In our condensed notation the whole infinite tower of DSEs is generated by either of the following functional equations:

$$\left(-\frac{\delta S}{\delta \phi_i} \left[\frac{\delta}{\delta j} \right] + j_i \right) Z[j] = 0 \quad (\text{for full Green's functions}), \quad (62)$$

$$-\frac{\delta S}{\delta \phi_i} \left[\frac{\delta W}{\delta j} + \frac{\delta}{\delta j} \right] + j_i = 0 \quad (\text{for connected Green's functions}), \quad (63)$$

$$\frac{\delta \Gamma[\phi]}{\delta \phi_i} - \frac{\delta S}{\delta \phi_i} \left[\phi + \frac{\delta^2 W}{\delta j \delta j} \frac{\delta}{\delta \phi} \right] = 0 \quad (\text{for proper Green's functions}). \quad (64)$$

This very dense notation²³ provides the guideline for the following derivations of the DSEs for specific Green's functions: Upon taking the n th derivative of the appropriate functional, the vacuum expectation values (setting all sources to zero) then yield the equation for the desired n -point function.

As a first example we will briefly review the derivation of the DSE for the photon propagator in QED with one species of fermions as given, *e.g.*, in ref. [2]. The DSE for the fermion propagator is of a structure equivalent to the one for the quark propagator in QCD discussed below. We will therefore not present its derivation separately here. In the linear covariant gauge the QED analogue of the Lagrangian (11), *i.e.*, without ghost fields and gauge field self-interactions, reads:

$$\mathcal{L}_{\text{QED}} = \frac{1}{2} A_\mu \left(-\partial^2 \delta_{\mu\nu} - \left(\frac{1}{\xi} - 1 \right) \partial_\mu \partial_\nu \right) A_\nu + \bar{q}(-\not{d} + m)q - ie \bar{q} \gamma_\mu q A_\mu. \quad (68)$$

To any order in perturbation theory one effectively employs a Gaussian measure in eq. (61) for which there is no need to worry about possible boundary terms in the derivation of DSEs. Quite likely, however, this might have to be reconsidered beyond perturbation theory [151]. Ignoring this potential subtlety and, in addition, also assuming multiplicative renormalizability, the renormalization constants are formally introduced by replacing the effective Lagrangian of eq. (68) with the renormalized one,

²³ It can also be applied to obtain an overview over generating identities reflecting symmetries other than field translations. For a symmetry of the action in the form $\frac{\delta S}{\delta \phi_i} F_i = 0$, one obtains the Ward identities from the functional relation

$$j_i F_i \left[\frac{\delta}{\delta j} \right] Z[j] = 0. \quad (65)$$

In presence of an anomaly the anomalous Ward identities can be inferred from

$$\left(j_i F_i \left[\frac{\delta}{\delta j} \right] - \frac{\delta F_i}{\delta \phi_i} \left[\frac{\delta}{\delta j} \right] \right) Z[j] = 0. \quad (66)$$

The functional Slavnov–Taylor identities can be derived using non-local transformations involving the Faddeev–Popov matrix \mathcal{M} ,

$$j_i F_i \left[\frac{\delta}{\delta j} \right] Z[j] = -j_i D_i \left[\frac{\delta}{\delta j} \right] \mathcal{M}^{-1} \left[\frac{\delta}{\delta j} \right] Z[j]. \quad (67)$$

$$\begin{aligned}\mathcal{L}_{\text{QED}} = Z_3 \frac{1}{2} A_\mu & \left(-\partial^2 \delta_{\mu\nu} - \left(\frac{1}{Z_3 \xi} - 1 \right) \partial_\mu \partial_\nu \right) A_\nu \\ & + Z_2 \bar{q}(-\partial + Z_m m) q - Z_{1F} i e \bar{q} \gamma_\mu q A_\mu.\end{aligned}\quad (69)$$

This defines the multiplicative constants for the photon wave function renormalization (Z_3), the fermion wave function renormalization (Z_2), the fermion mass renormalization (Z_m), and for the renormalization of the fermion-photon vertex (here denoted by Z_{1F} to adopt a unified naming of constants for QED and QCD). The variation of the action $S_{\text{QED}} := \int d^4x \mathcal{L}_{\text{QED}}$ with respect to the photon field yields

$$\frac{\delta S_{\text{QED}}}{\delta A_\mu(x)} = Z_3 \left(-\partial^2 \delta_{\mu\nu} - \left(\frac{1}{Z_3 \xi} - 1 \right) \partial_\mu \partial_\nu \right) A_\nu - Z_{1F} i e \bar{q} \gamma_\mu q. \quad (70)$$

One way to proceed here is to employ eq. (62): Replacing the photon field by a derivative with respect to the current j_μ , the fermion fields by derivatives with respect to their Grassmann sources (introduced as in eq. (2)), and applying these derivatives together with an appropriate combination of further derivatives with respect to these sources on the full generating functional Z yields the DSE for the full Green's function under consideration. For the photon propagator, with one additional derivative $\delta/\delta j_\nu(y)$ this amounts to

$$\left\langle \frac{\delta S_{\text{QED}}}{\delta A_\mu(x)} A_\nu(y) \right\rangle = \delta_{\mu\nu} \delta^4(x - y) \quad (71)$$

which could have been inferred directly from eq. (61) in this simple case. Inserting eq. (70) herein, one still has to work out the linked cluster theorem for the decomposition of the full Green's functions occurring in the DSE of the form (71) into 1-PI ones explicitly by hand, however. In general, this can be a quite tedious task, *e.g.*, when applied to the gluon propagator DSE in QCD which formally looks just as simple as eq. (71) at first.

It might therefore be more convenient to employ the generating identity for proper (*i.e.*, 1-PI) Green's functions of eq. (64) directly. In the present case, this leads to:

$$\left(\frac{\delta \Gamma_{\text{QED}}}{\delta A_\mu(x)} \right)_{\bar{q}=q=0} = Z_3 \left(-\partial^2 \delta_{\mu\nu} - \left(\frac{1}{Z_3 \xi} - 1 \right) \partial_\mu \partial_\nu \right) A_\nu - Z_{1F} i e \text{tr}(\gamma_\mu S(x, x, [A_\mu])). \quad (72)$$

Here, use has been made of the fact that one may set the fermionic fields to zero already at this stage in the derivation of the DSE for the photon propagator. We furthermore defined the fermionic propagator in an external photon field $A_\mu(x)$ as

$$S(x, y, [A_\mu]) = \left(\left(\frac{\delta^2 \Gamma_{\text{QED}}}{\delta \bar{q}(x) \delta q(y)} \right)_{\bar{q}=q=0} \right)^{-1}. \quad (73)$$

The fermion propagator in the vacuum is obtained from the one above for vanishing external

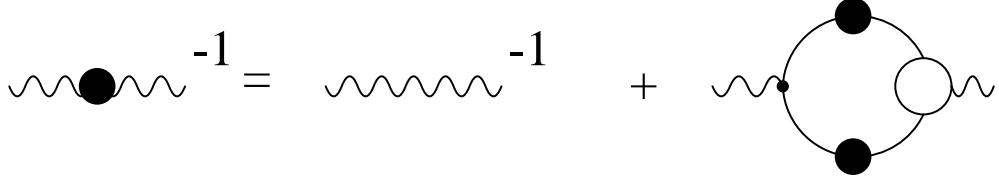


Fig. 2. Pictorial representation of the photon DSE (75).

photon field, $A_\mu = 0$, of course,

$$S(x, y) := S(x, y, [A_\mu = 0]) . \quad (74)$$

Applying a second derivative with respect to the photon field on eq. (72), and setting $A_\mu = 0$ afterwards, we arrive at the DSE for the photon propagator in the form,

$$D_{\mu\nu}^{-1}(x, y) := \left(\frac{\delta^2 \Gamma_{\text{QED}}}{\delta A_\mu(x) \delta A_\nu(y)} \right)_{A_\mu = \bar{q} = q = 0} = D_{(0)\mu\nu}^{-1}(x, y) + \Pi_{\mu\nu}(x, y) , \quad (75)$$

$$D_{(0)\mu\nu}^{-1}(x, y) = Z_3 \left(-\partial^2 \delta_{\mu\nu} - \left(\frac{1}{Z_3 \xi} - 1 \right) \partial_\mu \partial_\nu \right) \delta(x - y) , \quad (76)$$

where we introduced the inverse of the tree-level propagator, $D_{(0)\mu\nu}^{-1}(x, y)$, and the photon polarization tensor $\Pi_{\mu\nu}(x, y)$. Its explicit form,

$$\Pi_{\mu\nu}(x, y) = e^2 Z_{1F} \int d^4 u \int d^4 v \text{ tr}(\gamma_\mu S(x, u) \Gamma_\nu(y; u, v) S(v, x)) , \quad (77)$$

involves the proper fermion-photon vertex function defined as,

$$e\Gamma_\mu(x; y, z) := \left(\frac{\delta^3 \Gamma_{\text{QED}}}{\delta A_\mu(x) \delta \bar{q}(y) \delta q(z)} \right)_{A_\mu = \bar{q} = q = 0} . \quad (78)$$

In eqs. (75) and (77) the general structure of DSEs can be seen quite clearly, see also Fig. 2. Here, the DSE for the photon propagator $D_{\mu\nu}(x, y)$ contains the inverse of the tree-level propagator (76), the photon-fermion vertex (78), and the fermion propagator (74). This structure describes the way the photon propagates from y to x . In doing so, the photon either does not interact at all, reflected in the tree-level propagator (76), or it generates a fermion-antifermion pair in one elementary interaction which then propagates and recombines in all possible ways, *i.e.*, with all radiative corrections included. This is reflected by the fully dressed propagators (74) and the fully dressed vertex (78). Equivalently, in momentum space (see Appendix B for the definition of Green's functions in momentum space), the photon DSE reads,

$$\begin{aligned} D_{\mu\nu}^{-1}(k) &= D_{(0)\mu\nu}^{-1}(k) + \Pi_{\mu\nu}(k) , \\ \Pi_{\mu\nu}(k) &= -e^2 Z_{1F} \int \frac{d^4 p}{(2\pi)^4} \text{tr}(\gamma_\mu S(p) \Gamma_\nu(p, p - k) S(p - k)) . \end{aligned} \quad (79)$$

The gluon DSE in QCD is considerably more complicated due to the additional elementary (self)interactions of gluons, the elements therein are, however, all of this same general structure entailed by the combinatorics of these interactions.

As in QED, before we derive the DSEs of QCD, we replace the Lagrangian of the linear covariant gauge given in eq. (11) by its renormalized version,

$$\begin{aligned} \mathcal{L}_{\text{QCD}} = & Z_3 \frac{1}{2} A_\mu^a \left(-\partial^2 \delta_{\mu\nu} - \left(\frac{1}{Z_3 \xi} - 1 \right) \partial_\mu \partial_\nu \right) A_\nu^a \\ & + \tilde{Z}_3 \bar{c}^a \partial^2 c^a + \tilde{Z}_1 g f^{abc} \bar{c}^a \partial_\mu (A_\mu^c c^b) - Z_1 g f^{abc} (\partial_\mu A_\nu^a) A_\mu^b A_\nu^c \\ & + Z_4 \frac{1}{4} g^2 f^{abe} f^{cde} A_\mu^a A_\nu^b A_\mu^c A_\nu^d + Z_2 \bar{q} (-\partial + Z_m m) q - Z_{1F} i g \bar{q} \gamma_\mu t^a q A_\mu^a. \end{aligned} \quad (80)$$

This defines all multiplicative renormalization constants. In addition to the QCD counterparts of those introduced for QED in eq. (69) above, these are Z_1, Z_4, \tilde{Z}_3 and \tilde{Z}_1 for the gluonic selfinteractions and ghost terms. With the coupling renormalization defined by $Z_g g = g_0$ one all together has nine constants which are not independent of each other, of course. In particular, one has,

$$Z_{1F} = Z_g Z_2 Z_3^{\frac{1}{2}}, \quad Z_1 = Z_g Z_3^{\frac{1}{2}}, \quad \tilde{Z}_1 = Z_g \tilde{Z}_3 Z_3^{\frac{1}{2}}, \quad Z_4 = Z_g^2 Z_3^2. \quad (81)$$

These relations are maintained in the multiplicative renormalization as a result of the Slavnov-Taylor identities.

In the renormalization procedure for n -point functions one first considers the primitively divergent functions, *i.e.*, the ones with a tree-level counterpart in the Lagrangian. In QED these are the (inverse) propagators and the fermion-photon vertex, in QCD the primitively divergent n -point functions are the (inverse) quark, gluon and ghost propagators, and the 3-gluon, 4-gluon, ghost-gluon and quark-gluon vertex functions. These are the seven primitively divergent vertex functions of QCD with their respective renormalization constants $Z_2, Z_3, \tilde{Z}_3, Z_1, Z_4, \tilde{Z}_1$ and Z_{1F} defined in eq. (80) and constrained by the Slavnov-Taylor identities to obey the relations in (81). As we will see in the following chapters the determination of these renormalization constants in a non-perturbative approximation scheme is quite non-trivial. For all other n -point functions except the primitively divergent ones renormalization effectively amounts to replacing bare Green's functions by renormalized ones in their corresponding skeleton expansions (which contain only the primitively divergent Green's functions by construction).

The most simple example of a DSE in QCD is the one for the ghost propagator. Here we present its derivation based on eq. (61) directly as discussed below eq. (70). In this particular example, starting from eq. (62) for a (left) derivative of the action $S_{\text{QCD}} := \int d^4x \mathcal{L}_{\text{QCD}}$ with respect to the anti-ghost field \bar{c}^a , and with σ and $\bar{\sigma}$ denoting the sources for (anti)ghosts as before, acting on the full generating functional one obtains

$$\left(-\frac{\delta S_{\text{QCD}}}{\delta \bar{c}^a(x)} \left[\frac{\delta}{\delta j}, \frac{\delta}{\delta \bar{\sigma}} \right] + \sigma^a(x) \right) Z[j, \bar{\eta}, \eta, \bar{\sigma}, \sigma] \Big|_{\bar{\eta}=\eta=0} = \left\langle -\frac{\delta S_{\text{QCD}}}{\delta \bar{c}^a(x)} + \sigma^a(x) \right\rangle_{[j, \bar{\sigma}, \sigma]} = 0, \quad (82)$$

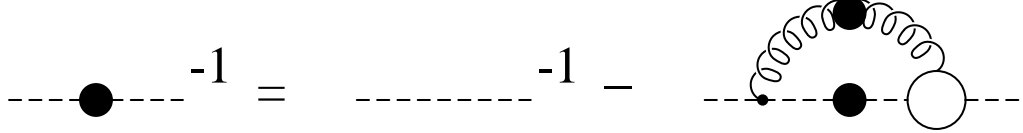


Fig. 3. Pictorial representation of the ghost DSE.

where the subscript $[j, \bar{\sigma}, \sigma]$ indicates which non-zero sources are retained for further derivatives. Acting with a further (right) derivative $\delta/\delta\sigma^b(y)$ on this equation, from (80) one explicitly obtains,

$$\left\langle \frac{\delta S_{\text{QCD}}}{\delta \bar{c}^a(x)} \bar{c}^b(y) \right\rangle = \delta^{ab} \delta^4(x - y) = \tilde{Z}_3 \left\langle \left(\partial_\mu D_\mu^{ac} c^c(x) \right) \bar{c}^b(y) \right\rangle, \quad (83)$$

where all sources are set to zero now. This is the equation of motion for the ghost propagator. We note here already that it will be used in the derivation of the gluon Slavnov–Taylor identity (96) in the next section. With $\langle c^a(x) \bar{c}^b(y) \rangle =: D_G^{ab}(x - y)$ denoting the ghost propagator, this DSE reads more explicitly,

$$\tilde{Z}_3 \partial^2 D_G^{ab}(x - y) - \tilde{Z}_1 g f^{acd} \int d^4 z d^4 z' \left(\partial_\mu^z \delta^4(z - x) \right) \delta^4(z - z') \times \langle c^c(z') \bar{c}^b(y) A_\mu^d(z) \rangle = \delta^{ab} \delta^4(x - y). \quad (84)$$

Again the general structure of DSEs is clearly visible. Here, the DSE for the ghost propagator D_G contains the inverse of the tree-level propagator, ∂^2 , the tree-level ghost-gluon vertex in coordinate space, $-\tilde{Z}_1 g f^{abc}(\partial_\mu^x \delta^4(x - y)) \delta^4(x - z)$, and the 3-point correlation function $\langle c^c(z) \bar{c}^b(y) A_\mu^a(x) \rangle$. As we used the full generating functional up to now, the latter correlation function, being a moment of $Z[j, \bar{\sigma}, \sigma]$, still is a full Green's function.

In the notation introduced at the beginning of this section the connected 3-point ghost-gluon correlation,

$$\langle c^c(z) \bar{c}^b(y) A_\mu^a(x) \rangle_{\text{conn.}} := \left. \frac{\delta^3 W[j, \bar{\sigma}, \sigma]}{\delta \sigma^b(y) \delta \bar{\sigma}^c(z) \delta j_\mu^a(x)} \right|_{\bar{\sigma}=\sigma=j=0}, \quad (85)$$

can be decomposed into the proper (1-PI) ghost–gluon vertex function,

$$G_\mu^{abc}(x, y, z) = \left. \frac{\delta^3 \Gamma[A, \bar{c}, c]}{\delta c^c(z) \delta \bar{c}^b(y) \delta A_\mu^a(x)} \right|_{c=\bar{c}=A=0}, \quad (86)$$

with ghost and gluon propagators, $D_G^{ab}(x)$ and $D_{\mu\nu}^{ab}(x)$, respectively, attached to its legs. In the covariant formalism full and connected 3-point functions are equivalent, and we thus obtain

$$\begin{aligned} \langle c^c(z) \bar{c}^b(y) A_\mu^a(x) \rangle &= \langle c^c(z) \bar{c}^b(y) A_\mu^a(x) \rangle_{\text{conn.}} = \\ &- \int d^4 u d^4 v d^4 w D_{\mu\nu}^{ad}(x - u) D_G^{ce}(z - v) G_\nu^{def}(u, v, w) D_G^{fb}(w - y). \end{aligned} \quad (87)$$

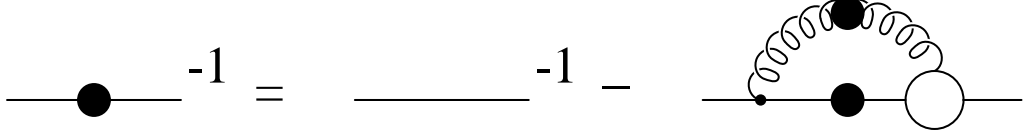


Fig. 4. Pictorial representation of the quark DSE.

From such decompositions of all connected correlations, the combinatorics of the possible interactions is reflected in the DSEs explicitly. For the ghost propagator $D_G(x - y)$, after rearranging eq. (84), this structure describes (similar to the general structure of the DSE for the photon propagator) the way a ghost field propagates from y to x (see also Fig. 3): it does it by either not interacting at all, reflected in the tree-level propagator $1/\partial^2$, or by generating a ghost-gluon pair in one elementary interaction which then propagates and recombines in all possible ways, *i.e.*, with all radiative corrections included. This is again reflected by the fully dressed propagators and the fully dressed vertex contained in the correlations (87) and thus in the DSE (84). In momentum space the ghost propagator DSE reads:

$$(D_G^{-1})^{ab}(k) = -\delta^{ab} \tilde{Z}_3 k^2 + g^2 f^{acd} \tilde{Z}_1 \int \frac{d^4 q}{(2\pi)^4} i k_\mu D_G^{ce}(q) G_\nu^{efb}(q, k) D_{\mu\nu}^{df}(k - q). \quad (88)$$

Analogous to the derivation of the ghost DSE (84), the DSE for the quark propagator, $S(x - y) := \langle q(x) \bar{q}(y) \rangle$, is obtained as follows,

$$\begin{aligned} \left\langle \frac{\delta S_{\text{QCD}}}{\delta \bar{q}(x)} \bar{q}(y) \right\rangle &= \mathbf{1} \delta^4(x - y) = Z_2 (-\not{\partial} + Z_m m) S(x - y) \\ &- Z_{1F} i g \int d^4 z d^4 z' \delta^4(x - z) \delta^4(x - z') (\gamma_\mu t^a) \langle q(z) \bar{q}(y) A_\mu^a(z') \rangle. \end{aligned} \quad (89)$$

Again, it contains the inverse tree-level propagator $(-\not{\partial} + m)$, the tree-level vertex, $\Gamma_\mu^{a\text{tl}}(x, y, z) = -Z_{1F} i g \gamma_\mu t^a \delta^4(y - x) \delta^4(z - x)$, and the full correlations $\langle q(z) \bar{q}(y) A_\mu^a(x) \rangle$. These are decomposed into the proper (1-PI) vertex function, $\Gamma_\mu^a(x, y, z)$, with quark/gluon propagators attached, in an analogous way as the correlations in eq. (87), see Fig. 4. For completeness we give the quark propagator DSE in momentum space:

$$S^{-1}(k) = Z_2 (-i k + Z_m m) + g^2 Z_{1F} \int \frac{d^4 q}{(2\pi)^4} t^a \gamma_\mu S(q) \Gamma_\nu^b(q, k) D_{\mu\nu}^{ab}(k - q). \quad (90)$$

A first idea of the complexity to expect in general (see, *e.g.*, sec. 3.3 on 3- and higher n-point Green's functions) can be obtained from the gluon DSE,

$$\begin{aligned} \left\langle \frac{\delta S_{\text{QCD}}}{\delta A_\mu^a(x)} A_\nu^b(y) \right\rangle &= \delta^{ab} \delta_{\mu\nu} \delta^4(x - y) \\ &= Z_3 \left(-\partial^2 \delta_{\mu\rho} - \left(\frac{1}{Z_3 \xi} - 1 \right) \partial_\mu \partial_\rho \right) \langle A_\rho^a(x) A_\nu^b(y) \rangle \\ &- \tilde{Z}_1 g f^{ade} \langle (\partial_\mu \bar{c}^d(x)) c^e(x) A_\nu^b(y) \rangle + Z_{1F} i g (\gamma_\mu t^a)_{ij} \langle q_j(x) \bar{q}_i(x) A_\nu^b(y) \rangle \end{aligned} \quad (91)$$

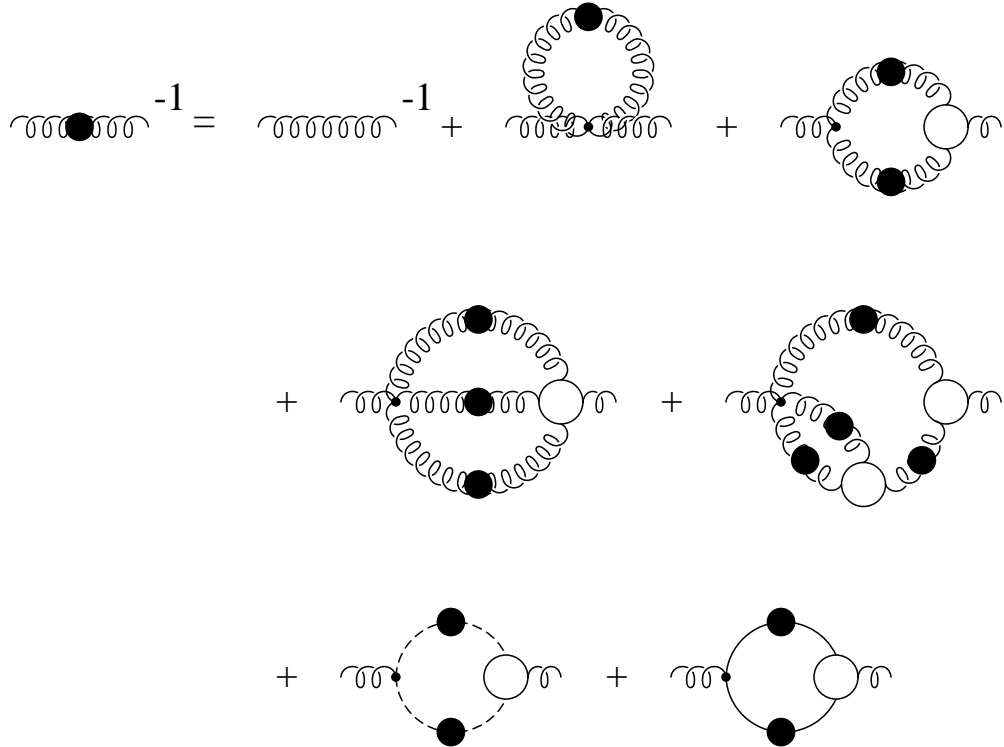


Fig. 5. Pictorial representation of the gluon DSE.

$$+ Z_1 g f^{ade} \langle \{(\partial A^d(x)) A_\mu^e(x) + (\partial_\mu A_\rho^d(x)) A_\rho^e(x) - 2(\partial_\rho A_\mu^d(x)) A_\rho^e(x)\} A_\nu^b(y) \rangle \\ + Z_4 g^2 f^{ack} f^{dek} \langle A_\rho^c(x) A_\mu^d(x) A_\rho^e(x) A_\nu^b(y) \rangle .$$

The full decomposition of all disconnected correlations herein blows up the notations considerably. It is straightforward but lengthy and is therefore given in Appendix C. The probably least suspicious term in the last line generates the majority of terms in this decomposition. It contains the tree-level 4-gluon vertex and gives rise to a tadpole as well as explicit 2-loop contributions to the gluon DSE. These will both not be included in the DSE solutions presented in sec. 5.3 below. The discussion and the necessary truncation of the DSEs for the propagators of QCD, derived formally here, is continued in Chapter 5. Before discussing some issues on DSEs for 3- and higher n -point functions in sec. 3.3 we will exploit their BRS invariance to derive the Slavnov-Taylor identities.

Despite the formal equivalence of the DSEs in different gauges their explicit form as integral equations are, of course, different. We would therefore like to add two comments on the gluon propagator in non-covariant gauges at the end of this section. One might think that the particular problem with ghosts in the Landau gauge can be avoided using gauges such as the axial gauge, in which there are no ghosts in the first place.²⁴ As for studies of the gluon DSE in the axial gauge, in which the gluon field is taken transverse to a fixed gauge vector t_μ , $t_\mu A_\mu^a = 0$, it is important to note that, so far, these rely on a simplifying assumption on the tensor structure of the gluon propagator [22,23,25,26,155]. In particular, an independent

²⁴ A further note of warning seems appropriate here. In a recent study it has been shown by using “interpolating” gauges that axial and light-like gauges are highly singular in the sense that infinite contributions to Feynman graphs are generated in the limit of a pure axial or light-like gauge [154].

additional term in the structure of the gluon propagator has not been included in presently available studies of the gluon DSE in axial gauge [27]. This term vanishes in perturbation theory, see Appendix C for an explicit definition of the corresponding tensor multiplying this term. If, however, the complete tensor structure of the gluon propagator in axial gauge is taken into account properly, one arrives at a coupled system of equations which is of considerably higher complexity than the ghost-gluon system in the Landau gauge, see section 5.2. Thus, despite the fact the gluon propagator DSE contains in axial gauge one term less than in linear covariant gauges (the ghost loop) its explicit form is much more complicated.

A final comment concerns the use of the Coulomb gauge in the present context. From the fact that the field gA_0 is invariant under renormalization in Coulomb gauge one concludes that the zero-zero component of the gluon propagator allows to extract the running coupling, see, *e.g.*, ref. [154] and the references therein. However, considerable complications due to the additional terms which arise in the proper Coulomb gauge Lagrangian as compared to a naive canonical quantization procedure [156,154], see also chapter 11 in [86], have meant that the non-perturbative gluon propagator has received very little attention in Coulomb gauge. While comprehensive studies of the gluon propagator in the Coulomb gauge are not available as yet, it has widely been used to study the quark propagator employing ansätze for the gluon propagator and the quark-gluon vertex, see refs. [157–164] as well as [165] for a recent discussion.

3.2 BRS Invariance of Green’s Functions

A classical gauge theory is by construction invariant under local gauge transformations. As discussed in the last chapter, quantizing a gauge theory necessitates gauge fixing and in general the introduction of Faddeev-Popov ghosts. We noted already that the BRS transformation (13) acting on gluons and quarks is nothing else than a gauge transformation with the ghost field as “gauge parameter”, and that the total Lagrangian is invariant under the global BRS transformations.

Here, we make use of the observation that the BRS invariance is an (unbroken) symmetry of the gauge fixed theory which, from eq. (46) in sec. 2.4.1, implies that all QCD Green’s functions are BRS invariant [56]. This provides the easiest way to derive the Slavnov–Taylor identities of QCD [16,17]. First, we introduce the renormalized BRS transformations for linear covariant gauges (*c.f.*, the unrenormalized ones in eqs. (13)) by defining $\delta\lambda_R := Z_3^{-1/2}\tilde{Z}_3^{-1/2}\delta\lambda$:

$$\begin{aligned}\delta_R A_\mu^a &= \tilde{Z}_3 D_\mu^{ab} c^b \delta\lambda_R, & \delta_R q &= -\tilde{Z}_1 i g t^a c^a q \delta\lambda_R, \\ \delta_R c^a &= -\tilde{Z}_1 \frac{g}{2} f^{abc} c^b c^c \delta\lambda_R, & \delta_R \bar{c}^a &= \frac{1}{\xi} \partial_\mu A_\mu^a \delta\lambda_R.\end{aligned}\tag{92}$$

Note that in non-linear gauges the last relation has to be replaced by

$$\delta_R \bar{c}^a = Z_3^{-1/2} \frac{1}{\xi} F^a [Z_3^{1/2} A] \delta\lambda_R\tag{93}$$

with F^a being the appropriate gauge fixing condition.

As the most elementary example to demonstrate how this symmetry constrains Green's functions we consider

$$\langle A^a(x) \bar{c}^b(y) \rangle := \left. \frac{\delta^2 Z[j, \bar{\eta}, \eta, \bar{\sigma}, \sigma]}{\delta \sigma(y) \delta j^a(x)} \right|_{j=\bar{\eta}=\eta=\bar{\sigma}=\sigma=0}. \quad (94)$$

From the BRS transformations given in eqs. (92) one obtains:

$$\delta_R \langle A^a(x) \bar{c}^b(y) \rangle = -\tilde{Z}_3 \langle (D_\mu^{ac} c^c(x)) \bar{c}^b(y) \rangle \delta \lambda_R + \frac{1}{\xi} \langle A_\mu^a(x) \partial_\nu A_\nu^b(y) \rangle \delta \lambda_R = 0. \quad (95)$$

Using the ghost DSE (83), $\tilde{Z}_3 \langle (\partial_\mu D_\mu^{ac} c^c(x)) \bar{c}^b(y) \rangle = \delta^{ab} \delta^4(x - y)$, it immediately follows from acting with ∂_μ on eq. (95) that the longitudinal part of the gluon propagator $D_{\mu\nu}^{ab}(x - y)$ is not modified by interactions,

$$\langle \partial A_\mu^a(x) \partial_\nu A_\nu^b(y) \rangle = -\partial_\mu \partial_\nu D_{\mu\nu}^{ab}(x - y) = \xi \delta^{ab} \delta^4(x - y). \quad (96)$$

This easiest example of a Slavnov–Taylor identity implies that, in Euclidean momentum space, the gluon propagator in the covariant gauge has the general structure,

$$D_{\mu\nu}^{ab}(k) = \delta^{ab} \left(\left(\delta_{\mu\nu} - \frac{k_\mu k_\nu}{k^2} \right) \frac{Z(k^2)}{k^2} + \xi \frac{k_\mu k_\nu}{k^4} \right), \quad (97)$$

involving one unknown invariant function, the gluon renormalization function $Z(k^2)$.

Obviously, an analogous statement is true for the photon propagator. In QED there is a Ward–Takahashi identity similar to eq. (96). This means that the Fourier transform of the photon polarization tensor (77),²⁵

$$\Pi_{\mu\nu}(k) = -e^2 Z_{1F} \int \frac{d^D p}{(2\pi)^D} \text{tr}(\gamma_\mu S(p) \Gamma_\nu(p, p - k)) S(p - k), \quad (98)$$

is purely transverse, $k_\mu \Pi_{\mu\nu}(k) = 0$. Defining the dimensionless function $\Pi(k^2)$ via the relation $\Pi_{\mu\nu}(k) = (k^2 \delta_{\mu\nu} - k_\mu k_\nu) \Pi(k^2)$ one finds that the general structures of the photon and the gluon propagator agree provided one identifies $Z(k^2) = 1/(1 + \Pi(k^2))$. Of course, the corresponding renormalization functions $Z(k^2)$ are obtained from their respective DSEs and will thus be completely different.

Similarly, other Slavnov–Taylor identities can be derived, most importantly, for 3-point correlation functions which typically relate their longitudinal pieces to the lower 2-point corre-

²⁵ As we will consider QED for different values of space-time dimensions in the next chapter we generalize here already from $D = 4$ to an arbitrary dimension D .

tions, *i.e.*, to the propagators. An important example is already provided by the Ward identity for the electron–photon vertex function in QED,

$$k_\mu \Gamma_\mu(p+k, p) = S^{-1}(p+k) - S^{-1}(k). \quad (99)$$

For $k \rightarrow 0$ the differential Ward identity results,

$$\Gamma_\mu(p, p) = \frac{\partial}{\partial p_\mu} S^{-1}(p). \quad (100)$$

Note that the differential identity also constrains the transverse parts of the electron-photon vertex function in this limit.

Another important example is provided by the derivation of a Slavnov–Taylor identity for the ghost-gluon vertex function obtained recently in ref. [49].²⁶ In order to construct a non-perturbatively dressed gluon-ghost vertex, one can start from the BRS invariance of the following particular correlator,

$$\delta_R \langle c^a(x) \bar{c}^b(y) \bar{c}^c(z) \rangle = 0, \quad (101)$$

from which one obtains with eqs. (92),

$$\tilde{Z}_1 \frac{1}{2} g f^{ade} \langle c^d(x) c^e(x) \bar{c}^b(y) \bar{c}^c(z) \rangle = \frac{1}{\xi} \langle c^a(x) (\partial A^b(y)) \bar{c}^c(z) \rangle - \frac{1}{\xi} \langle c^a(x) \bar{c}^b(y) (\partial A^c(z)) \rangle. \quad (102)$$

Note that this symbolic notation refers to full (and thus reducible) correlation functions. The two terms on the r.h.s. of eq. (102) can be decomposed in the gluon-ghost proper vertex and the respective propagators. The derivative on the gluon leg thereby projects out the longitudinal part of the gluon propagator which, by virtue of its own Slavnov-Taylor identity $k_\mu D_{\mu\nu}(k) = \xi k_\nu/k^2$, remains undressed in the covariant gauge, see eq. (97). The l.h.s. contains a disconnected part plus terms due to ghost-ghost scattering,

$$\langle c^d c^e \bar{c}^b \bar{c}^c \rangle = \langle c^e \bar{c}^b \rangle \langle c^d \bar{c}^c \rangle - \langle c^e \bar{c}^c \rangle \langle c^d \bar{c}^b \rangle + \langle c^d c^e \bar{c}^b \bar{c}^c \rangle_{\text{conn.}}. \quad (103)$$

If the truncating assumption is made at this point, and this is done consistently for all irreducible scattering kernels in the truncation scheme for the DSEs developed in ref. [49], that ghost-ghost scattering contributions to the vertex are neglected herein, only the reducible part of the correlation function on the l.h.s. of the Slavnov-Taylor identity in eq. (102) is maintained which corresponds to the disconnected ghost propagation. Decomposing the ghost-gluon 3-point correlation functions on the r.h.s of eq. (102) into the irreducible ghost-gluon vertex function $G_\mu^{abc}(x, y, z)$ and gluon and ghost propagators according to eq. (87) then yields,

²⁶ This vertex function will play a quite central role throughout the presentations of the solutions for the propagators of Landau gauge QCD in the following chapters.

$$\begin{aligned}
\tilde{Z}_1 \frac{1}{2} g f^{ade} \left\{ D_G^{eb}(x-y) D_G^{dc}(x-z) - D_G^{db}(x-y) D_G^{ec}(x-z) \right\} = \\
\frac{1}{\xi} \int d^4u d^4v d^4w \partial_\mu^z D_{\mu\nu}^{cd}(z-u) D_G^{ae}(x-v) G_\nu^{def}(u, v, w) D_G^{fb}(w-y) \\
-\frac{1}{\xi} \int d^4u d^4v d^4w \partial_\mu^y D_{\mu\nu}^{bd}(y-u) D_G^{ae}(x-v) G_\nu^{def}(u, v, w) D_G^{fc}(w-z). \quad (104)
\end{aligned}$$

Fourier transforming this expression one obtains,

$$\begin{aligned}
\tilde{Z}_1 \frac{1}{2} g f^{ade} (2\pi)^4 \delta^4(p+q+k) \left\{ D_G^{eb}(-q) D_G^{dc}(-k) - D_G^{db}(-q) D_G^{ec}(-k) \right\} = \\
\frac{1}{\xi} i k_\mu D_{\mu\nu}^{cd}(k) D_G^{ae}(p) G_\nu^{def}(k, p, -q) D_G^{fb}(-q) \\
-\frac{1}{\xi} i q_\mu D_{\mu\nu}^{bd}(q) D_G^{ae}(p) G_\nu^{def}(q, p, -k) D_G^{fc}(-k) \quad (105)
\end{aligned}$$

Therefore, when irreducible ghost-ghost correlations are neglected, the Slavnov-Taylor identity (102) yields an equation for the ghost-gluon vertex which relates its longitudinal part to a sum of inverse ghost propagators in some sense reminiscent of the Abelian Ward-Takahashi identities in QED. Separating the momentum conserving δ -function and the color structure from the ghost-gluon vertex (see below), and defining the ghost renormalization function $G(k^2)$, via

$$G_\mu^{abc}(k, q, -p) = (2\pi)^4 \delta^4(k+q+p) g f^{abc} G_\mu(q, -p), \text{ and } D_G^{ab}(p) = -\delta^{ab} G(p^2)/p^2, \quad (106)$$

respectively, one finally arrives at

$$i k_\mu G_\mu(p, -q) G(q^2) + i q_\mu G_\mu(p, -k) G(k^2) = p^2 \tilde{Z}_1 \frac{G(k^2) G(q^2)}{G(p^2)}, \quad (107)$$

where $p+q+k=0$. Note that this equation is valid for all ξ including $\xi=0$, *i.e.*, for Landau gauge in which one has $\tilde{Z}_1=1$, see sec. 5.3.3. A solution to this identity for the ghost-gluon vertex will be given in sec. 5.3.2.

Interestingly, the most simple solution to eq. (107) given by,

$$G_\mu(q, p) = i q_\mu \frac{G(k^2)}{G(q^2)}, \quad (108)$$

was employed also in ref. [166,167] in which solutions to the flow equations in Wilson's renormalization group approach were studied. As we will see in sec. 5.3.2, this solution admits a particularly simple solution also to the Slavnov-Taylor identity for the 3-gluon vertex function. However, it does not reflect the ghost-antighost symmetry of the Landau gauge, see appendix A. A ghost-antighost symmetric solution to eq. (107) which leads to the same 3-gluon vertex function [49] will be presented in sec. 5.3.2.

3.3 The Structure of Vertex Functions

DSEs for 3- and higher n -point functions become increasingly more complicated in structure, see ref. [168]. Before we continue their discussion, we first have to introduce some further definitions regarding the 3-point functions of QCD. The following notations are used to separate the structure constants f^{abc} of the gauge group $SU(N_c = 3)$ (and the coupling g) from the 3-gluon vertex function,

$$\Gamma_{\mu\nu\rho}^{abc}(k, p, q) = g f^{abc} (2\pi)^4 \delta^4(k + p + q) \Gamma_{\mu\nu\rho}(k, p, q) . \quad (109)$$

The arguments of the 3-gluon vertex denote the three outgoing gluon momenta according to its Lorentz indices (counter clockwise starting from the dot). With this definition, the tree-level vertex has the form,

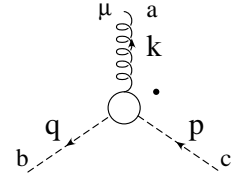
$$\Gamma_{\mu\nu\rho}^{(0)}(k, p, q) = -i(k - p)_\rho \delta_{\mu\nu} - i(p - q)_\mu \delta_{\nu\rho} - i(q - k)_\nu \delta_{\mu\rho} . \quad (110)$$

The possibility of color structures other than the perturbative ones assumed so far was recently assessed for the pure Landau gauge theory by lattice simulations in ref. [169]. In this study, the (gluon and ghost) propagators were found to be proportional to δ^{ab} to an accuracy of the order of 1%. For the 3-gluon Green's function, a possibly symmetric color structure $\sim d^{abc}$ was also verified to be negligible except at the very largest lattice momenta considered.

The arguments of the ghost-gluon vertex denote in the following order two outgoing momenta for gluon and ghost, and one incoming ghost momentum,

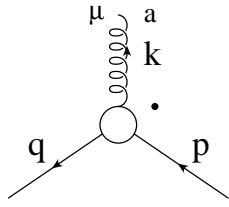
$$G_\mu^{abc}(k, q, p) = (2\pi)^4 \delta^4(k + q - p) G_\mu^{abc}(q, p) , \quad (111)$$

$$G_\mu^{abc}(q, p) = g f^{abc} G_\mu(q, p) = g f^{abc} i q_\nu \tilde{G}_{\mu\nu}(q, p) ,$$



where the tensor $\tilde{G}_{\mu\nu}(q, p)$ contains the ghost-gluon scattering kernel (for its definition see, *e.g.*, ref. [170]). At tree-level this kernel vanishes which corresponds to $\tilde{G}_{\mu\nu}(q, p) = \delta_{\mu\nu}$. Note that the color structure of the ghost and the gluon loop diagrams in the gluon DSE (C.4) as well as the one in the ghost equation (83) are simply given by $f^{acd} f^{bdc} = -N_c \delta^{ab}$. The quark loops involve the color generators in the fundamental representation t^a normalized to $\text{tr}(t^a t^b) = \delta^{ab}/2$ and giving rise to the quadratic Casimir operator $t^a t^a = C_f$ (with $C_f = 4/3$

for $N_c = 3$). The color structure of the quark-gluon vertex is made explicit by

$$\Gamma_\mu^a(k, q, p) = -igt^a (2\pi)^4 \delta^4(k + q - p) \Gamma_\mu(q, p) , \quad (112)$$


the convention for momentum arguments is analogous to the one adopted for the ghost-gluon vertex, and the tree-level vertex is given by $\Gamma_\mu(q, p) = \gamma_\mu$. The trivial color structure of the propagators $\sim \delta^{ab}$ is thus reproduced by the contractions in the loops.

In linear covariant gauges the Slavnov–Taylor identity for the 3-gluon vertex in momentum space is given by [170–172],

$$ik_\rho \Gamma_{\mu\nu\rho}(p, q, k) = G(k^2) \left\{ \tilde{G}_{\mu\sigma}(q, -k) \mathcal{P}_{\sigma\nu}(q) \frac{q^2}{Z(q^2)} - \tilde{G}_{\nu\sigma}(p, -k) \mathcal{P}_{\sigma\mu}(p) \frac{p^2}{Z(p^2)} \right\} , \quad (113)$$

where $\mathcal{P}_{\mu\nu}(k) = \delta_{\mu\nu} - k_\mu k_\nu / k^2$ is the transverse projector. A simple solution to (113) is possible if ghosts are neglected completely. However, this is not satisfactory for a complete truncation scheme including ghost contributions in linear covariant gauge neither does it account for the correct renormalization scale dependence of the 3-gluon vertex. We will therefore postpone a more complete discussion to sec. 5.3.2 where the inclusion of ghosts into the coupled gluon-ghost DSEs is discussed in detail.

One of the appealing aspects of the axial gauge is that the Slavnov–Taylor identity for the 3-gluon vertex $\Gamma_{\mu\nu\rho}$ in axial gauge has the comparatively simple form,

$$ik_\rho \Gamma_{\mu\nu\rho}(p, q, k) = \Pi_{\mu\nu}(q) - \Pi_{\mu\nu}(p) . \quad (114)$$

In particular, no unknown contributions from higher correlation functions such as the 4-point ghost-gluon scattering kernel as in linear covariant gauges enter in this axial gauge identity for the 3-gluon vertex. Retaining the most general tensor structure, however, its solution becomes quite involved. With the additional requirement that it should be free from kinematic singularities the solution was obtained in ref. [172]. Its rather complicated form is given in Appendix D. It should be emphasized that the solution D.2 for the longitudinal part of the 3-gluon vertex is not only free from singularities of the type $1/(p^2 - q^2)$ but also from the typical axial gauge singularities of the form $1/(pt)$ [172].

Of course, Slavnov–Taylor or Ward identities are only helpful in constructing the longitudinal parts of vertex functions (except at vanishing or infinite momenta where they also constrain the transverse components). In order to determine the full vertex functions one would have to

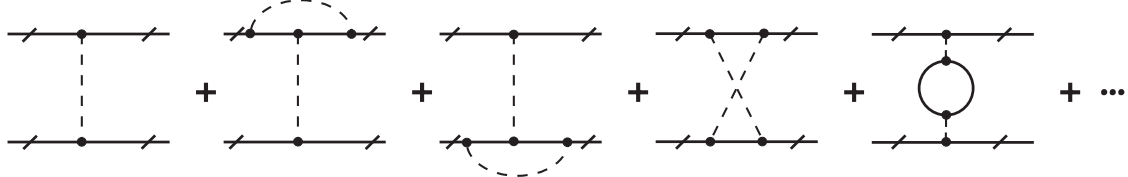


Fig. 6. Feynman diagrams of the first few terms in a perturbative expansion of the kernel K . Solid lines represent propagators of the constituents, dashed lines the propagator of the exchange particle, *i.e.* photons for QED and gluons for QCD.

solve their corresponding DSEs. Being the least complicated case we will discuss the fermion-photon vertex $\Gamma_\mu(k, q, p) = -ie(2\pi)^4\delta^4(k + q - p)\Gamma_\mu(q, p)$. Its DSE,

$$\Gamma_\mu(q, p) = Z_2\gamma_\mu + \int \frac{d^D l}{(2\pi)^D} S(q + l)\Gamma_\mu(q + l, p + l)S(p + l)K(p + l, q + l, l) , \quad (115)$$

is an inhomogenous Bethe-Salpeter equation [29]. The kernel K is defined as the sum of all amputated two-particle irreducible contributions, *i.e.*, it is the renormalized amputated fermion-antifermion scattering kernel.

It should be noted that the vertex function $\Gamma_\mu(q, p)$ can have a pole at $p^2 = -m^2$ corresponding to bound states of mass m with these particular quantum numbers. This is especially interesting when the fermions are not only interacting electromagnetically. It has been verified explicitly in the ladder-rainbow approximation using a model gluon propagator as interaction between quark and antiquark that the quark-photon vertex displays such a pole at the vector-meson mass [173,174].

The general form of the fermion-photon vertex can be decomposed into twelve linearly independent Lorentz covariants. Whereas the four longitudinal components are highly constrained by the Ward identity (99), for all photon momenta $k_\mu = p_\mu - q_\mu$ the eight transverse components are only affected by the differential Ward identity (100) at $k = 0$. The solution for the quark-photon vertex given in ref. [173] exhibits several interesting features. First, the longitudinal components agree perfectly with the Ball-Chiu ansatz [171] (see also the secs. 4.2 and 4.3 for its explicit form). Secondly, all eight transverse components were demonstrated clearly to contain the vector meson pole. We will discuss these issues further in sec. 6.2.4. Unfortunately, however, already the ladder-rainbow calculation presented in ref. [173] turned out to be technically quite involved.

An obvious complication for considering DSEs of vertex functions is the fact that the kernel K is defined in a diagrammatic language, a first few terms in a perturbative (or a skeleton) expansion which occur in QED and QCD are shown in fig. 6. Thus, a self-consistent treatment of vertex functions, especially in QCD, hardly seems feasible. It is therefore quite remarkable that the DSEs for all primitively divergent functions have been studied in the approximation scheme of ref. [142], see refs. [148,149]. As this approach will briefly be presented in sec. 5.4 below, we also postpone the corresponding discussion until then.

Some toy models have also been employed to solve DSEs of vertex functions. A simplified equation for the 3-gluon vertex has, *e.g.*, been solved in ref. [175] based on the so-called pinch technique, see refs. [176–178]. It might be interesting to note that an infrared singular 3-gluon vertex results in this study for massless gluons. In ref. [175] an explicit gluon mass was introduced to avoid this singularity. This ambiguity underlines the necessity to understand the qualitative behaviour of 2-point functions, *i.e.*, propagators, before a more systematic study of higher n -point functions can be attained.

4 Green's Functions of QED

4.1 1+1 Dimensional QED (Schwinger model): Dyson–Schwinger Equations in a Model with Instantons

QED with one massless fermion in 1+1 dimensions is called the Schwinger model [179]. There is an enormous number of papers on this exactly solvable model which displays phenomena like confinement and dynamical mass generation in a Kosterlitz–Thouless phase. It therefore serves as a “theoretical laboratory” (for a recent review see [180]). Here we are particularly interested in the aspect that instantons exist in the Schwinger model. In fact, an instanton vacuum is needed to obtain a consistent quantization. In the Schwinger model there is an infinite number of vacua labeled by the (integer) winding number n . As in QCD, instantons relate different vacua and the instanton number $k = n_+ - n_-$ can be calculated from the corresponding Pontryagin index density. Furthermore, a superposition of these vacua is introduced as the physical vacuum,

$$|\Theta\rangle = \sum_{n=-\infty}^{\infty} e^{in\Theta} |n\rangle, \quad (116)$$

which is characterized by a vacuum angle Θ .

It has been shown by explicit calculation [181] that the DSEs for the n -point functions of the Schwinger model hold separately in every instanton sector. This fact is related to the invariance of the model with respect to the vacuum angle Θ : For general Θ a Green's function would pick up a phase $\exp(ik\Theta)$ from a sector with instanton number k . If the DSEs were to enforce cancellations between different instanton sectors, the related conditions would acquire a Θ dependence. On the other hand, as the Schwinger model is invariant with respect to Θ the DSEs have to be, too. And the fact that the DSEs are separately fulfilled in every sector is the simplest possibility to ensure the required Θ invariance. Thus, at least for the Schwinger model, it has been demonstrated in ref. [181] that the DSEs can be extended to cases in which the true vacuum is not the perturbative one but a Θ vacuum (or a vacuum with a definite number of instantons).

Of course, the fact that the DSEs hold independently in each sector does not imply that the solutions to Green's functions are unaffected by the presence of instantons. This is demonstrated by an explicit solution for the fermion propagator and the 4-fermion Green's function in ref. [182]. The corrections due to the sectors with non-zero instanton number are shown to be just the terms allowed by the general structure of the DSEs. The Θ dependence of the Green's functions found in this calculation can be removed by a suitably chosen chiral transformation and is thus trivial. *E.g.*, the fermion propagator is of the form ($S_0(x)$ being the tree-level propagator)

$$S(x) = S_0(x) e^{-ie^2\beta(x)} + \frac{iee^{\gamma_E}}{4\pi^{3/2}} e^{-i\gamma_5\Theta} e^{ie^2\beta(x)} \quad (117)$$

where the first term is the one which would result in a calculation without instantons. Further details can be found in refs. [181,182]. Since we will not touch upon the issue about the influence of topological field configurations on DSEs for the rest of this review anymore, we would like to point out that the Schwinger model can be solved exactly by calculating its Green's functions using DSEs. Hereby, it is not only possible but also necessary to take all topological effects into account. Whereas the DSEs stay formally correct in different instanton vacua, the explicit expressions for Green's function acquire additional terms allowed by the DSEs. To our knowledge similar investigations in other models or theories are unavailable as yet: Possible complications due to a presence of topologically non-trivial configurations are usually not addressed in DSE based studies.²⁷

4.2 *Confinement in 2+1 Dimensional QED*

There are basically two different objectives in studies of the Green's functions in 2+1 dimensional QED. One line of research is based on applications to condensed matter systems. The systems of main interest are hereby high- T_c superconductors, see, *e.g.*, ref. [184] for a recent review in this direction. Other applications to condensed matter systems include the fractional quantum Hall effect by adding a Chern–Simons term to the action, for a summary of studies of the topological structure due to this term, see ref. [185].

On the other hand, and that will be the main issue discussed in this section, there also is a considerable number of investigations which employ 2+1 dimensional QED in order to study general aspects of DSEs in a confining and chiral symmetry breaking theory. Here we restrict to non-compact electrodynamics²⁸ at zero temperature. In 2+1 dimensional QED, fermions can be introduced by two- or four-component Dirac spinors, for details as well as a discussion of possible mass terms see below, where it will also become clear why we restrict to four-component spinors here,²⁹ with vanishing bare mass. The possibility to generate a parity invariant and chiral-symmetry breaking dynamical mass is still included, of course. Finally, having outlined the basis for the discussion of this subsection, we refer the reader to chapter 3 of the review in ref. [29] in which corresponding studies are summarized with status as of the early nineties in some detail. We therefore put the emphasis here on the developments since then.

²⁷ Note, however, that effects of Abrikosov–Nielsen–Olesen strings on the gauge boson propagator in the dual Abelian Higgs model have been considered in terms of an unknown string-string correlator in ref. [183] which nevertheless allows some general restrictions on the infrared behavior of the gauge boson propagator. In particular, it was demonstrated that an infrared enhanced gauge boson propagator is excluded by confinement in this model.

²⁸ The difference between a compact and a non-compact U(1) gauge theory is best understood on the lattice: There it amounts to allow for gauge transformations to be valued on a circle or on the real line, respectively [186]. In the continuum this translates, roughly speaking, into the question whether monopole field configurations are in principle allowed or not.

²⁹ Studies of DSEs in two-component 2+1 dimensional QED exist with Chern–Simons term included, see ref. [187], and without, see [188]. The main motivation for both these studies are applications to condensed matter systems.

The coupling in 2+1 dimensional QED, e^2 has the dimension of mass. The theory is super-renormalizable, and no new scale needs to be introduced during renormalization. The dynamical generation of a fermion mass, *i.e.*, the dynamical breaking of chiral symmetry (DB χ S), is thus directly related to the scale provided by e^2 . An order parameter for DB χ S is provided by the fermion condensate $\langle \bar{\psi} \psi \rangle = -\text{tr}S(x)$ in the case of vanishing bare mass in the Lagrangian. As mentioned already, two-component spinors are sufficient to describe “Dirac” fermions in three dimensions. Furthermore, there are two inequivalent 2×2 representations of the Clifford algebra $\{\gamma_\mu, \gamma_\nu\} = 2\delta_{\mu\nu}$.³⁰ Using two-component spinors, however, any mass term, whether explicit or dynamically generated, is odd under parity transformations. Furthermore, for the two-component fermion which belongs to the irreducible spinor representation in three dimensions, chiral symmetry cannot be well-defined. These features are unacceptable in studies of three-dimensional QED as a testing ground for (four-dimensional) QCD. An alternative is provided by using four-component spinors or, phrased otherwise, an even number of flavors of two-component fermions. The Euclidean Clifford algebra $\{\gamma_\mu, \gamma_\nu\} = 2\delta_{\mu\nu}$ can be realized by employing three of the Dirac matrices conventionally used in four dimensions, *e.g.*, $\gamma_1, \gamma_2, \gamma_4$. Since both $\gamma_5 := -\gamma_1 \gamma_2 \gamma_4$ and γ_3 anticommute with these three matrices the massless theory is invariant under an $U(2N_f)$ group of chiral transformations where N_f is the number of (four-component) flavours. The four generators of this group (per flavor) are the unit matrix, γ_3, γ_5 and $\frac{1}{2}[\gamma_3, \gamma_5]$. One way to construct a mass term is given by $\tilde{m}\bar{\psi}\frac{1}{2}[\gamma_3, \gamma_5]\psi$ which is invariant under chiral transformations but not under parity. This is obviously not the analogue of a Dirac mass in four dimensions, and we will not consider it here. The term $\tilde{m}\bar{\psi}\psi$ on the other hand does have the desired transformation properties: It is invariant under parity but not under chiral transformations. The generation of a parity-invariant dynamical mass breaks the $U(2N_f)$ symmetry down to $U(N_f) \times U(N_f)$. This leads to $2N_f^2$ Nambu–Goldstone bosons, N_f^2 scalars and N_f^2 pseudoscalars.

The fermion DSE is given by (*c.f.*, the quark DSE in eq. (90))

$$S^{-1}(p) = Z_2(i\cancel{p} + Z_m m) + e^2 Z_{1F} \int \frac{d^3 q}{(2\pi)^3} \gamma_\mu S(q) \Gamma_\nu(q, p) D_{\mu\nu}(p - q). \quad (118)$$

Besides the full photon propagator $D_{\mu\nu}(k)$ it contains the fermion-photon vertex function $\Gamma_\nu(q, p)$. During the past years some effort has been put in finding suitable Ansätze for this fermion-photon vertex with the intention to minimize the gauge dependence of the results for observables. To this end, the so-called *transverse* condition has been suggested and employed in an explicit construction of the vertex function, *e.g.*, see refs. [189, 190]. It was pointed out, however, that this transverse condition is violated at two-loop level in perturbation theory in ref. [191]. This might be an indication that the vertex does contain transverse parts which cannot be determined from properties of the single particle propagators alone. We will return to this issue in the next section where we discuss four-dimensional QED.

On the other hand, in ref. [192] it was observed that the detailed structure of the vertex does not play a too significant role in the solution of the coupled DSEs for fermion and photon propagator in three-dimensional QED, both in the massless and in the massive phase. Despite the fact that only a quite restricted class of Ansätze has been used in this study, it nevertheless

³⁰ As before, we adopt a positive definite Euclidean metric $g_{\mu\nu} = \delta_{\mu\nu}$ with hermitean Dirac matrices.

shows that maintaining consistency at the level of the propagators does somewhat improve the robustness of the solutions with respect to truncations in higher order n -point functions. In the following we briefly summarize the work presented in ref. [192]. In three-dimensional QED in Landau gauge $Z_2 = Z_{1F} = 1$ is finite, and starting with bare mass $m = 0$ the renormalization constant Z_m is irrelevant. Assuming that parity is not broken dynamically one can decompose the fermion propagator as usual,

$$S^{-1}(p) = i\cancel{p}A(p^2) + B(p^2). \quad (119)$$

With this decomposition one obtains from eq. (118),

$$A(p^2) = 1 + \frac{e^2}{p^2} \int \frac{d^3q}{(2\pi)^3} \frac{1}{4} \text{tr}[\cancel{p} \gamma_\mu S(q) \Gamma_\nu(q, p) D_{\mu\nu}(p - q)], \quad (120)$$

$$B(p^2) = e^2 \int \frac{d^3q}{(2\pi)^3} \frac{1}{4} \text{tr}[\gamma_\mu S(q) \Gamma_\nu(q, p) D_{\mu\nu}(p - q)]. \quad (121)$$

The DSE of the photon propagator which occurs in these equations was solved simultaneously in ref. [192]. It is fully determined by the transverse part of the photon polarization tensor (see the discussion below eq. (98)),

$$D_{\mu\nu}^{-1}(k) = D_{(0)\mu\nu}^{-1}(k) + \Pi_{\mu\nu}(k) \quad (122)$$

with

$$\Pi_{\mu\nu}(k) = (k^2 \delta_{\mu\nu} - k_\mu k_\nu) \Pi(k^2) = -e^2 Z_{1F} \int \frac{d^3q}{(2\pi)^3} \text{tr}(\gamma_\mu S(q) \Gamma_\nu(q, q - k) S(q - k)). \quad (123)$$

In principle, a gauge-invariant regularization scheme is required here, because of an ultraviolet divergence in the longitudinal part of the photon polarization tensor. Note that one possible source of spurious longitudinal terms in the photon (or gluon) DSE can be the regularization by an $O(d)$ -invariant Euclidean cutoff Λ . This regularization violates the residual invariance under gauge transformations generated by harmonic gauge functions ($\partial^2 \Lambda(x) = 0$) in linear covariant gauges. A straightforward elimination of spurious longitudinal terms by contracting with the transverse projector $\mathcal{P}_{\mu\nu}(k)$ is known to result in quadratically ultraviolet divergent contributions which are of course artifacts of the regularization not being gauge invariant. As observed in ref. [193], in general, quadratic ultraviolet divergences can occur only in the term proportional to $\delta_{\mu\nu}$. Therefore, this part cannot be determined unambiguously, its finite part necessarily also depends on the momentum routing in the loop integration. An unambiguous procedure is, however, to isolate the part free of quadratic ultraviolet divergences by contracting with the projector

$$\mathcal{R}_{\mu\nu}(k) = \delta_{\mu\nu} - d \frac{k_\mu k_\nu}{k^2} = \delta_{\mu\nu} - 3 \frac{k_\mu k_\nu}{k^2}, \quad (124)$$

which is constructed such that $\mathcal{R}_{\mu\nu}(k) \delta^{\mu\nu} = 0$, and therefore the ambiguous term proportional to $\delta_{\mu\nu}$ is projected out. Thus, in the numerical solution of the DSEs, the problem introduced by

the gauge non-invariant cutoff regularization can be avoided in contracting $\Pi_{\mu\nu}(k)$ with $\mathcal{R}_{\mu\nu}(k)$ to project onto the unambiguous and finite part of the polarization tensor, even though gauge invariance is in principle broken by the sharp cutoff.³¹ The coupled equations for the photon and fermion propagator form a set of three non-linear equations for three scalar functions, and the only unknown therein is the full vertex function. Up to this point the DSEs for the fermion propagator and the photon propagator are, in principle, exact. As discussed in the last chapter the vertex satisfies its own DSE which could in principle be solved in some approximation. In the exploratory study of ref. [192], on the other hand, the following Ansätze were investigated:

$$\Gamma_\mu(p, k) = f(A(p^2), A(k^2), A((p - k)^2)) \gamma_\mu, \quad (125)$$

with

$$f(A(p^2), A(k^2), A((p - k)^2)) = \begin{cases} 1 \\ \frac{1}{2}(A(p^2) + A(k^2)) \\ A(p^2)A(k^2)/A((p - k)^2) \\ \frac{1}{4}(A(p^2) + A(k^2))^2 \end{cases}.$$

The coupled equations for N_f different fermion flavours,

$$A(p^2) = 1 + \frac{2e^2}{p^2} \int \frac{d^3k}{(2\pi)^3} \frac{A(k^2)(p \cdot q)(k \cdot q)/q^2}{A^2(k^2)k^2 + B^2(k^2)} \frac{f(A(p^2), A(k^2), A(q^2))}{q^2(1 + \Pi(q^2))}, \quad (126)$$

$$B(p^2) = 2e^2 \int \frac{d^3k}{(2\pi)^3} \frac{B(k^2)}{A^2(k^2)k^2 + B^2(k^2)} \frac{f(A(p^2), A(k^2), A(q^2))}{q^2(1 + \Pi(q^2))}, \quad (127)$$

$$\begin{aligned} \Pi(q^2) = 4N_f e^2 \int \frac{d^3k}{(2\pi)^3} & \left(k^2 + 2k \cdot q - 3 \frac{(k \cdot q)^2}{q^2} \right) \frac{A(k^2)}{A^2(k^2)k^2 + B^2(k^2)} \\ & \times f(A(p^2), A(k^2), A(q^2)) \frac{A(p^2)}{A^2(p^2)p^2 + B^2(p^2)}, \end{aligned} \quad (128)$$

(with $q = p - k$) were solved for both, the chirally symmetric and the broken phase.

The most important result of this study is a critical number for chiral symmetry breaking, $N_{crit} \approx 3.3$ such that dynamical mass generation occurs for $N_f < N_{crit}$; above this critical number, only the chirally symmetric solution exists. This is in qualitative agreement with studies based on the $1/N_f$ expansion of the DSEs employing a bare vertex and assuming no wavefunction renormalization ($A(p^2) \equiv 1$) [197,198].³² This result is in contradiction to previous claims, however, that the effect of wavefunction renormalization would lead to DB χ S for all N_f , see the discussion in section 3.5 of the review [29] as well as references therein. What the results of ref. [192] thus seem to tell us is that the photon polarization is very important here. Without it, *i.e.*, in the quenched approximation, the occurrence of DB χ S is sensitive to the wavefunction renormalization and to the particular Ansatz employed for the fermion-photon vertex function. Quite in contrast to this situation, the solutions to the complete system of

³¹ In a gauge-invariant regularization this problem is avoided all together, of course. As such, dimensional regularization was employed for the fermion propagator DSE in four-dimensional QED in refs. [194–196] as discussed in the next section.

³² This phase transition is of infinite order and resembles a conformal phase transition, see ref. [199]. Adding a Chern–Simons term, however, the phase transition becomes one of first order [200].

coupled DSEs for the propagators do not seem to be overly sensitive at all to the precise assumptions made to truncate the system at the level of the vertex function.

In the chirally broken phase one has an infrared vanishing photon polarization, and thus logarithmic confinement as might be expected from dimensional reasons. In the chirally symmetric phase, an infrared divergent photon polarization function $\Pi(q^2)$ is found [192].³³ This leads to screening instead of confinement. The infrared behavior of the fermion propagator in the chirally symmetric phase is determined by an exponent η indicative of a conformal regime: The wavefunction renormalization $A(p^2)$ (being approximately equal to one in the ultraviolet as required by perturbation theory) vanishes with positive exponent η in the infrared. From fig. 3 of ref. [192] one might estimate,

$$S^{-1}(p) = A(p^2) \not{p} \xrightarrow{p^2 \rightarrow 0^+} \left(\frac{p}{N_f e^2 / 8} \right)^\eta \not{p} \quad \text{with} \quad \eta = \frac{8}{3N_f \pi^2}. \quad (129)$$

This same exponent was obtained from inverse Landau–Khalatnikov transformations in ref. [201], and it has furthermore been verified in a recent calculation [202] to a very high precision. Note that for all possible values of N_f which lead to the chirally symmetric phase, η is an irrational number much smaller than one. This is very likely to lead to a cut (with infinitely many Riemann sheets, *i.e.*, logarithmic-like) in the fermion propagator. This cut on the time-like p^2 -axis is, at least in principle, understandable from the existence of massless photons. The infrared behavior of the photon propagator is of the form $\text{const.}/q = \text{const.}/\sqrt{q^2}$ and thus indicates that the photon propagator has a two-fold cut. One might interpret this cut as being generated by the massless fermions. The chirally symmetric phase is often called the Coulomb phase for this reason. We would also like to emphasize here that the infrared behavior of the propagators as well as their analytic structures related to this behavior reflect the physics of a given phase, as this explicit example demonstrates.

The analytic structure of the propagators is much more interesting in the confining phase, of course. In the chirally broken and confining phase $A(p^2)$ is not of the order one either, but considerably smaller in this case. As the number of fermion flavors approaches the critical number N_{crit} (from below), $A(0)$ tends to go to zero. This behavior suggests the conjecture that $A(p^2)$ might vanish by an irrational power at the zeros of the denominator $A^2(p^2)p^2 + B^2(p^2)$ for $N_f < N_{\text{crit}}$. This would imply that the fermion propagator had no isolated poles in the confining phase. This hypothesis is currently being investigated more closely [202]. Results in this direction based on simultaneous solutions of the coupled photon *and* fermion DSEs are not available yet, however.

Studies of singularities of the fermion propagator in the complex p^2 plane are available only for solutions to fermion DSEs with assuming different Ansätze for the photon polarization and the fermion-photon vertex [203,52]. Not too surprisingly, however, the locations of the poles then depend strongly on the Ansatz for the vertex function [203]. Improving the vertex

³³ Note that a somewhat unconventional definition of the photon polarization, by the denominator $q^2 + \Pi(q)$ in the photon propagator, was adopted in ref. [192]. In order to compare to the dimensionless polarization defined by $q^2(1 + \Pi(q))$ herein, eq. (28) in ref. [192] has to be replaced by $\Pi_{\text{pert}} = \alpha/q$. Some typos in ref. [192] can easily be identified by comparing to the formulas given above.

function such that, *e.g.*, Ward identities are satisfied, the poles of the fermion propagator are found to occur much closer to the time-like real axis as compared to the cases in which bare vertices are employed. This might be taken as an evidence that the (unknown) full renormalized fermion propagator does have singularities on time-like axis despite confinement. Independent of this, however, in connection with the results for QCD presented in chapter 5 below, it seems interesting to note that the fermion propagator does violate reflection positivity in all the cases for which the underlying Ansätze lead to fermion confinement [52]. This result was established by two different methods: One method is to solve the fermion DSE for complex values of p^2 in order to determine the singularities of the propagator directly. The other method is based on studying the Fourier transform of the fermion propagator at large (Euclidean) times. As a central result of ref. [52], oscillations in the Fourier transform of the fermion propagator as a function of time t are observed clearly. This result thus demonstrated the violation of positivity quite unambiguously. It would therefore seem to be interesting to perform an analogous investigation of positivity on possible solutions for the fermion propagator as obtained from the coupled fermion and photon DSEs. Such a study was initiated during the write-up of this review [202].

Summarizing this subsection we conclude that in non-compact four-component massless three-dimensional QED with $N_f < N_{crit}$ flavors D χ SB and confinement are realized.³⁴ In this phase fermions acquire a dynamical mass and decouple from the infrared dynamics. The resulting potential thus grows at large separation similar to the tree-level one leading to logarithmic confinement. The corresponding analytic structure of the fermion propagator is, however, not known in detail. Nevertheless, based on the investigations reported in refs. [203,52] it seems safe to conclude that *the fermion propagator of three-dimensional QED in the confining phase violates reflection positivity*. For $N_f > N_{crit}$ a Coulomb phase with massless fermions and photons is found in a solution of the coupled photon and fermion DSEs. This result agrees qualitatively with the leading order in the $1/N_f$ expansion. This well understood case serves as an explicit example of how the infrared behavior of the propagators, as well as their analytic structures related to this behavior, have a direct interpretation in terms of the physics of this phase which is characterized by massless, interacting fermions and photons.

As stated in the beginning of this section, three-dimensional QED was analyzed here as a “toy model” for four-dimensional QCD. To this end we have to learn the lesson that even the qualitative behavior of DSE solutions can be sensitive to the truncations employed. A nevertheless encouraging lesson is, however, that those truncations which are complete at the level of the propagators lead to fairly stable results. In particular, the qualitative behavior of the corresponding solutions is then found to be quite insensitive to modifications in the 3-point vertex function. As a result, a consistent picture of the two-phase structure of this theory emerges: For a large number of flavors one has a Coulomb phase, whereas for a small number of flavors D χ SB and confinement occur.

³⁴ The investigations described above start from a vanishing bare mass. In the limit of infinitely heavy fermion masses, on the other hand, it was proposed from bosonization techniques in ref. [204] that one should always obtain screening instead of confinement. This can be related to the occurrence of a massive pole in the effective bosonic action found in ref. [205]. One should keep in mind, however, that these bosonization technique are applicable only if the dimensionless parameter e^2/m is small. This condition is certainly always violated for sufficiently small or vanishing bare fermion masses m .

4.3 Dynamical Chiral Symmetry Breaking in 3+1 Dimensional QED

In the sense of Wilson's renormalization group, full 3+1 dimensional QED is most likely to be trivial: It has only an infrared fixed point, see, *e.g.*, chapter 16 in ref. [111] for a pedagogical discussion and ref. [112] for a non-perturbative verification based on a lattice calculation. As a matter of fact, the underlying goals when studying the Green's functions of QED are based on the observation that massless QED with N_f flavors possesses the same chiral symmetry as QCD. Therefore the quark DSE in 3+1 dimensional QED has been used to study technical questions like: the analytic structure of propagators, numerical cancellations of divergences, gauge dependencies introduced by numerical cutoffs, and the question of gauge covariance in general. Obviously, with this restriction in mind in most cases it is sufficient to consider the quenched approximation.³⁵

$\text{DB}\chi\text{S}$ has been discussed in detail in the review [29] and in the book [30]. We briefly summarize the corresponding knowledge and describe the progress made since then in some more detail (parts of the material presented here follow ref. [207]). Of course, the generation of a dynamical mass for fermions with bare mass zero is a genuinely non-perturbative problem. Note that it is not possible to put massless fermions on a lattice. Thus every lattice calculation which wants to include $\text{DB}\chi\text{S}$ has to rely on extrapolations provided, *e.g.*, by “chiral perturbation theory” or other continuum techniques. (Note also that “chiral perturbation theory” describes $\text{DB}\chi\text{S}$ rather than explaining its origin.) Studying this issue with non-perturbative methods based on a continuum formulation is therefore required. Already the very simplest truncation of the fermion propagator DSE does provide for a dynamically generated mass. Replacing the photon propagator and the fermion-photon vertex by their tree-level forms, $D_{\mu\nu}(k) \rightarrow D_{(0)\mu\nu}(k)$ and $\Gamma_\mu(p, q) \rightarrow \gamma_\mu$, *i.e.*, applying the so-called rainbow approximation together with the quenched approximation,³⁶ one obtains

$$A(p^2) = 1 + \xi \frac{e^2}{p^2} \int \frac{d^4 q}{(2\pi)^4} \frac{A(q^2)(p \cdot (p - q))(q \cdot (p - q))}{A^2(q^2)q^2 + B(q^2)} \frac{1}{(p - q)^4},$$

$$= 1 + \xi \frac{e^2}{(4\pi)^2} \int dq^2 \frac{A(q^2)}{A^2(q^2)q^2 + B(q^2)} \left(\Theta(p^2 - q^2) \frac{q^2}{p^2} + \Theta(q^2 - p^2) \right), \quad (130)$$

$$B(p^2) = Z_m m + (3 + \xi) e^2 \int \frac{d^4 q}{(2\pi)^4} \frac{B(q^2)}{A^2(q^2)q^2 + B(q^2)} \frac{1}{(p - q)^2},$$

$$= Z_m m + (3 + \xi) \frac{e^2}{(4\pi)^2} \int dq^2 \frac{B(q^2)}{A^2(q^2)q^2 + B(q^2)} \left(\Theta(p^2 - q^2) \frac{q^4}{p^4} + \Theta(q^2 - p^2) \right). \quad (131)$$

The bare mass $m_0 = Z_m m$ is sent to zero by an appropriately defined limit in studies of $\text{DB}\chi\text{S}$.

³⁵ There are very few unquenched calculations. The only one to our knowledge in which the quadratic divergence in the vacuum polarization was treated correctly is that of ref. [206].

³⁶ Diagrammatically the use of a bare vertex in the fermion DSE amounts to a summation of horizontal arrays of “rainbows” of parallel photon exchanges. In many-body theory this is identical to the Green's function formulated Hartree–Fock approximation, see *e.g.* ref. [162]. Bosonization techniques as employed, *e.g.*, in the “Global Colour Symmetry Model” [208] (see also the reviews [29,28,209] and references therein) naturally lead to this approximation also.

One furthermore observes that in this approximation there is no wave function renormalization, *i.e.*, $A(p^2) = 1$ for the choice of the Landau gauge $\xi = 0$. In this gauge, and with introducing an $O(4)$ -invariant Euclidean momentum cutoff Λ_{UV} , the equation for the dynamical mass function $M(p^2) \equiv B(p^2)/A(p^2) = B(p^2)$ reads:

$$M(p^2) = m_0 + \frac{3e^2}{(4\pi)^2} \int_0^{p^2} dq^2 \frac{q^2}{p^2} \frac{M(q^2)}{q^2 + M(q^2)} + \frac{3e^2}{(4\pi)^2} \int_{p^2}^{\Lambda_{UV}^2} dq^2 \frac{M(q^2)}{q^2 + M(q^2)}. \quad (132)$$

This equation obviously has the trivial solution $M(p^2) = 0$ in the chiral limit $m_0 = 0$. The interesting question is, however: Under what circumstances can the solution for $M(p^2)$ be non-vanishing in the chiral limit? The simplicity of eq. (132) allows one to convert it into a differential equation,

$$\frac{d}{dp^2} \left(p^4 \frac{d}{dp^2} M(p^2) \right) = -\frac{3e^2}{(4\pi)^2} \frac{p^2 M(p^2)}{p^2 + M(p^2)}, \quad (133)$$

together with the *boundary conditions* that,

$$\lim_{p^2 \rightarrow 0} \left(\frac{d}{dp^2} (p^4 M(p^2)) \right) = 0 \quad \text{and} \quad \lim_{p^2 \rightarrow \Lambda_{UV}^2} \left(\frac{d}{dp^2} (p^2 M(p^2)) \right) = m_0. \quad (134)$$

For large p^2 , *i.e.*, $p^2 \gg M^2(p^2)$, one has $p^2 + M^2(p^2) \approx p^2$ and the differential equation can be linearized. The Ansatz $M(p^2) \propto (p^2)^a$ then yields $a(a+1) = -3e^2/(4\pi)^2$. Writing the corresponding roots in terms of the fine structure constant $\alpha = e^2/(4\pi)$ and defining $\alpha_c := \frac{\pi}{3}$,

$$a = -\frac{1}{2} \pm \frac{1}{2} \sqrt{1 - \frac{\alpha}{\alpha_c}}, \quad (135)$$

one realizes that solutions of qualitatively different character arise in the two distinct cases $\alpha < \alpha_c$ and $\alpha > \alpha_c$. In the latter case, having a complex power a , the solution oscillates at large p^2 . This oscillatory behavior makes it possible to obey the boundary condition at the ultraviolet cutoff, even in the limit $m_0 \rightarrow 0$. Having the real power for $\alpha < \alpha_c = \pi/3$ this is not the case, and DB χ S is excluded. This is a nice and quite intuitive result: Only if the interaction is sufficiently strong, and this is the case for a fine structure constant larger than the critical value of the order one, a mass will be generated dynamically [210].

It is instructive to plot the numerical result for the dynamical mass (with $\alpha > \pi/3$) as a function of p^2 on a logarithmic scale, see fig. 7. At large p^2 the numerical solution reproduces the (analytically obtained) asymptotic behavior quite well. Note that the plot in fig. 7 is extended beyond the ultraviolet cutoff where the mass function is set to $m_0 = 0$ in order to demonstrate the oscillatory behavior. At small p^2 the mass function is almost momentum independent and approaches a constant value. This indicates that an analytic continuation of the mass function (and thus the propagator) to time-like momenta $p^2 < 0$ might be possible.

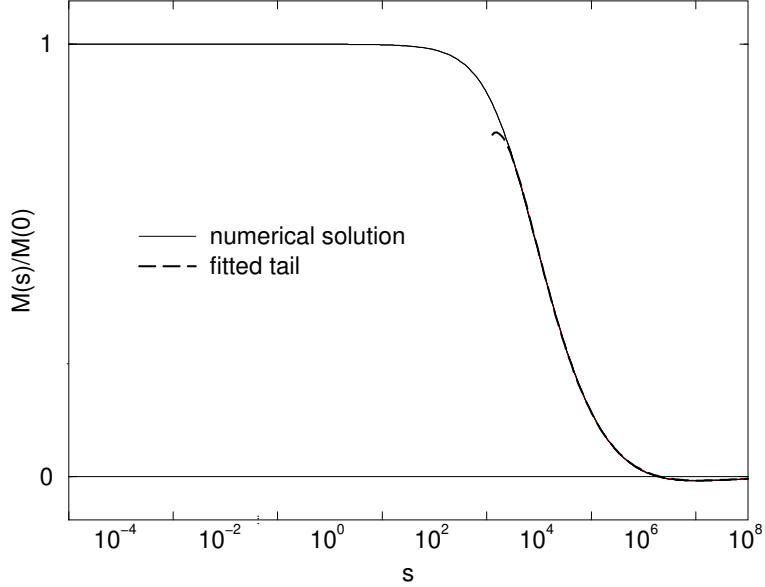


Fig. 7. The mass function $M(s)$ ($s = p^2/\mu^2$ with μ being some arbitrary numerical scale) for some coupling ($\alpha = 1.6$) above the critical value. Also shown is the asymptotic behaviour according to the linearized differential equation.

It would then furthermore be quite evident that the position of the pole should approximately be determined by $M(0)$, *i.e.*, $p_{\text{pole}}^2 \approx -M^2(0)$.

For a coupling smaller than its critical value, the boundary condition (134) cannot be fulfilled for $m_0 = 0$, and thus only the trivial solution is possible. At the critical coupling the solution bifurcates: One still has the trivial solution which is unstable, however. The chiral symmetry breaking solution with $M(p^2) > 0$ is energetically favoured as can be seen by analyzing the Cornwall–Jackiw–Tomboulis action [211]. (There exists a third solution with $M(p^2) < 0$ which is only a mirror of the massive solution with positive mass function. This third solution is excluded if one considers $m_0 \rightarrow 0^+$ instead of putting $m_0 = 0$ immediately.)

As discussed above a non-vanishing mass function implies a non-vanishing pole mass. As the latter is an observable and thus a gauge-independent quantity, the critical coupling has to be gauge invariant also. However, in the rainbow approximation this is not the case within the class of linear covariant gauges. Using, *e.g.*, the Feynman gauge ($\xi = 1$) instead of Landau gauge ($\xi = 0$), the value of the critical coupling increases by approximately fifty percent. As the use of a bare vertex violates Ward identities this should be no big surprise. Requiring that (i) the vertex function solves the Ward identity (99), that (ii) it is free of kinematical singularities (*i.e.*, that $\Gamma_\mu(p, q)$ has a unique limit for $p^2 \rightarrow q^2$), that (iii) it has the same transformation properties as the bare vertex under parity, time reversal and charge conjugation invariances, and that (iv) it reduces to the bare vertex γ_μ for a vanishing coupling, the longitudinal part of the vertex function is completely fixed in terms of the fermion propagator [171]:

$$\Gamma_\mu^{\text{BC}}(p, q) = \frac{1}{2}(A(p^2) + A(q^2))\gamma_\mu + \frac{1}{2}\Delta A_{pq}(p+q)_\mu(p + q) + i\Delta B_{pq}(p+q)_\mu \quad (136)$$

with

$$\Delta A_{pq} = \frac{A(p^2) - A(q^2)}{p^2 - q^2}, \quad \Delta B_{pq} = \frac{B(p^2) - B(q^2)}{p^2 - q^2}, \quad (137)$$

and where p and q are the momenta attached to the fermion legs. As stated in Sect. 3.3 in an explicit solution of the DSE for the vertex function, the form (136) for its longitudinal part is *exactly* reproduced.

If one refrains from solving the vertex function DSE, on the other hand, the transverse part of the vertex function has to be modelled. Transverse part here refers to those contributions transverse to the photon momentum $k = q - p$, *i.e.*, $(p - q)_\mu \Gamma_\mu^T(p, q) = 0$, which, in addition, satisfy the requirement that $\Gamma_\mu^T(p, p) = 0$. This additional requirement results from the differential Ward identity (100). The general form of the fermion-photon vertex can be decomposed into twelve linearly independent Lorentz covariants, four of them are longitudinal and eight are transverse. As the Ward identity has no $\sigma_{\mu\nu}$ component one coefficient is zero, and one obtains the three terms given in eq. (136) for the longitudinal part. As a further constraint, the condition that the propagators and vertices should be gauge covariant can then be imposed on the coefficients of the transverse parts. Restricting to the purely longitudinal vertex (136), however, the mass generation mechanism is still gauge dependent. This is related to the fact that a consistent regularization and renormalization of the fermion propagator DSE cannot be achieved unless the fermion propagator is multiplicatively renormalizable. Note that proofs of the gauge independence of the pole mass implicitly use this property, *e.g.*, see [212,60]. Since multiplicative renormalizability and gauge covariance are satisfied order by order in perturbation theory,³⁷ the perturbative result is a good starting point to resolve this issue [213]. Renormalizability is related to the ultraviolet behavior of the loop, and it is thus sufficient to consider momenta $p^2 \gg q^2$. In this limit the transverse part of the vertex function to $\mathcal{O}(e^2)$ is given by³⁸

$$\Gamma_\mu^{\text{T,1-loop}}(p, q) = \frac{e^2 \xi}{32\pi^2} \left(\gamma_\mu - \frac{p_\mu p}{p^2} \right) \log \frac{p^2}{q^2}. \quad (138)$$

On the other hand, taking the limit $p^2 \gg q^2$ in the purely longitudinal vertex (136) one then realizes that a non-perturbative expression for the transverse part has to include the functions $A(p^2)$ and $A(q^2)$. These considerations have been the underlying motivation for Curtis and Pennington to suggest the following form for the fermion-photon vertex [213],

$$\begin{aligned} \Gamma_\mu^{\text{CP}}(p, q) &= \Gamma_\mu^{\text{BC}}(p, q) \\ &- \frac{1}{2} \Delta A_{pq} \frac{(p^2 + q^2)(p^2 - q^2)}{(p^2 - q^2)^2 + (M^2(p^2) + M^2(q^2))^2} \left(\gamma_\mu(p^2 - q^2) - (p + q)_\mu(\not{p} - \not{q}) \right). \end{aligned} \quad (139)$$

³⁷ In perturbation theory this just means that violations of gauge covariance are of higher order than the highest one taken into account in a given approximation.

³⁸ The complete one-loop form of the fermion-photon vertex is given in ref. [214]. This reference also gives a list of minor errors in ref. [171].

To understand how multiplicative renormalizability constrains the transverse part of the vertex it is instructive to study the function $A(p^2)$ in the massless, *i.e.*, the chirally symmetric phase. A leading logarithmic expansion of $A(p^2)$ has the form

$$A(p^2) = \sum_{n=0}^{\infty} c_n (e^2)^n \log^n \left(\frac{p^2}{\Lambda_{\text{UV}}^2} \right). \quad (140)$$

In the chirally symmetric phase of the quenched approximation $A(p^2)$ is the only quantity which has to be renormalized. Therefore, the coefficients have to be of the form $c_n = c_1^n / n!$ in order to ensure multiplicative renormalizability. Then the series (140) can be summed, and using the 1-loop perturbative result one obtains

$$A(p^2) = \left(\frac{p^2}{\Lambda_{\text{UV}}^2} \right)^\eta \quad \text{with} \quad \eta = \frac{e^2 \xi}{16\pi^2}. \quad (141)$$

Since there is only one scale in the problem, Λ_{UV} , a power-law is indeed inevitable:

$$A(p^2) = \left(\frac{p^2}{\Lambda_{\text{UV}}^2} \right)^\gamma. \quad (142)$$

Using the vertex (139,136) $A(p^2)$ turns out to be of the form (142) with the difference $\gamma - \eta$ being of the order e^4 . This demonstrates explicitly that the transverse part of the vertex function is sufficient to maintain multiplicative renormalizability.

If the vertex function (139,136) is employed in the quark DSE, *i.e.*, with this particular transverse part included, the critical coupling above which $D\chi\text{SB}$ occurs becomes almost independent of the gauge parameter ξ [215,216]. For $0 \leq \xi \leq 20$ it varies by less than ten percent, see fig. 1 of ref. [195]. From this figure it can also be seen that imposing the transverse condition [217] leads to slightly different values for the critical coupling. This condition (which has been mentioned already in the last section) is imposed in order to remove gauge-covariance violating terms. An explicit solution to this condition is given in ref. [189]. It should also be mentioned that some of the simplifying assumptions used there have been questioned [218,219]. The interesting point here is that the values of the critical coupling obtained when imposing the transverse condition show an even stronger variation with the gauge parameter, *e.g.*, dropping from $\alpha_c = 0.933$ in Landau gauge to $\alpha_c \approx 0.80$ at $\xi = 5$. Note that for small values of the gauge parameter ξ these results have been verified in a direct numerical calculation in ref.[220]. Using a bifurcation analysis [216] it is straightforward to show that the critical coupling α_c^{CP} based on the Curtis–Pennington vertex (136,139) is related to the critical coupling α_c^{TC} , if the transverse condition is enforced. In particular, one obtains [195],

$$\alpha_c^{TC} = \frac{\alpha_c^{CP}}{1 + \xi \alpha_c^{CP} / 8\pi}. \quad (143)$$

Note that both values coincide in Landau gauge $\xi = 0$. For large positive values of ξ , however, the difference becomes large.

Identifying the regularization with the help of an Euclidean momentum cutoff as a source of gauge-invariance violating terms, the fermion propagator DSE of quenched four-dimensional QED has been studied using dimensional regularization in refs. [194–196]. Note that the use of dimensional regularization increases the numerical effort considerably. The values for the critical coupling are within numerical errors equal to the ones obtained by using cutoff schemes [195].

Thus we have to report that the goal to maintain gauge covariance by a suitable choice of the fermion-photon vertex has not fully been achieved. Nevertheless, the qualitative conclusions are unaffected: Above the critical coupling any vertex which satisfies the Ward identity and leads to multiplicative renormalizability will lead to a diverging mass function for quenched QED in four dimensions [221]. This supports the conjecture mentioned in the beginning of this subsection that four-dimensional QED might not have a non-trivial continuum limit.

Finally, we emphasize the special role that the Landau gauge plays here amongst the linear covariant gauges. Even in the most simple truncation, the rainbow approximation, it provides a reasonably accurate value for the critical coupling. As we have to acknowledge that even gauge-invariant observables can be sensitive to the details of the truncation (in this example the Ansatz for the fermion-photon vertex), and that they can furthermore depend on technicalities such as the choice of the regularization within a certain renormalization scheme, it seems worthwhile to remember that most approximations (and truncations) can best be justified in combination with the Landau gauge. This remark seems especially appropriate in view of the Green's functions in QCD discussed in the next chapter.

5 The Infrared Behavior of QCD Green's Functions

In this chapter the present knowledge on the infrared behavior of QCD Green's functions is summarized. As we will see, most of the results are obtained in the Landau gauge. This might seem somewhat surprising at first, as studies of Green's functions in Landau gauge should include the Faddeev–Popov ghosts. Thus, it could seem more natural to employ the axial gauge. And indeed, especially the gluon propagator has been subject to a considerable number of investigations in the axial gauge. Before discussing the corresponding results, however, a few general remarks on the infrared behavior of the gluon propagator are in order.

5.1 “Confined” or “Confining” Gluons?

In the literature one sometimes finds the distinction between *confined* and *confining* gluons (see, *e.g.*, ref. [222] and references therein). The first phrase is usually attributed to a gluon propagator which is infrared suppressed. The underlying idea is simply that under these circumstances the gluons themselves do not propagate over long distances. It is also clear that an infrared suppressed propagator almost necessarily violates reflection positivity, and we will present the quite convincing evidence for exactly that picture later in this chapter. Infrared enhanced gluonic correlations have, on the other hand, been referred to as confining gluons. As we describe below, if the gluon propagator was as singular in the infrared as $1/k^4$ in some gauge, this alone would establish an area law and the linearly rising interquark potential. Thus, such gluon (2-point) correlations alone would suffice to generate quark confinement in a simple and intuitive picture which was frequently connected with the notion of *infrared slavery* in the past. As will become clear in the course of this chapter, there is increasing evidence nowadays, however, that this is actually not what happens in QCD. And neither would it fit into the formal development of the covariant description of confinement outlined in sec. 2.4. It is important to realize that the more complicated picture emerging for QCD in the covariant gauge can certainly accommodate confined (but not confining) gluons in coexistence with an effective quark interaction which is confining, however.

Since the intuitive picture of confining gluons had quite a long history, we will describe some of its implications and applications first in the following. Despite the necessity of a reinterpretation about the origin of effective quark interactions, especially the applications thereby continue to provide many interest aspects.

As stated, by infrared enhanced gluonic correlations one usually refers to a gluon two-point function which (in momentum space) is more singular than a massless free particle pole in the infrared. In particular, for the gluon propagator in the Landau gauge,

$$D_{\mu\nu}(k) = \left(\delta_{\mu\nu} - \frac{k_\mu k_\nu}{k^2} \right) \frac{Z(k^2)}{k^2}, \quad (144)$$

this implies that the invariant function $Z(k^2)$ diverges for $k^2 \rightarrow 0$. The most singular behavior that does not lead too obviously to contradictions in the theory is given by $Z(k^2) \rightarrow \sigma/k^2$.

Such a behavior can, of course, at best be meaningful when supplemented by a prescription to define this singularity in the sense of distributions. An early Lagrangian model of confinement was given in ref. [223], the dipole gluon model which uses the derivative of the principal value prescription, $P \frac{1}{k^4} := -\frac{d}{dk^2} P \frac{1}{k^2}$. However, this model is in quite obvious conflict with causality.

Other frequently adopted prescriptions designed to subtract the leading singularity in $Z(k^2)$ at $k^2 = 0$ are the $[\sigma/k^2]_+$ prescription used in ref. [20] which is defined as acting on a function F by,

$$\int_0^\infty dx \left[\frac{1}{x} \right]_+ F(x, y) = \int_0^\infty dx \frac{1}{x} (F(x, y) - \theta(y - x)F(0, y)) , \quad (145)$$

and a prescription leading to a 3-dimensional Fourier transform corresponding to a linear rising potential $V(r) = \sigma r$ (in instantaneous approximation, $k_0 \rightarrow 0$),

$$8\pi \left[\frac{\sigma}{k^4} \right] := \lim_{\mu \rightarrow 0} \left\{ \frac{8\pi\sigma}{(k^2 + \mu^2)^2} - C(k_0, \mu) \delta^3(\vec{k}) \right\} , \quad C(k_0, \mu) = \int \frac{d^3k}{(2\pi)^3} \frac{8\pi\sigma}{(k^2 + \mu^2)^2} , \quad (146)$$

with $C = \sigma/\sqrt{k_0^2 + \mu^2}$ introduced to implement the regularity of the potential at $r \rightarrow 0$, *i.e.*, $\int d^3q V(q) = 0$ [224]. The need for such a prescription introduces an additional ambiguity as this can usually not be determined from the numerical solutions of the gluon propagator DSE. The more dramatic problem with such an infrared enhanced propagator, however, is that the σ/k^4 behavior cannot be well-defined as a distribution over a finite neighborhood of the origin in the Euclidean momentum space by simply providing a small mass $\mu^2 \rightarrow 0$. This is most clearly seen from eq. (146). The regularity constraint on its Fourier transform results in the necessity to subtract a term which is not a well-defined distribution but a more singular object in the limit $\mu \rightarrow 0$ (the contribution one subtracts for $k_0 = 0$ is essentially proportional to $\delta^3(\vec{k})/\mu$ while for $k_0 \neq 0$ it can be cast into the form $\propto \delta^4(k) \sqrt{k_0^2 + \mu^2}/\mu$).

While this is a serious conceptual problem, infrared enhanced gluon correlations have been phenomenologically quite successful, *e.g.*, in describing quark confinement by infrared slavery [225, 9, 113]. This term refers to the possible existence of severe infrared singularities, *i.e.*, infrared singularities which cannot be removed from the S -matrix by virtue of the Kinoshita–Lee–Nauenberg theorem in analogy to those arising from soft photons in QED.³⁹ Occurring in the inverse (ultraviolet renormalized) propagator of interacting quark fields, these divergences can then remove asymptotic states with quark quantum numbers from the asymptotic Hilbert space.

It will be corroborated repeatedly in the following that the effective interaction thereby arises from combinations of different contributions. This holds independently of whether that combination in the end gives rise to an interaction as strong as the $\sim \sigma/k^4$ infrared-slavery model or not. In particular, in covariant gauges it already follows from the necessity of renormalization

³⁹ As mentioned in the introduction, such severe infrared singularities do not arise at any finite order in perturbation theory in QCD.

group invariance of the color octet quark-current interactions that these interactions are mediated by both, gluon and ghost correlations. An infrared enhancement of these interactions, *e.g.*, the two-current interaction of the “Global Color Model” [208,29,28,209], thus is still a viable possibility even though the elementary gluon and ghost correlations should separately give rise to tempered distributions and show the corresponding analyticity properties in the noncoincident Euclidean domain.

By the same remark, such effective quark-current interactions should replace the literal meaning of a gluon propagator in the following argument: Infrared enhanced correlations $\propto \sigma/k^4$ in the purely gluonic Yang–Mills theory are known to provide sufficient damping in expectation values of large Wilson loops to give rise to an area law in analogy to the $1/k^2$ behavior of photons in the 2-dimensional Schwinger model. For the non-Abelian Yang–Mills theory in four dimensions this would follow from an infrared enhanced gluon propagator. The gluonic correlations besides being gauge and, in general, also renormalization scale dependent give rise to the following upper bound on the behavior of large Wilson loops with contour C [226],

$$W(C) = \left\langle P \exp \left\{ ig \oint_C A_\mu dx_\mu \right\} \right\rangle \leq \exp \left\{ -g^2 N_c C_f \oint_C dx_\mu dy_\nu D_{\mu\nu}(x - y) \right\}. \quad (147)$$

Note that a gluon propagator which is an analytic function for all noncoincident Euclidean $x \neq y$ cannot provide the sufficient damping to lead to an area law. Under those circumstances, its upper bound on Wilson loops is thus likely to be useless. The argument can, however, be strengthened by the replacement of the gluon propagator with an effective current interaction as mentioned above, and a stronger bound might be obtained from that renormalization group invariant combination of contributions here also. This seems plausible, in particular, since the expectation values of Wilson loops are physical objects and should as such have renormalization scale invariant bounds. Gauge invariance in this context simply means that such bounds from gauge covariant correlations will in general depend on the specific gauge employed in their derivation. Judging from nowadays’ knowledge, the original intention in ref. [226] to obtain the area law from the gauge dependent upper bound by demonstrating the existence of an infrared enhanced 2-point correlator in just one specific gauge, seems too optimistic.

An example in which the infrared behavior of the 2-point ghost correlations provide the essential infrared strength for the area law was given in ref. [93]. Assuming that configurations close to the Gribov horizon overcompensate the suppression from the Faddeev–Popov determinant and dominate the Yang–Mills partition function, an infrared enhanced ghost propagator was conjectured. Together with additional ghost fields which were introduced into the action via a Boltzmann factor this led to the following estimate for the Wilson loop,

$$W(C) \propto \exp -c\sigma^2 \oint_C dx_\mu dy_\nu \int d^4u d^4v g^2 D_{\mu\rho}(x - u) g^2 D_{\nu\rho}(y - v) D_G(u - v). \quad (148)$$

The dimensionless constant c herein is related to the leading infrared behavior of the gluon and ghost propagators, $D_{\mu\nu}(k) \propto 1/\sigma$ and $D_G(k) \propto \sigma/k^4$ for $k^2 \rightarrow 0$, respectively, as suggested by the estimates in this approach. The renormalization group invariance of this bound is somewhat unclear here again. Naively, one would at least expect the constant c to have a suitable scale

dependence to compensate the one of the other factors in the exponent in order to obtain an invariant string tension. At least in the Landau gauge the particular combination of ghost and gluon propagators does certainly not compensate the scale dependence of the explicit couplings (the factor g^4). A second question is, of course, whether it is more acceptable for the ghost correlations to violate temperedness than it is for the gluons. However, this example once more demonstrates that ghosts can provide for the infrared dominant correlations in large Wilson loops in covariant gauges. As will be discussed in sec. 5.5, a behavior of the gluon and ghost propagators, $D(k) \propto 1/\sigma$ and $D_G(k) \propto \sigma/k^4$ for $k^2 \rightarrow 0$, is not incompatible with present lattice data.

After these cautioning remarks on a possible σ/k^4 behavior for any two-point correlations in a sensible quantum field theory, in the next sections early studies of the gluon Dyson–Schwinger equation will be described in which exactly such an infrared enhancement was obtained. It will become clear in the sequel that ghosts affect this conclusion. We reiterate that this alone would not necessarily exclude a σ/k^4 behavior for the effective interactions of quarks in the infrared.

5.2 The Gluon Propagator in Axial Gauge

Historically, an infrared enhanced gluon propagator $\propto \sigma/k^4$ was first obtained in the covariant gauge much before the importance of ghosts became evident which had been neglected in the approximation summarized in sec. 5.3.1 below. The same infrared behavior was confirmed in the early studies of the gluon DSE in the axial gauge [22–24]. In this section we will discuss why it now seems plausible that these axial gauge results are just as inconclusive, since they were based on a simplifying assumption quite analogous to disregarding the ghosts of the covariant gauge.

5.2.1 Dyson–Schwinger Equation Studies

In the axial gauge the gluon field is taken transverse to a fixed gauge vector t_μ , *i.e.* $t_\mu A_\mu^a = 0$. The tensorial structure of the gluon propagator in this gauge is given in eq. (C.6) in Appendix C. Note that two independent tensor structures and therefore two scalar functions $f(p^2, (pt)^2)$ and $g(p^2, (pt)^2)$ are involved. The tree-level propagator is recovered from setting $g(p^2, (pt)^2) \equiv 1$ and $f(p^2, (pt)^2) \equiv 0$. A corresponding construction [172] of the longitudinal part of the 3-gluon vertex with the help of the Slavnov–Taylor identity relating this vertex to the gluon propagator is summarized in Appendix D. Note that in this gauge the Slavnov–Taylor identity reduces to a kind of Ward identity. In particular, no unknown contributions from higher correlation functions such as the 4-point ghost-gluon scattering kernel in covariant gauges enter in this axial gauge identity for the 3-gluon vertex given in eq. (114). Nevertheless, keeping the full tensor structure of the gluon propagator leads to a longitudinal part of the 3-gluon vertex which is of an enormous complexity, however.

The DSE for the gluon propagator is given explicitly in eq. (C.5) and pictorially represented in fig. (C.1) in Appendix C. Of course, the ghost loop does not contribute in axial gauge.

As already mentioned in section 3.1, studies of the axial-gauge gluon DSE [22–26,155] rely on a simplifying assumption on the tensor structure of the gluon propagator. That particular term which strength is parametrized by the function $f(p^2, (pt)^2)$, and that can only be non-vanishing non-perturbatively, has not been included in presently available studies of the gluon DSE in axial gauge [27]. The original studies of the axial-gauge gluon DSE assumed that a possibly infrared enhanced part of the gluon propagator has the same structure as the tree-level propagator, *i.e.*, $f = 0$ was set for simplification and the structure corresponding to the function f had been dismissed. This also simplifies the longitudinal part of the 3-gluon vertex considerably: Only with the approximation $f = 0$, and with assuming, in addition, $g(p^2, (pt)^2) \rightarrow g(p^2)$ in eq. (D.2), *i.e.*, that the function g is independent of t , this solution reduces to the simple form used in refs. [22,23]. It was further noted that upon contracting the axial gauge gluon Dyson–Schwinger equation for the vacuum polarization tensor $\Pi_{\mu\nu}$ with the tensor $t_\mu t_\nu$ only the 3-gluon loop plus a tadpole term give non-vanishing contributions to a single integral equation for the one scalar function $g(p^2)$ of this approximation scheme. And it was found numerically that $g(p^2) \propto p^2/\sigma$, *i.e.*, the solution gives rise to an infrared enhanced gluon propagator $\propto \sigma/p^4$.

Before discussing some implications of this approximation scheme in the following subsection we will comment on a further simplification: In ref. [25] the t -dependence (that had anyhow been disregarded in the solution for the 3-gluon vertex) has been consistently neglected also in the Dyson–Schwinger equation. Then the tadpole contribution disappears in addition to the other contributions with 4-gluon vertices [222]. Furthermore, a one-dimensional approximation and subtractions have been employed to ensure the masslessness condition

$$\lim_{k^2 \rightarrow 0} D_{\mu\nu}^{-1}(k^2) = 0. \quad (149)$$

This masslessness condition follows from the axial gauge Slavnov–Taylor identity (114) in the limit $k \rightarrow 0$ with assuming that the vertex does not have massless poles in the external momenta.⁴⁰ The resulting equation, of a structure similar to the Mandelstam euqation to be discussed in sec. 5.3.1, was found to confirm the findings of refs. [22,23] with respect to the infrared behavior of the solution.

Subsequent studies based on the identical approximation scheme for the axial gauge came to a somewhat dissentive conclusion proposing the possibility of a gluon propagator less singular than a massless free particle pole $1/p^2$ in the infrared [26]. This possibility was, however, later attributed to a sign error in the resulting equation [27,222]. The infrared soft solution to the approximate gluon DSE of ref. [25] for this wrong sign also yields the wrong sign in the well-known perturbative contributions valid at high momenta [222]. In ref. [222] a detailed comparison of the approximate gluon DSEs of the axial gauge (in the scheme of ref. [25]) with the Mandelstam approximation to the Landau gauge DSE (see sec. 5.3.1 below) showed some analogies in these two schemes. In light of this, it might thus not be too surprising anymore that previous DSE studies of the gluon propagator in both these gauges seemed to agree in

⁴⁰ This condition was in some older studies assumed to hold also for the Landau gauge. In sec. 5.3.2 it will be demonstrated, however, that ghosts change this conclusion and that the masslessness condition in the present form (149) does not hold in general in Landau gauge.

indicating an infrared enhancement of the gluon propagator, $D(k) \propto \sigma/k^4$ for $k^2 \rightarrow 0$.⁴¹

Studies of the gluon Dyson–Schwinger equation using the light-cone gauge, $t^2 = 0$, in which the second tensor structure (as well as the spurious gauge singularities $\propto 1/(kt)^2$, see the next section) are obviously avoided, seem to come to similar conclusions, see refs. [227–229]. The light-cone gauge has its own problems, however, for an extensive discussion see, *e.g.*, ref. [230]. Here it suffices to mention that ghost fields are indispensable in light-cone gauges, see ref. [231] and references therein for the recent developments concerning this issue.

5.2.2 The Spectral Representation

On one hand, an infrared enhanced gluon propagator is known to lead to an area law for expectation values of large Wilson loops [226], on the other hand it was pointed out in ref. [108] that a full axial gauge gluon propagator more singular than $1/k^2$ in the infrared violates positivity of the norm in the corresponding Hilbert space. Such an infrared enhanced behavior is thus generally excluded for physical correlation functions, see also sec. 5.3.4. We will therefore discuss the possibilities to infer positivity violations of transverse gluon states from the axial-gauge propagator in the following two subsections.

The spectral representation for the gluon propagator in the (spacelike) axial gauge involving the spectral functions ρ_g and ρ_f corresponding to the two different tensor structures is given by [108],

$$D_{\mu\nu}(k) = \int_0^\infty d\mu^2 \left\{ \frac{\rho_g(\mu^2, kt)}{k^2 + \mu^2} \mathcal{M}_{\mu\nu}(k) - \frac{\rho_f(\mu^2, kt)}{k^2 + \mu^2} \mathcal{P}_{\mu\nu}(t) \right\}. \quad (150)$$

Imposing equal-time canonical commutation relations in the standard way, one obtains their respective spectral sum rules as follows,

$$\int_0^\infty dq^2 \rho_g(q^2, qt) = 1 \quad (151)$$

$$\int_0^\infty dq^2 \rho_f(q^2, qt) = -\frac{g^2}{3} \int_{-\infty}^\infty dl \epsilon(l) e^{-il(qt)} \langle A_i^a(l\hat{t}) A_i^a(0) \rangle, \quad \hat{t}_\mu = t_\mu/t^2, \quad (152)$$

where $\epsilon(l)$ is the signature function. For the interacting theory modifications are necessary since equal-time commutation relations are lost in general, see sec. 2.3. Note though that quite interestingly a finite value for the integral of the second spectral function, the r.h.s in eq. (152), might be used to obtain a bound on the coupling g^2 for finite $\langle A_i^a A_i^a \rangle$.

The positivity of the two spectral functions separately being affected by the axial gauge singularity (see the next section), for the difference of these spectral functions it was shown

⁴¹ It is nevertheless not entirely trivial that the solutions to different non-linear integral equations, may they look similar or not, show this same behavior.

unambiguously in ref. [108] that positive definiteness in a space of physical gluon states in the axial gauge would imply the positivity condition,

$$\rho_g(k^2, kt) - \rho_f(k^2, kt) \geq 0. \quad (153)$$

To see how this generalizes the analogous condition for QED, recall that in QED the field strengths are gauge invariant and thus, in particular, independent of the gauge vector t in axial gauge from which it can be inferred that $\rho_f \equiv 0$ as well as $\rho_g(k^2, kt) \equiv \rho_g(k^2)$ which is identical to the spectral density $\rho(k^2)$ in the covariant gauge. Then, $\rho_g(k^2) \geq 0$ from eq. (151) implies Källén screening for the renormalized (physical) charge (to be smaller than the bare charge), and the gauge invariance of $\rho_g(k^2)$ reflects the invariance of the Coulomb potential.

From the discussion above it is clear that the assumptions underlying the studies of refs [22–27], of the gluon DSE in axial gauge can be thought of as an Abelian approximation to the more general structures that can occur in the non-Abelian theory. QED does provide an example to demonstrate, on the other hand, that it is the coefficient of the metric tensor (here the Euclidean $\delta_{\mu\nu}$) in the spectral representation of the photon which is gauge invariant and which thus has a physical interpretation. For the full non-Abelian structure of the axial gauge gluon propagator and its corresponding spectral condition (150) this coefficient is given by $\rho_g(k^2, kt) - \rho_f(k^2, kt)$, and the positivity condition (153) certainly suggests to study this difference. Therefore, the possibility of the additional tensor structure introduced by $f \neq 0$ should be considered not only to explore physical consequences such as long range forces but to first of all assess the question of positivity. Whether or not the gluonic degrees of freedom in the axial gauge have a particle interpretation cannot be decided from the results of [22,23] for $g(k^2)$ alone.

This clearly demonstrates that progress is desirable in axial gauge. Another important prerequisite for this will be a proper treatment of the spurious infrared divergences which are well-known to be present in axial gauge due to the zero modes of the covariant derivative [230]. This can be achieved by either introducing redundant degrees of freedom, *i.e.*, ghosts, also in this gauge [232] (by which it obviously loses its particular advantage) or by using a modified axial gauge [121,233], which is specially designed to account for those zero modes. Ultimately, progress in more than one gauge will be the only reliable way to assess the influence of spurious gauge dependencies.

5.2.3 Positivity in Axial Gauge

The same contradiction between positivity and antiscreening as discussed in sec. 2.3 applies to the axial gauge (here with $\gamma = 1$ and $Z_3^{-1} \rightarrow 0$), if it can be shown that positivity of the norm implies not only the inequality in (153) but also the stronger condition $\rho_g(k^2, kt) \geq 0$. It was argued in ref. [108] that this condition is generally not satisfied in the axial gauge, however. In particular, for large k^2 , *i.e.*, in the ultraviolet, which for dimensional reasons corresponds to very small kt in the spectral function, it depends on the prescription adopted for the gauge singularities $\sim 1/(kt)$. This argument is based on the observation that positivity of the norm of the states in axial gauge (spacelike corresponding to Euclidean $t^2 > 0$) actually implies the

modified condition,

$$\frac{t^2}{(kt)^2} \rho_g(k^2, kt) \geq 0. \quad (154)$$

Accordingly, the positivity of ρ_g depends on the positivity of the prescription adopted for the gauge singularity [230]. In particular, for the principal value prescription (which is *not* positive) it follows that $\rho_g(k^2, 0) \leq 0$ which in generalization of the perturbative argument given in ref. [234] would be sufficient to resolve the contradiction between positivity and asymptotic freedom in the axial gauge. It is clear that this resolution of the issue of positivity is itself based on an artifact of the principal value prescription, however. In fact, it is known by now that defining the square of the principal value prescription (usually denoted by square brackets) in the gluon propagator through its derivative,

$$\frac{1}{kt} \rightarrow P \frac{1}{kt} =: \frac{1}{[kt]}, \quad \text{and} \quad \frac{1}{(kt)^2} \rightarrow -\frac{d}{d(kt)} \frac{1}{[kt]}, \quad (155)$$

results in loosing positivity of the polarization sum at the Feynman poles of the tree-level gluon propagator. This demonstrates that such a prescription in fact introduces unphysical degrees of freedom also in the axial gauge [235,236]. Exactly this prescription was also employed, however, for the double pole in the spectral representation of the full propagator in ref. [108]. As a result, the resolution of the Oehme–Zimmermann paradox proposed in ref. [108] is most likely itself based on the presence of negative norm states. It is thus inconclusive. In contrast to this, other prescriptions such as the positive Mandelstam–Leibbrandt prescription or the planar gauge choice naturally lead to redundant degrees of freedom as a result of the impossibility to fully eliminate $t_\mu A_\mu^a$. These degrees of freedom give rise to negative norm states. Their elimination by projection onto a subspace of semi-definite norm suffices to recover Gauss' law and unitarity and, in addition, canonical quantization then results in a free (tree-level) gluon propagator without double pole of the form $1/(kt)^2$ [236]. While the method of canonical quantization may not be too appropriate for interacting theories, this nevertheless suggests that the stronger positivity condition

$$\rho_g(k^2, kt) \geq 0 \quad (156)$$

should also hold in the axial gauge, implying that the Oehme–Zimmermann superconvergence relation (30) does as well.

In either case, the considerations based on the principal value prescription cannot establish positivity in the axial gauge. Note however, that the positivity condition for the difference of the spectral functions (153) is unaffected by this, *i.e.*, by the question whether the stronger condition (156) has to hold in general or not. The relevance of the second tensor structure in the axial gauge gluon propagator as emphasized in refs. [27,222] holds independent of the artifacts of the principal value prescription for the gauge singularity. In addition, this singularity is less relevant for the infrared behavior than it is in the ultraviolet, as the limit $k^2 \rightarrow 0$ can be studied for $kt > 0$. On the other hand, the typical zero modes of QCD in the axial gauge make

an important difference as compared to QED: these zero modes prevent the spectral density $\rho_g(k^2, kt)$ from being independent of the gauge vector t_μ [108].

As a result, it seems fair to say that available studies of the gluon propagator from the axial gauge DSE cannot be regarded any more conclusive than those of the Mandelstam approximation to the Landau gauge DSE, see sec. 5.3.1 below. As for the Landau gauge, it will be demonstrated in sec. 5.3.2 that, instead of the gluon propagator, the previously neglected ghost propagator assumes an infrared enhancement similar to what was then obtained for the gluon. It is certainly not inconceivable that the additionally possible structure in the axial gauge has some similar effect there, too. To this end it is interesting to note that a study of the gauge boson propagator of the dual Abelian Higgs model in axial gauge does lead to a non-vanishing function $f(p^2, (pt)^2)$ [183]. Herein, an infrared suppressed gauge boson propagator has been obtained, and an inspection of the signs involved in the functions $f(p^2, (pt)^2)$ and $g(p^2, (pt)^2)$ reveals that this gauge boson propagator does indeed violate positivity also in the axial gauge.

5.3 Truncation Schemes for Propagators in Landau Gauge

In this section we present a truncation scheme for the Landau gauge QCD Green's functions which is complete at the level of two-point functions, *i.e.*, the propagators. The corresponding system of DSEs whose derivation has been reviewed in sec. 3.1 is diagrammatically represented in fig. 8. In addition to the emphasis on maintaining the correct infrared properties as much as possible, the known ultraviolet behavior of the Green's functions provides another important guideline in the assumptions employed to simplify the system. Hereby we start with a discussion of the gluon DSE. In a first step towards its truncation consider the terms containing explicit four-gluon vertices. These are the momentum independent tadpole term, an irrelevant constant which vanishes perturbatively in Landau gauge, as well as explicit two-loop contributions to the gluon DSE. A possibly non-vanishing contribution from the tadpole term beyond perturbation theory can nevertheless be eliminated from the equation upon contraction of the free Lorentz indices with momentum projector $\mathcal{R}_{\mu\nu}(k) = \delta_{\mu\nu} - 4k_\mu k_\nu/k^2$, see sec. 4.2. For the explicit two-loop terms one first notes that these are subdominant in the ultraviolet. Possible solutions can therefore be expected to resemble the correct leading perturbative behavior for asymptotically high momenta also without those terms. It should be kept in mind though that these terms will have an effect, *e.g.*, on the running QCD coupling, at next to leading order in perturbation theory. While this can partially be compensated for by an adjustment of the scale parameter of the subtraction scheme as will be discussed in sec. 5.3.3 below, discrepancies with two-loop perturbative results in the energy range where these are phenomenologically well supported serve as one indicator of the quantitative effects of the truncations.

Secondly, and more importantly, for the infrared behavior it has been argued that the singularity structure of the two-loop terms does not interfere with that of the one-loop terms [237]. The argument is based on studies of certain Ansätze for the leading infrared behavior of all correlation functions and their self-reproduction in the coupled equations. A dimensional regularization was adopted and integer powers of the invariant momenta for these Ansätze were studied with the result that the explicit two-loop contributions to the gluon DSE turn out

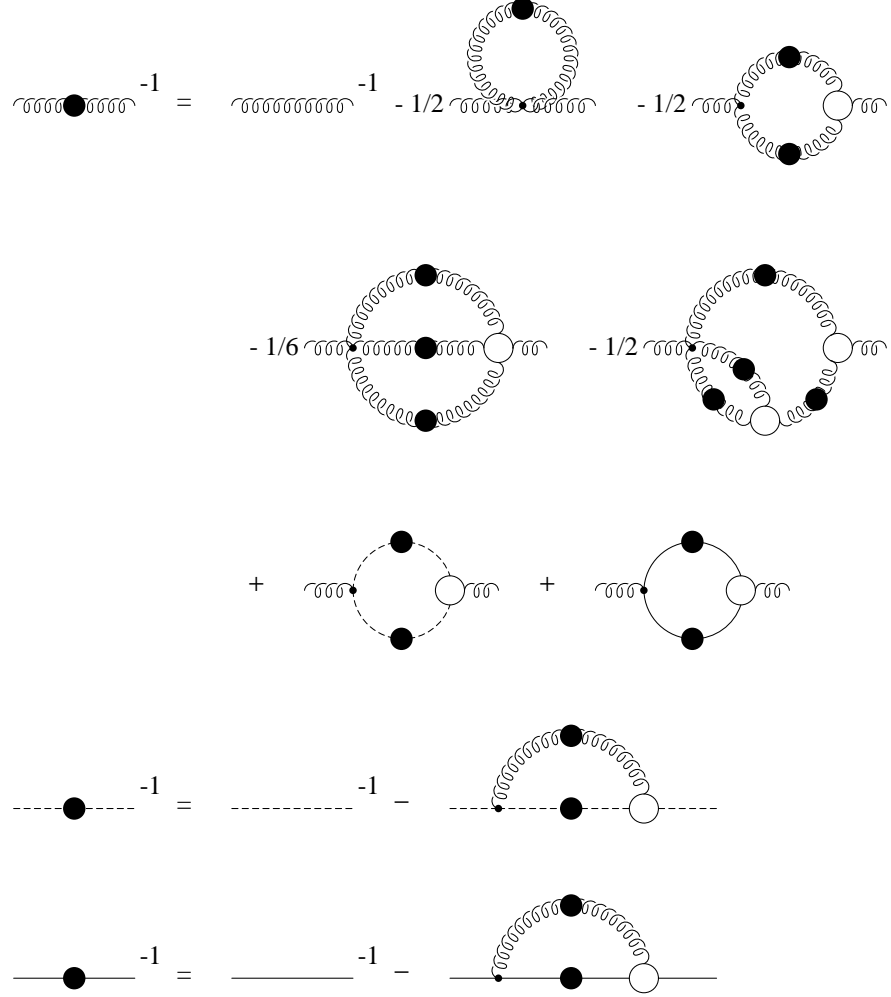


Fig. 8. Diagrammatic representation of the gluon, ghost and quark DSEs of QCD. The wiggly, dashed and solid lines represent glue, ghosts and quark, respectively. Filled blobs stand for fully dressed propagators and open circles for one-particle irreducible vertices.

to be subleading in the infrared and do not influence the leading contributions from the one-loop terms. The conditions for self-reproduction of the respective contributions (with different exponents) in the gluon DSE were found to decouple from each other. This argument is unfortunately still incomplete, however, because the possibility for non-integer exponents in the leading infrared behavior was not considered. The solutions to the coupled system of gluon and ghost equations as presented below in this section provide strong evidence for precisely such an infrared behavior determined by a non-integer exponent. For this type of solutions, however, it has been verified a posteriori by an explicit calculation that the two-loop terms are subleading in the infrared [238].

In light of this evidence and of the tremendously rich structure of the non-perturbative 4-gluon vertex function introducing a whole new degree of complexity, it seems reasonable to study the non-perturbative behavior of the gluon propagator in the infrared without explicit contributions from four-gluon vertices, *i.e.*, without the two-loop diagrams in fig. 8. The renormalized Dyson–Schwinger equation for the inverse gluon propagator $D_{\mu\nu}^{-1}$ in Euclidean momentum space with positive definite metric, $g_{\mu\nu} = \delta_{\mu\nu}$, (color indices suppressed) then simplifies as

follows,

$$\begin{aligned}
D_{\mu\nu}^{-1}(k) = & Z_3 D_{\mu\nu}^{\text{tl}}(k) - g^2 N_c \tilde{Z}_1 \int \frac{d^4 q}{(2\pi)^4} i q_\mu D_G(p) D_G(q) G_\nu(p, q) \\
& - g^2 Z_{1F} N_f \frac{1}{2} \int \frac{d^4 q}{(2\pi)^4} \text{tr}(\gamma_\mu S(p) \Gamma_\nu(p, q) S(q)) \\
& + g^2 N_c Z_1 \frac{1}{2} \int \frac{d^4 q}{(2\pi)^4} \Gamma_{\mu\rho\alpha}^{\text{tl}}(k, -p, q) D_{\alpha\beta}(q) D_{\rho\sigma}(p) \Gamma_{\beta\sigma\nu}(-q, p, -k) ,
\end{aligned} \tag{157}$$

where $p = k + q$, D^{tl} and Γ^{tl} are the tree-level propagator and three-gluon vertex, D_G is the ghost propagator, S the quark propagator, and Γ and G are the respective fully dressed 3-point vertex functions. The DSEs for the ghost propagator and the quark propagator, formally without any truncations, will be used as given in eqs. (88,90).

In order to arrive at a closed set of equations for these functions, it is still necessary to specify the form of the three remaining vertex functions, the ghost-gluon, the quark-gluon and the 3-gluon vertex functions. As discussed in sec. 3.3 little is known about possible solutions to their corresponding DSEs. For the 3-gluon vertex, independent of the presence of quarks, a general procedure to construct a solution to its Slavnov–Taylor identity (113) is in principle possible [170–172]. Since this procedure involves unknown contributions from the ghost-gluon scattering kernel, it cannot be readily applied to express the vertex functions entirely in terms of the ghost and gluon renormalization functions G and Z . To achieve this one has to make additional assumptions on the scattering kernel. Since this kernel is related to the ghost-gluon vertex the construction of the latter via the identity (107) should be done before explicitly solving the Slavnov–Taylor identity (113) for the 3-gluon vertex. Noting that a simple solution to eq. (113) is possible if ghosts are neglected completely [170–172] we will digress briefly in order to discuss the historically first and particularly drastic approximation to the gluon DSE.

5.3.1 The Mandelstam Approximation

The first approximation scheme for the gluon DSE in Landau gauge was originally proposed by Mandelstam [18]. The essential truncating assumption is, even though working in Landau gauge, to neglect all ghost contributions to the gluon DSE of pure QCD (without quarks). As a justification for this, it was usually referred to perturbative calculations which yield numerically small ghost contributions to the gluon self-energy. Even though there was never any doubt about the importance of ghosts for fundamental reasons such as transversality of the gluon propagator and unitarity, it was asserted that their quantitative contributions to many hadronic observables might remain negligible even beyond perturbation theory. It will be seen later on in this section that presently available solutions to the coupled system of gluon and ghost DSEs yield qualitatively quite different results as compared to the Mandelstam approximation, and are thus counterexamples to this assertion. The exact implications of the importance of ghosts, in particular, in the infrared, on the effective interactions of quarks and on hadronic observables are more subtle as will be discussed in detail in the appropriate context of later sections.

As already stated, without ghosts the solution of Slavnov–Taylor identity (113) assumes a particularly simple form [170–172]:

$$\begin{aligned} \Gamma_{\mu\nu\rho}(p, q, k) &= -A_+(p^2, q^2) \delta_{\mu\nu} i(p - q)_\rho - A_-(p^2, q^2) \delta_{\mu\nu} i(p + q)_\rho \\ &- 2 \frac{A_-(p^2, q^2)}{p^2 - q^2} (\delta_{\mu\nu} p q - p_\nu q_\mu) i(p - q)_\rho + \text{cyclic permutations} , \\ \text{with } A_\pm(p^2, q^2) &= \frac{1}{2} \left(\frac{1}{Z(p^2)} \pm \frac{1}{Z(q^2)} \right) . \end{aligned} \quad (158)$$

Assuming that the gluon renormalization function $Z(p^2)$ is a slowly varying function one may then approximate this solution by

$$\Gamma_{\mu\nu\rho}(p, q, k) = A_+(p^2, q^2) \Gamma_{\mu\nu\rho}^{\text{tl}}(p, q, k) . \quad (159)$$

While this form for the full three-gluon vertex simplifies the 3-gluon loop in the gluon DSE even more than the use of another bare vertex, which corresponded to setting $\Gamma \equiv \Gamma^{\text{tl}}$, the approximation (159) was observed by Mandelstam to be superior to the latter since it accounts for some of the dressing of the vertex as it results from the corresponding Slavnov–Taylor identity. The nature of this dressing is such that it cancels the dressing of one of the gluon propagators in the 3-gluon loop, and without ghost contributions the gluon DSE in the Mandelstam approximation assumes the comparatively simple form

$$\begin{aligned} D_{\mu\nu}^{-1}(k) &= Z_3 D_{\mu\nu}^{\text{tl}-1}(k) \\ &+ g^2 N_c \frac{1}{2} \int \frac{d^4 q}{(2\pi)^4} \Gamma_{\mu\rho\alpha}^{\text{tl}}(k, -p, q) D_{\alpha\beta}(q) D_{\rho\sigma}^{\text{tl}}(p) \Gamma_{\beta\sigma\nu}^{\text{tl}}(-q, p, -k) \end{aligned} \quad (160)$$

where $p = k + q$. This equation, the Mandelstam equation, is schematically depicted in fig. 9. It was already pointed out by Mandelstam that in order to solve this equation selfconsistently it is necessary to implement an additional constraint: Without ghosts the Slavnov–Taylor identity for the 3-gluon vertex and its solution (158) for $p^2 \rightarrow 0$ entail the masslessness condition (149) which may be written explicitly as

$$\lim_{k^2 \rightarrow 0} \frac{k^2}{Z(k^2)} = 0 . \quad (161)$$

While imposing this additional condition seems consistent with the other assumptions in the Mandelstam approximation, it has to be emphasized that concluding (161) as a result of (158) relies solely on neglecting all ghost contributions in covariant gauges.

The Mandelstam equation in its original form is obtained from eq. (160) upon contraction with the transversal projector $\mathcal{P}_{\mu\nu}(k) = \delta_{\mu\nu} - k_\mu k_\nu / k^2$. As stated in the last chapter in connection with the discussion of the photon DSE, this leads to an ambiguity in combination with an ultraviolet momentum cutoff which violates gauge invariance. The correponding quadratic

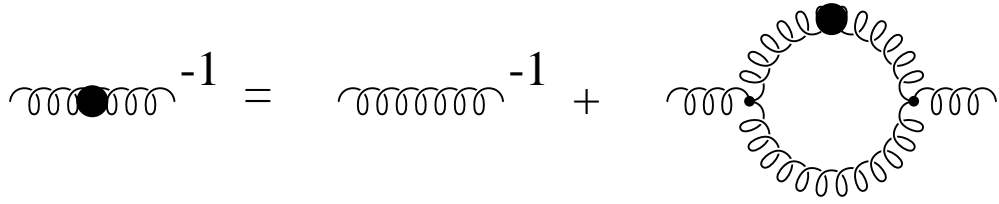


Fig. 9. Diagrammatic representation of the gluon Dyson–Schwinger equation in Mandelstam’s approximation.

ultraviolet divergence has in the early studies been absorbed by a suitably added counter term introduced in order to account for the masslessness condition (161), see refs. [18,19]. The solution to this equation proposed by Mandelstam’s infrared analyses proceeds briefly as follows: Assume $Z(k^2) \sim 1/k^2$. This exclusively yields contributions which violate the masslessness condition (161). Such terms have to be subtracted. Since the kernel of Mandelstam’s equation is linear in Z , this is achieved by simply subtracting the corresponding contribution from Z in the integrand. Thus defining

$$Z(k^2) = \frac{b}{k^2} + C(k^2), \quad b = \text{const.}, \quad (162)$$

and retaining only the infrared subleading second term in the integrals, one obtains a solution to this equation, which can be shown to vanish in the infrared by some non-integer exponent of the momentum [18],

$$C(k^2) \sim (k^2)^{\gamma_0}, \quad \gamma_0 = \sqrt{\frac{31}{6} - 1} \simeq 1.273, \quad \text{for } k^2 \rightarrow 0. \quad (163)$$

Subsequently, an existence proof, a discussion of the singularity structure and an asymptotic expansion of the solution generalizing Mandelstam’s discussion of the leading behavior of $C(k^2)$ in the infrared was given by Atkinson et al. [19].

Contracting instead of the transversal projector $\mathcal{P}_{\mu\nu}(k) = \delta_{\mu\nu} - k_\mu k_\nu / k^2$ with $\mathcal{R}_{\mu\nu}(k) = \delta_{\mu\nu} - 4k_\mu k_\nu / k^2$ leads to a somewhat modified equation for the gluon renormalization function, in particular, without quadratically ultraviolet divergent terms [20]. The solution to this equation has an infrared behavior quite similar to the solution of Mandelstam’s original equation [21]. In particular, explicitly separating the leading infrared contribution according to (162) one obtains a unique solution of the form

$$C(k^2) \sim (k^2)^{\gamma_0}, \quad \gamma_0 = \frac{2}{9} \sqrt{229} \cos \left(\frac{1}{3} \arccos \left(-\frac{1099}{229\sqrt{229}} \right) \right) - \frac{13}{9} \simeq 1.271, \quad (164)$$

for $k^2 \rightarrow 0$. Both equations can be solved using a combination of numerical and analytic methods [239]. In the infrared, the asymptotic expansion technique of ref. [19] is applied to calculate successive terms recursively. The asymptotic expansions obtained this way were then

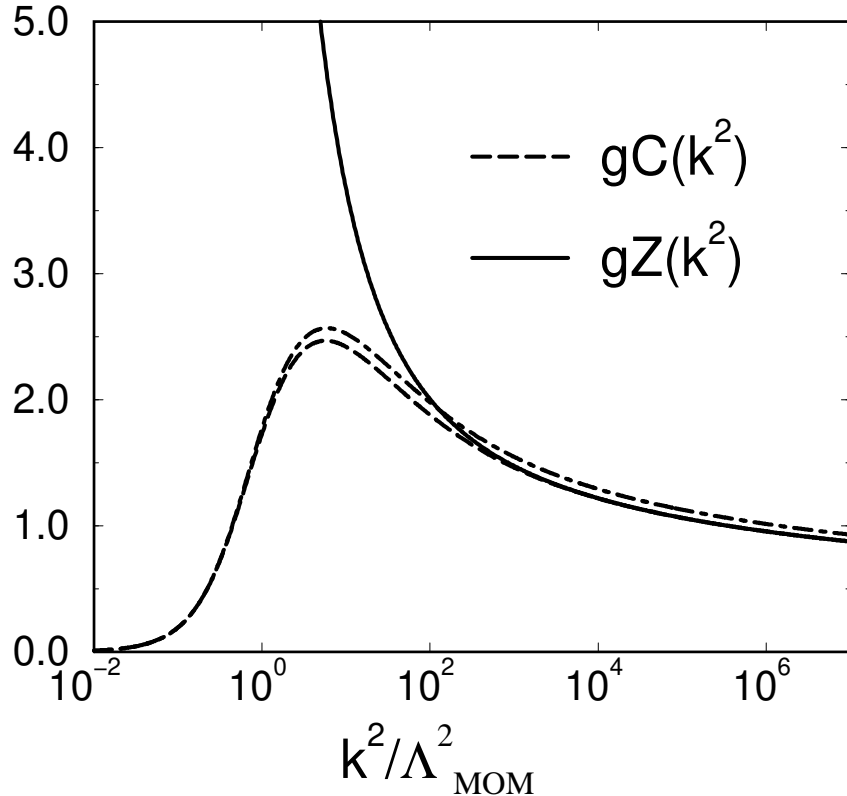


Fig. 10. The gluon renormalization function $gZ(k^2) = 8\pi\sigma/k^2 + gC(k^2)$ for Mandelstam's equation projected with $\mathcal{R}_{\mu\nu}$. The dashed lines show the corresponding function $gC(k^2)$ for this equation and Mandelstam's original equation (projected with $\mathcal{P}_{\mu\nu}$).

matched to the iterative numerical solution (see ref. [239] for details). As can be seen from fig. 10 the solutions to both versions of Mandelstam's equation are very similar to each other.

A remark concerning the renormalization of Mandelstam's equation is in order. Logarithmic ultraviolet divergences are absorbed in the gluon renormalization constant Z_3 which can be shown to obey the identity $Z_g Z_3 = 1$ in Mandelstam approximation [21]. This entails that the product of the coupling and the gluon propagator, $gD_{\mu\nu}(k)$, does not acquire multiplicative renormalization in this approximation scheme. Using a non-perturbative momentum subtraction scheme corresponding to the renormalization condition $Z(k^2 = \mu^2) = 1$ for some arbitrary renormalization point $\mu^2 > 0$, the resulting equation can in both cases be cast in a renormalization group invariant form determining the renormalization group invariant product $gZ(k^2)$ which is equivalent to the running coupling $\bar{g}(t, g)$ of the scheme,

$$gZ(k^2) = \bar{g}(t_k, g) , \quad t_k = \frac{1}{2} \ln k^2/\mu^2 . \quad (165)$$

The scaling behavior of the solution near the ultraviolet fixed point is determined by the coefficients $\beta_0 = 25/2$ and $\gamma_A^0 = 25/4$ for Mandelstam's original equation or $\beta_0 = 14$ and $\gamma_A^0 = 7$ for the equation projected with $\mathcal{R}_{\mu\nu}$. These values are reasonably close to the perturbative values for $N_f = 0$, *i.e.*, $\beta_0 = 11$ and $\gamma_A^0 = 13/2$, the difference being attributed to neglected ghost contributions.

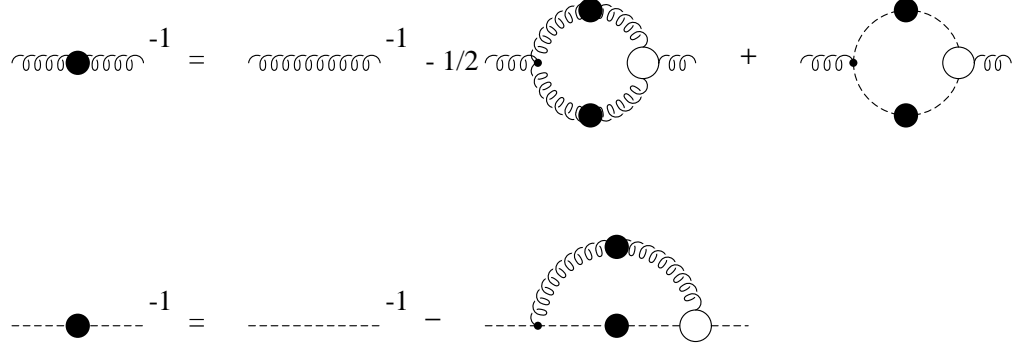


Fig. 11. Diagrammatic representation of the gluon and ghost Dyson–Schwinger equations of QCD without quarks. In the gluon DSE terms with four-gluon vertices have been dismissed.

The most important feature of the results concerning the Mandelstam approximation is the infrared enhancement of the gluon propagator. With ghosts completely neglected one obtains then an infrared enhanced quark-antiquark interaction

$$gD_{\mu\nu}(k) = \mathcal{P}_{\mu\nu}(k) \left(\frac{8\pi\sigma}{k^4} + \frac{gC(k^2)}{k^2} \right) \quad (166)$$

which is renormalization group invariant in the present approximation. It especially allows to identify the string tension σ and relate it to the scale Λ_{MOM} of the subtraction scheme [21].

5.3.2 Including Ghosts

In this subsection it will be demonstrated that the inclusion of ghosts change the solution for the gluon propagator drastically. This can be seen from the simultaneous solution of the coupled subsystem of gluon and ghost DSEs (eqs. (157) and (88)) without quarks, as depicted in figure 11, see refs. [49,240]. These solutions were obtained using the Landau gauge ($\xi = 0$) in which one has $\tilde{Z}_1 = 1$ [16]. Therefore, for the ghost-gluon vertex the choice of its tree-level form in the DSEs might seem justified as a first truncating assumption at least to the extend that the asymptotic behavior of the solutions in the ultraviolet does not imply the necessity of renormalization scale dependence by radiative corrections of the ghost-gluon vertex in this gauge. This is in contrast to the other vertex functions in QCD which have to be dressed at least in such a way as to account for their anomalous dimensions, if the solutions to the DSEs in terms of propagators are expected to resemble their leading perturbative behavior at short distances. A good way to achieve this is in general is to construct vertex functions from their respective Slavnov–Taylor identities which of course respect the relations between the anomalous dimensions of vertex functions and propagators, *i.e.*, their respective renormalization scale dependences.

As stated in chapter 3 already, the Slavnov–Taylor identities generally fail, however, to fully constrain the vertex functions. We have seen in the last chapter that, *e.g.*, methods of refinement of such constructions from implications of multiplicative renormalizability have been developed for the fermion-photon vertex in QED. In the present context, one can furthermore make use of the fact that the 3-gluon vertex has a considerably higher symmetry than fermion

vertices. This symmetry, namely its full Bose symmetry, alleviates the problem of unconstraint terms considerably and the results are not expected to be overly sensitive to such terms in the 3-gluon vertex.

At first sight it might seem appealing to retain the tree-level form of the ghost-gluon vertex while taking the presence of the ghost renormalization function $G(k^2)$ into account in solving the Slavnov–Taylor identity (113) for the 3-gluon vertex. This can be shown to lead to a contradiction: The STI for the 3-gluon vertex has no fully Bose symmetric solution with this Ansatz [49]. One possibility to resolve this problem is to add structure to the ghost-gluon scattering kernel. Its minimal modification necessary to admit a symmetric solution to the Slavnov–Taylor identity for the 3-gluon vertex while retaining the tree-level ghost-gluon vertex is (transverse in q_ν),

$$\tilde{G}_{\mu\nu}(q, p) = \delta_{\mu\nu} + \frac{1}{q^2} \frac{G(k^2) - G(q^2)}{G(p^2)} \left(\delta_{\mu\nu} p q - p_\nu q_\mu \right). \quad (167)$$

The requirement that the anomalous dimension of the ghost-gluon scattering kernel is zero fixes its dependence on the renormalization functions of ghosts and gluons to a dependence on ratios $G(k^2)/G(p^2)$ and $Z(k^2)/Z(p^2)$ with varying arguments. Interestingly, one further simplifying Ansatz, namely that this dependence be at most linear in such ratios, suffices to fully determine the kernel to be of the form (167), see App. B in [49].

This procedure is certainly not unambiguous, more complex structure to the above scattering kernel cannot be excluded. It furthermore seems inconsistent to neglect explicit one-particle irreducible four-gluon interactions while resorting to some non-trivial but quite *ad hoc* assumption on the ghost-gluon scattering kernel which also represents a sort of one-particle irreducible four-point interactions.

Therefore a truncation based on using the tree-level form for the ghost-gluon vertex function, $G_\mu(q, p) = iq_\mu$, while compatible with the desired short distance behavior of the solutions, at the same time implies that some non-trivial assumptions on the otherwise unknown ghost-gluon scattering kernel have to be made in order to solve the Slavnov–Taylor identity for the 3-gluon vertex.

In light of this, a closer look at the ghost-gluon vertex function seems necessary. A suitable source of information is provided by the identity (107) involving the ghost-gluon vertex directly. Note that the derivation presented in sec. 3.3 proceeds not only via the usual BRS invariance but also requires neglecting irreducible ghost-ghost scattering. This identity has the advantage that it allows to express the ghost-gluon vertex in terms of the ghost renormalization function $G(k^2)$. The vertex constructed this way has the correct short distance behavior and therefore no anomalous dimension. It is compatible with the perturbative one-loop result, but some incompatibilities arise at two-loop level [238]. Furthermore, the result suffices to constrain $\tilde{G}_{\mu\nu}(q, p)$ just enough to admit a simple solution to the 3-gluon Slavnov–Taylor identity (113) without any further assumptions [49].

In ref. [49] the ghost-gluon vertex $G_\mu(q, p)$ has been constructed explicitly using the approximation described above. The corresponding form of G_μ follows from $\tilde{G}_{\mu\nu}(q, p)$ as given

by,

$$\tilde{G}_{\mu\nu}(q, p) = \frac{G(k^2)}{G(q^2)} \delta_{\mu\nu} + \left(\frac{G(k^2)}{G(p^2)} - 1 \right) \frac{p_\mu q_\nu}{q^2}, \quad \text{and} \quad G_\mu(q, p) = i q_\nu G_{\mu\nu}(q, p). \quad (168)$$

Additional contributions to $\tilde{G}_{\mu\nu}(q, p)$ which are purely transverse in q_ν can arise from the ghost-gluon scattering kernel. Such terms cannot be constraint from the form of the ghost-gluon vertex. In contrast to the truncation scheme based on the tree-level ghost-gluon vertex as mentioned above, where precisely such terms are necessary to solve the 3-gluon Slavnov–Taylor identity, unknown contributions from the ghost-gluon scattering kernel can be neglected also for the 3-gluon STI (113). Thus, using (168) in (113) one obtains,

$$ik_\rho \Gamma_{\mu\nu\rho}(p, q, k) = G(k^2) \left(\mathcal{P}_{\mu\nu}(q) \frac{q^2 G(p^2)}{G(q^2) Z(q^2)} - \mathcal{P}_{\mu\nu}(p) \frac{p^2 G(q^2)}{G(p^2) Z(p^2)} \right). \quad (169)$$

Using the symmetry of the vertex the solution to (169) fixes the vertex up to completely transverse parts. It can be derived straightforwardly along the lines of the general procedure outlined in [171,172]. This leads to the following solution to (169):

$$\begin{aligned} \Gamma_{\mu\nu\rho}(p, q, k) = & -A(p^2, q^2; k^2) \delta_{\mu\nu} i(p - q)_\rho - B(p^2, q^2; k^2) \delta_{\mu\nu} i(p + q)_\rho \\ & - 2 \frac{C(p^2, q^2; k^2)}{p^2 - q^2} (\delta_{\mu\nu} p q - p_\nu q_\mu) i(p - q)_\rho + \text{cyclic permutations}, \end{aligned} \quad (170)$$

with $A = A_+$, $B = C = A_-$, and

$$A_\pm(p^2, q^2; k^2) = G(k^2) \frac{1}{2} \left(\frac{G(q^2)}{G(p^2) Z(p^2)} \pm \frac{G(p^2)}{G(q^2) Z(q^2)} \right). \quad (171)$$

For comparison, the solution which results from using the non-trivial ghost-gluon scattering kernel (167) together with the tree-level ghost-gluon vertex reads, $A = A_+$, $C = A_-$, with

$$A_\pm(p^2, q^2; k^2) = G(k^2) \frac{1}{2} \left(\frac{1}{Z(p^2)} \pm \frac{1}{Z(q^2)} \right), \quad B(p^2, q^2; k^2) = \frac{1}{2} \left(\frac{G(q^2)}{Z(p^2)} - \frac{G(p^2)}{Z(q^2)} \right) \quad (172)$$

These two solutions differ by ratios of ghost renormalization functions. It has to be emphasized though that the tree-level ghost-gluon vertex corresponding to the latter solution (172) only solves the ghost-gluon Slavnov–Taylor identity (107) if at the same time a tree-level ghost propagator is assumed. It is thus inconsistent to insist on the tree-level ghost-gluon vertex (even by modifying the ghost-gluon scattering kernel instead to solve the 3-gluon STI) as this implies a trivial ghost propagator ($G(k^2) = 1$). In fact, if ghost contributions in Landau gauge are neglected completely, *e.g.*, in the Mandelstam approximation, in which case this is consistent at the level of Slavnov–Taylor identities, the solution for the 3-gluon vertex is obtained from the above solutions by replacing all $G \rightarrow 1$. If ghost contributions are to be

taken into account, however, then also the ghost-gluon vertex has to be dressed. Or else, Slavnov–Taylor identities are manifestly violated.

As for undetermined transverse terms in the vertex functions of the ghost-gluon system, first note that the STI for the ghost-gluon vertex leaves the following transverse contribution undetermined:

$$\begin{aligned} G_\mu(q, p) &= iq_\nu \mathcal{M}_{\mu\nu}(q, p) = \left\{ iq_\mu(p^2 - pq) + ip_\mu(q^2 - pq) \right\} 2f(k^2; p^2, q^2) \\ &= i(p+q)_\mu k^2 f(k^2; p^2, q^2) - i(p-q)_\mu (p^2 - q^2) f(k^2; p^2, q^2), \end{aligned} \quad (173)$$

for some function f (symmetric in its last two arguments). The different factors in this transverse contribution are chosen such that it escapes the construction based on symmetry arguments.⁴² In the present truncation scheme such a contribution is dismissed as corresponding to a non-trivial contribution to the neglected ghost-gluon scattering kernel of the form

$$\mathcal{M}_{\mu\nu}(q, p) = \left\{ \delta_{\mu\nu} (p^2 - q^2) - (p+q)_\mu (p-q)_\nu \right\} 2f(k^2; p^2, q^2). \quad (174)$$

Furthermore, there are 4 purely transverse terms in the 3-gluon vertex involving two more functions in the parameterization of [171] adopted here,

$$\begin{aligned} \Gamma_{\mu\nu\rho}^{\text{tr}}(p, q, k) &= -i H(p^2, q^2, k^2) (p_\rho q_\mu k_\nu - p_\nu q_\rho k_\mu) + \\ &\quad \left(i(F(p^2, q^2; k^2)(\delta_{\mu\nu}pq - p_\nu q_\mu) + H(p^2, q^2, k^2)\delta_{\mu\nu}) (p_\rho qk - q_\rho pk) + \text{cycl. perm.} \right). \end{aligned} \quad (175)$$

H is fully symmetric in all its arguments, and F is symmetric in the first two. These 4 additional independent terms are the only undetermined terms out of a total of 14 in the Lorentz structure of the 3-gluon vertex (the others being fixed by the form (170) of the solution). In contrast to fermion vertices in QED and QCD, in which the 8 transverse terms out of 12 independent Lorentz tensor terms in an analogous parameterization [171] are known to be important [241], the Slavnov-Taylor identity for the 3-gluon vertex when combined with its full Bose (exchange) symmetry puts much tighter constraints on the 3-gluon vertex than the Ward–Takahashi/Slavnov–Taylor identities do on the fermion-photon/gluon vertices. Furthermore, the infrared limit of the 3-gluon STI (169), *i.e.*, the limit $k \rightarrow 0$ for any of the three gluon momenta, puts additional constraints on all Lorentz tensors. These constraints are saturated by the solution in the form (170). As a result, the transverse terms (175) have to vanish in this limit.

Another important difference between fermion vertices and the 3-gluon vertex function is that transverse terms in the vertices of (electrons) quarks are of particular importance due to their coupling to transverse (photons) gluons in the Landau gauge. In contrast, for the 3-gluon vertex function to be used in truncated gluon DSEs, it is well-known that the relevant (unambiguous) contribution to the 3-gluon loop is longitudinal in the external gluon momentum [193]. This

⁴²The possibility of such a term was not noticed in [49], where it was incorrectly asserted that, due to its symmetry, there would be no such undetermined transverse terms in the ghost-gluon vertex.

implies that even though the two gluons within the loop are transverse in Landau gauge, the third (external) leg of the 3-gluon vertex *must not* be connected to a transverse projector.⁴³ The unconstraint terms of the 3-gluon vertex (175) are, however, transverse with respect to *all three* gluon momenta.

The DSEs (157) and (88) with the vertex functions given by (168) and (170/171) build a closed system of equations for the renormalization functions $G(k^2)$ and $Z(k^2)$ of ghosts and gluons. Thereby explicit 4-gluon vertices (in the gluon DSE (C.5)), irreducible 4-ghost correlations (in the identity for the ghost-gluon vertex (107)) and contributions from the ghost-gluon scattering kernel (to the Slavnov–Taylor identity (113) as well as to transverse parts of the ghost-gluon vertex) have been neglected. This is the basic idea of the truncation scheme at the propagator level of the pure gauge theory without quark. Its solution in an one-dimensional approximation [49,240] will be presented below.

To extend this scheme and include the quark Dyson–Schwinger equation, the quark-gluon vertex $\Gamma_\mu^a(p, q)$ has to be specified in addition. Its the Slavnov–Taylor identity reads [168],

$$G^{-1}(k^2) ik_\mu \Gamma_\mu^a(p, q) = (gt^a - B^a(k, q)) iS^{-1}(p) - iS^{-1}(q) (gt^a - B^a(k, q)), \quad k = p - q. \quad (176)$$

Here, t^a is the $SU(3)$ generator in the fundamental representation, and $B^a(k, q)$ is the ghost-quark scattering kernel which again represents irreducible 4-point correlations. In the present truncation scheme in which such 4-point correlations are consistently neglected, the solution to this Slavnov–Taylor identity is obtained from a particularly simple extension to the construction of Ball and Chiu for the solution to the analogous Ward–Takahashi identity of Abelian gauge theory [171]. For $B^a(k, q) = 0$ the Slavnov–Taylor identity for the quark-gluon vertex (176) is solved by

$$\begin{aligned} \Gamma_\mu^a(p, q) = -gt^a G(k^2) & \left\{ \frac{1}{2} (A(p^2) + A(q^2)) i\gamma_\mu + \frac{p_\mu + q_\mu}{p^2 - q^2} \left((A(p^2) \right. \right. \\ & \left. \left. - A(q^2)) \frac{i\cancel{p} + i\cancel{q}}{2} - (B(p^2) - B(q^2)) \right) \right\} + \text{transverse terms}. \end{aligned} \quad (177)$$

This is furthermore justified for a study with emphasis on the infrared behavior of the propagators even beyond the present truncation scheme, because it has been shown that $B^a(k, q) \rightarrow 0$ for $k \rightarrow 0$ in Landau gauge [16]. Note that the only difference to the Abelian case considered in [171] at this point is the presence of the ghost renormalization function appearing in the quark-gluon vertex in Landau gauge. This being a minor modification to the structure of the vertex, the ghost renormalization function in (177) is, however, crucial for the vertex to resemble its correct anomalous dimension in the perturbative limit. Furthermore, the presently available solutions demonstrate that the ghost renormalization function $G(k^2)$, being infrared

⁴³ It has to be contracted with $R_{\mu\nu}$ which projects onto terms longitudinal in the external momentum, see sec. 4.2. This also removes the tadpole term as mentioned above.

enhanced as we will see below, can give an essential contribution to the effective interaction of quarks as part of the quark-gluon vertex also in the infrared.

At this point, additional unconstrained transverse terms in the vertex can be significant. As discussed in the last chapter the transverse part of the fermion-photon vertex in QED is crucial for multiplicative renormalizability [241,213]. Similar constructions to fix transverse pieces of the vertices in QCD is still lacking. It is observed however, that an analogous transverse term in the quark-gluon vertex is necessary in order to recover the correct ultraviolet behavior in the solution to the quark DSE in Landau gauge. First, in perturbation theory at 1-loop level the quark field renormalization constant $Z_2 = 1$ in Landau gauge. This means that there should be no ultraviolet divergence at this level in the loop integral of the quark DSE either. Obviously, this leading perturbative feature will be manifest in the rainbow approximation, *i.e.*, the relativistic Hartree–Fock approximation for quarks, which is obtained from replacing the quark-gluon vertex by its tree-level form $\Gamma_\mu(q, p) = \gamma_\mu$. At the level of renormalization group improvements at one-loop perturbation theory, however, this is already inconsistent because of the non-vanishing anomalous dimension of the vertex. One has $Z_{1F} = \tilde{Z}_3^{-1}$ in Landau gauge which implies that the renormalization scale dependence of the quark-gluon vertex is governed essentially by the one of the ghost renormalization function. This is explicitly verified by the solution to its Slavnov–Taylor identity (177). It can, on the other hand, be explicitly verified that the longitudinal pieces given in eq. (177) change the divergence structure of the equation, in particular, leading to a necessarily non-trivial $Z_2 \neq 1$. Secondly, a careful discussion of the leading perturbative behavior of the quark mass function reveals that with the Ball–Chiu form for the vertex (177) alone the leading perturbative behavior of the running current quark mass cannot be reproduced either.

In the solution of the coupled gluon, ghost and quark DSE (or already in the quenched solution to the quark DSE) presented in sec. 5.3.5 below the following transverse extension to the vertex (177), which is analogous to the Curtis–Pennington vertex (139) [213], will be seen to cure these problems,

$$\Gamma_\mu^{\text{tr}}(p, q) = G(k^2) \frac{1}{2} \left(A(p^2) - A(q^2) \right) \frac{(\gamma_\mu(p^2 - q^2) - (p + q)_\mu(p - q))(p^2 + q^2)}{(M^2(p^2) + M^2(q^2))^2 + (p^2 - q^2)^2} \quad (178)$$

Here, $M(p^2) := B(p^2)/A(p^2)$. With this form there will be a) no quark field renormalization necessary, *i.e.*, $Z_2 = 1$ in Landau gauge; b) the leading contribution to the current mass in the ultraviolet will resemble perturbation theory; and c) the correct scale dependence of the renormalization group improvement will be incorporated by the same explicit overall factor $G(k^2)$, the ghost renormalization function, as present in the longitudinal pieces (177). To justify these observations on a more sound basis for the quark vertex of Landau gauge QCD in analogy to the available QED studies will be another important goal for future studies.

With the form (177) for the vertex function in the quark DSE, improved by the additional transverse terms of (178), the present truncation scheme is extended to a closed set of equations for all propagators of Landau gauge QCD as parameterized by the four functions $Z(k^2), G(k^2), A(k^2)$ and $B(k^2)$. Its simultaneous solution represents for the first time a systematic and complete solution to the DSEs of QCD at the level of propagators [242].

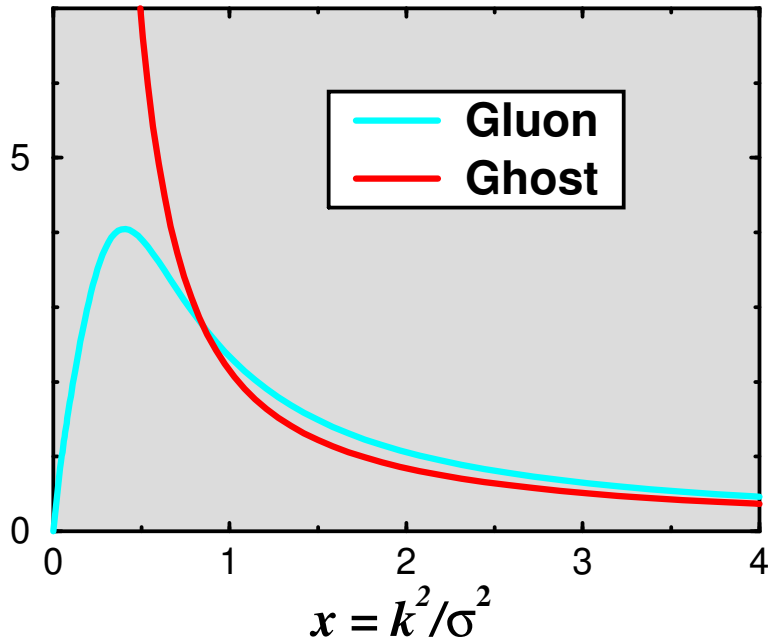


Fig. 12. The renormalization functions $Z(x)$ and $G(x)$.

However, before turning to the very recent results including quarks it is illustrative to discuss the solution of the coupled gluon-ghost system. The non-linear integral equations for the renormalization functions Z and G of gluons and ghosts have been solved employing angle approximations [49,240], see fig. 12. Such an approximation is as yet necessary in order to allow for an analytic infrared expansion of the solutions. This technique of asymptotic infrared expansions which was originally developed for and applied to the Mandelstam approximation [19,21] and subsequently extended to the coupled system of gluon and ghost DSEs [49,240] proved to be a necessary prerequisite to finding numerically stable solutions. An analogous expansion will most likely have to be developed also for the four-dimensional equations before the one-dimensional approximation can be abandoned. Some preliminary progress towards solutions not relying on one-dimensional approximations was obtained in a truncation scheme for gluons and ghosts with bare vertices and considering in the gluon DSE the ghost loop only in ref. [243]. The modified angle approximation approximation used in refs. [49,240] to arrive at the one-dimensional system of equations is designed to preserve the leading order of the integrands in the infrared limit of integration momenta. At the same time, it accounts for the correct short distance behavior of the solutions, *i.e.*, the behavior at large integration momenta. Nevertheless, due to induced singularities some terms have to be dismissed, see refs. [49,244] for a discussion. The relative importance of such a term was assessed in [49] where the integral has been calculated without using an angle approximation from the self-consistent solutions for $Z(k^2)$ and $G(k^2)$ as obtained without this term. For all momenta the resulting contribution was found to be negligible as compared to the other terms retained in the solution to gluon DSE. Though even small terms can, in principle, have a considerable effect on the non-linear self-consistency problem, this supports the additional approximation to dismiss such terms. Of course, progress on this issue is highly desirable.

The leading infrared behavior of the gluon and ghost renormalization function can be extracted

analytically. To this end one employs an Ansatz for these functions of the form,

$$Z(k^2) \sim (k^2)^\alpha \quad \text{and} \quad G(k^2) \sim (k^2)^\beta. \quad (179)$$

A complete analysis in Landau gauge based on this ansatz and keeping the vertex functions as general as possible can be found in ref. [238]. The important point which makes such an analysis feasible is the non-renormalization of the ghost-gluon vertex, $\tilde{Z}_1 = 1$. Then three possible solutions are found: $\beta = 0$, $\beta = -1$ and $2\beta = -\alpha$ with $\beta > -1$. The first two solutions require, in addition, that the ultraviolet part of the integrals involved contributes to the infrared power thereby spoiling the renormalization group behavior of, *e.g.*, the running coupling, see the next section. The third solution $2\beta = -\alpha > 2$ is, however, quite general.

As a matter of fact, such a solution has been obtained from the coupled gluon system [48] before the analysis in ref. [238] had been started. Defining $x := k^2/\sigma \rightarrow 0$ (for some scale σ) and using $Z(x)G(x) \sim x^\kappa$ in the gluon DSE immediately yields

$$G(x) \sim x^{-\kappa} \quad \text{and} \quad Z(x) \sim x^{2\kappa} \quad \text{as} \quad x \rightarrow 0. \quad (180)$$

Furthermore, in order for a positive definite function $G(x)$ to result for positive x and assuming a positive definite $Z(x)$, as $x \rightarrow 0$, one obtains the necessary condition $1/\kappa - 1/2 > 0$ which is equivalent to

$$0 < \kappa < 2. \quad (181)$$

The special case $\kappa = 0$ leads to a logarithmic singularity in the gluon DSE for $x \rightarrow 0$. In particular, assuming that $ZG = c$ with some constant $c > 0$ and $x < x_0$ for a sufficiently small x_0 , one obtains $G^{-1}(x) \rightarrow c(3N_c g^2 / 64\pi^2) \ln(x/x_0) + \text{const}$ and thus $G(x) \rightarrow 0^-$ for $x \rightarrow 0$, showing that no positive definite solution can be found in this case either.

From the gluon DSE one obtains

$$G(x) \rightarrow \left(g^2 \gamma_0^G \left(\frac{1}{\kappa} - \frac{1}{2} \right) \right)^{-1} c^{-1} x^{-\kappa}, \quad \gamma_0^G = \frac{1}{16\pi^2} \frac{3N_c}{4}, \quad (182)$$

$$Z(x) \rightarrow \left(g^2 \gamma_0^G \left(\frac{1}{\kappa} - \frac{1}{2} \right) \right) c^2 x^{2\kappa}, \quad 0 < \kappa < 2, \quad (183)$$

where γ_0^G is the leading order perturbative coefficient of the anomalous dimension of the ghost field. Accordingly, the ghost-loop gives infrared singular contributions $\sim x^{-2\kappa}$ to the gluon equation while the 3-gluon loop yields terms proportional to x^κ as $x \rightarrow 0$, which are thus subleading contributions to the gluon equation in the infrared. With eq. (182) the leading asymptotic behavior of the ghost equation for $x \rightarrow 0$ provides

$$Z(x) \rightarrow g^2 \gamma_0^G \frac{9}{4} \left(\frac{1}{\kappa} - \frac{1}{2} \right)^2 \left(\frac{3}{2} \frac{1}{2-\kappa} - \frac{1}{3} + \frac{1}{4\kappa} \right)^{-1} c^2 x^{2\kappa} \quad (184)$$

and mutual consistency between the gluon and ghost equation requires

$$\left(\frac{3}{2}\frac{1}{2-\kappa} - \frac{1}{3} + \frac{1}{4\kappa}\right) \stackrel{!}{=} \frac{9}{4}\left(\frac{1}{\kappa} - \frac{1}{2}\right) \Rightarrow \kappa = \frac{61 - \sqrt{1897}}{19} \stackrel{(+)}{\simeq} 0.92. \quad (185)$$

Note that one of the roots is excluded by the range allowed to κ .

This leading behavior of the gluon and ghost renormalization functions and thus their propagators is entirely due to ghost contributions. The details of the treatment of the 3-gluon loop have no influence on above considerations. This is in remarkable contrast to the Mandelstam approximation, in which the 3-gluon loop alone determines the infrared behavior of the gluon propagator and the running coupling in Landau gauge [18–21,239]. As a result of this, the running coupling as obtained from the Mandelstam approximation is singular in the infrared [21,239]. As will be shown in the next section, the infrared behavior derived from the present truncation scheme implies an infrared stable fixed point. This is certainly a counter example to the frequently quoted assertion that the presence of ghosts in Landau gauge may have negligible influence on physical observables at hadronic energy scales.

The qualitative infrared behavior of ghosts and gluons reported in refs. [48,49] and the conclusions on the dominance of the ghost contributions in Landau gauge as described above were also confirmed in ref. [244] where the same qualitative behavior was obtained neglecting the 3-gluon loop completely. A tree-level ghost-gluon vertex together with a naive angle approximation in this case led to a numerical value of $\kappa \simeq 0.77$ for the same exponent determining the infrared behavior of gluons and ghosts [244]. In the same approximation but with no angle approximation employed a solution for $\kappa = 1^-$ is reported in ref. [244]. ($\kappa = 1^-$ has to be interpreted as $\kappa = 1 - \epsilon$, $\epsilon \rightarrow 0^+$. Thus, this result already provides a regularization for the infrared singular ghost renormalization function.) Such forms (for $\kappa = 1$) have been discussed in the literature before, independently in the two completely different approaches of refs. [245,92] and refs. [141,142] respectively. However, the evidence for the $\kappa = 1$ solutions has since disappeared in both these approaches again [93,148]. For the DSE study of ref. [243], it cannot be excluded that the $\kappa = 1$ behavior obtained there might be an artifact of the *ghost-loop only approximation* and/or the use of a tree-level vertex.

For the infrared behavior of gluon and ghost propagators as described above, a comment on its implications for the vertex functions is in order. Starting with the ghost-gluon vertex one realizes that the limit of vanishing ghost momenta is regular:

$$G_\mu(q, p) \rightarrow -ik_\mu \quad \text{for } p \rightarrow 0 \quad (186)$$

$$G_\mu(q, p) \rightarrow 0 \quad \text{for } q \rightarrow 0, \quad (187)$$

where it was used that $G(k^2) \sim (k^2)^{-\kappa}$ for $k^2 \rightarrow 0$. On the other hand, for vanishing gluon momentum $k \rightarrow 0$ the vertex diverges as

$$G_\mu(q, p) \rightarrow 2ip_\mu \frac{G(k^2)}{G(p^2)} \sim \frac{2ip_\mu}{G(p^2)} \frac{1}{(k^2)^\kappa} \quad \text{for } k \rightarrow 0. \quad (188)$$

Since the exponent κ is a (positive) irrational number, see eq. (185), the corresponding divergence cannot be easily interpreted. This divergence is in fact weaker than a massless particle pole ($\kappa < 1$) and presumably lacking a physical interpretation.

Similarly, the 3-gluon vertex as given in eqs. (170), (171) shows analogous infrared divergences resulting from the infrared enhanced ghost renormalization function,

$$\begin{aligned} \Gamma_{\mu\nu\rho}(p, q, k) \rightarrow & G(k^2) \left\{ \left(ip_\mu \delta_{\nu\rho} + ip_\nu \delta_{\mu\rho} - 2ip_\rho \delta_{\mu\nu} \right) \frac{1}{Z(p^2)} \right. \\ & \left. + 2ip_\rho p^2 \mathcal{P}_{\mu\nu}(p) \left(\frac{2G'(p^2)}{G(p^2)Z(p^2)} + \frac{Z'(p^2)}{Z^2(p^2)} \right) \right\} \quad \text{for } k \rightarrow 0. \end{aligned} \quad (189)$$

Note that such a limit usually implies some mild regularity restrictions on the functions A , B and C of eq. (170). In particular, the form of (189) above is obtained from eqs. (170), (171) provided that in addition,

$$q^2 C(p^2, q^2; k^2) \rightarrow 0, \quad \text{for } q^2 \rightarrow 0. \quad (190)$$

This result, eq. (189), then agrees with the differential Slavnov–Taylor identity as obtained directly from eq. (169) in the limit $k \rightarrow 0$. In the previous studies of the gluon DSE in the Mandelstam approximation [18–21], the analogous requirement for the 3-gluon vertex function to obey the differential Slavnov–Taylor identity led to the so-called masslessness condition, eq. (149), $p^2/Z(p^2) \rightarrow 0$ for $p^2 \rightarrow 0$. In absence of ghost contributions, the gluon DSE had to be supplemented by this as an additional constraint. This original condition is violated by the infrared behavior of the gluon propagator found in [48], *i.e.*, $Z(x) \rightarrow x^{2\kappa}$. The correct replacement of this condition for the present case results from eq. (190). With $C = A_-$ from eq. (171) one thus obtains,

$$p^2 G(p^2) \rightarrow 0 \quad \text{and} \quad \frac{p^2}{G(p^2)Z(p^2)} \rightarrow 0 \quad \text{for } p^2 \rightarrow 0. \quad (191)$$

These two necessary conditions are obeyed by the infrared behavior presented above without further adjustments, *i.e.*, $G(x) \sim 1/(G(x)Z(x)) \sim x^{-\kappa}$ for $x \rightarrow 0$ (with $\kappa \simeq 0.92$). One realizes, however, that the original bounds on κ obtained from the consistency of the ghost DSE, when combined with conditions (191), have to be restricted further to $0 < \kappa < 1$. The possibility that the masslessness condition in its original form might not hold for non-Abelian gauge theories has been pointed out in the literature before [118,246]. The present results support this conjecture.

Finally, since quarks cannot screen the divergence in the ghost renormalization function, see below, its presence in the quark-gluon vertex function, see eq. (177), has a similar effect there, too. It will be demonstrated on the example of the running coupling in the next section, how these apparently unphysical divergences in the elementary correlation functions of gluons, ghosts and quarks can, in principle, nevertheless cancel in physical quantities. The lack of a physical interpretation of these divergences (other than maybe reflecting confinement) should,

however, not be too surprising for a Euclidean field theory violating reflection positivity. Note also that in all skeletons of the kernels in relativistic bound state equations for hadrons, the combination of dressed quark-gluon vertices with the non-perturbative gluon propagator will give contributions of the form

$$\sim g^2 G^2(k^2) D_{\mu\nu}(k) \Gamma_\nu^{\text{CP}}(p, p - k) \otimes \Gamma_\mu^{\text{CP}}(q - k, q) , \quad (192)$$

where Γ_μ^{CP} is the vertex function given in eq. (139) for QED, here corresponding the sum of the terms in eqs. (177) and (178) without ghost renormalization function, coupling and color factors. The resulting combination of the ghost and gluon renormalization functions, $g^2 G^2(k^2) Z(k)$, to this skeleton of the quark interaction kernel is free of unphysical infrared divergences for $k \rightarrow 0$. It is furthermore independent of the renormalization scale in Landau gauge and suited to define a non-perturbative running coupling as will be discussed in the next section.

Generally, on external gluon lines the divergent contributions to scattering amplitudes induced by the ghost renormalization function in the vertex functions will be over-compensated by the attached gluon propagators. These divergences thus do not give rise to massless asymptotic gluon states. In internal gluon lines from one-particle reducible contributions, the divergence of the two vertex functions is exactly compensated by the gluon propagator leaving one single “massless” pole, since with some dimensionless constant $a > 0$, $g^2 G^2(k^2) D(k) \rightarrow a/k^2$ for $k^2 \rightarrow 0$. If this behavior corresponding to a finite infrared fixed point should persist such a massless pole contribution to quark and gluon scattering amplitudes in the Mandelstam variables could nevertheless be compensated by an analogous pole from 1-PI contributions in a way analogous to the mechanism described in sec. 2.5 in the context of the non-perturbative approximation scheme of ref. [142]. For this scheme it was demonstrated quite generally in refs. [148,149] how these unphysical but necessarily arising *shadow-poles* in Mandelstam variables that appear in 1-PI correlations as well as in one-particle reducible contributions mutually cancel in scattering amplitudes (introducing the notion of *extended irreducibility*).

The present situation is different, however, as far as the ghost fields are concerned. The infrared enhanced ghost propagator will result in an infrared divergence of external ghost legs which is too strong for a particle interpretation. Note that a particle interpretation for ghost degrees of freedom is, of course, anyhow precluded as they lead to negative norm states. Furthermore, the infrared enhanced ghost propagator results in non-decoupling of ghost clusters at large separations. For example, already in the disconnected contributions to 4-point ghost correlations, for no pair of (space-time) arguments with comparatively small separation will the 2-point correlations connecting this pair decouple from those connected to the other largely (spacelike) separated pair. At that point it is interesting to note that lattice calculations provide evidence that in Coulomb gauge not only the ghost propagator but also the time-time component of the gluon propagator is infrared enhanced [247]. (The space-space components of the gluon propagator are infrared suppressed.) Therefore, it is quite plausible that in Coulomb gauge this non-decoupling of clusters also applies to the Coulomb gluons (being also negative norm states).

Another example for the implications of the infrared divergences induced by the ghosts which requires a more careful analysis is provided by ghost-box contributions to 4-point gluon corre-

lations. In particular, in color singlet channels it is expected that no long range correlations in contradiction with cluster separation occur in these correlations. This will have to be studied in more detail. There is no obvious conflict at least, as the Mandelstam variables in such a case do not coincide with the momenta of the infrared enhanced ghost 2-point correlations. Further damping of these enhanced 2-point correlations in such contributions is provided by the ghost-gluon vertices which yield vanishing transverse contributions for vanishing ghost leg momenta, as is seen from (187) above. However, this example demonstrates that, with loosing the cluster decomposition in general, the important question arises how to recover it for color singlet clusters.

5.3.3 Subtraction Scheme and Running Coupling

Before the non-perturbative running coupling can be discussed, some introductory remarks on the choice of the non-perturbative subtraction scheme and its relation to the definition of the running coupling are necessary. In particular, it will become clear that the preliminary infrared discussion of last section already yields an important first result: it implies the existence of an infrared fixed point.

The starting point is the following identity for the renormalization constants

$$\tilde{Z}_1 = Z_g Z_3^{1/2} \tilde{Z}_3 = 1, \quad (193)$$

which holds in the Landau gauge [16]. It follows that the product $g^2 Z(k^2) G^2(k^2)$ is renormalization group invariant. In absence of any dimensionful parameter this (dimensionless) product is therefore a function of the running coupling \bar{g} ,

$$g^2 Z(k^2) G^2(k^2) = f(\bar{g}^2(t_k, g)), \quad t_k = \frac{1}{2} \ln k^2 / \mu^2. \quad (194)$$

Here, the running coupling $\bar{g}(t, g)$ is the solution of $d/dt \bar{g}(t, g) = \beta(\bar{g})$ with $\bar{g}(0, g) = g$ and the Callan–Symanzik β -function $\beta(g) = -\beta_0 g^3 + \mathcal{O}(g^5)$. The perturbative momentum subtraction scheme is asymptotically defined by $f(x) \rightarrow x$ for $x \rightarrow 0$. This is realized by independently setting

$$Z(\mu^2) = 1 \quad \text{and} \quad G(\mu^2) = 1 \quad (195)$$

for some asymptotically large subtraction point $k^2 = \mu^2$. If the renormalization group invariant product $g^2 Z(k^2) G^2(k^2)$ is to have a physical meaning, *e.g.*, in terms of a potential between static color sources, it should be independent under changes $(g, \mu) \rightarrow (g', \mu')$ according to the renormalization group for arbitrary scales μ' . Therefore,

$$g^2 Z(\mu'^2) G^2(\mu'^2) \stackrel{!}{=} g'^2 = \bar{g}^2(\ln(\mu'/\mu), g), \quad (196)$$

and, $f(x) \equiv x, \forall x$. This can thus be adopted as a physically sensible definition of a non-perturbative running coupling in the Landau gauge.

Note that this definition is an extension to the one used in the Mandelstam approximation, eq. (165). In ref. [21] the identity $Z_g Z_3 = 1$ has been obtained for this approximation (without ghosts) implying that $gZ(k^2)$ would be the renormalization group invariant product in this case. Its according identification with the running coupling $gZ(k^2) = \bar{g}(t_k, g)$ is equivalent to the non-perturbative renormalization condition $Z(\mu^2) = 1(\forall \mu)$ which turns out to be possible in the Mandelstam approximation (in which there is no ghost renormalization function).

In the present case, it is not possible to realize $f(x) \equiv x$ by simply extending the perturbative subtraction scheme (195) to arbitrary values of the scale μ , as this would imply a relation between the functions Z and G which is inconsistent with the leading infrared behavior of the solutions discussed in the last section. For two independent functions the condition (195) is in general too restrictive to be used for arbitrary subtraction points. Rather, in extending the perturbative subtraction scheme, one is allowed to introduce functions of the coupling such that

$$Z(\mu^2) = f_A(g) \quad \text{and} \quad G(\mu^2) = f_G(g) \quad \text{with} \quad f_G^2 f_A = 1 , \quad (197)$$

and the limits $f_{A,G} \rightarrow 1$, $g \rightarrow 0$. Using this it is straightforward to see that for $k^2 \neq \mu^2$ one has $(t_k = (\ln k^2/\mu^2)/2)$,

$$\begin{aligned} Z(k^2) &= \exp \left\{ -2 \int_g^{\bar{g}(t_k, g)} dl \frac{\gamma_A(l)}{\beta(l)} \right\} f_A(\bar{g}(t_k, g)) , \\ G(k^2) &= \exp \left\{ -2 \int_g^{\bar{g}(t_k, g)} dl \frac{\gamma_G(l)}{\beta(l)} \right\} f_G(\bar{g}(t_k, g)) . \end{aligned} \quad (198)$$

Here $\gamma_A(g)$ and $\gamma_G(g)$ are the anomalous dimensions of gluons and ghosts respectively, and $\beta(g)$ is the Callan–Symanzik β -function. eq. (193) corresponds to the following identity for these scaling functions in Landau gauge:

$$2\gamma_G(g) + \gamma_A(g) = -\frac{1}{g} \beta(g) . \quad (199)$$

One thus verifies that the product $g^2 Z G^2$ indeed gives the running coupling (*i.e.*, eq. (194) with $f(x) \equiv x$). Perturbatively, at one-loop level eq. (199) is realized separately, *i.e.*, $\gamma_G(g) = -\delta \beta(g)/g$ and $\gamma_A(g) = -(1 - 2\delta) \beta(g)/g$ with $\delta = 9/44$ for $N_f = 0$ and arbitrary N_c . Non-perturbatively one can still separate these contributions from the anomalous dimensions by introducing an unknown function $\epsilon(g)$,

$$\gamma_G(g) =: -(\delta + \epsilon(g)) \frac{\beta(g)}{g} \Rightarrow \gamma_A(g) = -(1 - 2\delta - 2\epsilon(g)) \frac{\beta(g)}{g} . \quad (200)$$

This allows to rewrite eqs. (198) as follows:

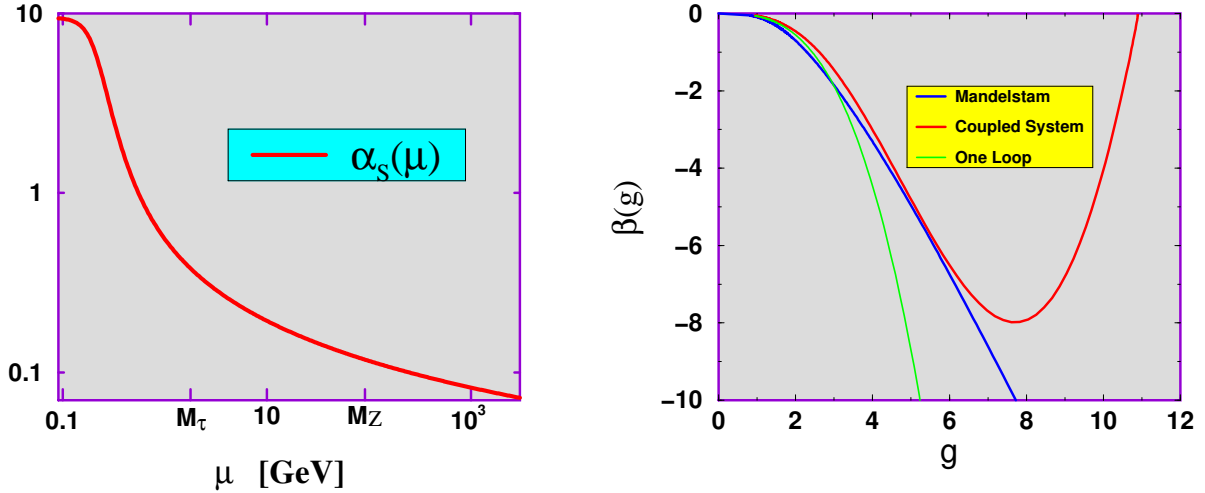


Fig. 13. The running coupling $\alpha_S(\mu)$ for $t = 0$ (left), and the corresponding β -function (right) in comparison with its leading perturbative form (one-loop) and the β -function as a result of the Mandelstam approximation from ref. [21].

$$Z(k^2) = \left(\frac{\bar{g}^2(t_k, g)}{g^2} \right)^{1-2\delta} \exp \left\{ -4 \int_g^{\bar{g}(t_k, g)} dl \frac{\epsilon(l)}{l} \right\} f_A(\bar{g}(t_k, g)) , \quad (201)$$

$$G(k^2) = \left(\frac{\bar{g}^2(t_k, g)}{g^2} \right)^\delta \exp \left\{ 2 \int_g^{\bar{g}(t_k, g)} dl \frac{\epsilon(l)}{l} \right\} f_G(\bar{g}(t_k, g)) .$$

This is generally possible, *i.e.*, also in the presence of quarks. In this case one has $\delta = \gamma_0^G / \beta_0 = 9N_c/(44N_c - 8N_f)$ for N_f flavors in Landau gauge. The above representation of the renormalization functions expresses clearly that regardless of possible contributions from the unknown function $\epsilon(g)$, the resulting exponentials cancel in the product $G^2 Z$. For a parameterization of the renormalization functions, these exponentials can of course be absorbed by a redefinition of the functions $f_{A,G}$. The only effect of such a redefinition is that the originally scale independent functions $f_{A,G}(\bar{g}(t_k, g))$ will acquire a scale dependence by this, if $\epsilon \neq 0$.

For the present truncation scheme it is possible, however, to obtain explicitly scale independent equations thus showing that the solutions for the renormalization functions G and Z obey one-loop scaling at all scales [49]. In particular, this implies that the products $g^{2\delta} G$ and $g^{2(1-2\delta)} Z$ are separately renormalization group invariants that scheme (as they are at one-loop level). As for the renormalization scale dependence, the non-perturbative nature of the result is therefore buried entirely in the result for the running coupling.

The implications of the preliminary results for the infrared behavior of the solutions G and Z as given in the last section can now be discussed without actually solving the gluon and ghost DSEs. From eqs. (182) and (183) for $k^2 \rightarrow 0$ one finds,

$$g^2 Z(k^2) G^2(k^2) = \bar{g}^2(t_k, g) \xrightarrow{t_k \rightarrow -\infty} \left(\gamma_0^G \left(\frac{1}{\kappa} - \frac{1}{2} \right) \right)^{-1} =: g_c^2 . \quad (202)$$

The critical coupling scales with the number of colors as $g_c^2 \sim 1/N_c$ implying that $g_c^2 N_c$ is

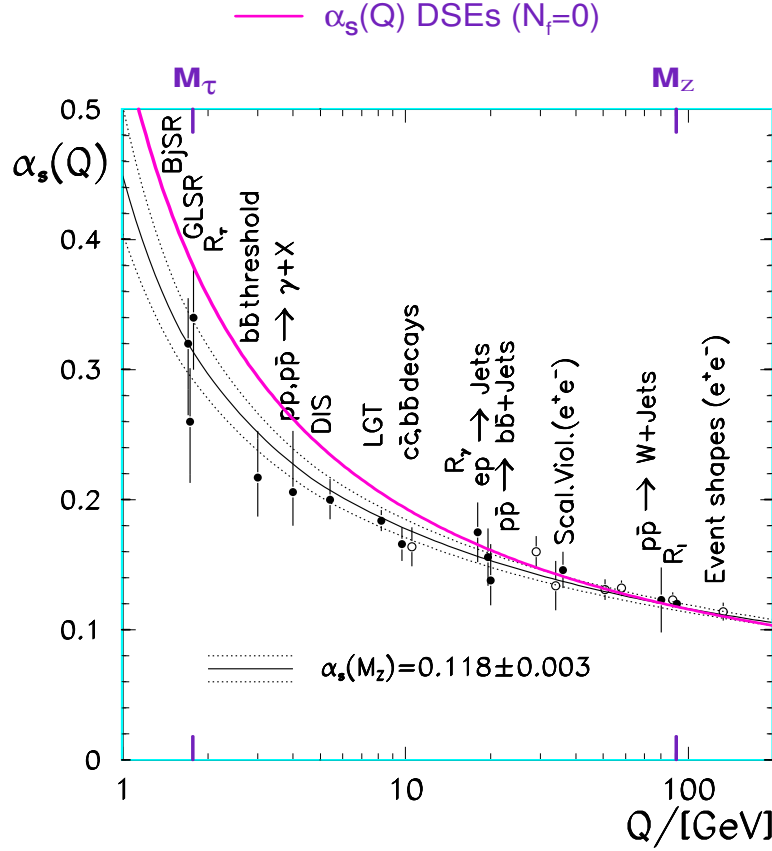


Fig. 14. The running coupling α_s from the Dyson–Schwinger equations of pure QCD compared to the collection of the *world's* experimental data assembled by M. Schmelling in ref. [249]. The open dots result from global event shape variables.

constant in the present approach. This agrees with the general considerations of the large N_c -limit in which $g^2 N_c$ is kept fixed as N_c becomes large [248]. For $N_c = 3$ and with eq. (185) for κ one obtains $g_c^2 \simeq 119.1$ which corresponds to a critical coupling $\alpha_c = g_c^2/(4\pi) \simeq 9.48$. This is a remarkable result in its own, if compared to the running coupling as it was analogously obtained from the Mandelstam approximation [21]. The dynamical inclusion of ghosts changes the infrared singular coupling of the Mandelstam approximation to an infrared finite one implying the existence of an infrared stable fixed point.

The running coupling as calculated from the coupled gluon and ghost DSEs, see fig. 13, involves an arbitrary scale σ related to the infrared behavior of the propagators. Note that this is a non-perturbative realization of dimensional transmutation. The phenomenologically well-known value of the running coupling $\alpha_s(M_Z) = 0.118$ at the mass of the Z -boson, $M_Z = 91.2$ GeV [250] can be used to fix the overall momentum scale σ directly which yields $\sigma \simeq (350\text{MeV})^2$. For completeness, from the rough estimate of the leading logarithmic behavior of the renormalization functions Z and G at high momenta, this corresponds to a perturbative scale Λ_{QCD} in $250 \sim 300$ MeV. This is not a very significant result, however, since the value for Λ_{QCD} depends on the number of quarks N_f , and the order of the perturbative expansion, the scheme etc.. In particular, in the present framework one expects it to change when quarks are included.

Once the momentum scale is fixed, it is of course possible to extract the corresponding value of

the running coupling at other values of the momentum scale. Phenomenologically, the running coupling is remarkably well known from a variety of experiments in the range from around the Z -masses down to the mass M_τ of the τ -Lepton (at about 1.78 GeV). In fig. 14 the recent collection by M. Schmelling of the available measurements is shown. These range from deep-inelastic sum rules (BjSR, GLSR), scaling violations in deep-inelastic scattering (DIS), hadronic τ decays (R_τ), and Υ ($b\bar{b}$) spectroscopy and decays in the energy range $Q \sim 1.6 - 10$ GeV, to measurements of total cross sections, jet rates and global event shapes in e^+e^- , $p\bar{p}$ and ep collisions determining α_S at higher energies typically in $Q \sim 30 - 130$ GeV (see ref. [249] for details). Several of the points in this figure represent hundreds of independent measurements, and the agreement with the next-to-next-to-leading order evolution is a truly remarkable success for perturbative QCD.

The running coupling from the Dyson-Schwinger equations in this same energy range agrees far less with the experimental data, remarkably only that it does much better than it actually should. From the ratio of the Z - to the τ -mass, $M_Z/M_\tau \simeq 51.5$ (and $\alpha_S(M_Z) = 0.118$), one obtains the value $\alpha_S(M_\tau) = 0.38$ which within errors might still be acceptable experimentally [250]. The running coupling of the present DSE solutions compares surprisingly well with the data of fig. 14. For $N_f = 0$ and with using Λ_{QCD} in $250 \sim 300$ MeV, as a result of the estimate from the anomalous dimensions given in the last section, such good agreement with the data is actually not expected for a perturbative QCD coupling at one, two or three loops. Even though the estimate of Λ_{QCD} used here is certainly not reliable, to parameterize the running coupling of the present scheme by the $N_f = 0$ perturbative (two- or three-loop) form would require Λ_{QCD} to rather be in $0.8 - 1.2$ GeV. This mismatch of estimates might demonstrate the limitations of the present calculation better than the compelling agreement with the experimental data (which should thus be taken with a grain of salt).

Maybe more significantly, the running coupling over the full momentum range, including the occurrence of the fixed point for $\mu \rightarrow 0$, is shown in fig. 13 with the momentum range of fig. 14 marked by M_τ and M_Z . The right panel of figure 13 shows the corresponding β -function with its two fixed points in the ultraviolet at $g = 0$ and in the infrared at $g = g_c \simeq 10.9$. For comparison the leading perturbative form for $g \rightarrow 0$ (and $N_f = 0$), $\beta(g) \rightarrow -\beta_0 g^3 = -11/(16\pi^2) g^3$, is added to the figure as well as the infrared singular non-perturbative result obtained from the analogous subtraction scheme in the Mandelstam approximation according to sec. 5.3.1 (see also refs. [21,239]). The solution to the coupled system of gluon and ghost Dyson-Schwinger equations yields better agreement with the leading perturbative form at small g than the Mandelstam approximation, since for the latter, due to neglecting ghosts, the leading coefficient $\beta_0 = 14/(16\pi^2)$ differs from its corresponding perturbative value. While this might still be regarded as small quantitative discrepancy, the significant difference between the present result and the Mandelstam approximation occurs for $g > 6$, once more demonstrating the importance of ghosts in Landau gauge, in particular, in the infrared.

5.3.4 Confined Gluons and Positivity

It has been mentioned in sec. 2.3 already that contradictions to positive (semi)definiteness of the norm of gluonic states (in the ghost free subspace) arise from the superconvergence relations in the asymptotically free, BRS invariant theory for not too many flavors ($N_f < 10$).

While this might still be a reincarnation of Haag's theorem occurring already at the level of perturbative interactions, full non-perturbative results as obtained from DSEs or lattice simulations allow to assess their implications on positivity more directly.

As one is dealing with Euclidean Green's functions, or Schwinger functions, for the elementary correlations (of gluons, ghost and quarks) in QCD, the most fundamental way to investigate a possible particle interpretation for these degrees of freedom is to resort to the Osterwalder–Schrader reconstruction theorem which states that a Gårding–Wightman relativistic quantum field theory can be constructed from a set of Schwinger functions if those Euclidean correlation functions obey certain conditions, the Osterwalder–Schrader axioms [3]. In particular, the axiom of *reflection positivity* for Euclidean Green's functions is thereby the Euclidean counterpart to the positive definiteness of the norm in the Hilbert space of the corresponding Gårding–Wightman quantum field theory. This general Euclidean positivity condition involves arbitrary partial sums of n -point correlation functions. To prove positivity of a theory based on these conditions is a mathematically very hard task which has generally been possible only in very few special cases [38]. Here, the converse is used. One counter example suffices to demonstrate the violation of positivity.

For the special case of a single propagator $D(x - y)$, *i.e.*, for the lowest partial sum, reflection positivity reads,

$$\int d^4x d^4y \bar{f}(-x_0, \mathbf{x}) D(x - y) f(y_0, \mathbf{y}) \geq 0 \quad (203)$$

where $f \in \mathcal{S}_+(\mathbb{R}^4)$ is a complex valued test (Schwartz) function with support in $\{(x_0, \mathbf{x}) : x_0 > 0\}$. This special case of reflection positivity can be shown to be a necessary *and* sufficient condition for the existence of a Källén–Lehmann representation, *i.e.* a spectral representation of the propagator as given in eq. (26) with positive spectral function. Therefore, the construction of a counter example to this condition (by a suitable choice of f) is a possibility to demonstrate that, as one manifestation of confinement, the particular Euclidean correlations can have no interpretation in terms of stable particle states.

Heuristically, after three dimensional Fourier transformation condition (203) can be written,

$$\int_0^\infty dt' dt \bar{f}(t') D(-(t' + t), \mathbf{p}) f(t) \geq 0, \quad (204)$$

where $D(x_0, \mathbf{p}) := \int d^3x D(x_0, \mathbf{x}) e^{i\mathbf{p}\mathbf{x}}$, and a separated momentum dependence of the analogous Fourier transform of the test function f has to provide for a suitable smearing around the three-momentum \mathbf{p} .

In Figure 15 this Fourier transform of (essentially the trace of) the gluon propagator,

$$D(t, \mathbf{p}^2) := \int \frac{dp_0}{2\pi} \frac{Z(p_0^2 + \mathbf{p}^2)}{p_0^2 + \mathbf{p}^2} e^{ip_0 t}, \quad (205)$$

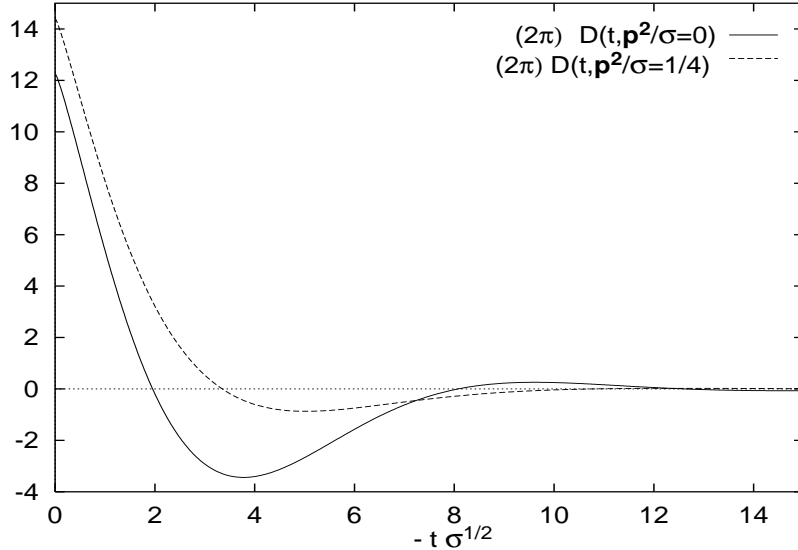


Fig. 15. The one-dimensional Fourier transform of the gluon propagator, $D(t, \mathbf{p}^2)$.

is plotted for $\mathbf{p}^2 = 0$ and $\mathbf{p}^2 = \sigma/4$. The fact that the DSE solution for sufficiently small \mathbf{p} is negative over finite intervals in the Euclidean time in this case shows trivially that reflection positivity is violated for the gluon propagator.

Another way to understand this connection between positivity and the Euclidean correlation functions is based on an argument which was first given by Mandula and Ogilvie [251] and is phrased most clearly in ref. [252]. The domain of analyticity of propagators in a Gårding–Wightman quantum field theory allows to write the spectral representation for the (Euclidean) propagator $D(p)$ in the form,

$$D(p) = \int_0^\infty dm^2 \frac{\rho(m^2)}{p^2 + m^2} , \quad (206)$$

which gives rise to the Fourier transform,

$$D(t, \mathbf{p}^2) = \int_0^\infty dm^2 \rho(m^2) \frac{1}{2\omega} \exp\{-\omega t\} , \quad \text{with } \omega = \sqrt{\mathbf{p}^2 + m^2} \quad (207)$$

$$= \int_{\sqrt{\mathbf{p}^2}}^\infty d\omega \rho(\omega^2 - \mathbf{p}^2) \exp\{-\omega t\} . \quad (208)$$

For a positive spectral function, $\rho(m^2) \geq 0$, it is therefore clear that $\ln D(t, \mathbf{p}^2)$ has to be a convex function of the Euclidean time,⁴⁴

$$\frac{d^2}{dt^2} \ln D(t, \mathbf{p}^2) \equiv \langle \omega^2 \rangle_{t, \mathbf{p}^2} - \langle \omega \rangle_{t, \mathbf{p}^2}^2 \geq 0 , \quad (209)$$

⁴⁴ Just as the free energy is a convex function of the external fields in statistical mechanics.

because $\langle \omega \rangle_{t,\mathbf{p}^2}$ and $\langle \omega^2 \rangle_{t,\mathbf{p}^2}$ are the moments of a positive measure for all \mathbf{p}^2 .

Even though no negative $D(t, \mathbf{p}^2)$ have been reported in the lattice calculations yet, the available results, refs. [94, 95, 53], agree in indicating that the gluon propagator is not a convex function of the Euclidean time and thus that positivity is indeed violated for gluonic correlations. The corresponding results will be discussed in sec. 5.5, a summary of lattice results on the gluon propagator can be found on ref. [253].

The ghost propagator in Euclidean momentum space, being negative for positive renormalization functions $G(k^2) > 0$, of course, is not reflection positive either. This is due to the wrong spin-statistics of the ghost field and is the case at tree-level already.

Besides this somewhat trivial minus sign, two general remarks on an infrared enhanced propagator (as the one obtained for the ghost field here) might be interesting to add. First, it is important to note that a propagator with an infrared divergence $\propto 1/(k^2)^{1+\kappa}$ as found for the ghost solution here (with $\kappa \simeq 0.93$), does not violate temperedness, as long as $\kappa < 1$. Secondly, the Fourier transform $I_\kappa(t, \omega)$ of correlations of a form $\propto 1/(p^2 + m^2)^{1+\kappa}$ (with $\kappa > -1$, $\omega = \sqrt{\mathbf{p}^2 + m^2}$, and not necessarily $m = 0$) in Euclidean momentum space generically reads,

$$\begin{aligned} I_\kappa(t, \omega) &:= \int \frac{dp_0}{2\pi} \frac{\omega^{2\kappa}}{(p_0^2 + \omega^2)^{1+\kappa}} e^{ip_0 t} \\ &= \frac{(\omega t)^\kappa}{2^\kappa \Gamma(1 + \kappa)} \frac{1}{\omega} \sqrt{\frac{\omega t}{2\pi}} K_{\kappa+\frac{1}{2}}(\omega t) \xrightarrow{\omega t \gg |\kappa|} \frac{(\omega t)^\kappa}{2^\kappa \Gamma(1 + \kappa)} \frac{1}{2\omega} \exp\{-\omega t\}. \end{aligned} \quad (210)$$

The limit of large ωt shows that $\ln I_\kappa(t, \omega)$ is not a convex function of t , if $\kappa > 0$.⁴⁵ More generally, from the Bessel function (of the second kind) $K_n(x)$, one indeed verifies that $\ln I_\kappa(t, \omega)$ is a convex function of t , if and only if $\kappa \leq 0$.

Euclidean correlations of a form (210), *i.e.*, modifications of free particle propagators by an additional exponent $0 < \kappa < 1$, in particular, infrared enhanced correlations (for $m = 0$) are thus an example of a manifest violation of positivity. However, they can in principle have all the other necessary and important properties of a local quantum field theory. These are for example temperedness which is necessary to define Fourier transforms, or also, importantly, the expected domain of holomorphy of the Green's functions which implies in particular that propagators are analytic functions in the cut complex k^2 -plane with singularities occurring on the timelike real axis only. This is crucial for the incorporation of timelike momenta in the analytically continued Euclidean formulation, *e.g.*, to describe bound states. The general analyticity properties of the Green's functions should therefore better be unaffected by possible violations of positivity. The nature of these violations for propagators is thus restricted to allowing the discontinuity at the cut, $\rho(k^2)$, to be of indefinite sign. This is in complete agreement with the local description of covariant gauge theories on indefinite metric spaces, see sec. 2.4.

From all the evidence presented here as well as in sec. 2.3, it seems quite settled that the

⁴⁵ For $\kappa = 0$ the limit $\omega t \gg |\kappa|$ (indicated by the arrow in (210)) becomes an identity, and thus $\ln I_0(t, \omega)$ linear in t (with slope $-\omega$).

requirement of positivity on the level of the elementary QCD correlations has to be abandoned anyway. Technically, this is fortunately the one property to give up with the least consequences of all. This minimal relaxation of the axioms of quantum field theory seems necessary in describing confining theories in which the elementary fields as the carriers of charges may serve to implement locality but are not directly associated with the observed particles.

Concluding this section, a last remark concerns the occurrence of zeros in the Fourier transform of the gluon propagator as a function of t , eq. (205), for sufficiently small \mathbf{p}^2 . This implies that the gluon propagator in coordinate space cannot have a well defined inverse for all (t, \mathbf{x}) . While the corresponding singularities in $G^{-1}(t, \mathbf{x})$ will cause problems in a Hubbard–Stratonovich transformation to bosonize effective non-local quark theories as the Global Color Model, see ref. [28], the same comment that was given at the end of the last subsection applies here again. The infrared structure of the vertex functions, renormalization group invariance and the existence of zeros in the gluon propagator, all lead to the same conclusion: The combination of ghosts and gluons, $g^2 G^2(k^2) Z(k^2)/k^2 = 4\pi\alpha_S(k^2)/k^2$ is the physically important quantity which determines the interactions of quarks in Landau gauge (and the current-current interaction of the Global Color Model, see the next section). It can be verified explicitly that the Fourier transform of $\alpha_S(k^2)/k^2$ is free of such zeros and positive.

5.3.5 *Dynamical Chiral Symmetry Breaking and Quark Confinement*

The studies of DB χ S via the study of the quark propagator DSE are numerous, see refs. [29] and [30] for a corresponding survey. Almost all of these studies used a highly infrared singular kernel for the quark DSE in order to implement confinement. On the other hand, until recently the ghost contribution in the quark-gluon vertex as discussed at the beginning of this section have not been taken into account. In this section we will shortly review a few selected calculations used later in studies of meson properties. It has to be noted, however, that the most recent of these calculations do not employ an infrared singular kernel. In addition, we will also comment on results for the coupled gluon-ghost-quark DSEs in Landau gauge. Please note that these are preliminary, and some of them are yet to be published [242].

One model of quark confinement is based on the idea that thresholds associated with quark production can be avoided in hadronic processes by assuming that the momentum space quark propagator has no singularities on (or near) the real axis in the complex k^2 -plane which precludes a Källén–Lehmann representation. The most simple realization of this, being given by entire functions of k^2 , is often adopted in phenomenological applications. In complex directions, singularities with timelike real part might technically seem acceptable, if they are sufficiently far away from the origin so as to not interfere with the hadronic processes considered. This introduces an upper bound on the momentum range for the applicability of such a model. Such a qualitative behavior can in fact be obtained from the quark DSE, *e.g.*, in the very simple model of gluonic interactions mimicked by a 4-dimensional δ -function in Euclidean momentum space [254].⁴⁶

In phenomenological applications of Bethe–Salpeter equations for mesonic bound states sim-

⁴⁶This quite useful toy-model has been used, *e.g.*, in a study of diquark confinement which will be discussed in sec. 7.1.

ilar entire function forms of the quark propagators are frequently also parameterized with quite remarkable success, see chapter 6. Typical forms of such parameterizations of the quark structure functions involve entire functions in the k^2 -plane (with essential singularities at infinity) and 3 – 7 parameters for the light quark sector which are then fitted to static meson properties, see *e.g.* [31,255,145,256] and references therein.

With respect to phenomenological applications it is thereby interesting to compare the different quark DSE models in quenched approximation to collect further evidence on the origin, interpretation and justification of the various models to be used in meson and baryon physics, see the next two chapters. The probably most obvious question at this point is the role of ghosts. In this chapter it became evident that their contributions cannot be neglected in Landau gauge. The open question can thus be phrased as to whether some of the more successful models might nevertheless be able to model their influence without taking these contributions into account explicitly.

To clarify this, consider the quark-current interaction of the Global–Color–Model which is motivated as being the result of an expansion in the color-octet quark currents $j_\mu^a(x)$ of the effective quark theory given by the Feynman–Schwinger functional $Z_{\text{YM}}[j]$ of the pure gauge theory with these currents as the external fields.⁴⁷ The term quadratic in the quark-currents of this functional is inevitably given by,

$$\ln Z_{\text{YM}}^{(2)}[j] := -\frac{1}{2} \int d^4x d^4y j_\mu^a(x) G_{\mu\nu}^{(2)ab}(x-y) j_\nu^b(y) , \quad (211)$$

which defines the interaction of the GCM. Obviously, the resulting current interaction cannot be gauge invariant. It is only invariant under global color rotations which is reflected in the model’s name. The interpretation of this model interaction, also called the Abelian approximation, is motivated from analogy to what would occur in QED. The central idea behind this approximation can be traced to the assumption that, as follows from gauge invariance for QED, the renormalization constant of the gauge field is related to the inverse coupling renormalization by $Z_g^2 Z_3 = 1$. This implies in particular for the gauge field propagator that

$$G_{\mu\nu}^{(2)ab}(x-y) = \delta^{ab} g^2 D_{\mu\nu}(x-y) , \quad (212)$$

with D being the gauge boson propagator,

$$g^2 D_{\mu\nu}(k) = \left(\delta_{\mu\nu} - \frac{k_\mu k_\nu}{k^2} \right) \frac{g^2 Z(k^2)}{k^2} + g^2 \xi \frac{k_\mu k_\nu}{k^4} , \quad (213)$$

and thus $g^2 Z(k^2)$, is a renormalization group invariant which can be identified with the running coupling in QED (as compared to $gZ(k^2)$ in the Mandelstam approximation for QCD, see sec. 5.3.1). Perturbative QCD does not show this behavior. But again, neglecting the ghosts

⁴⁷ As the measure in this gluonic functional of the quark-currents is not Gaussian, of course, this can at best be understood in the sense of Gell-Mann and Low’s “magic formula of perturbation theory” [257].

of the non-Abelian theory in the covariant gauge, the Abelian approximation at this point effectively might include some of their contributions. Within this approximation, asymptotic freedom is put in by replacing the infrared stable running coupling of QED with the asymptotically free one of QCD (with N_f quark flavors and N_c colors),

$$g^2 Z(k^2) \equiv \bar{g}^2(t_k, g^2) \rightarrow \frac{48\pi^2}{11N_c - 2N_f} \frac{1}{\ln(k^2/\Lambda^2)}, \quad \text{for } k^2 \gg \Lambda^2, \quad (214)$$

where Λ denotes the QCD scale parameter. In the infrared the interaction is then chosen such that phenomenologically acceptable models arise. Especially, a certain strength of the interaction is needed to imply DB χ S.

In the non-Abelian theory, the situation is of course different. In particular, in the covariant gauges ghost contributions enter in this effective interaction. Even though this might seem to be evident from its definition, consider perturbation theory to demonstrate this fact explicitly. The symmetry currents $j_\mu^a(x)$ not being renormalized, their interaction $G^{(2)}$ has to be renormalization group invariant as is the case for the expression (212) in QED, of course. In perturbative QCD in Landau gauge, however, the product $g^2 D$ has an anomalous dimension γ which is different from unity for all numbers of colors and all numbers of flavors, and it is thus not renormalization group invariant. Near the ultraviolet fixed point, this anomalous dimension is given by

$$\gamma(g) \xrightarrow{g \rightarrow 0} \frac{\gamma_A^0}{\beta_0} = \frac{(13/2)N_c - 2N_f}{11N_c - 2N_f} \stackrel{!}{=} \begin{cases} 1, & \text{AA, not possible for } N_c, N_f \in \mathbb{N} \\ \frac{1}{2}, & \text{MA, } \rightarrow N_f = N_c \end{cases} \quad (215)$$

with γ_A^0 and β_0 being the leading coefficients of the gluon anomalous dimension and the β -function. Note that in contrast to the Abelian approximation (AA) the result of the Mandelstam approximation (MA), *c.f.* sec. 5.3.1, that gD is renormalization group invariant without ghosts, happens to resemble the perturbative result for $N_f = N_c$. The effect of neglecting ghosts seems to have canceled with neglecting $N_f = N_c$ quark flavor at this point. Of course, the quark loops as well as the ghost loop both contribute with a negative sign to the perturbative divergences. The different strengths of these contributions nevertheless make their compensation in the ratio γ_A^0/β_0 possible.

While it thus seems impossible to neglect ghosts consistently, ghosts do implicitly enter in quark-gluon vertices, and that the interaction of the GCM might be justified from a dressed-ladder exchange, *e.g.* as given in eq. (192). For the GCM the quantity $G^{(2)}$ may in turn serve to define a non-perturbative running coupling, *e.g.*, from its part proportional to the metric $\delta^{ab}\delta_{\mu\nu}$ by,

$$\frac{1}{3(N_c^2 - 1)} \delta^{ab} \delta_{\mu\nu} G_{\mu\nu}^{(2)ab}(k) =: -\frac{4\pi\alpha(k^2)}{k^2}. \quad (216)$$

Perturbatively (at next-to-leading order) this is equivalent to the definition for the running coupling adopted in sec. 5.3.3. Non-perturbatively, the definition (216) should, in principle,

be obtainable from the term of the quark-gluon vertex $\propto \gamma_\mu$ in a symmetric momentum subtraction scheme in a quenched lattice approximation. It would be interesting to assess, from such a lattice calculation, possible indications towards the phenomenologically successful infrared enhancement for the GCM coupling (216). The simulation of ref. [258] seems to indicate to the contrary. It is, however, obtained from an asymmetric subtraction scheme and thus is very likely inconclusive, see sec. 5.5. The effective interaction of the GCM in the covariant gauges, whatever it is, is *not* the gluon propagator alone as suggested by eq. (212). Ghosts contribute to the current-current interaction in eq. (211) as they are an unavoidable part of the (perturbative) definition of $Z_{\text{YM}}[j]$.

The quark DSE (90) (with $S_{\text{tl}}(k) = 1/(-ik + Z_m m)$ denoting the tree-level propagator),

$$S^{-1}(k) = Z_2 S_{\text{tl}}^{-1}(k) + g^2 Z_{1F} \frac{4}{3} \int \frac{d^4 q}{(2\pi)^4} \gamma_\mu S(q) \Gamma_\nu(q, k) D_{\mu\nu}(k - q) , \quad (217)$$

in the Abelian rainbow approximation effectively simplifies to

$$S^{-1}(k) = Z_2 S_{\text{tl}}^{-1}(k) + \frac{16\pi}{3} \int \frac{d^4 q}{(2\pi)^4} \alpha((k - q)^2) \gamma_\mu S(q) \gamma_\nu D_{\mu\nu}^{\text{free}}(k - q) . \quad (218)$$

“Effective running couplings” $\alpha((k - q)^2)$ employed in the study of meson properties can be found, *e.g.*, in eqs. (252,267) in the next chapter. Whereas the interaction in (252) contains a δ -function in momentum space, the form (267) is infrared finite. Nevertheless, the results for the quark propagator are very similar. This can be seen *e.g.* from the fact that the quark condensate (renormalized at 1 GeV) for both interaction types is very close to the phenomenological value,

$$\langle \bar{q}q \rangle(\mu = 1\text{GeV}) = (0.240\text{GeV})^3 . \quad (219)$$

This condensate can be extracted either from mass function or by integrating the trace of the quark propagator. Parametrizing the general form of the quark propagator in Euclidean momentum space,

$$S(p) = \frac{1}{-i\cancel{p}A(p^2) + B(p^2)} = \frac{Z_q(p^2)}{-i\cancel{p} + M(p^2)} , \quad (220)$$

the mass function $M(p^2) = B(p^2)/A(p^2)$ is proportional to the quark condensate at large p^2 ,

$$M(p^2) \simeq m - \frac{4\pi\alpha(p^2)}{3p^2} \left(\frac{\alpha(p^2)}{\alpha(\mu^2)} \right)^{-d_m} \langle \bar{q}q(\mu^2) \rangle , \quad (221)$$

where $d_m = 12/(11N_c - 2N_f)$ is the anomalous dimension of the quark mass and μ is large Euclidean renormalization point.

The mass functions for the three light flavors and in the chiral limit obtained in ref. [259] are displayed in fig. 16. Clearly one sees the phenomenon of DB χ S. The authors of ref. [259]

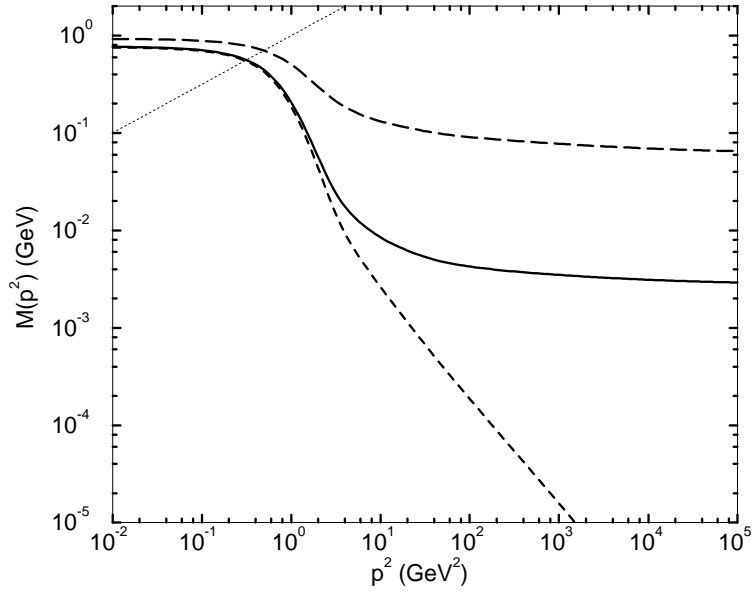


Fig. 16. The renormalised dressed-quark mass function, $M(p^2)$, obtained by solving the quark DSE with the interaction (252): u/d -quark (solid line); s -quark (long-dashed line); and chiral limit (dashed line). The renormalisation point is $\mu = 19$ GeV. The intersection of the line $M^2(p) = p^2$ (dotted line) with each curve defines the Euclidean constituent-quark mass, M^E . (Adapted from ref. [259].)

introduce as measure the Euclidean mass M^E defined by $(M^E)^2 = M((M^E)^2)$. It has to be noted, however, that the corresponding quark propagator does not possess poles for time-like (real) p^2 . Instead singularities for complex values at p^2 are present.

Recently the coupled ghost, gluon and quark DSEs have been solved [242]. Before commenting on this solution it is illustrative to study the quark DSE in quenched approximation using the ghost and gluon propagators of ref. [49] discussed in the last sections together with its implied form for the quark-gluon vertex. The related truncation scheme is based on the solution to the simplified Slavnov–Taylor identity obtained from eq. (176) by neglecting the quark-ghost scattering kernel,

$$G^{-1}(k^2) k_\mu \Gamma_\mu(p, q) = iS^{-1}(p) - iS^{-1}(q) , \quad k = p - q . \quad (222)$$

This identity being of analogous form as the Abelian Ward–Takahashi identity but with the important additional ghost factor $G(k^2)$. The corresponding solution given in eqs. (177,178) is then employed in the quark DSE. The resulting effective quark interaction is only slightly infrared singular and even integrable. This allows, *e.g.*, to use the Landshoff–Nachtmann model for the pomeron in this approach. From the solution a pomeron intercept of approximately 2.7/GeV [260,261] has been estimated as compared to the typical phenomenological value of 2.0/GeV [262]. The resulting quark mass functions are shown in fig. 17. It is reassuring that in this approach, where the only parameter, the scale generated by dimensional transmutation, is fixed from the behavior of the running coupling at large momenta, DB χ S occurs. It has to be emphasized that except for lattice calculations this phenomenon has been found in an *ab initio* calculation for the first time, *i.e.* without any explicit assumptions or modeling of

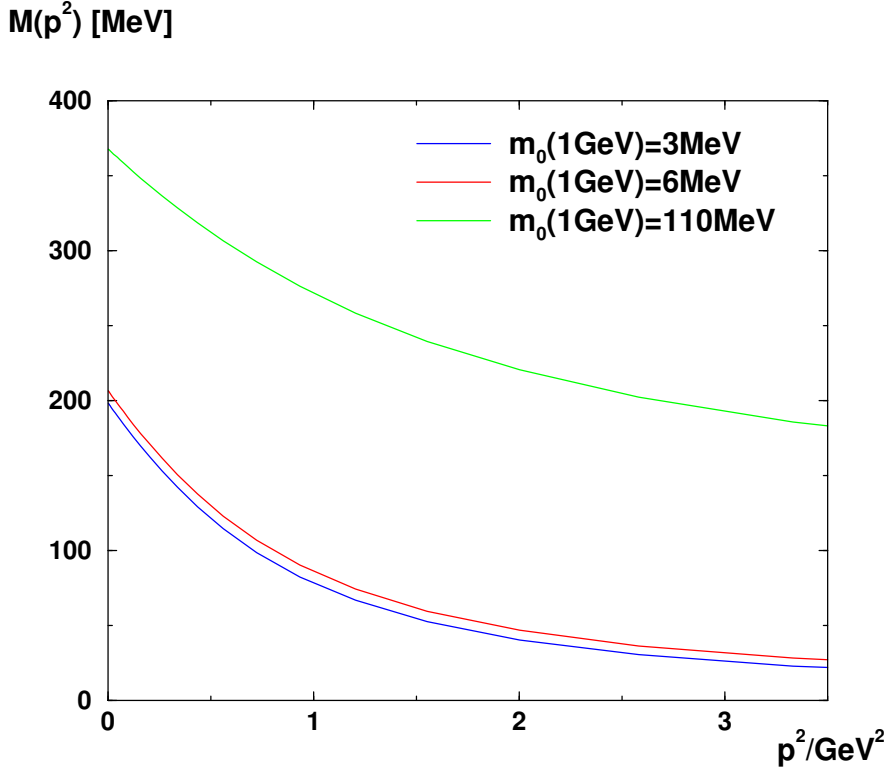


Fig. 17. Quark mass functions $M(p^2)$ for various current masses from the quenched approximation (with $\bar{\beta}_0 = 11$).

the effective infrared quark interaction. However, fig. 17 also makes clear that the calculated mass functions are smaller than phenomenologically required. This is especially pronounced in the quark condensate. At a renormalization scale of 1 GeV the calculated value is $\langle \bar{q}q \rangle(\mu = 1\text{GeV}) = (0.1\text{GeV})^3$ and thus an order of magnitude smaller than the empirical value.

This problem becomes even worse beyond the quenched approximation. First, it has to be noted that only a solution for the coupled systems of propagator equations has been found where the quark propagator resembles qualitatively the one in quenched approximation [242]. This does not exclude that other solutions exists, and as a matter of fact, such a solution with non-trivial infrared behavior of the quark renormalization function $Z_q(p^2)$ seems possible. Concentrating on the solution found so far, one notes that the quark loop in the gluon DSE is screening and thus the effective quark-quark interaction becomes smaller. This effect is somewhat weakened due to the back-reaction via the quark DSE. But nevertheless the quark mass function and correspondingly the quark condensate become even smaller. There is, however, an interesting feature not present in the quenched approximation (where $Z_q(p^2)$ is only slightly suppressed in the infrared): The calculated quark renormalization function $Z_q(p^2)$ displays a very pronounced dip in the infrared dropping to $Z_q(0) \approx 0.7$ slightly dependent on the number of active flavors. This is for two reasons interesting: First, as can be seen from fig. 21 such a behavior is found in the most recent lattice calculations. Furthermore, as an increase in the numerical effort makes this dip even more pronounced currently a solution with an infrared vanishing quark renormalization function $Z_q(p^2)$ is put into the quark DSE via a power ansatz and an infrared asymptotic expansion. Therefore, the hope is that despite the numerical mismatch for the amount of DB χ S, this and related investigations will shed light on the question of quark confinement in linear covariant gauges.

5.4 A Non-Perturbative Expansion Scheme in Landau Gauge QCD

The results on the infrared behavior of the gluon propagator in Landau gauge with or without ghosts differ as much as possible. Certainly, including ghosts provides DSEs which are consistent at the level of propagators. Nevertheless, it is of utter importance to have some other non-perturbative scheme to compare with. In the next section we will contrast the DSE solutions with lattice results. As already mentioned in sec. 2.5 there is an alternative approach to the DSEs in Landau gauge QCD [141,142]. A brief description of this approach in this section will supplement the study of the infrared behavior of the Green's functions in Landau gauge QCD as inferred from the already presented truncation schemes. As such it adds some new aspects while some others are given less emphasis in this somewhat complementary approach to the Dyson–Schwinger hierarchy.

This approach is based on the observation that an exact vertex function and its perturbative estimate differ by expressions which, in general, contain essential singularities in the coupling of the same structure as in the spontaneous mass scale, see eq. (1). The idea therefore is to improve the perturbative expansion in approximating the Euclidean proper vertices Γ by a double series in the coupling as well as in the degree of a rational approximation with respect to the spontaneous mass scale Λ being non-analytic in g^2 . The proper vertices are thereby approximated by a truncated double series in functions $\Gamma^{(r,p)}$ where r denotes the degree of the rational approximation while p represents the order of perturbative corrections in g^2 calculated from $\Gamma^{(r,0)}$ instead of $\Gamma_{pert.}^{(0)}$, see ref. [142]. The requirement that these non-perturbative terms reproduce themselves in the Dyson–Schwinger equations is then used to extract constraints on the finite set of dimensionless coefficients that are used to parameterize the rational approximants.

To be specific, consider the 1-PI gluon 2-point function, *i.e.* the inverse gluon propagator. It is transverse in Landau gauge and its functional dependence on the gluon momentum and the spontaneous mass scale Λ is parameterized by a rational function with denominator of degree r , introducing $2r + 1$ dimensionless coefficients $\{\zeta_i\}$, $\{\eta_i\}$,

$$\Gamma^{(r,0)}(k^2) = \frac{(k^2)^{r+1} + \zeta_1 \Lambda^2 (k^2)^r + \dots \zeta_{r+1} (\Lambda^2)^{r+1}}{(k^2)^r + \eta_1 \Lambda^2 (k^2)^{r-1} + \dots \eta_r (\Lambda^2)^r}. \quad (223)$$

The idea here is to account for the polynomial dependence on Λ and thus on k^2 to parameterize non-perturbative effects such as the condensate contributions of the operator product expansion. The logarithmic Λ dependences have to be generated from radiative corrections, *i.e.*, from higher perturbative orders ($p \geq 1$).

The lowest rational approximation $r = 0$ describes the dynamical generation of a Schwinger mass [263], $m^2 = \zeta_1 \Lambda^2$, from the gluon DSE. Generally, for even orders r there will be at least one “physical particle” pole on the (negative) real k^2 -axis in the propagator. In a situation like this one would expect a lowest isolated pole to stabilize as r is increased, and a sequence of real zeros and poles to develop and approximate the branch cut describing multi-particle production for a propagator of physical degrees of freedom, *i.e.*, one with a Källén–Lehmann representation. As this is not anticipated for the elementary degrees of freedom in QCD, it

was further concentrated on the odd sequence of rational approximations, *i.e.* an even number of generally complex poles⁴⁸ which have been interpreted as describing unstable short lived excitations [142]. For asymptotically large $k^2 \gg \Lambda^2$ one imposes the boundary condition that the rational approximants reduce to the tree-level vertices, *e.g.*, for the gluon, $\Gamma^{(r,0)}(k^2) \rightarrow k^2$. The power corrections to this limit can furthermore be compared to condensate contributions in a corresponding operator product expansion. The perturbative logarithms of the coefficient functions could in principle be obtained analogously from $\Gamma^{(r,p)}(k^2)$ for successively higher p .

The practical calculations in this approach are thus far restricted to the lowest non-trivial degree $r = 1$ in the odd rational approximation. The general idea of the approach will be sketched for this most simple order in the following. The 2-point gluon vertex function then has the structure,

$$\Gamma^{(1,0)}(k^2) = k^2 + u_1 \Lambda^2 + \frac{u_3}{k^2 + u_2 \Lambda^2}, \quad (224)$$

with one simple pole, and some linear combinations u_i , $i = 1 \dots 3$, of the $r = 1$ coefficients introduced above. One can then infer from the hierarchical coupling to the higher vertex functions in DSEs together with the exchange symmetry of these higher vertices that analogous simple poles have to occur also in the momentum variables corresponding to each of their external legs [142]. For example, the part of the 3-gluon vertex that replaces the tree-level vertex is found to have the following structure ($A(x, y; z) = A(y, x; z)$, and $A = 1$ at tree-level),

$$\Gamma_{\mu\nu\rho}(p, q, k) = -A(p^2, q^2; k^2) \delta_{\mu\nu} i(p - q)_\rho + \text{cyclic permutations}, \quad (225)$$

containing poles and a polynomial numerator N in the momenta and Λ^2 of the form,

$$A(p^2, q^2; k^2) = \frac{N(p^2, q^2; k^2)}{(p^2 + u_2 \Lambda^2)(q^2 + u_2 \Lambda^2)(k^2 + u_2 \Lambda^2)}. \quad (226)$$

The additional requirement (besides the symmetry of N) that these vertex functions, when replacing the tree-level vertices, should not change the superficial degree of divergence of any diagram, is then used to constrain the numerator polynomials further.⁴⁹

These rational approximants for the 1-PI vertices at lowest perturbative order $p = 0$, *i.e.* order zero in the coupling g^2 , replace the tree-level vertices in a modified perturbative expansion. Combined with the operator product expansion, this scheme corresponds to a Padé approximation with respect to the high momentum power corrections by condensates [150]. Its actual use goes far beyond this, however. Dyson–Schwinger equations are used to determine

⁴⁸ This means that poles occur only as complex conjugate pairs (for real coefficients). The occurrence of an even number of real poles is rejected as being exotic. In particular, those closest to the origin in the complex k^2 -plane are assumed to come as complex pair.

⁴⁹ One might think that this requirement is contained already in the asymptotic condition for the vertex to reduce to tree-level at high momenta, in general however, some additional restrictions are necessary [142].

these approximants self-consistently. The inhomogeneities of the DSEs, being the tree-level vertices, lead to the following question: How can the difference between these and the rational approximants at zeroth perturbative order, *e.g.* for inverse the gluon propagator,

$$\Delta\Gamma(k^2) := \Gamma^{(1,0)}(k^2) - \Gamma_{pert.}^{(0)}(k^2) = u_1\Lambda^2 + \frac{u_3}{k^2 + u_2\Lambda^2}, \quad (227)$$

be generated from loop-integrals containing explicit orders of the (bare) coupling g_0^2 ? This mechanism can be understood qualitatively as follows: Due to the presence of the mass scale Λ there will be new types of logarithmic ultraviolet divergences generated in the loops. These contain factors

$$\propto \gamma_0 g_0^2 \ln(\Lambda_{UV}^2/\Lambda^2), \quad (228)$$

where the renormalization group invariant (since physical) mass scale Λ replaces the momentum variables that occur in analogous perturbative divergences in which the constant γ_0 would be identified with the leading coefficient of the corresponding anomalous dimension. For perturbative divergences, the cutoff Λ_{UV} dependence is traded for a renormalization scale μ dependence by subtracting $\gamma_0 g^2 \ln(\Lambda_{UV}^2/\mu^2)$ with a suitable counter term which is done successively order by order in the coupling. Here on the other hand, it is used that, heuristically, the bare coupling is the running coupling at the cutoff scale, $\bar{g}^2(\Lambda_{UV}) \rightarrow g_0^2$, which tends to zero in the scaling limit ($\Lambda_{UV} \rightarrow \infty$), *c.f.*, eq. (1),

$$\bar{g}^2(\mu) = \frac{1}{\beta_0 \ln(\mu^2/\Lambda^2)}, \quad \text{hence: } \gamma_0 g_0^2 \ln(\Lambda_{UV}^2/\Lambda^2) \rightarrow \frac{\gamma_0}{\beta_0}. \quad (229)$$

In this way the contributions giving rise to the non-analyticities in $g_0^2 = 0$, and which thus cannot be taken care of by an asymptotic expansion in the coupling, have to reproduce themselves in the equations at every order in this expansion. This argument can be made more rigorous using dimensional regularization and the particular subtraction scheme of ref. [142]. At one-loop this mechanism has been demonstrated to generate the rational structure $\Delta\Gamma$ for the (inverse) gluon propagator as well as the corresponding $r = 1$ structure of the remaining six superficially divergent vertex functions of Landau gauge QCD explicitly in refs. [141,142,148,149].⁵⁰

Furthermore, the non-linear structure of the DSEs is then used to determine the coefficients of the approximants by comparing their poles and residues on one side of the equations with those generated from the one-loop divergence structure on the other side as outlined above. One conclusion from the resulting conditions is for example that the pole positions in identical types of external legs of different proper vertex functions have to be identical, *e.g.*, $p_2 = -u_2\Lambda^2$ in the gluonic 2-point vertex as well as in the 3-point vertex as given above. Together with additional constraints from the exchange symmetries as well as from the form of the perturbative divergences the systems of equations that determine the coefficients of the approximants

⁵⁰ It is intuitively clear from the above that this generation of rational structure at lowest order $\Gamma^{(r,0)}$ is restricted to the seven primitively divergent vertices.

are highly over-determined. Some violations of exchange symmetries and some additional contributions to the perturbative divergences have thus to be taken into account and minimized for a given set of solutions that can be obtained in absence of these additional constraints. The remaining violations can then serve as an indicator for the quality of the particular level of approximation. The present results suggest that the $r = 1$ level describes the system of gluon and ghost 2-point and 3-point functions quite consistently [142,148]. And the results obtained for this subsystem of the superficially divergent vertices in which the influence of the 4-gluon vertex function is parameterized by additional free coefficients, are furthermore confirmed reasonably well from a decoupled study of the Dyson–Schwinger equation for the 4-gluon vertex [149]. The violations mentioned above become more drastic, however, when quarks are included. Also, the study of the 4-gluon equation so far yields results which seems to be difficult to reconcile with those of the 2-point and 3-point subsystem in presence of quarks. So the question whether the approach is a viable possibility beyond a quenched approximation remains somewhat unclear. There is certainly the possibility that the situation improves considerably at much higher orders in r , given the complexity of the approach at the presently employed order, however, this conclusion would nevertheless cast some doubt on its practical use. Beyond the question of practicability this approach has added something conceptually new, namely a mechanism of compensating singularities, see sec. 2.5. Due to its importance we will shortly reiterate on this point below.

One previously raised criticism [264] concerning the apparently unphysical singularities in the proper vertex functions which are induced by the zeros in the propagators, and which are a feature inherent in the approach, has now been clarified [148]. As seen from the structure of the gluon 3-point vertex function given above, the hierarchical coupling of the different vertex functions implies common poles in external momenta. Therefore these poles in the 2-point vertices which are zeros in the propagators reappear in all higher vertex functions. It follows that poles in the external lines are compensated by the corresponding zeros of the propagators attached to these lines when computing scattering amplitudes and will not give rise to unphysical asymptotic particles. As discussed in sec. 2.5 the related poles on internal lines are also automatically canceled in this approximation scheme [148,149]: The necessary pole contributions reproduce themselves in the hierarchy. What still needs to be shown is that colorless hadrons do appear as asymptotic states.

5.5 Lattice Results

In this section we will discuss the results for QCD Green's functions as obtained from lattice calculations. As we will see results from the lattice and from DSEs are complementary. DSEs have to rely on truncation schemes. Therefore, to be at least able to judge their validity it is mandatory to confront them with some other non-perturbative methods. It is especially helpful to compare DSE results with the one of lattice calculations. Whereas the latter cannot investigate the deep infrared region they nevertheless allow to distinguish between infrared suppressed and infrared enhanced functional forms for propagators. Also the conclusion, that the gluon propagator in Landau gauge violates positivity, can be drawn quite reliably from lattice data [253].

As we will see lattice results provide evidence for an infrared suppressed gluon and an infrared enhanced ghost propagator. Thus it is natural to compare the DSE results of ref. [49] with lattice results available for the gluon [94,95,50] as well as for the ghost propagator [96]. These calculations use lattice versions to implement the Landau gauge condition supplemented by different procedures to eliminate Gribov copies (at least approximately). Recently, for the pure $SU(2)$ lattice gauge theory, the influence of such copies of gauge equivalent configurations present in the conventional Landau gauge, has been systematically investigated for gluons and ghosts in [97].

Due to different normalizations, lattice sizes and, in general, differing values of the lattice coupling β , it is not quite obvious that all presently available lattice data sets for the gluon propagator in Landau gauge from different groups are indeed consistent *e.g.*, compare refs. [94] and [95]. Since it is not possible to compare these different data sets without manipulating their scales, we will present results only for a very recent and accurate lattice calculation for the gluon propagator in Landau gauge. In fig. 18 the lattice data of ref. [50] are shown. For comparison the DSE solution (with normalization $Z(x = 1) = 1$) of ref. [49] is also included. The momentum scale in the results, chosen to yield $\alpha_S(M_Z) = 0.118$ as described above, is not used as a free parameter and is thus not adjusted. Rather, the gluon propagator for this fixed momentum scale is plotted as a function of the invariant momentum $x = k^2 a^2$ in units of the inverse lattice spacing with $a^{-1} = 1.9\text{GeV}$ from lattice phenomenology corresponding to the value $\beta = 6.0$ for $SU(3)$ which was used in this particular simulation. Note that these lattice results obtained on an anisotropic $32^3 \times 64$ lattice with $\beta = 6.0$ are without significant statistical errors for momenta down to as low as 0.4 GeV. A very recent investigation [51] using an improved action and an improved gauge fixing unambiguously demonstrates that the infrared suppression of the gluon propagator is not a finite size effect. This at least indicates towards a common trend for the gluon propagator to be very weak in the infrared. The influence of Gribov copies on these lattice calculation is as yet not entirely clear (nor is it on the presently available DSE solutions, of course). However, the same qualitative behavior and a very similar quantitative behavior, in particular in the infrared, was reported for the gluon propagator from a lattice calculation employing the Laplacian gauge⁵¹ in [267].

In fig. 19 the infrared enhanced ghost propagator with normalization such that $G(x = 1) = 1$ is compared to the results of ref. [96] obtained on a symmetric 24^4 and a non-symmetric $16^3 \times 32$ lattice for $SU(3)$ at $\beta = 6.0$ from fig. 1 in ref. [96] up to $x = 1.5$. Identical results modulo finite size effects were obtained for an 8^4 lattice (see ref. [96]). Again, $x = k^2 a^2$ with $a^{-1} = 2\text{GeV}$ and the momentum scale in the DSE result, fixed from the Z -mass, is *not* adjusted.

The data extracted from the long direction of the $16^3 \times 32$ lattice might indicate the existence of a finite maximum in the ghost propagator at very low momenta. The fact that the two lowest data points in this set lie significantly below their neighbors of the 24^4 lattice was interpreted by the authors of ref. [96] as a genuine signal rather than a finite size effect. The reason for this being that, on the small 8^4 lattice, an enhancement was observed for the lowest point (and attributed to the finite size) in contrast to the shift downwards of the two points from the 32 direction of the non-symmetric lattice. However, no such maximum was observed on any of

⁵¹ The Laplacian gauge also reduces to the Landau gauge in the continuum, it was proposed as an effective procedure of finding absolute minima, however [265,266].

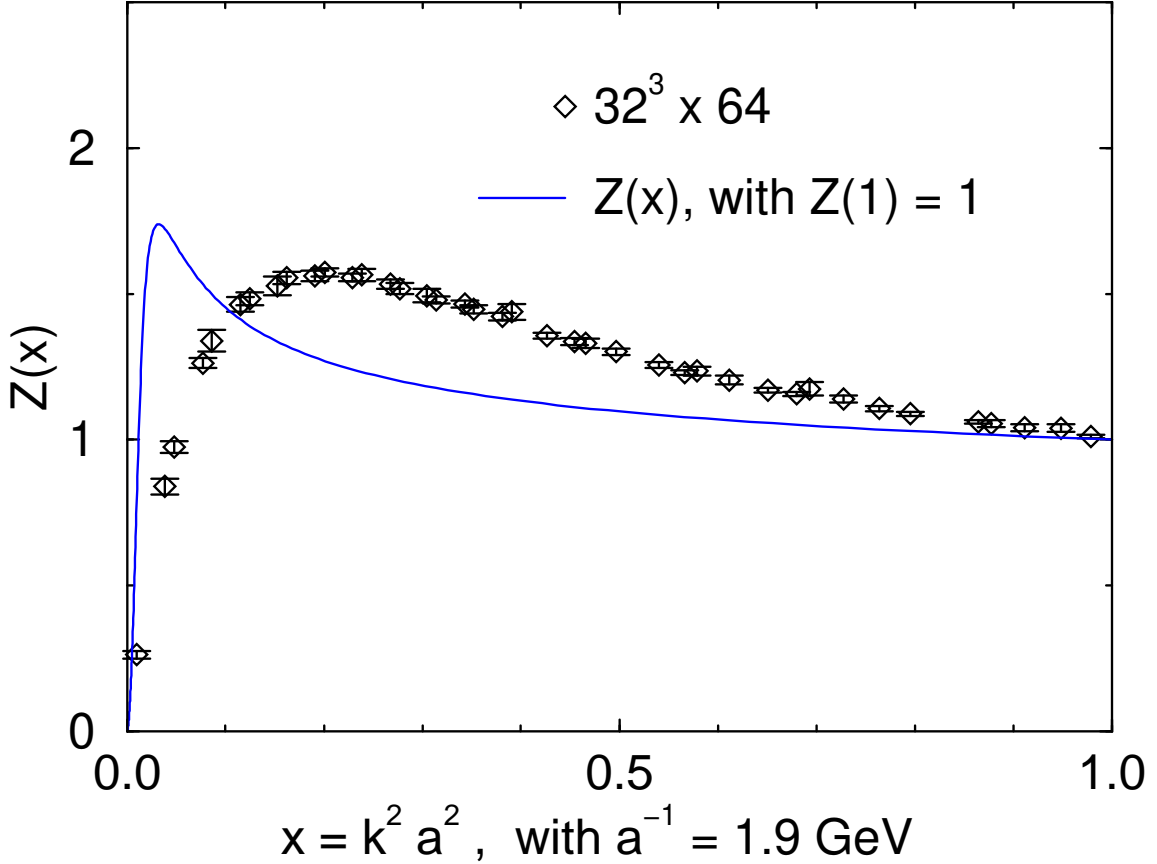


Fig. 18. The gluon renormalization function from Dyson–Schwinger equations compared to the corresponding lattice data from [50].

the smaller lattices. The present DSE results do not confirm the existence of such a maximum in the ghost propagator but coincide nicely with all those data points of the differently sized lattices that lie on a universal curve. In addition, note that the 24^4 and $16^3 \times 32$ lattices are of roughly the same size as the asymmetric $16^3 \times 48$ and $24^3 \times 48$ lattices used for the gluon propagator in ref. [95]. Considering their estimate of finite size effects based on deviations between different components of the gluon propagator at small momenta, one might be led to question the significance of the maximum in the ghost propagator observed for the one particular data set of ref. [96] at momenta too low to yield finite size independent results for the gluon propagator, *c.f.*, ref. [95], on even larger lattices.

It is quite amazing to observe that the numerical DSE solution fits the lattice data at low momenta ($x \leq 1$) significantly better than the fit to an infrared singular form with integer exponents, $D_G(k^2) = c/k^2 + d/k^4$, as given in ref. [96]. Clearly, low momenta ($x < 2$) were not included in this fit, but the authors conclude that no reasonable fit of such a form is possible if the lower momentum data is to be included. Therefore, apart from the question about a possible maximum at the very lowest momenta, the lattice calculation seems to confirm the existence of an infrared enhanced ghost propagator of the form $D_G \sim 1/(k^2)^{1+\kappa}$ with a non-integer exponent $0 < \kappa < 1$. The same qualitative conclusion has in fact been obtained in a more recent lattice calculation of the ghost propagator in $SU(2)$ [97], where its infrared

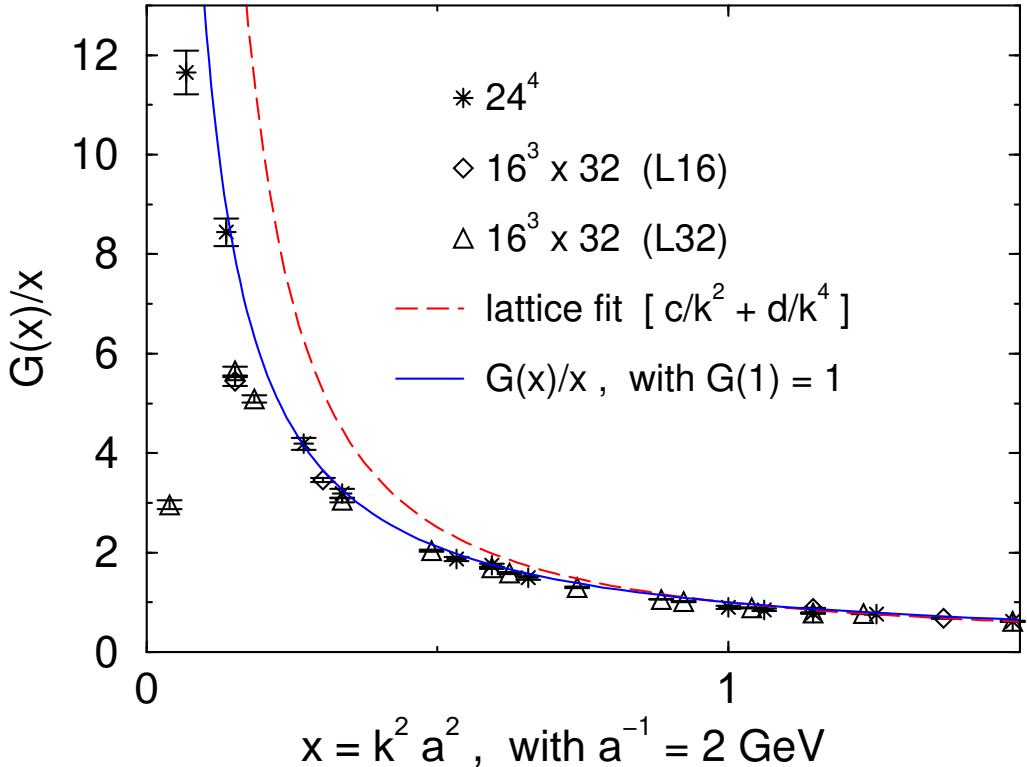


Fig. 19. The ghost propagator from Dyson–Schwinger equations (solid line) compared to data from fig. 1 in ref. [96] for 24^4 and $16^3 \times 32$ lattices, and a fit of the form $c/x + d/x^2$ (with $c = 0.744$, $d = 0.256$) as obtained in ref. [96] for $x \geq 2$ (dashed line).

dominant part was fitted best by $D_G \sim 1/(k^2)^{1+\kappa}$ for an exponent κ of roughly 0.3 (for $\beta = 2.7$). This also is in qualitative agreement with the $SU(2)$ calculations of ref. [96], again, with the exception of one single data point for the smallest lattice momentum possible.

Furthermore, in refs. [96,97] the Landau gauge condition was supplemented by algorithms to select gauge field configurations from the fundamental modular region which is done to eliminate systematic errors that might occur due to the presence of Gribov copies.⁵² Thus, the good agreement of the DSE result with these lattice calculations suggests that the existence of such copies of gauge configurations might have little effect on the solutions to Landau gauge Dyson–Schwinger equations. This would also help to understand the similarity of these solutions to the qualitative behavior obtained by Zwanziger for gluon and ghost propagators from implications of complete gauge fixings [92,93].

Having seen that lattice data provide evidence for an infrared enhanced ghost propagator and an infrared suppressed gluon propagator the question arises whether lattice calculations support also the idea that the gluon propagator does violate reflection positivity. Even though no negative $D(t, \mathbf{p}^2)$ have been reported in the lattice calculations yet, the available results, refs. [94,95,53], agree in indicating that the gluon propagator is not a convex function of the

⁵² An investigation of the effectiveness of the stochastic overrelaxation method to achieve this is given in ref. [97]

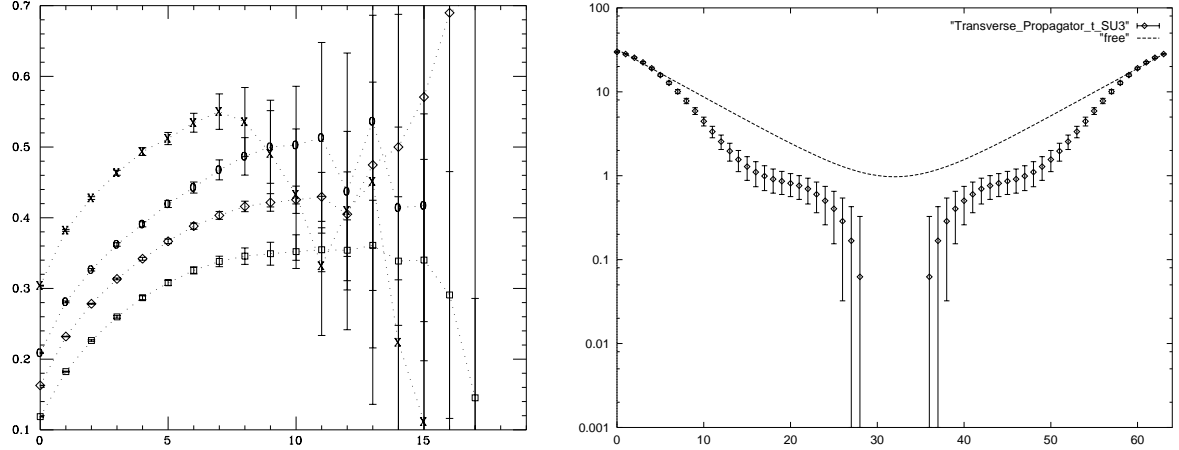


Fig. 20. Lattice results of the effective energy $\omega_{\text{eff}}(t, \mathbf{p})$ at $(a\mathbf{p}) = 0, (2\pi/24, 0, 0), (2\pi/24, 2\pi/24, 0), (4\pi/24, 0, 0)$ on a $24^3 \times 48$ lattice at $\beta = 6.0$ (left, fig. 1 of ref. [95]), and $D(t, \mathbf{p})$ at $(a\mathbf{p}) = (2\pi/48, 0, 0)$ for $\beta = 6.8$ on a $48^3 \times 64$ lattice (right, fig. 2 of ref. [53]).

Euclidean time and thus that positivity is indeed violated for gluonic correlations. In the right graph of fig. 20, the result of ref. [95] for the effective energy,

$$\omega_{\text{eff}}(t, \mathbf{p}) = \langle \omega \rangle_{t, \mathbf{p}^2} := - \frac{d}{dt} \ln D(t, \mathbf{p}^2), \quad (230)$$

is plotted which is clearly not the monotonically decreasing function of t it would be for a positive gluonic spectral function. Similarly, the left graph of fig. 20 shows the result of refs. [53, 252] for $D(t, \mathbf{p}^2)$ together with the free propagator $\propto \exp(-\omega t)$ which for $\mathbf{p} = (2\pi/(48a), 0, 0)$ and with periodic boundary conditions has the form

$$D(t) \propto \cosh(2\pi(t - N_t/2)/48). \quad (231)$$

The logarithmic plot again indicates quite clearly that this result is not a convex function of t . Note that for a scale given by roughly $a^{-1} \simeq 6\text{GeV}$ at $\beta = 6.8$ the lowest momentum $2\pi/(48a)$ corresponds to about 780MeV . Using for the scale $\sigma \simeq (300\text{MeV})^2$ as in previous sections, one can estimate that the lattice result therefore compares to a spatial momentum $\mathbf{p}^2/\sigma \gg 1$ for which the Fourier transform of the DSE solution, eq. (205), is found to no longer be negative as a function of the Euclidean times t either. The qualitative behavior as shown in fig. 15 is obtained for spatial momenta $\mathbf{p}^2/\sigma < 1$. The results of the lattice simulation are thus not incompatible with the DSE solution. A closer comparison might therefore be interesting. Good fits to the gluon data of ref. [53] have been obtained in ref. [252] from parameterizations based on the two lowest order rational approximants of the scheme described in sec. 5.4.

As noted already in sec. 2.4.2 the Kugo–Ojima Green’s function has been calculated on the lattice [231, 137]. It is interesting to note that in these calculations also an infrared suppressed gluon and an infrared enhanced ghost propagator have been found.

Lattice calculations of the infrared behavior of the quark propagator are still in a very preliminary stage [269–271, 268]. This first data provide evidence that the quark renormalization

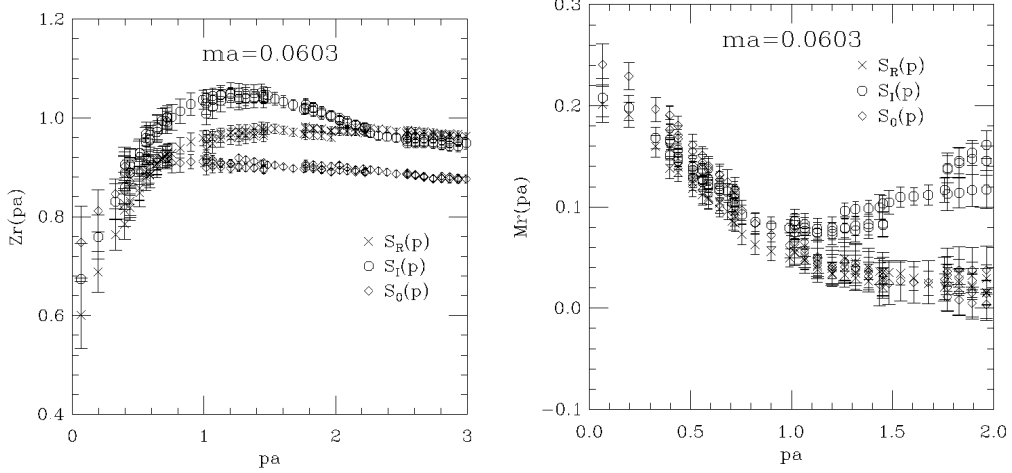


Fig. 21. *Left panel*: Lattice result for $Z_q(pa)$, where $a \simeq 2.0 \text{ GeV}^{-1}$ is the lattice spacing, calculated with $ma = 0.0603$. *Right panel*: Analogous plot for the mass function. (Adapted from ref. [268].)

function $Z_q(p^2)$ is infrared suppressed, *i.e.* the vector self-energy function $A(p^2)$ is infrared enhanced, and the mass function $M(p^2) = B(p^2)/A(p^2)$ approaches a value of $300 \pm 30 \text{ MeV}$ at $p^2 = 0$. The mass function $M(p^2)$ is a monotonically decreasing function of p^2 and the only surprise, if any, is given by the fact that $M(p^2)$ decreases more slowly than expected. The results of the most recent calculations are shown in fig. 21.

Recent lattice calculations of the running coupling are reported in refs. [272,169] based on the 3-gluon vertex, and ref. [258] on the quark-gluon vertex. The non-perturbative definitions of these couplings are related but manifestly different from the one adopted in sec. 5.3.3. The most recent result from the 3-gluon vertex shown in the right graph of fig. 22, is obtained from an asymmetric momentum subtraction scheme according to non-perturbatively requiring that the transverse part of the 3-gluon vertex at the renormalization point be given by,

$$\Gamma_{\mu\nu\rho}^T(p, -p, 0) := \mathcal{P}_{\mu\kappa}(p) \Gamma_{\kappa\sigma\rho}(p, -p, 0) \mathcal{P}_{\sigma\nu}(p) \quad (232)$$

$$\Gamma_{\mu\nu\rho}^T(p, -p, 0)|_{p^2=\mu^2} = \frac{1}{Z^{3/2}(\mu^2)} 2ip_\rho \mathcal{P}_{\mu\nu}(p) . \quad (233)$$

Comparing to the according $k \rightarrow 0$ limit of the vertex as given in sec. 5.3.2, one finds that this corresponds to a definition of the running coupling \bar{g}_{3GVas}^2 which can explicitly be related to the one of sec. 5.3.3 ($\bar{g}^2(t, g)$ with $t = \ln \mu'/\mu$ and $g := g(\mu)$),

$$\bar{g}^2(t, g^2)_{3GVas} = \bar{g}^2(t, g^2) \lim_{s \rightarrow 0} \frac{G^2(s)}{G^2(\mu'^2)} \left(1 - \frac{\beta(\bar{g}(t, g))}{\bar{g}(t, g)} \right)^2 , \quad (234)$$

where according to eq. (196) in sec. 5.3.3 it was used that,

$$\bar{g}^2(t, g^2) = g^2 G^2(\mu'^2) Z(\mu'^2) , \quad \mu'^2 \frac{d}{d\mu'^2} \left(\frac{2G'(\mu'^2)}{G(\mu'^2)} + \frac{Z'(\mu'^2)}{Z(\mu'^2)} \right) = \frac{d}{dt} \ln \bar{g}(t, g^2) . \quad (235)$$

An inessential difference in these two definitions of the running coupling is the last factor in

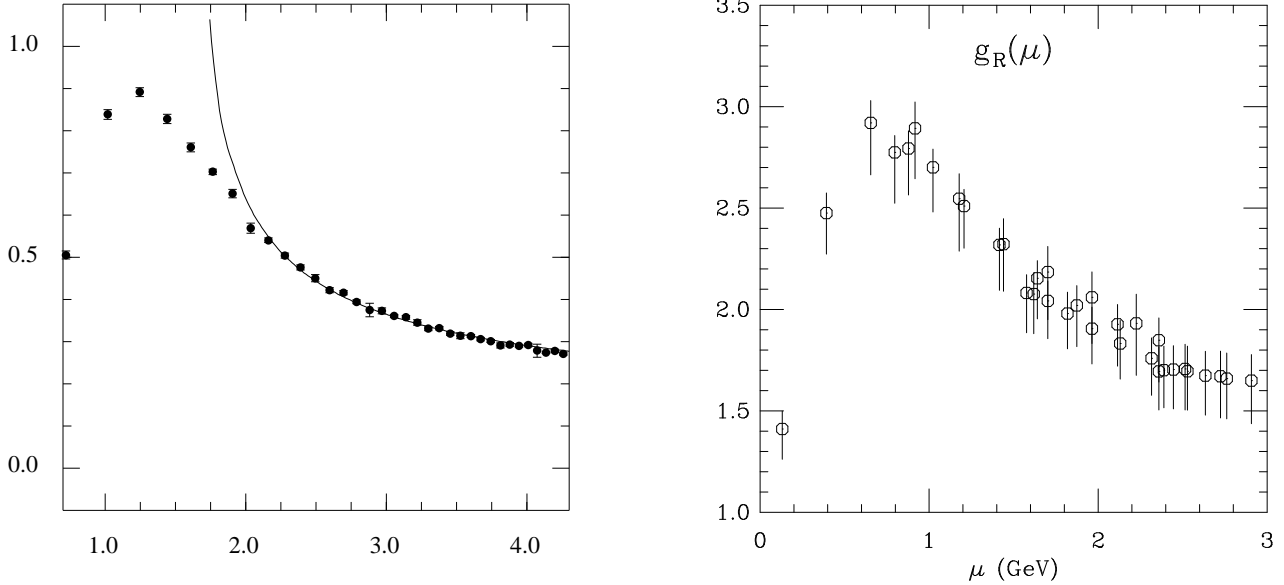


Fig. 22. Lattice results of the running coupling from the 3-gluon vertex (left, together with a 3-loop fit, fig. 1 of ref. [169]), and from the quark-gluon vertex for $\beta = 6.0$ on a $16^3 \times 48$ lattice (right, fig. 2 of ref. [258]).

brackets in eq. (234) which is what arises typically by choosing the 3-gluon vertex instead of the ghost-gluon vertex as is done here. This could of course be accounted for in comparing the results of the different schemes.⁵³ However, the crucial difference is the ratio of ghost renormalization functions $G(s \rightarrow 0)/G(\mu'^2)$. Of course, the lowest lattice momentum used in the calculation is not strictly zero but corresponds to some s_{min} . However, the considerations above show that the asymmetric scheme can be extremely dangerous if infrared divergences occur in vertex functions as the coupled system of DSEs indicates due to the infrared enhancement of the ghost propagator in Landau gauge. In particular, a large numerical factor arising from a large $G(s_{min})$ should thereby result in a quite different scale $\Lambda_{\tilde{MOM}}$ for the asymmetric scheme. The additional μ' -dependence from the ratio $G(s_{min})/G(\mu'^2)$ is harder to understand.⁵⁴ Clearly, from the infrared enhanced ghost renormalization function this scale dependence could account for the infrared suppressed couplings which seem to be found in the asymmetric schemes.

Similarly, the results from the quenched calculation of the quark-gluon vertex of ref. [258] given in the right graph of fig. 22 are obtained from an analogous asymmetric scheme (with the gluon momentum set to zero). It is thus expected to have the same problems in taking the possible infrared divergences of the vertices into account which arise in both, the 3-gluon and the quark-gluon vertex, as a result of the infrared enhancement of the ghost propagator, *c.f.* sec. 5.3.2.

⁵³ Differences in these definitions should actually occur at order g^6 , *i.e.*, at 3-loop level. Here they seem to occur at two-loop level. This is likely to be an artifact of the truncation scheme in the DSEs.

⁵⁴ Note that the perturbative limit, strictly speaking being *all* momenta timelike and large, is never really reached if one momentum is put to zero as in the asymmetric schemes. Therefore, one cannot expect to recover the perturbative anomalous dimension for the vertex in the asymmetric limit $\mu \rightarrow \infty$.

Furthermore, definitions of the coupling which lead to extrema at finite values of the scale correspond to double valued β -functions with artificial zeros. If the maxima in the couplings of the asymmetric schemes at finite scales $\mu = \mu_0$, as shown in fig. 22, are no lattice artifacts, these results seem to imply that the asymmetric schemes are less suited for a non-perturbative extension of the renormalization group to all scales $\mu \geq 0$. Indeed, the results for the running coupling from the 3-gluon vertex obtained for the symmetric momentum subtraction scheme in ref. [169] differ from those of the asymmetric scheme, in particular, in the infrared. The suppression of the coupling seems to be much weaker if not absent in the symmetric scheme. These results would be better to compare to the DSE solution, however, they unfortunately seem to be much noisier thus far (see ref. [169]).

The ultimate lattice calculation to compare to the present DSE coupling would be obtained from a pure QCD calculation of the ghost-gluon vertex in Landau gauge with a symmetric momentum subtraction scheme. This is unfortunately not available yet.

With regard to a later chapter, (*c.f.*, sec. 7.1), it is interesting to note that there exist a lattice calculation of diquark masses [273]. Hereby the nucleon, delta, quark and diquark correlation functions in Landau gauge are analyzed in order to extract information on the spin dependence of the quark-quark interaction. Evidence was found that the nucleon-delta mass splitting can be attributed to the spin dependence of the interaction between quarks in a colour anti-triplet state with spin 0 and 1, respectively. The lightest diquark excitations are observed in the S=0 channel, $m_{0^+} \approx 620$ MeV in the chiral limit. The mass of the spin 1 diquark as been estimated to be 730 MeV. In view of a quark constituent mass of approximately 310 MeV as found in the same calculation, however, no evidence for a deeply bound diquark state has been found.

6 Mesons as Quark–Antiquark Bound States

Mesons are bound states of quarks and antiquarks. Hereby the pions as (would-be) Goldstone bosons of the dynamically broken chiral symmetry play a special role. Resolving this dichotomous nature of the pions provides a strong constraint on an unified description of mesons. In the chiral limit quarks acquire a dynamical (constituent) mass. Then a method is required which respects chiral symmetry such that the pions become massless bound states. Phrased otherwise, the binding energy between quarks and antiquarks in the pion channel has to match exactly two times the constituent quark mass. It is obvious that only a fully Lorentz covariant scheme can yield a satisfactory representation of pions. We will see in this chapter that this is indeed possible.

6.1 Bethe–Salpeter Equation for Mesons

Applications of the QCD propagators in Bethe–Salpeter (BS) equations [274] have progressed during the last few years considerably. One caveat has to be mentioned, however. Almost all of these investigations rely on the rainbow–ladder approximation of the systems of DSEs and BS equations. One important exception will be discussed in detail in sec. 7.1 where it will be demonstrated that the rainbow–ladder scheme is a less dangerous approximation for pseudoscalar and vector meson calculations than for diquark calculations. Nevertheless, including a non–trivial quark–gluon vertex function in a way that is chiral symmetry preserving is highly desirable but nobody succeeded yet in such an undertaking. In ref. [275] a general scheme for a consistent treatment of DSEs and BS equations has been formulated, however, it has not been realized with a realistic quark–gluon vertex constructed from the Slavnov–Taylor identities. Therefore, in the following subsections we will discuss the generalized ladder BS equation, *i.e.* with dressed propagators, for mesons.

6.1.1 Derivation of the Ladder Bethe–Salpeter Equation

The important step in the derivation of the homogeneous BS equation from the inhomogeneous one is to realize that two–particle bound states can be identified through the occurrence of poles in the corresponding four–point Green’s function. From the homogeneous BS equation which assumes the form of an eigenvalue problem in the ladder approximation one can determine the bound state masses and covariant wave functions. Hereby the bound state mass has to be tuned such that the BS eigenvalue equals the given value of the coupling constant. The covariant wave functions are then determined as the eigenfunctions of the system.

Restricting ourselves to the rainbow–ladder approximation the fermion–antifermion BS equations for QED and QCD are identical up to straightforwardly computable colour algebra factors. Thus the derivation presented in this section is equally valid for QED and QCD. Hereby the starting point is the generating functional as given in sec. 2.1. In sec. 3.3 we have already discussed an inhomogeneous BS equation. Deriving the effective action Γ_{QED} with respect to the gauge boson, the fermion and the antifermion field defines the fermion–photon vertex (78)

whose DSE (115) is the inhomogeneous BS equation:

$$\Gamma_\mu(q, p) = Z_2 \gamma_\mu + \int \frac{d^4 l}{(2\pi)^4} S(q + l) \Gamma_\mu(q + l, p + l) S(p + l) K(p + l, q + l, l). \quad (115)$$

The kernel K is defined as the sum of all amputated two-particle irreducible contributions and is pictorially represented in fig. 6. As described in sec. 3.3 the transverse part of the quark-photon vertex has a pole at momenta corresponding to the vector meson mass. Of course, one can derive inhomogeneous BS equations for the scalar, pseudoscalar, axialvector and tensor channel of the quark-antiquark bound state. These vertex functions will have poles related to the respective meson masses. This property can be exploited to derive the homogeneous BS equation.

In order to keep the following discussion as transparent as possible we will demonstrate the underlying principle using scalar fields. We assume to deal with three types of scalar fields. The two constituents are supposed to have masses m_1 and m_2 and self-energies Σ_1 and Σ_2 . The four-point function $G^{(4)}(x_1, x_2, y_1, y_2)$ describing the scattering of these two constituents fulfills the inhomogeneous Bethe-Salpeter equation

$$\begin{aligned} & \left((\partial_\mu \partial^\mu)_{x_2} + m_2^2 - \Sigma_2 \right) \left((\partial_\mu \partial^\mu)_{x_1} + m_1^2 - \Sigma_1 \right) G^{(4)}(x_1, x_2, y_1, y_2) = \\ & \delta^{(4)}(x_1 - y_1) \delta^{(4)}(x_2 - y_2) + \delta^{(4)}(x_1 - y_2) \delta^{(4)}(y_1 - x_2) \\ & + \int d^4 z_1 d^4 z_2 K(x_1, y_1, z_1, z_2) G^{(4)}(z_1, z_2, y_1, y_2). \end{aligned} \quad (236)$$

As already stated the kernel K is the sum of all amputated two-particle irreducible contributions, see fig. 6. Note that the introduction of the relative coordinate $x = x_1 - x_2$ allows an arbitrary parameter $\eta_P \in [0, 1]$ in defining the coordinate $X = \eta_P x_1 + (1 - \eta_P) x_2$ which results after transforming to momentum space in the corresponding momenta

$$p_1 = \eta_P P + p \quad \text{and} \quad p_2 = (1 - \eta_P) P - p \quad (237)$$

for the constituents in terms of the total and relative momenta, P and p , respectively. Fourier transforming eq. (236) leads to

$$\int \frac{d^4 p'}{(2\pi)^4} [D(p, p', P) + K(p, p', P)] G^{(4)}(p', p'', P) = \delta^{(4)}(p - p''), \quad (238)$$

where

$$D(p, p', P) := (2\pi)^4 \delta^{(4)}(p - p') \left(G_1^{(2)} \right)^{-1}(p_1) \left(G_2^{(2)} \right)^{-1}(-p_2) \quad (239)$$

is defined in terms of the inverse two-point Green's functions of the constituents.

The crucial step from the inhomogeneous to the homogeneous Bethe-Salpeter equation consists in assuming a bound state reflecting itself in a pole in the four-point Green's function for an

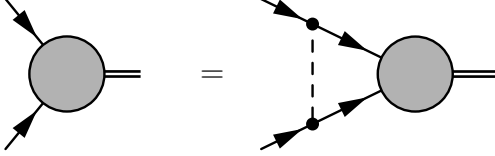


Fig. 23. Pictorial representation of the homogeneous Bethe–Salpeter equation in ladder approximation.

on–shell momentum P_{os} , with $P_{os}^2 = -M^2$

$$G^{(4)}(p, p', P_{os}) = \frac{-i}{(2\pi)^4} \frac{\chi(p, P_{os}) \bar{\chi}(p', P_{os})}{2\omega(P^0 - \omega + i\epsilon)} + \text{reg. terms}, \quad \omega := \sqrt{\mathbf{P}^2 + M^2}. \quad (240)$$

Here we introduced the definition of the Bethe–Salpeter amplitudes

$$\begin{aligned} \chi(x_1, x_2, P) &:= \langle 0 | T \{ \Phi(x_1) \Phi(x_2) \} | P \rangle, \\ \bar{\chi}(x_1, x_2, P) &:= \langle 0 | T \{ \Phi^\dagger(x_1) \Phi^\dagger(x_2) \} | P \rangle, \end{aligned} \quad (241)$$

together with their Fourier transforms

$$\begin{aligned} \chi(x_1, x_2, P) &=: e^{-iPX} \int \frac{d^4 p}{(2\pi)^4} e^{-ipx} \chi(p, P), \\ \bar{\chi}(x_1, x_2, P) &=: e^{+iPX} \int \frac{d^4 p}{(2\pi)^4} e^{-ipx} \bar{\chi}(p, P). \end{aligned} \quad (242)$$

Hereby $|0\rangle$ denotes the ground state (vacuum) and $|P\rangle$ the bound state. Very close to the pole the regular terms can be safely neglected and the dependence of the four–point function on the relative momenta p and p' can be separated. Expanding $G^{(4)}$ and $[D - K]$ in the inhomogeneous Bethe–Salpeter equation in powers of $(P^0 - \omega)$ yields the homogeneous Bethe–Salpeter equation and the normalisation condition for the amplitude. The order $(P^0 - \omega)^{-1}$ provides

$$\int \frac{d^4 p'}{(2\pi)^4} [D(p, p', P_{os}) + K(p, p', P_{os})] \chi(p, P_{os}) = 0, \quad (243)$$

whereas to $\mathcal{O}((P^0 - \omega)^0)$ one obtains

$$\begin{aligned} \int \frac{d^4 p}{(2\pi)^4} \frac{d^4 p'}{(2\pi)^4} \text{tr} \left(\bar{\chi}(p, P_{os}) \frac{\partial}{\partial P^0} (D(p, p', P) + K(p, p', P)) \Big|_{P^0=\omega} \chi(p', P_{os}) \right) \\ = 2i\omega. \end{aligned} \quad (244)$$

This ensures the residue to be equal to 1 at the bound state pole.

The homogeneous Bethe–Salpeter equation (243) is a linear integral equation for the amplitude χ whose overall normalisation is fixed by (244). Approximating the kernel by the one–boson–

exchange depicted in the first diagram of fig. 6, eq. (243) can be cast into an eigenvalue problem for the coupling constant by using the vertex function $\Gamma(p_1, p_2)$ instead of the amplitude:

$$\chi(p, P) =: G_1(p_1) G_2(p_2) \Gamma(p_1, p_2) . \quad (245)$$

In the context of BS equations it is advantageous to use the total and relative momenta, see eq. (237), as arguments of the vertex functions, $\Gamma(p_1, p_2) \rightarrow \Gamma(p; P)$. The homogeneous BS equation (243) then in terms of the vertex function then reads

$$\Gamma(p; P_{os}) = - \int \frac{d^4 p'}{(2\pi)^4} K(p, p', P_{os}) G_1(p'_1) G_2(p'_2) \Gamma(p'; P_{os}) . \quad (246)$$

In the ladder approximation the kernel K is set equal to the propagator of the exchange particle multiplied with the coupling constant for each vertex, *i.e.* with g^2 . On inspection one finds that (246) is an eigenvalue problem for g^2 if G_1 and G_2 are the bare propagators of the constituents. The ladder approximation to the BS equation is pictorially represented in fig. 23. If a parameter pair $(g^2, P^0 = M)$ exists the pole assumption is *a posteriori* justified and M is the bound state mass with χ being the corresponding amplitude (wave function) as can be inferred from eq. (240) which reflects, of course, nothing else than the Lehmann representation of the four-point function.

The description of mesons, and especially the one of pions, requires to use a generalized ladder approximation: The intrinsically non-perturbative nature of bound-state problems, and the complex structure of the QCD vacuum, necessitates that one employs non-perturbative gluon and quark propagators in the BSE kernel. There have been many studies of meson spectroscopy using this framework; summaries can be found in refs. [28–30]. Typically, such studies employ an ansatz for the gluon propagator in solving the rainbow-approximation quark DSE and pair the input gluon propagator and calculated quark propagator to construct the non-perturbatively dressed-ladder approximation kernel for the meson BS equation. The resulting BS equation is then solved to obtain the spectrum. This rainbow-ladder truncation has the feature that Goldstone’s theorem is manifest; *i.e.* in the chiral limit, when the current quark mass $m_q = 0$, the pion is a zero-mass bound state in strongly dressed quark-antiquark correlations [276]. As we will see in the following, with few-parameter models for the gluon propagator, this can be used to provide fair descriptions of the light-light, light-heavy and heavy-heavy meson spectra and decays.

In order to keep the notation readable we introduce “multiple indizes” $E = \{i_c, i_f, i_D\}$ associated with the color, flavor and Dirac structure of the amplitude. The homogenous BS equation for the vertex function Γ_M , the subscript M denoting meson, then reads:

$$\begin{aligned} \Gamma_M^{EF}(p; P) = & \\ \int \frac{d^4 k}{(2\pi)^4} K_M^{EF; GH}(k, p; P) \left(S(k + \frac{1}{2}P) \Gamma_M(k; P) S(k - \frac{1}{2}P) \right)^{GH} , \end{aligned} \quad (247)$$

where we have symmetrized the momenta of the quark legs for reasons which will become obvious soon. The rainbow approximation to the quark DSE is defined by using a bare quark

gluon vertex ($\Gamma_\mu(k, p) \equiv \gamma_\mu$). The corresponding generalized ladder approximation is given by the by the choice

$$\begin{aligned} K_M^{EF;GH}(k, p; P) & \left(S(k + \frac{1}{2}P) \Gamma_M(k; P) S(k - \frac{1}{2}P) \right)^{GH} \\ & \equiv -g^2 D_{\mu\nu}(p - k) \left(\gamma_\mu \frac{\lambda^a}{2} S(k + \frac{1}{2}P) \Gamma_M(k; P) S(k - \frac{1}{2}P) \gamma_\nu \frac{\lambda^a}{2} \right)^{EF} \end{aligned} \quad (248)$$

for the kernel in eq. (247). This form of the kernel together with the rainbow quark DSE preserve the Goldstone boson character of the pion. In the chiral limit $m_q = 0$ this can be demonstrated by substituting in the rainbow DSE for the quark self-energy (defined by $S^{-1}(p) =: i\gamma \cdot p + \Sigma(p)$),

$$\Sigma(p) = m_q + g^2 \frac{4}{3} \int \frac{d^4 k}{(2\pi)^4} \gamma_\mu S(k) \gamma_\nu D_{\mu\nu}(p - k), \quad (249)$$

the expression

$$\gamma_\mu S(k) \gamma_\nu \rightarrow \gamma_\mu S(k + P/2) \Gamma_M(k, P) S(k - P/2) \gamma_\nu. \quad (250)$$

Straightforward algebra leads then to the BS equation in the pseudoscalar channel with $P^2 = 0$ [276].⁵⁵ Therefore, in the chiral limit a massless bound state is found in the pion channel when employing the rainbow-ladder scheme. An equivalent derivation can be based on the observation that in the chiral limit the pion vertex function at total momentum $P = 0$ can be obtained via an infinitesimal chiral rotation of the quark self-energy,

$$\tau_{ij}^a \Gamma^{ij}(p, P = 0) = -i \frac{d}{d\alpha^a} \left(e^{i\alpha^a \frac{1}{2}\tau^a \gamma_5} \Sigma(p) e^{i\alpha^a \frac{1}{2}\tau^a \gamma_5} \right)_{\alpha^a=0} = \frac{1}{2} \tau^a \{ \gamma_5, \Sigma(p) \} \quad (251)$$

where a and ij are obvious flavour indices.

Before we are going to discuss the solutions of the ladder BS equations for the ground state mesons two comments on general properties are, however, in order.

6.1.2 Solutions of the Ladder Bethe-Salpeter Equation in Minkowski Space

An Euclidean formulation is used throughout this review which, as described in the beginning of chapter 2, has its justification in the fact that the domain of holomorphy for the Green's function of a quantum field theory (fulfilling the usual axioms) allows a complex extension of the Euclidean space. The on-shell momenta of bound states introduced in the last section are time-like and have to be represented as complex four-vectors in an analytically continued Euclidean formulation. Being justified formally, at least for quantum field theories without

⁵⁵ An extension of this constructive way to preserve the Goldstone boson character of the pion will be presented in sec. 7.1.1.

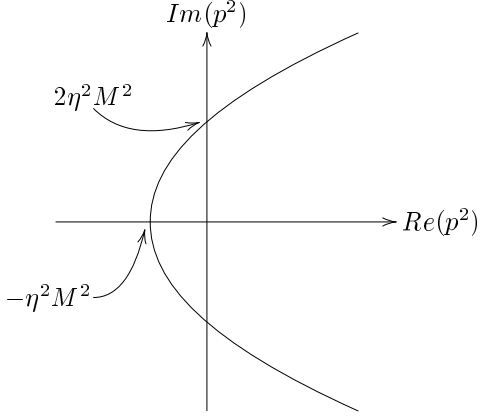


Fig. 24. Plot of the complex p^2 plane. The interior of the parabola shows the subset of the complex plane where the BS equation 'probes' the propagators of the constituents. M is the mass of the bound state and η is the momentum partitioning parameter.

complications like confinement, there are inherent practical difficulties, however. Looking at eq. (247) one realizes that the quark propagators have to be known in a parabolic region of the complex p^2 -plane. This region includes the real positive p^2 (half-)axis, and it extends to $p^2 = -M^2/4$ on the negative real axis and to $p^2 = \pm iM^2/2$ on the imaginary axes, see fig. 24. (Of course, this region depends on the momentum partitioning parameter η_P . It extends either to $p^2 = -M^2/\eta_P^2$ or $p^2 = -M^2/(1 - \eta_P)^2$ such that the case $\eta_P = 1/2$ is the one where least of the complex p^2 plane has to be known.) If the kernel of the quark DSE, *i.e.* in rainbow approximation the gluon propagator, is a known analytic function in this parabolic region it is possible to solve the BS equation without further approximation, see sec. 6.2 for a discussion of such calculations. If, however, the kernel of the quark DSE is known only numerically on the spacelike p^2 -axis, or if there are singularities in these parabolic region (note that the point $p^2 = 0$ is contained in this region for all bound state masses), or if both these statements are true, a reliable evalution of the (ladder) BS kernel is virtually impossible.

Thus a solution of the DSE directly in Minkowski space might provide some new insight. Rewriting the integrals in the fermion DSE in rainbow aproximation with the help of dispersion relations it is possible to solve this equation directly in Minkwoski space [277]. However, for the extraction of the imaginary part it has been a necessary prerequisite that the analytic structure of the kernel is known explicitely. In ref. [277] either a bare gauge boson propagator or a bare gauge boson propagator multiplied with a logarithmically running coupling has been used. Of course, the obtained results are in accordance with the one obtained from the Euclidean DSE. Another Minkowski space study of DSEs is employing the perturbation theory integral representation (see below) in scalar ϕ^3 theory [278]. This work is, however, still unpublished.

In refs. [279,280] the ladder BS equation for a scalar–scalar bound state with scalar exchange has been solved in Minkowski space using the perturbation theory integral representation

[281]. This representation is an extension of the spectral representation for two-point Green's functions. Hereby, for the relatively simple kernels tested so far, the results for bare and dressed ladder kernels are in complete agreement with the results obtained from an Euclidean approach and Wick rotation. The main advantage of this method would, however, become vital when using non-ladder kernels. Note that beyond ladder approximation the naive Wick rotation is not possible, *i.e.* one has to choose much more complicated integration contours. Furthermore, the method is quite general and also applicable if no Wick rotation is possible at all. Also in these cases it could provide the vertex function and the amplitude for the entire allowed range of momenta. Therefore, progress in this direction would be highly desirable.

6.1.3 (In-)Consistency of the Relativistic Description of Excited States

At first sight the BS equation seems very suited to describe excited states. Interpreting the spectrum of the homogeneous BS equation is, however, far from being trivial [282]. Common to the analytical⁵⁶ and the numerical solutions is the existence of abnormal states which have led to controversial discussions regarding their physical interpretation [283–285]. Even worse, for the case of constituents with unequal masses some eigenvalues of the homogeneous Bethe–Salpeter equation become complex [286,287]. Clearly, such a behavior is unexpected and has to be understood. It has been usually attributed to the use of the ladder approximation [283] which destroys crossing symmetry from the very beginning. This conjecture in its strict form is, however, refuted: Going beyond ladder approximation and employing also crossed ladder exchanges the abnormal states still exists [288]. In this section we will provide evidence that the use of a dressed ladder kernel is absolutely required if one wants to interpret the spectrum of the BS equation [282].

The abnormal solutions are “excitations in relative time”. They will obviously not appear in a purely non-relativistic treatment where the constituents are considered for equal times only.⁵⁷ In the Wick–Cutkosky model [283,284] with constituents of equal masses $m_1 = m_2 = m$ these abnormal states are easily identified: They only exist for certain values of the coupling constant ($\lambda := g^2/16\pi^2m^2 > \lambda_c = 1/4$). If the binding energy becomes very small the corresponding coupling constant λ vanishes for the normal solutions, *i.e.* $\lambda \rightarrow 0$, whereas $\lambda \rightarrow \lambda_c = 1/4$ for the abnormal states. The latter behavior is completely unexpected, a vanishing binding energy should be related to no coupling at all. It can be shown that in this model the abnormal solutions possesses nodes when plotted as a function of the relative time. For all normal solutions, including the ground state, there are no nodes in relative time. It has to be noted, however, that for a general BS equation there is no known method to identify abnormal states.

The appearance of complex eigenvalues is related to a crossing of an abnormal with a normal

⁵⁶ The only analytically solvable example of a BS equation is the one for two (massive) scalar particles bound by the ladder approximation to the exchange of a massless scalar field [283–285]. Despite its relative simplicity as compared to realistic systems this model, the Wick–Cutkosky model, displays already the advantages (*e.g.* full covariance) as well as the shortcomings (*e.g.* the existence of abnormal states) inherent to almost all Bethe–Salpeter based approaches used until today.

⁵⁷ However, not all abnormal solutions necessarily vanish in a three-dimensional reduction of the BS equation [289]. On the contrary, the spectrum of a three-dimensionally reduced equation will contain remnants of these abnormal states.

M, μ	symmetry group	BS amplitude
$M = 0, \mu = 0$	$O(5)$	$\chi \propto Z_{nklm}(\Omega_5)$
$M = 0, \mu \neq 0$	$O(4)$	$\chi \propto Z_{klm}(\Omega_4)$
$M \neq 0, \mu = 0$	$O(4)$	$\chi \propto Z_{klm}(\Omega_4)$
$M \neq 0, \mu \neq 0$	$O(3)$	$\chi \propto Y_{lm}(\Omega_3)$
$\mu \rightarrow \infty$	$O(4)$	$\chi \propto Z_{klm}(\Omega_4)$

Table 1

Summary of the symmetries of the scalar BS equation in ladder approximation. μ denotes the mass of the exchange particle and M is the Mass of the bound state. The functions Z (or Y) denote the spherical harmonics for the corresponding n -sphere Ω_n . (Adopted from ref. [282].)

(or abnormal) state [282]. Therefore, this problem is related to the existence of abnormal states. It occurs for a wide range of parameters. Increasing the mass of the exchange particle the higher lying eigenvalues tend to become real again. This can be understood from the fact that for an infinitely heavy exchange particle the BS equation assumes an $O(4)$ symmetric form as in the case of an massless exchange particle, see also table 1 which summarises the symmetries of the scalar ladder BS equation. It is interesting to note that the ladder BS spectrum of QED also shows such a phenomenon [282]. First, one has to note that for QED in Feynman gauge there exists a continuum of solutions for $\alpha = e^2/4\pi > \pi/4 := \alpha_c$ [290]. Using a finite mesh for the numerical calculation this continuum of eigenvalues⁵⁸ is represented by discrete eigenvalues which become more dense for a finer mesh. In this continuum there are abnormal states and there occur crossings between these states, *i.e.* complex eigenvalues.⁵⁹

The important point to notice is that the scalar model possesses a critical coupling beyond which the one-particle propagators are not renormalizable [293,282]. For acceptable values of the coupling no abnormal solutions to the BS equation exists. As for quenched QED one has to notice that the critical value of the coupling for DB χ S is $\alpha_c = \pi/4$ in Feynman gauge. Furthermore, from the discussion in sec. 4.3 it is clear that in quenched QED in rainbow approximation no finite mass solution for the fermion DSE exists for values of the coupling exceeding the critical one. On the other hand, for couplings below the critical coupling no

⁵⁸ This continuum of eigenvalues should be not confused with a physical continuum, *i.e.* the existence of scattering solutions. Here we are discussing the formal spectrum of the BS equation. The Goldstein continuum discussed here would imply (if taken at face value) that for all couplings $\alpha > \pi/4$ normalizable solutions with any bound state mass between zero and two times the constituent mass should exist.

⁵⁹ The existence of complex eigenvalues has also been observed for an axialvector state in the ladder BS equation of 2+1-dimensional QED with one four-component flavour, *i.e.* in the confining phase [291]. The poles of the fermion propagator (calculated in the corresponding rainbow approximation) come in complex conjugate pairs thereby signaling violation of positivity. It is suggestive that the complex eigenvalues of the BS equation appear for values of the fermion bare mass m for which $-\text{Re}(p_{\text{pole}}^2) > \text{Im}(p_{\text{pole}}^2)$ as can be inferred by comparing table I in ref. [292] with table II in ref. [291]. On the other hand, in the non-relativistic limit $m \gg e^2$ this state exists again and becomes degenerate with the positive parity scalar state. Furthermore, in ref. [291] unnatural parity states have been observed. It is quite likely that these states are abnormal states, *i.e.* excitations in relative time.

abnormal states appear in the spectrum of the BS equation. Therefore, this two examples provide evidence that there is no problem with abnormal states as long as one applies the BS equation only for values of the coupling constant where the underlying theory is renormalizable and the full renormalized two-point functions are well-defined [282]. The important warning to keep in mind, however, is: Calculating excited states from the BS equation (or from a three-dimensional reduction of it) one first has to clarify the issue of abnormal states. On the other hand, the use of the BS equation for the corresponding ground states is quite safe.

6.2 Ground State Mesons

6.2.1 The Goldstone Boson Sector

Pions (and kaons) are very special. First of all, they are the lightest hadrons and therefore play a significant role in nuclear physics as they provide the long-range part of the nucleon-nucleon interaction. Furthermore, they are produced in almost all reactions involving hadrons ranging from intermediate energy electron-nucleon to ultrarelativistic heavy ion collisions. As stated already in the last section their low mass can be understood from the approximate chiral symmetry of QCD. Furthermore, symmetry considerations provide the BS amplitude in the chiral limit, see eq. (251). However, in the real world with explicit current quark masses the situation is much more complex as revealed by the up to now most complete study of the pion and kaon BS amplitudes [259].

The considerations in the last section demonstrated that the quark self-energy has to be determined first. Identical kernels of the quark rainbow DSE and the meson ladder BSE have hereby to be chosen. The authors of ref. [259] employed a model kernel of the form $4\pi\alpha(k^2)/k^2$ with

$$\alpha(k^2) = 2\pi^3 D k^2 \delta^{(4)}(k) + \pi D \frac{k^4}{\omega^6} e^{-k^2/\omega^2} + \frac{\pi \gamma_m (1 - \exp(-k^2/4m_t^2))}{\frac{1}{2} \ln \left[\tau + \left(1 + k^2/\Lambda_{\text{QCD}}^2 \right)^2 \right]} \quad (252)$$

where $\gamma_m = \frac{12}{33-2N_f} = \frac{12}{25}$ is the anomalous dimension of the quark mass ($N_f = 4$ has been used in ref. [259]), and a value of $\Lambda_{\text{QCD}}^{N_f=4} = 0.234 \text{ GeV}$ has been assigned. The parameter $\tau = e^2 - 1$ is chosen such that the perturbative Landau pole is screened and the denominator of the last term in eq. (252) becomes identical to one as k^2 vanishes. Obviously, this last term is proportional to k^2 for low momenta and identical to the known 1-loop behaviour at large k^2 . The parameter m_t has hereby been fixed to be $m_t = 0.5 \text{ GeV}$. The second term is modeled to provide interaction strength at intermediate momenta of a few hundred MeV. To achieve this, values $\omega = 0.3 \text{ GeV}$ and $D = 0.781 \text{ GeV}^2$ have been used in ref. [259]. The first term, being a delta function (adopted from ref. [254]), leads to a quark propagator with complex conjugate poles, *i.e.* to a positivity violating one. Choosing at a scale of 1 GeV the current masses to be $m_u^{1 \text{ GeV}} = 5.5 \text{ MeV}$, $m_s^{1 \text{ GeV}} = 130 \text{ MeV}$ “Euclidean” constituent masses of 560 MeV for up/down and 700 MeV for strange quarks are obtained.

The ladder BS equation in the pseudoscalar channel is an eigenvalue for the vertex function.

This vertex function does not only involve a pseudoscalar term as in eq. (251) but has the general form [294]

$$\begin{aligned}\Gamma_H(k; P) = & T^H \gamma_5 \left[iE_H(k; P) + \gamma \cdot P F_H(k; P) \right. \\ & \left. + \gamma \cdot k k \cdot P G_H(k; P) + \sigma_{\mu\nu} k_\mu P_\nu H_H(k; P) \right],\end{aligned}\quad (253)$$

where T^H is the flavour Gell–Mann matrix for the meson H , *e.g.* $T^{K^+} = \frac{1}{2}(\lambda^4 + i\lambda^5)$. For bound states with equal mass constituents the scalar functions E_H , F_H , G_H and H_H are even under $k \cdot P \rightarrow -k \cdot P$. In general, the subleading Dirac components of $\Gamma_H(k; P)$ and therefore the functions $F_H(k; P)$, $G_H(k; P)$ and $H_H(k; P)$ are nonzero.

To understand the relation of these functions to the quark propagator one considers the renormalised axial–vector Ward–Takahashi in the chiral limit

$$-iP_\mu \Gamma_{5\mu}^H(k; P) = S^{-1}(k_+) \gamma_5 \frac{T^H}{2} + \gamma_5 \frac{T^H}{2} S^{-1}(k_-). \quad (254)$$

In the chiral limit the axial–vector vertex has the form

$$\begin{aligned}\Gamma_{5\mu}^H(k; P) = & \frac{T^H}{2} \gamma_5 \left[\gamma_\mu F_R(k; P) + \gamma \cdot k k_\mu G_R(k; P) - \sigma_{\mu\nu} k_\nu H_R(k; P) \right] \\ & + \tilde{\Gamma}_{5\mu}^H(k; P) + f_H \frac{P_\mu}{P^2} \Gamma_H(k; P),\end{aligned}\quad (255)$$

where F_R , G_R , H_R and $\tilde{\Gamma}_{5\mu}^H$ are regular as $P^2 \rightarrow 0$. Note that $P_\mu \tilde{\Gamma}_{5\mu}^H(k; P) \sim \mathcal{O}(P^2)$, and $\Gamma_H(k; P)$ is the pseudoscalar BS amplitude of eq. (253). The residue of the pseudoscalar pole in the axial–vector vertex is f_H , the leptonic decay constant of the meson H . The chiral limit axial–vector Ward–Takahashi identity (254) imply

$$f_H E_H(k; 0) = B(k^2), \quad (256)$$

$$F_R(k; 0) + 2f_H F_H(k; 0) = A(k^2), \quad (257)$$

$$G_R(k; 0) + 2f_H G_H(k; 0) = 2A'(k^2), \quad (258)$$

$$H_R(k; 0) + 2f_H H_H(k; 0) = 0, \quad (259)$$

where $A(k^2)$ and $B(k^2)$ are the quark propagator functions. Note that eq. (256) is identical to eq. (251). Surprisingly, these equations, however, imply that the subleading Dirac structures are non–vanishing in the chiral limit.

The BS equation has been solved in ref. [259] by a direct numerical solution of the multidimensional integral equation and by employing an expansion of the functions E , F , G and H in Chebyshev polynomials in $k \cdot P / \sqrt{k^2 P^2}$. This expansion converges quickly, and two moments are sufficient to obtain an accurate solution. This is also seen from the fact that physical observables calculated with these solutions are independent of the arbitrary momentum partitioning parameter η_P , see eq. (237). Note that this has been considered problematic in older

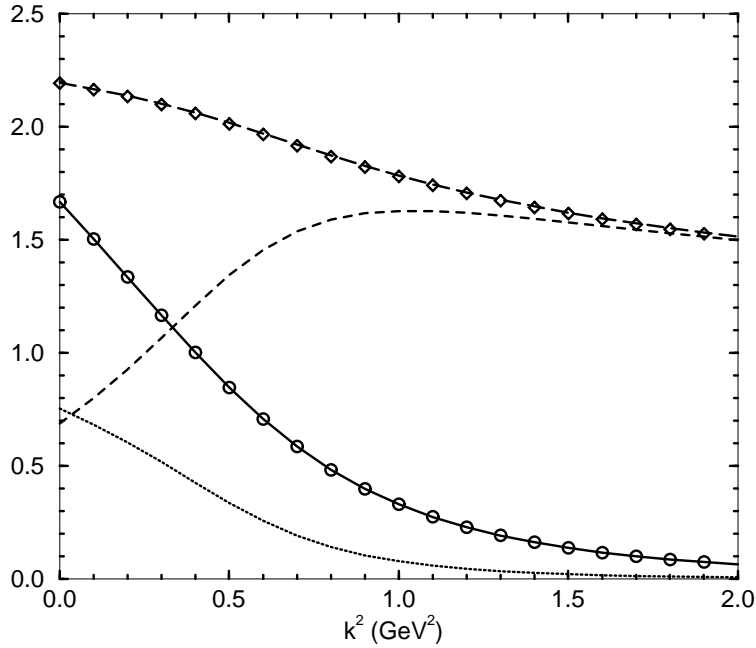


Fig. 25. An illustration of the realisation of the identities eqs. (256) and (257), which are a necessary consequence of preserving the axial vector Ward-Takahashi identity. Shown is $f^0 E_H(k; 0)$ (GeV, solid line); $F_R(k; 0)$ (dimensionless, dashed line); $f^0 F_H(k; 0)$ (dimensionless, dotted line); and $F_R(k; 0) + 2 f_H F_H(k; 0)$ (long-dashed line). In each curve the plotted points represent the right-hand-side of these equations as obtained in the solution of the chiral-limit quark DSE: $B(k^2)$ (GeV, \circ); $A(k^2)$ (dimensionless, \diamond). (Adapted from ref. [259].)

studies of the BS equation [295] where only the leading order Chebyshev moments have been kept in the numerical solution.

The Goldstone boson character of the flavour–nonsinglet pseudoscalar has been made explicit in the BS description as relativistic QCD bound states. Hereby the axial–vector Ward–Takahashi identity is the key to realize the importance of the non–leading Dirac invariants in the pseudoscalar BS amplitudes [259,296,297]. This axial–vector Ward–Takahashi identity is in turn then seen in the numerical solution, see fig. 25. Thus we summarize this subsection by stating that reliable BS amplitudes for pions and kaons are available. As we will see in the following this is very helpful for calculating observables in hadronic processes.

6.2.2 A Dynamical η' Mass

In the preceding subsection the flavour–singlet pseudoscalar meson, the η' , has not been considered. Of course, due the anomalous, *i.e.* explicit, breaking of the $U_A(1)$ chiral symmetry the η' is not a Goldstone boson.

More than twenty years ago Kogut and Susskind pointed out that for dimensional reasons a non–vanishing contribution to the mass of the pseudo–scalar flavor–singlet meson in the chiral

limit can result from its mixing with two non-perturbatively infrared enhanced gluons, corresponding to a momentum space propagator $D(k) \sim \sigma/k^4$ for $k^2 \rightarrow 0$ [298]. The identification of the string tension σ shows that effects due to infrared enhanced gluons can be expected to be complementary to instanton models. In particular, a description of the $\eta - \eta'$ mixing driven by the string tension [299,300], provides an interesting alternative to the standard solution of the $U_A(1)$ problem by instantons.

Phenomenologically, this mixing is described by the $\eta_8 - \eta_0$ mass matrix [301,302],

$$\frac{1}{2} \begin{pmatrix} \eta_8 & \eta_0 \end{pmatrix} \begin{pmatrix} \frac{4}{3}m_K^2 - \frac{1}{3}m_\pi^2 & \frac{2}{3}\sqrt{2}(m_\pi^2 - m_K^2) \\ \frac{2}{3}\sqrt{2}(m_\pi^2 - m_K^2) & \frac{2}{3}m_K^2 + \frac{1}{3}m_\pi^2 + \frac{2N_f}{f_0^2}\chi^2 \end{pmatrix} \begin{pmatrix} \eta_8 \\ \eta_0 \end{pmatrix} \quad (260)$$

where the screening mass in the flavor-singlet component, $m_0^2 := 2N_f\chi^2/f_0^2$, is given by a non-vanishing topological susceptibility,

$$\chi^2 := \frac{g^2}{(32\pi^2)^2} \int d^4x \langle \tilde{G}G(x) \tilde{G}G(0) \rangle \quad \text{with} \quad (261)$$

$$\tilde{G}G = \epsilon^{\mu\nu\rho\sigma} 2\partial_\mu \text{tr}(A_\nu \partial_\rho A_\sigma - ig \frac{2}{3} A_\nu A_\rho A_\sigma) .$$

In the Instanton Liquid Model the topological susceptibility, given by the density of instantons, is $\chi^2 \approx 1\text{fm}^{-4}$, and the mass eigenvalues are $m_\eta \approx 530\text{MeV}$, $m_{\eta'} \approx 1170\text{MeV}$ together with a mixing angle of $\theta \approx -11.5^\circ$ [303]. This has to be compared with the experimental values $m_\eta = 547\text{MeV}$ and $m_{\eta'} = 959\text{MeV}$.

Recently, indirect $SU(3)$ flavor breaking in the pseudoscalar meson mass matrix has been considered [304], *i.e.* the assumption that the topological susceptibility leads only to a flavor-singlet component of the mass matrix has been relaxed. Hereby, the corresponding “weakening” parameter in the strange sector, $X = 0.663$, has been determined from the two-photon amplitudes $\pi^0, \eta, \eta' \rightarrow \gamma\gamma$ calculated in a DSE based approach (see also Sect. 6.2.5 below). The corresponding results are $m_\eta = 588\text{MeV}$, $m_{\eta'} = 933\text{MeV}$ and $\theta = -13.4^\circ$. One sees that this indirect flavor symmetry breaking improves the agreement with the phenomenological η and η' masses considerably. On the other hand, as this effect is of quantitative importance only we will ignore it in the rest of this section and discuss the qualitative features.

To explore the effect of infrared enhanced quark interactions, one concentrates on the mixing of the flavor-singlet pseudo-scalar with two uncorrelated gluons. According to the Kogut-Susskind argument, for infrared enhanced gluons $\sim \sigma/k^4$, the corresponding diagram, see Fig. 26, can contribute to the topological susceptibility for the meson momentum $P \rightarrow 0$. Of course, this diagram is not the only one capable of providing such a contribution [305], however, the consideration of this leading term should be sufficient to demonstrate the effect qualitatively and to provide a semi-quantitative estimate. To explore the Kogut-Susskind conjecture, the following model interaction for quarks in the Landau gauge has been used in

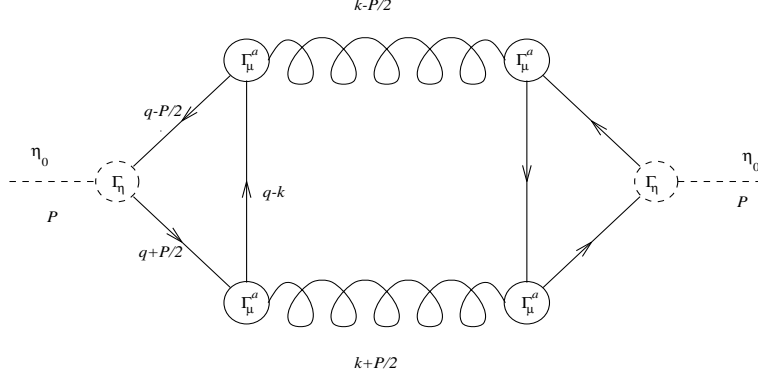


Fig. 26. The diamond diagram $\Pi(P^2)$. (A factor 2 arises from crossed gluon exchange.)
ref. [299,300],

$$g^2 D_{\mu\nu}(k) = P_{\mu\nu}(k) \left(\frac{8\pi\sigma}{k^4} + \frac{16\pi^2/9}{k^2 \ln(e + k^2/\Lambda^2)} \right). \quad (262)$$

The second term, subdominant in the infrared, was added to simulate the effect of the leading logarithmic contribution of perturbative QCD for $N_f = 3$. As mentioned at the beginning of this chapter, a quark interaction of the form (262) can, strictly speaking, not arise from gluons alone in Landau gauge, since the product $g^2 D_{\mu\nu}$ is not renormalization group invariant for any finite number of flavours or colours. Even though this is assumed in the Abelian approximation, ghost contributions do implicitly enter in the RG invariant interaction by the dressing of the quark-gluon vertex function as has been discussed in previous chapters.

From the axial anomaly, the quark triangle $\Gamma_{\mu\nu}^{ab}$ in Fig. 26 has the limit,

$$P \rightarrow 0, k^2 = 0 : \quad \Gamma_{\mu\nu}^{ab} \rightarrow \delta^{ab} \epsilon_{\mu\nu\rho\sigma} k^\rho P^\sigma \frac{\sqrt{N_f} g^2}{f_0 8\pi^2}, \quad (263)$$

with f_0 being the flavor-singlet decay constant. This model independent form, determining the coupling of two gluons to the pseudoscalar flavor-singlet bound state in the infrared, is particularly suited for the present calculation, since the contribution to χ^2 is obtained from $P \rightarrow 0$, and since the gluon interaction (262) weights the integrand so strongly in the infrared ($\sim \sigma/(k \pm P/2)^4$). With this, all contributions containing ultraviolet dominant terms of the interaction (262) vanish for $P \rightarrow 0$, and one obtains [299,300],

$$m_0^2 = \lim_{P^2 \rightarrow 0} \Pi(P^2) = \frac{2N_f}{f_0^2} \chi^2 = \frac{3N_f}{f_0^2} \frac{\sigma^2}{\pi^4}. \quad (264)$$

The phenomenological string tension $\sigma = 0.18 \text{ GeV}^2$ and $f_0 \approx f_\pi = 93 \text{ MeV}$ thus yield $m_0^2 \approx 0.346 \text{ GeV}^2$, and the physical mass eigenstates are, $m_{\eta'} \approx 810 \text{ MeV}$ and $m_\eta \approx 430 \text{ MeV}$, with a corresponding mixing angle $\theta \approx -30^\circ$. Furthermore, using $f_0^2 \simeq f_\pi^2 (1 + \Pi'(P^2)|_{P^2 \rightarrow 0})$ with $\Lambda \approx 500 \text{ MeV}$ in (262), one obtains an additional contribution to the decay constant of the flavor-singlet of about 30% as compared to the pion [299].

As these values are reasonably close to experiment, one might conclude that the $U_A(1)$ –anomaly can be encoded in the infrared behavior of QCD Green’s functions. Whether the Kogut–Susskind mechanism or the instanton based solution to the $U_A(1)$ problem is realized in nature, can be assessed from their respective temperature dependences. If the origin of the η' mass is predominantly due to instantons, the $\eta - \eta'$ mixing angle is expected to vary exponentially with temperature, leading to a significant change of η and η' production rates in relativistic heavy ion collisions [306]. On the other hand, lattice calculations indicate that the string tension is almost temperature independent up to the deconfinement transition. This offers the possibility to study the physics of the $U_A(1)$ anomaly experimentally.

6.2.3 An Unified Description of Light and Heavy Mesons

In sec. 3.3 we have described a solution for the DSE of the quark–photon vertex function and remarked that its transverse part possesses a pole at the vector meson mass [173]. Following the derivation of the homogenous BS equation it is quite obvious then that the transverse part of the quark–photon vertex fulfills eq. (247). As stated in sec. 3.3 in general twelve independent Dirac tensors are needed to describe a vector vertex, four of them are longitudinal with respect to the photon and/or vector meson momentum, eight are transverse. For a physical on–shell vector meson the corresponding BS vertex function is transverse,

$$\left(P_\mu \Gamma_\mu^V(p; P) \right)_{P^2 = -m_V^2} = 0. \quad (265)$$

Therefore eight independent functions have to be determined in the solution of the vector meson BS amplitudes [294]:

$$\Gamma_\mu^V(p; P) = \sum_{i=1}^8 F_i(p^2, p \cdot P; P^2) T_\mu^i(p; P) = \gamma_\mu^T F_1(p^2, p \cdot P; P^2) + \dots, \quad (266)$$

where $\gamma_\mu^T = \gamma_\mu - P_\mu (P \cdot \gamma) / P^2$ is the transverse projection of the four–vector γ_μ . Not surprisingly, the amplitude F_1 is quantitatively the most important one [307].

The study in ref. [307] uses a kernel very similar to the one used ref. [259], only the delta–function has been omitted, *i.e.*

$$\alpha(k^2) = \pi D \frac{k^4}{\omega^6} e^{-k^2/\omega^2} + \frac{\pi \gamma_m (1 - \exp(-k^2/4m_t^2))}{\frac{1}{2} \ln \left[\tau + \left(1 + k^2/\Lambda_{\text{QCD}}^2 \right)^2 \right]} \quad (267)$$

and ω and D are treated as free parameters. Please note that the coupling (267) is vanishing in the extreme infrared. On the other hand, it is very strongly enhanced for momenta $p^2 \approx \omega^2$. Table 2 (adapted from ref. [307]) shows that pion and kaon masses are described also very well.

In ref. [307] it has been found that only five of the eight covariants are important for the vector meson masses and decay constants, see table 3. (Two warnings are here in order. First, the

	experiment (estimates)	Ref. [259]	$\omega = 0.3 \text{ GeV}$ $D = 1.25 \text{ GeV}^2$	$\omega = 0.4 \text{ GeV}$ $D = 0.93 \text{ GeV}^2$	$\omega = 0.5 \text{ GeV}$ $D = 0.79 \text{ GeV}^2$
- $\langle \bar{q}q \rangle_{\mu=1 \text{ GeV}}^0$	$(0.236 \text{ GeV})^3$	$(0.241 \text{ GeV})^3$	0.242	0.241	0.243
$m_{\mu=1 \text{ GeV}}^{u=d}$	5 - 10 MeV	5.5 MeV	5.54	5.54	5.35
$m_{\mu=1 \text{ GeV}}^s$	100 - 300 MeV	130 MeV	124	125	123
m_π	0.1385 GeV	0.1385	0.139	0.138	0.138
f_π	0.1307 GeV	0.1307	0.130	0.131	0.131
m_K	0.496 GeV	0.497	0.496	0.497	0.497
f_K	0.160 GeV	0.154	0.154	0.155	0.157

Table 2

Calculated values of the properties of light pseudoscalar mesons for the parameterization of the effective coupling (267), using three different parameter sets, and also for the parameterization of ref. [259]. (Adapted from ref. [307].)

	ρ		K^*		ϕ	
	m_ρ	f_ρ	m_{K^*}	f_{K^*}	m_ϕ	f_ϕ
experiment	0.770	0.216	0.892	0.225	1.020	0.236
All amplitudes $F_1 \dots F_8$						
$\omega = 0.3 \text{ GeV}, D = 1.20 \text{ GeV}^2$	0.747	0.197	0.956	0.246	1.088	0.255
$\omega = 0.4 \text{ GeV}, D = 0.93 \text{ GeV}^2$	0.742	0.207	0.936	0.241	1.072	0.259
$\omega = 0.5 \text{ GeV}, D = 0.79 \text{ GeV}^2$	0.74	0.215	0.94	0.25	1.08	0.266
amplitudes $F_1 \dots F_5$ only						
$\omega = 0.3 \text{ GeV}, D = 1.20 \text{ GeV}^2$	0.737	0.192	0.942	0.235	1.080	0.247
$\omega = 0.4 \text{ GeV}, D = 0.93 \text{ GeV}^2$	0.729	0.199	0.919	0.229	1.062	0.250
$\omega = 0.5 \text{ GeV}, D = 0.79 \text{ GeV}^2$	0.731	0.207	0.926	0.237	1.072	0.259

Table 3

Comparison of the results for the vector mesons for the three different parameter sets for the effective interaction, using all eight BS amplitudes (top) or the five leading ones (bottom). (Adapted from ref. [307].)

relative importance of amplitudes depends in general on the observable under consideration. Second, in an other basis for the eight independent covariants the number of relevant covariants might be different.) Furthermore, for the ρ and the ϕ meson the truncation to the leading Chebyshev moment leads to very similar results. It is interesting to note that the leading amplitudes for the pion (*i.e.* E_π which is related to the scalar part of the quark self-energy in the chiral limit) and for the ρ are very much alike. Up to now it is unknown whether this is a more general relation or only valid for the interaction (267) with the chosen parameters. Note also that in this calculation the ρ and the ω are degenerate. It is usually assumed that this degeneracy will be lifted by the coupling to pions, see sec. 6.2.5.

As we have seen in the sector with light, *i.e.* up and down, and strange quarks the pseudoscalar and vector mesons can be understood quite well based on solutions of the ladder BS equation. An investigation of scalar mesons with the same quality as for pseudoscalar and vector mesons is not available, see, however, ref. [295] for a study which considers also scalar mesons. There are indications that the ladder truncation is not a good approximation for scalar mesons. The coupling of scalar mesons to two pseudoscalar mesons is very strong complicating this issue enormously. There is evidence from lattice calculations that scalar mesons are more like $\bar{q}^2 q^2$ than $\bar{q}q$ states [308]. Interpretations of scalar mesons range accordingly from them being unitarized $\bar{q}q$ states to being ‘molecules’ of two pseudoscalars, see *e.g.* refs. [309–312]. For the scalar–isoscalar mesons there is in addition the issue of mixing with glueballs and/or annihilation into timelike gluons. Due to this a straightforward application of the ladder BS equation to the scalar mesons is certainly not adequate.

The rainbow DSE and ladder BS formalism is straightforwardly applicable to mesons with heavy quarks [255]. First of all, the constituent quark mass functions for charm and bottom quarks is almost trivial, at large momenta they obey the perturbative RG behaviour, and in the infrared they display a slight enhancement. As the function $A(p^2)$ does also not deviate much from its perturbative value the corresponding propagators can be approximated very well by the free ones with a constant mass. Due to this the consequences of heavy–quark symmetry are reproduced in this approach, *e.g.* in the heavy–quark limit pseudoscalar meson masses grow linearly with the mass of their heaviest constituent, $m_P \propto \hat{m}_Q$.⁶⁰ A note of warning is, however, in order: For the solutions of the BS equation it is not only required that the binding energy is much smaller than the quark mass but also the momentum space width of the amplitudes have to be significantly less than the quark mass. Note that in ref. [255] a parameterization of these amplitudes have been used. (Also the propagators of the light quarks have been parameterized as entire functions.) These were then used to calculate heavy–meson leptonic decays, semileptonic heavy–to–heavy and heavy–to–light transitions ($B \rightarrow D^*$, D , ρ , π ; $D \rightarrow K^*$, K , π), radiative and strong decays ($B_{(s)}^* \rightarrow B_{(s)}\gamma$; $D_{(s)}^* \rightarrow D_{(s)}\gamma$, $D\pi$), and the rare $B \rightarrow K^*\gamma$ flavour–changing neutral–current process.

The leptonic decay constants are given by

$$f_P = f_V = \frac{\kappa_f}{\sqrt{m_H}} \frac{N_c}{2\sqrt{2}\pi^2} \int_0^\infty du \left(\sqrt{u} - E_H \right) \varphi_H(z) \left\{ \sigma_S^f(z) + \frac{1}{2} \sqrt{u} \sigma_V^f(z) \right\},$$

$$\frac{1}{\kappa_f^2} = \frac{N_c}{4\pi^2} \int_0^\infty du \varphi_H^2(z) \left\{ \sigma_S^f(z) + \sqrt{u} \sigma_V^f(z) \right\},$$

where $z = u - 2E_H\sqrt{u}$, f labels the meson’s lighter quark and $\varphi_H(z)$ is the scalar function characterising the dominant Dirac–covariant in the heavy–meson’s BS amplitude, *e.g.* the term proportional to γ_5 for the pseudoscalar and to γ_μ for the vector mesons. $\sigma_{S(V)}^f(z)$ is the scalar (vector) part of the quark propagator with flavour f . The semileptonic heavy–to–heavy pseudoscalar transition form factors ($P_1 \rightarrow P_2 \ell \nu$) acquire a particularly simple form in the heavy–quark symmetry limit:

⁶⁰ For a review on heavy–quark symmetry see *e.g.* ref. [313].

$$f_{\pm}(t) := \frac{m_{P_2} \pm m_{P_1}}{2\sqrt{m_{P_2}m_{P_1}}} \xi_f(w), \quad (268)$$

$$\xi_f(w) = \kappa_f^2 \frac{N_c}{4\pi^2} \int_0^1 \frac{\tau}{W} \int_0^\infty du \varphi_H^2(z_W) \left[\sigma_S^f(z_W) + \sqrt{\frac{u}{W}} \sigma_V^f(z_W) \right], \quad (269)$$

with $W = 1 + 2\tau(1 - \tau)(w - 1)$, $z_W = u - 2E_H\sqrt{u/W}$ and

$$w = \frac{m_{P_1}^2 + m_{P_2}^2 - t}{2m_{P_1}m_{P_2}} = -v_{P_1} \cdot v_{P_2}. \quad (270)$$

The normalisation of the BS amplitude automatically ensures that the Isgur–Wise function $\xi_f(w)$ [314] fulfills

$$\xi_f(w = 1) = 1 \quad (271)$$

in the heavy–quark limit. Furthermore, one obtains from eq. (269) that

$$\rho^2 := - \left. \frac{d\xi_f}{dw} \right|_{w=1} \geq \frac{1}{3}. \quad (272)$$

Similar analysis for the heavy–to–heavy transitions with vector mesons in the final state and for heavy–to–light transitions yields relations between the form factors that coincide with those observed in ref. [314]: In the heavy–quark limit also these form factors are expressible solely in terms of $\xi_f(w)$.

In ref. [255] the model parameters were fitted to a total of 42 light and heavy meson observables, see table 4 for the corresponding heavy meson quantities. The fitted constituent–heavy–quark masses are

$$\hat{M}_c = 1.32 \text{ GeV} \text{ and } \hat{M}_b = 4.65 \text{ GeV}. \quad (273)$$

This entails that the heavy–meson binding energy is large:

$$\begin{aligned} E_D &:= m_D - \hat{M}_c = 0.67 \text{ GeV}, \\ E_B &:= m_B - \hat{M}_b = 0.70 \text{ GeV}, \end{aligned} \quad (274)$$

i.e. $E_D/\hat{M}_c = 0.51$ and $E_B/\hat{M}_b = 0.15$. This provides an indication that while an heavy–quark expansion is applicable for the b -quark it will provide a poor approximation for the c -quark. The constituent–heavy–quark–masses in eq. (273) obtained in the Poincaré covariant approach [255], are, respectively, $\sim 25\%$ and $\sim 10\%$ smaller than the values used in nonrelativistic models.

Table 4

The 26 dimensionless quantities used in χ^2 -fitting the model parameters. The light-meson electromagnetic form factors are calculated in impulse approximation and $\xi(w)$ is obtained from $f_+^{B \rightarrow D}(t)$ via eq. (268). (Table adapted from Ref. [255].)

	Obs.	Calc.		Obs.	Calc.
$f_+^{B \rightarrow D}(0)$	0.73	0.58	$f_\pi r_\pi$	0.44 ± 0.004	0.44
$F_\pi(3.3 \text{ GeV}^2)$	0.097 ± 0.019	0.077	$B(B \rightarrow D^*)$	0.0453 ± 0.0032	0.052
ρ^2	1.53 ± 0.36	1.84	$\alpha^{B \rightarrow D^*}$	1.25 ± 0.26	0.94
$\xi(1.1)$	0.86 ± 0.03	0.84	$A_{\text{FB}}^{B \rightarrow D^*}$	0.19 ± 0.031	0.24
$\xi(1.2)$	0.75 ± 0.05	0.72	$B(B \rightarrow \pi)$	$(1.8 \pm 0.6) \times 10^{-4}$	2.2
$\xi(1.3)$	0.66 ± 0.06	0.63	$f_+^{B \rightarrow \pi}(14.9 \text{ GeV}^2)$	0.82 ± 0.17	0.82
$\xi(1.4)$	0.59 ± 0.07	0.56	$f_+^{B \rightarrow \pi}(17.9 \text{ GeV}^2)$	1.19 ± 0.28	1.00
$\xi(1.5)$	0.53 ± 0.08	0.50	$f_+^{B \rightarrow \pi}(20.9 \text{ GeV}^2)$	1.89 ± 0.53	1.28
$B(B \rightarrow D)$	0.020 ± 0.007	0.013	$B(B \rightarrow \rho)$	$(2.5 \pm 0.9) \times 10^{-4}$	4.8
$B(D \rightarrow K^*)$	0.047 ± 0.004	0.049	$f_+^{D \rightarrow K}(0)$	0.73	0.61
$\frac{V(0)}{A_1(0)} D \rightarrow K^*$	1.89 ± 0.25	1.74	$f_+^{D \rightarrow \pi}(0)$	0.73	0.67
$\frac{\Gamma_L}{\Gamma_T} D \rightarrow K^*$	1.23 ± 0.13	1.17	$g_{B^* B \pi}$	23.0 ± 5.0	23.2
$\frac{A_2(0)}{A_1(0)} D \rightarrow K^*$	0.73 ± 0.15	0.87	$g_{D^* D \pi}$	10.0 ± 1.3	11.0

Table 5

Calculated values of a range of observables not included in fitting the model's parameters. (Table adapted from ref. [255].)

	Obs.	Calc.		Obs.	Calc.
$f_K r_K$	0.472 ± 0.038	0.46	$-f_K^2 r_{K^0}^2$	$(0.19 \pm 0.05)^2$	$(0.10)^2$
$g_{\rho \pi \pi}$	6.05 ± 0.02	5.27	$\Gamma_{D^{*0}}$ (MeV)	< 2.1	0.020
$g_{K^* K \pi^0}$	6.41 ± 0.06	5.96	$\Gamma_{D^{*+}}$ (keV)	< 131	37.9
g_ρ	5.03 ± 0.012	5.27	$\Gamma_{D_s^* D_s \gamma}$ (MeV)	< 1.9	0.001
f_{D^*} (GeV)		0.290	$\Gamma_{B^{*+} B^+ \gamma}$ (keV)		0.030
$f_{D_s^*}$ (GeV)		0.298	$\Gamma_{B^{*0} B^0 \gamma}$ (keV)		0.015
f_{B_s} (GeV)	0.195 ± 0.035	0.194	$\Gamma_{B_s^* B_s \gamma}$ (keV)		0.011
f_{B^*} (GeV)		0.200	$B(D^{*+} \rightarrow D^+ \pi^0)$	0.306 ± 0.025	0.316
$f_{B_s^*}$ (GeV)		0.209	$B(D^{*+} \rightarrow D^0 \pi^+)$	0.683 ± 0.014	0.683
f_{D_s}/f_D	1.10 ± 0.06	1.10	$B(D^{*+} \rightarrow D^+ \gamma)$	$0.011^{+0.021}_{-0.007}$	0.001
f_{B_s}/f_B	1.14 ± 0.08	1.07	$B(D^{*0} \rightarrow D^0 \pi^0)$	0.619 ± 0.029	0.826
f_{D^*}/f_D		1.36	$B(D^{*0} \rightarrow D^0 \gamma)$	0.381 ± 0.029	0.174
f_{B^*}/f_B		1.10	$B(B \rightarrow K^* \gamma)$	$(5.7 \pm 3.3)_{10^{-5}}$	11.4

With the model's parameters fixed it is possible to calculate a wide range of other light- and heavy-meson observables. Some of the results are summarised in table 5, more results may be found in ref. [255]. It is also possible to check the fidelity of heavy-quark symmetry limits. The universal function characterising semileptonic transitions in the heavy-quark symmetry limit, $\xi(w)$, can be obtained with least uncertainties from $B \rightarrow D, D^*$ transitions. Using Eq. (268) to extract it from $f_+^{B \rightarrow D}(t)$ one obtains

$$\xi^{f_+}(1) = 1.08, \quad (275)$$

which is a measurable deviation from Eq. (271). Note that corrections to the heavy-quark symmetry limit of the order of 30% are encountered in $b \rightarrow c$ transitions and that these corrections can be as large as a factor of two in $c \rightarrow d$ transitions. The investigation carried out in ref. [255] indicates that heavy and light mesons are both simply finite-size bound states of dressed quarks and antiquarks.

To summarize this subsection: The elements of the Poincaré-covariant DSE framework are rich enough to account for the qualitative structure of almost all mesons. Of course, possibilities for improvements are numerous. The most wanted one, however, is in the treatment of the BS equation. The construction of a BS kernel that respects Slavnov-Taylor and Ward-Takahashi identities would be a significant improvement. Especially, it would allow one consistent route from the underlying properties of QCD Green's functions to meson structure. Nevertheless, the level of understanding achieved so far justifies studies of dynamical properties of mesons in this framework.

6.2.4 Electromagnetic Coupling: Form Factors and Decay

As described in subsection 6.2.1 the static properties of pions and kaons such as the mass and decay constants have been studied at a fairly fundamental level. Dynamic properties and scattering observables are much less understood even though they are not less important. In this respect the elastic electromagnetic form factors of pions and kaons are a very interesting next step. First of all, there are accurate data for F_π at low Q^2 to confront theoretical calculations with, and the charge radii r_π^2 , $r_{K^+}^2$, and $r_{K^0}^2$ are experimentally known. Currently, there are several experiments to determine both the pion and the kaon form factor in the range up to 3 GeV^2 to better accuracy, see *e.g.* Jlab experiments E93-018 (Spokesperson O. K. Baker) and E93-021 (Spokesperson D. Mack). Also the pion polarizabilities, *i.e.* the second moment of the form factor at $Q^2 = 0$, will be measured to a higher precision, see *e.g.* experiments at MAMI in Mainz (Spokesperson R. Beck).

In refs. [173,315] the electromagnetic form factors of pions and kaons have been calculated based on the solutions for the meson BS amplitudes and the quark-photon vertex of the homogeneous and inhomogeneous ladder BS equations, respectively. As in the study of light vector mesons the required dressed quark propagators are obtained from solutions of the quark DSE in rainbow truncation using the effective interaction (267). Hereby the model parameters are all fixed [307] and constrained only by m_π , m_K , f_π and $\langle \bar{q}q \rangle$. As can be inferred from sects. 3.3 and 6.2.3 non-analytic effects from vector mesons are automatically taken into account: the vector $\bar{q}q$ bound states appear as poles in the quark-photon vertex solution [173]. As a matter

of fact, in the domain $-m_V^2 < Q^2 < 0.2\text{GeV}^2$ the quark–photon vertex is well described by the sum of the Ball–Chiu vertex plus a second term containing an explicit pole at the vector meson mass $p^2 = -m_V^2$ [173]. This splitting yields (via the impulse approximation to be discussed below) a charge form factor for the pion that can be expressed as

$$F_\pi(Q^2) \approx F_\pi^{\text{BC}}(Q^2) - \frac{g_{\rho\pi\pi} F_{V\pi\pi}(Q^2) Q^2}{g_\rho(Q^2 + m_\rho^2)}, \quad (276)$$

where $F_\pi^{\text{BC}}(Q^2)$ is the result from the Ball–Chiu vertex. The combination $g_{\rho\pi\pi} F_{V\pi\pi}$ represents the $\pi\pi$ coupling to the vector $\bar{q}q$ correlation as present in the resonant term in the quark–photon vertex. The second term on the l.h.s. of eq. (276) is written such that $F_{V\pi\pi}(-m_\rho^2) = 1$. As off–shell mesons are unphysical, $F_{V\pi\pi}(Q^2 \neq -m_\rho^2)$ does not correspond to a physical process. Nevertheless, it is an interesting quantity when discussing the relation of the approach presented here to Vector Meson Dominance (VMD). To this end we note that the departure of $F_{V\pi\pi}(Q^2)$ from unity is a measure of the difference in $\pi\pi$ coupling experienced by the effective vector $\bar{q}q$ correlation away from the ρ mass–shell compared to the physical $\rho\pi\pi$ coupling. On the other hand, using VMD (in the form as reviewed *e.g.* in ref. [316]), where $\rho - \gamma$ coupling is described by the contraction of the two field strength tensors $\rho^{\mu\nu} F_{\mu\nu}$, the pion form factor is given by

$$F_\pi(Q^2) \approx 1 - \frac{g_{\rho\pi\pi} Q^2}{g_\rho(Q^2 + m_\rho^2 - im_\rho \Gamma_\rho(Q^2))}. \quad (277)$$

The non–resonant constant term “1” arises from the photon coupling to the charge of a point pion. The resonant, Q^2 -dependent term stems from $\rho - \gamma$ coupling and vanishes at $Q^2 = 0$ in accordance with gauge invariance. The width Γ_ρ is non–vanishing due to $\pi\pi$ production only, and thus the form factor is real for $Q^2 > -4m_\pi^2$. (In the model of refs. [173,315] this width is neglected which is, however, only of minor importance for the argument presented here.) Employing VMD the charge radius $r_\pi^2 = -6F'_\pi(0)$ comes entirely from the resonant term and is $6g_{\rho\pi\pi}/(m_\rho^2 g_\rho) = 0.48 \text{ fm}^2$, which compares favorably with the experimental value 0.44 fm^2 .

As the pion is a $\bar{q}q$ bound state, eq. (277) cannot be the full truth for $F_\pi(Q^2)$ at spacelike Q^2 . The photon couples only to quark currents in the pion, and the vector meson bound state is not a well–defined concept away from its pole. Adressing this question within the two contributions in the dressed quark–photon vertex, eq. (276) is employed to split also the pion charge radius into a Ball–Chiu and a resonant contribution. The latter one is given by

$$\frac{6 g_{\rho\pi\pi} F_{V\pi\pi}(0)}{m_\rho^2 g_\rho}, \quad (278)$$

and comparison to eq. (277) reveals that $F_{V\pi\pi}(0)$ characterizes the necessary weakening of the VMD mechanism for r_π^2 to account for the distributed $\bar{q}q$ substructure. The numerical value obtained in ref. [173] based on the solution of the quark–photon vertex DSE is 0.58, or phrased otherwise, approximately half of the pion radius is due to the vector meson contribution and the other half is due to the longitudinal part of the quark–photon vertex reflecting the

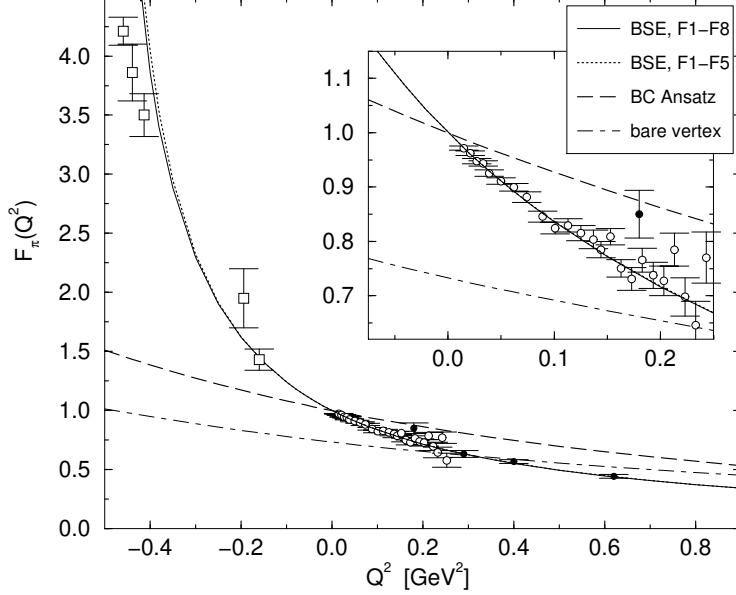


Fig. 27. The pion charge form factor $F_\pi(Q^2)$ as obtained from different treatments of the quark-photon vertex. The inset shows the Q^2 region relevant for the charge radius. (Adapted from ref. [173].)

Table 6

Calculated charge radii compared with the experimental values. (Adapted from ref. [315].)

charge radii	experiment	calculated
r_π^2	$0.44 \pm 0.01 \text{ fm}^2$	0.45 fm^2
$r_{K^+}^2$	$0.34 \pm 0.05 \text{ fm}^2$	0.38 fm^2
$r_{K^0}^2$	$-0.054 \pm 0.026 \text{ fm}^2$	-0.086 fm^2

electromagnetic Ward identity at the level of quarks. Note that this implies that $g_{\rho\pi\pi}$ has to decrease also by approximately 50% when extrapolated from the physical value at the ρ meson mass shell to the soft point $Q^2 = 0$. Of course, away from the mass shell $g_{\rho\pi\pi}$ has not the meaning of a physical coupling constant. At $Q^2 = 0$ the photon couples not to a physical meson but to a distributed, interacting $\bar{q}q$ correlation and a large part of this coupling is already accounted for by the Ward-identity-preserving Ball-Chiu part of the vertex. Thus, the results presented in ref. [173] nicely reconciles the VMD picture with one based on the quark substructure of pions.

The main result of ref. [173] is represented in fig. 27. Given the fact that the parameters have been fixed in the study of vector mesons [307] the result is quite impressive. In ref. [315] the calculation of the pion form factor has been extended up to 4 GeV^2 . Given the uncertainty of the experimental data this calculation has to be considered as a prediction. It is interesting to note that above 3.5 GeV^2 the result for the pion form factor starts to deviate from the monopole fit. In ref. [315] also the kaon charge form factors have been calculated. The K^+ form factor at several GeV^2 looks similar to the pion one, at low momenta it is in agreement with the experimental data which possess, however, large errors. The charge radii are given in table 6.

In ref. [317] the electromagnetic form factors of light vector mesons, $G_E(Q^2)$, $G_M(Q^2)$ and $G_Q(Q^2)$, have been calculated in a DSE based approach. Hereby an algebraic model for the quark propagator has been used. For the vector meson BS amplitudes only the leading Dirac covariant have been taken into account, and the corresponding scalar function has been chosen to be of the functional form of the leading pion BS amplitude, however, the parameters have been adjusted by a fit to some observables. The calculated static properties include the charge radii $\langle r_{\rho^+}^2 \rangle^{1/2} = 0.61\text{fm}$, $\langle r_{K^{*+}}^2 \rangle^{1/2} = 0.54\text{fm}$ and $\langle r_{K^{*0}}^2 \rangle = -0.048\text{fm}^2$; the magnetic moments $\mu_{\rho^+} = 2.69e/2m_\rho$, $\mu_{K^{*+}} = 2.37e/2m_{K^{*+}}$ and $\mu_{K^{*0}} = -0.40e/2m_{K^{*0}}$; and the quadrupole moment $\bar{Q}_\rho = 0.055\text{fm}^2$.

We close this section by noting that in ref. [318] the dipole moments of the ρ meson has been calculated through the inclusion of an electric dipole moments for quarks, *i.e.* physics beyond the standard model. The interesting observation which has been made in ref. [318] is that the use of non-perturbative quark propagators (reflecting confinement) significantly enhances the dipole moments calculated for the ρ meson.

6.2.5 Meson Interactions

The approach presented here is in principle capable of treating the interaction of mesons with other mesons and photons. However, for an increasing number of particles in the initial and final states the practical difficulties will rise enormously. Due to this such investigations will be restricted to cases which are of special interest. In this subsection we will review investigations of the coupling of the ρ meson to two pions in order to demonstrate how a finite width for a hadronic resonance is generated in this approach. The calculation of the $\gamma\pi\rho$ form factor serves as an example that the presented approach is able to provide information needed in nuclear physics. The considerations of the $\pi\gamma\gamma$ and $\gamma\pi\pi\pi$ form factors, on the other hand, provide some insight in some fundamental quantum field theoretic phenomenon, the anomaly.

Restricting oneself to the leading Dirac covariant for the ρ meson BS amplitude the $\rho\pi\pi$ vertex function can in principle be obtained directly from the $\gamma\pi\pi$ vertex function, *i.e.* the pion charge form factor, discussed in the last subsection. Since only the isovector part of the photon-quark vertex contributes to the pion form factor the $\rho^0\pi\pi$ vertex can be obtained by replacing $\Gamma_\mu/2$ in the expression for the $\gamma\pi\pi$ vertex with $\gamma_\mu^T V_\rho(q; Q)$ for the ρ^0 in the $\rho\pi\pi$ vertex. This has been the calculational scheme in ref. [319], however, as this most recent study of the $\rho\pi\pi$ coupling in the DSE approach predates the solution of the photon-quark DSE the corresponding calculation is not as sophisticated as the corresponding one for the pion form factor in the last subsection. For the pion only the leading Dirac covariant in the chiral limit has been used, $E_\pi(q; P) = B(q^2, m)/f_\pi$, and the ρ amplitude has been parameterized as a Gaussian, $\Gamma^\rho(p^2) \propto e^{-p^2/a^2}$. The width a of this Gaussian has been fixed by fitting empirical value of $\rho\pi\pi$ at the ρ meson mass shell, $g_{\rho\pi\pi}^{\text{expt}} = 6.05$. This phenomenologically successful ansatz has also been employed in studies of other processes such as $\rho - \omega$ mixing [320] and the $\rho \rightarrow e^+ e^-$ decay [321]. The resulting $\rho \rightarrow \pi\pi$ decay width, given by

$$\Gamma_{\rho \rightarrow \pi\pi} = \frac{g_{\rho\pi\pi}^2}{4\pi} \frac{m_\rho}{12} \left[1 - \frac{4m_\pi^2}{m_\rho^2} \right]^{3/2}, \quad (279)$$

is 151 MeV. The calculated form factor $F_{\rho\pi\pi}(Q^2)$ decreases rapidly with increasing Q^2 [319]. At the soft point its value is approximately 3, *i.e.* half the value at the ρ meson pole. Therefore, the main result of ref. [319] is a clear warning: an approximation in which the $\rho\pi\pi$ vertex function is evaluated at the soft point and not at the pole can induce an 100% error. Of course, these investigations are exploratory in the sense that an independently calculated ρ BS amplitude including subleading covariants will change the results. On the other hand, the strong suppression as Q^2 increases from the mass-shell point to the spacelike region indicates that the effective coupling strength $g_{\rho\pi\pi}(Q^2)$ appropriate to the ρ contribution to the pion charge form factor and radius is significantly smaller than what is assumed in the standard VMD approach. This is consistent with findings which have been discussed in the last subsection and which are based on a much more sophisticated calculation.

The parameterization invoked in ref. [319] enables a prediction for the $\gamma\pi\rho$ vertex. This provides a check on the internal consistency of this approach to meson physics beyond phenomena dictated by chiral symmetry. Within nuclear physics the associated isoscalar $\gamma^*\pi\rho$ meson-exchange current contributes significantly to electron scattering from light nuclei and is thus of phenomenological interest. Furthermore, it is an anomalous process, *i.e.* it can only occur due to the chiral anomaly of QCD. As will be detailed below this implies that independent of the model form of the quark propagator the corresponding coupling constant at the soft point is $g_{\gamma\pi\rho} = 0.5$. Comparing to the empirical value $g_{\gamma\pi\rho}^{\text{expt}} = 0.54 \pm 0.03$ obtained from the experimental $\rho^+ \rightarrow \pi^+\gamma$ partial width (67 ± 7 keV) indicates that the effects of the momentum dependence the effective coupling are much weaker for this process. The calculated $\gamma\pi\rho$ form factor obtained with on-mass-shell π and ρ is much softer than the one obtained in a VMD approach [28].

Hadronic processes involving an odd number of pseudoscalar mesons are of particular interest because they are intimately connected to the anomaly structure of QCD. The decay $\pi^0 \rightarrow \gamma\gamma$ is the primary example of such an anomalous process. That such processes occur in the chiral limit ($m_\pi^2 = 0$) is a fundamental consequence of the quantisation of QCD; *i.e.*, of the non-invariance of the QCD measure under chiral transformations even in the absence of current quark masses [2]. The $\pi^0 \rightarrow \gamma\gamma$ decay rate can be calculated from a quark triangle diagram and agreement with the observed rate requires that the number of colours, N_c , equal three. The transition form factor for the related process $\gamma^*\pi^0 \rightarrow \gamma$ can be measured experimentally and has attracted a lot of theoretical interest (see *e.g.* [322–325,304,326] and references therein) because it involves only one hadronic bound state and provides a good test of QCD-based models and their interpolation between the soft and hard domains. Another anomalous form factor, accessible to experiment, is that which describes the transition $\gamma\pi^* \rightarrow \pi\pi$. This provides additional constraints on DSE based models not only because three hadronic bound states are involved but also the pion BS amplitudes are tested at time-like momenta [327–329].

An important point in the treatment of anomalous processes in a DSE based approach is the following: Using a quark-photon vertex that obeys the Ward identity (*e.g.* the Ball-Chiu vertex) and a pion BS amplitude with the correct chiral limit, the integral appearing in the amplitude for anomalous process in the chiral limit at the soft point can be solved analytically. First of all, as the longitudinal part of the quark-photon vertex and the chiral limit pion BS amplitude can be expressed in terms of the functions appearing in the quark propagator, $A(p^2)$ and $B(p^2)$, the corresponding integrand contains exactly these functions. Introducing

$C(s) = B(s)^2/(s A(s)^2) = M(s)^2/s$ the effective $\pi^0\gamma\gamma$ coupling in the chiral limit can be written as

$$g_{\pi^0\gamma\gamma}^{(0)}(0) = - \int_0^\infty ds \frac{C'(s)}{(1+C(s))^3} = \int_0^\infty dC \frac{1}{(1+C)^3} = \frac{1}{2} \quad (280)$$

since $C(s)$ is a monotonic function for $s \geq 0$ with $C(s=0) = \infty$ and $C(s=\infty) = 0$. Hence, the chiral limit value [2] is reproduced *independent* of the details of the quark propagator. The same trick can be applied when considering the same limits (soft point and massless pion) in the $\gamma \rightarrow 3\pi$ amplitude:

$$F^{3\pi}(0,0,0) = - \frac{eN_c}{2\pi^2} \int_0^\infty ds \frac{C'(s)C(s)}{(1+C(s))^4} = \frac{eN_c}{2\pi^2 f_\pi^3} \int_0^\infty dC \frac{C}{(1+C)^4} = \frac{eN_c}{12\pi^2 f_\pi^3} . \quad (281)$$

In order to obtain these results it is essential that the electromagnetic and chiral Ward identities are satisfied by the vertex functions. The subtle cancellations that are required to obtain these results also make clear that they cannot be obtained in model calculations where an arbitrary cutoff function is introduced into each integral. The fact that the pion BS amplitude is proportional to the scalar part of the quark self energy in the chiral limit is crucial. Of course, these results remain valid with the subleading Dirac covariants in the pion BS amplitude taken into account [324]. Note also that the independence from the detailed form of the quark propagator is also to be seen in the calculation of the Wess–Zumino five pseudoscalar term [330]. It is a generic feature of the DSE based approach which respects the underlying symmetry structure of QCD as close as possible.

Away from the soft point and for a realistic pion mass the corresponding form factors are, of course, model dependent. Especially for large momentum transfers they are predictions which will be tested in the near future experimentally. For more details we refer to the literature [323,304,327,329].

6.2.6 Pion Loops

The meson fields have been treated so far as ladder $\bar{q}q$ bound states whose structure and interactions are determined by dressed quarks. Of course, these mesons interact at a purely hadronic level. To describe this type of interactions meson loops have to be taken into account. As we will see in this section meson loop effects are in most cases of interest numerically small. The main reason to review some work in this direction is to provide a qualitative demonstration that it is in principle possible to bridge the gap from QCD Green's functions to hadronic interactions.

To describe the finite lifetime of the ρ meson it is mandatory to couple it to the two-pion channel [319,28]. We will discuss here the most recent corresponding study [331] which uses an algebraic parameterization of the quark propagator and the light pseudoscalar and vector meson BS amplitudes. Note that such a parameterization has also been used in ref. [317] to calculate the electromagnetic form factors of the light vector mesons. As the on-shell $\rho\pi\pi$

coupling is fitted to the experimental value, $g_{\rho\pi\pi} = 6.03$, the correct ρ width of 150 MeV is reproduced. The corresponding polarization operator displays the emergence of an imaginary part for $q^2 < -m_\rho^2$ with the expected non-analytic behaviour. The real part of this polarization operator lead to mass shifts for the vector mesons. These contributions to the self-energies of the ρ and the ω mesons due to several pseudoscalar–pseudoscalar and pseudoscalar–vector loops are less than 10% of the “bare” mass generated by the quark core. A mass splitting $m_\omega = m_\rho \approx 25$ MeV is found from the $\pi\pi$, $K\bar{K}$, $\omega\pi$, $\rho\pi$, $\omega\eta$, $\rho\eta$ and K^*K channel. Despite the fact that this value is twice as large as the experimental value (12 MeV) this nicely demonstrates the effectiveness of this approach which has neglected direct isospin breaking effects due to different up and down quark masses. Thus, the inclusion of meson loops is on the one hand capable to describe qualitative effects like the ρ width and the $\omega - \rho$ mass splitting quantitatively and on the other hand it yields only a small correction to the predominant valence quark–antiquark structure of the vector meson. This is emphasized by the fact that the two-pion loop provides a modest increase for the ρ charge radius from 0.61 fm, calculated from the quark core only, to 0.67 fm when the pion loop is included in the calculation.

Despite this robustness of the ladder $\bar{q}q$ bound state picture when using a physical pion mass there is a question of fundamental interest concerning the chiral limit. To this end one has to note that the non-analytic behaviour underlying chiral perturbation theory is generated solely by pion loops [332,333]. Therefore the question arises whether the approach presented here is capable of producing this chiral limit divergencies. This question has been exemplified in the case of the pion charge radius [334]. Chiral Perturbation Theory can be understood as the study of the necessary consequences of the chiral Ward Identities via the construction of an effective action, using field variables with pionic quantum numbers, in such a way as to ensure that these identities are realised. It should be noted that in this approach the pseudoscalar Lagrangean field has no physical significance: it is merely an auxiliary field and should not be identified with the physical pion. At first nonleading order in Chiral Perturbation Theory, $O(E^4)$, the effective action is only completely determined once the effect of one-pion loops, generated by the $O(E^2)$ part of the action, is included. The regularisation of the divergence of each of these loops introduces ten arbitrary parameters at this level. The action at $O(E^4)$ is completely specified once the effect of the $O(E^2)$ loops is taken into account and the 10 parameters fixed by comparison with experimental data. These pseudoscalar loops are characteristic of the approach and, indeed, are sometimes regarded as being the dominant feature. The expression for every physical observable receives a contribution from such loops which depends on the mass of the particle in the loop and which diverges in the chiral limit. For example, in the case of the electromagnetic pion charge radius, $\langle r_\pi^2 \rangle \sim \ln m_\pi$. In ref. [334] the importance of these loop contributions, evaluated at the real pion mass, relative to that of the core of dressed-quarks, which is the dominant contribution at large spacelike- q^2 , has been estimated for the pion charge radius.

Hereby an ansatz for the quark propagator and the leading Dirac covariant for the pion BS amplitude has been used. The photon coupling has been described using the Ball–Chiu form of the quark–photon vertex. Neglecting pion off-mass-shell effects the electromagnetic pion form factor can be written in the form

$$F_\pi(Q^2) = F_\pi^{\text{quark core}}(Q^2) \left\{ 1 + I(Q^2, m_\pi^2)/f_\pi^2 \right\} \quad (282)$$

where $I(Q^2, m_\pi^2)$ is a lengthy integral stemming from the pion loop. The factorization of $F_\pi^{\text{quark core}}(Q^2)$ can be understood from the fact that the pion loop contribution to the pion–photon coupling is nothing else than the convolution of the quark–core pion–photon coupling with the $\pi\pi$ scattering amplitude. It is obvious that the pion loop describes some additional structure of the pion in addition to the quark core. However, the one-pion-loop corrected value of the pion decay constant differ at most by 2% (slightly depending on the parameters for the quark propagator) from its quark core value. The one-pion-loop corrected value of the pion charge radius has been found between 6 and 14% larger than its meson–tree–level value. To discuss the chiral divergencies one may set the mass of all the external pions to zero so that the contribution of the loop–pions in the chiral limit is easily identified when their mass m_π^L vanishes: $m_\pi^L \rightarrow 0$. The quark core contribution, $r_\pi^{\text{quark core}}$, is regular in the chiral limit and only weakly dependent on the current quark mass. At $m_\pi^L \approx 0.14$ GeV the dominant contribution to the pion charge radius is provided by the dressed–quark core. It is not until m_π^L becomes very small, ~ 10 MeV, that the pion cloud contribution becomes as important as the quark core, and this contribution is well described by the form

$$(r_\pi^2)^{\text{div}} = (r_\pi^2)^{\text{quark core}} \left[0.73 - 0.082 \ln \left(\frac{(m_\pi^L)^2}{m_\rho^2} \right) \right], \quad (283)$$

for $m_\pi^L < 0.14$ GeV.

In Chiral Perturbation Theory the corresponding result reads [335]

$$\langle r^2 \rangle_\pi = \frac{12 L_9^r}{F_0^2} - \frac{1}{32\pi^2 F_0^2} \left(2 \ln \left[\frac{m_\pi^2}{\mu^2} \right] + \ln \left[\frac{m_K^2}{\mu^2} \right] + 3 \right) \quad (284)$$

where μ^2 is the loop regularisation scale and L_9^r is one of the ten standard low energy constants in the effective action of Chiral Perturbation Theory into which an infinity from the divergence of the pseudoscalar loop has been absorbed. Using accepted values for L_9^r the first term in eq. (284) provides 84 to 90 % of the total value. One sees that at the physical value of the pion mass, and with an accepted value of the renormalisation scale, the main contribution to the charge radius is hidden in the parameter L_9^r ; it is not provided by the “chiral logarithm”. This can be interpreted as a strong indication of the importance of the underlying quark-gluon degrees of freedom.

However, some warning is here in order. The parameter L_9^r cannot be directly related to our dressed–quark core. The flaw in such an identification is obvious if one considers the scalar radius of the pion. In this case the analogous parameter in ChPT is L_4^r , which is inferred, from fits to data, to be smaller than the “chiral logarithm”. Nevertheless the scalar radius of the pion also receives its main contribution from the dressed–quark core.

In the DSE based approach the charge radius of the pion receives a contribution from its dressed–quark core, from pion loops, from ρ_μ - A_ν mixing, etc., each of which can be identified and calculated in a systematic manner. The quark core contribution is finite in the chiral limit and, at $m_\pi = 0.14$ GeV, it is the dominant determining characteristic of the pion, with the pion-loop contribution being a small, finite, additive correction of less than 15%. The fact

that the pion loop contribution is ultraviolet finite is a general property of the DSE approach: it is due to the internal quark core structure which provides a natural cutoff in all integrals that arise. Nevertheless the origin of the chiral divergence in the charge radius of the pion is identified as arising from the pion loop. This feature is present in the DSE approach as an higher order correction, as are all meson loop effects.

In this chapter we have reviewed the progress made in the last years in describing meson as quark–antiquark bound states within the DSE approach. The main missing link to the direct use of QCD Green’s functions is the fact that still one is not able to include non–trivial quark–gluon vertex functions fulfilling the Slavnov–Taylor identities of QCD in the BS equation. As we will see in the next section this is not only a matter of principles but also a main obstacle in this approach to describe baryons as bound states of confined quarks and confined two–quark–correlations, the “diquarks”.

7 Baryons as Diquark–Quark Bound States

Many baryon models, too numerous to mention them all, exist. These range from various sorts of bag [336], and skyrmion/soliton models [337–342], to non-relativistic [343–345] as well as relativistic potential models [346]. In addition, hybrid models exist which combine complementary aspects of the previous models. Examples are the chiral bag [347,348], or also a recent hybrid model combining the NJL soliton picture of baryons with the quark–diquark BS bound state description within the NJL model [349].

The naturally embedded framework in the present context is the description of hadrons as bound states in relativistic Bethe–Salpeter/Faddeev equations for particle poles in quark correlation functions (in the color singlet channel), the 4–point quark–antiquark Green’s function for mesons, and the 6–quark Green’s function for baryons.

The aim is, of course, to use the results from DSEs, in particular the ones for the quark correlations, in the relativistic bound state equations for baryons in a similar manner as for mesons. However, for baryons, in the simplest case the nucleons, the relativistic bound state description is considerably less understood, even on the phenomenological level. Their description as relativistic quark–diquark BS bound states has been studied in the NJL model in refs. [350–358] and in the Global Colour Model in refs. [359,360]. Other studies of nucleon properties have simply parameterized the nucleon’s Faddeev amplitudes [361,362]. Some recent developments in the quark–diquark bound state picture from more realistic models of quark interactions can be found in refs. [363–369]. While these latter studies still entirely rely on simple model assumptions for the quark correlations, the mechanism modeled is sufficiently general to accommodate a more detailed knowledge of the underlying dynamics of quarks and gluons as this emerges. The hope is also here, of course, that the present gap between the studies of quark and gluon correlations and the description of baryonic bound states from these correlations will be closed in future. Until then, it will be important to improve the understanding of the relativistic 3–quark bound state problem from simple model assumptions, not for technical reasons alone. These assumptions can then be replaced by more realistic ones successively.

While the non-relativistic Faddeev equation can be solved numerically in potential models, see, *e.g.*, ref. [370], the bound state problem of 3–quark correlations in quantum field theory has to be truncated. At present, the widely employed assumption is that the diquark correlations are separable which allows to reduce the Faddeev problem to an effective Bethe–Salpeter equation for the quark–diquark system. Separable diquark correlations are obtained from the lowest lying poles in the particular channel. The assumption therefore is that these pole contributions might dominate the diquark correlations in the kinematic regime relevant within baryons at not too high energies. However, as we will see in the following section repulsive contributions to the quark–quark scattering kernel beyond the ladder approximation are likely to prevent poles on the timelike P^2 –axis for diquark states.

7.1 Goldstone Theorem and Diquark Confinement

Besides the knowledge of the analytic structure of quark and gluon propagators and an understanding of the absence of quark and transverse gluon production thresholds in the S -matrix of hadronic color–singlet processes, a complete description of confinement also has to explain the absence of colored composite states. In particular, the existence of bound states from BS equations for colored channels gives rise to the question, why such states cannot be produced either?

A natural explanation might be obtained from a rigorous connection between the representations of the gauge group and the sign of the BS norm. It might for instance be established that color non–singlet bound states necessarily have to have negative norm and thus correspond to abnormal solutions.

In this section it is demonstrated that there are important differences between otherwise analogous color–singlet and non–singlet channels beyond ladder approximation [371,372]. In a simple toy model of confinement and chiral symmetry breaking [254] it can be explicitly verified that these differences suffice to remove the colored partner of physical mesons from the spectrum that would otherwise be bound in the ladder approximation [371]. This same mechanism has been verified to have the same effect in a diametrically different model of chiral symmetry breaking, the Nambu–Jona–Lasinio (NJL) model with infrared cutoff [372]. This suggests, that the general mechanism as described below, indeed has the expected effect beyond the simple model used for its demonstration at work.

In the last chapter it has become clear that the homogeneous BS equation for relativistic bound states is derived under the assumption that the associated two–body T –matrix has a pole in a given channel. The absence of a solution contradicts this assumption and establishes that no bound–state exists with the quantum numbers of the channel under consideration.

As noted in the last chapter a description of mesons in the rainbow–ladder DSE–BS equation approach is extremely rich and surprisingly successful. However, it has the defect that it admits $(\bar{3})_c$ –diquark bound states [360]. Clearly, such colored states have not been observed. Recently, a truncation scheme has been developped [371] that allows for a systematic improvement in the kernels of the quark DSE and the meson as well as the diquark BS equation. In this procedure the pion remains a Goldstone boson at every order. The first correction to the rainbow–ladder approximation is found to introduce a repulsive term in the BS kernel. Using a model gluon propagator, singular in the infrared and with no Lehmann representation, the quark DSE yields a quark propagator that also has no Lehmann representation. Pairing these gluon and quark propagators in the meson channel, the repulsive term is almost canceled by attractive terms of the same order and therefore the higher order terms are verified to only lead to very small changes in the meson masses. However, due to the color algebra of $SU(3)_c$, the repulsive term is considerably stronger in the diquark channel and is not canceled by the attractive terms. This suffices to establish that the color anti–triplet 4–point Green’s function does not have a spectral representation with single particle bound state poles, and that there are no corresponding diquark bound states in this model. These arguments can be generalized to an arbitrary number of colours [372]. The case $N_c = 2$ is special: The diquarks are then the

(bosonic) baryons. Accordingly, the repulsive term does not overwhelm the attractive one. On the other hand, for $N_c \rightarrow \infty$ the attractive interaction is completely negligible, and there are no diquark correlations. Note that such a picture is in complete agreement with the general arguments of the $1/N_c$ expansion [248,301].

7.1.1 Beyond Rainbow–Ladder Approximation

First, we will have a look at the ladder diquark BS equation. The analogue of the meson BS equation eq. (247) for quark–quark systems is

$$\Gamma_D^{EF}(p; P) = \int \frac{d^4 k}{(2\pi)^4} K_D^{EF;GH}(k, p; P) \left(S(k + \frac{1}{2}P) \Gamma_D(k; P) S^T(-k + \frac{1}{2}P) \right)^{GH}, \quad (285)$$

where “ T ” denotes matrix–transpose and the subscript D denotes diquark. $K_D(k, p; P)$ is the kernel, P is the total momentum of the system, k, p are the internal and external relative quark–quark momenta, and the superscripts are associated with the color, flavor and Dirac structure of the amplitude; *i.e.*, $E = \{i_c, i_f, i_D\}$. The absence of a solution to this equation entails that diquarks do not appear in the strong–interaction spectrum.

In the iso–vector channel, each contribution to $K_M^{EF;GH}(k, p; P)$ is matched by a direct analogue in $K_D^{EF;GH}(k, p; P)$ that can be obtained via the replacement

$$S(k) \gamma_\mu \frac{\lambda^a}{2} \rightarrow \left[\gamma_\mu \frac{\lambda^a}{2} S(-k) \right]^T, \quad (286)$$

for each antiquark in the meson kernel. This means that a general one–to–one correspondence between every contribution to the interaction kernels in the (iso–scalar) diquark channels and the (iso–vector) meson channels (with opposite parity) can be established. This procedure breaks down only for the iso–scalar meson channels which can mix with purely gluonic correlations, and which have thus no partner in the diquark correlations. In particular, for two flavours the corresponding pairs of $(\bar{3})_c$ diquarks versus $(1)_c$ mesons thereby are: the iso–scalar scalar(pseudo–scalar) diquarks versus the iso–triplet pseudo–scalar(scalar) mesons, and the iso–vector axial–vector(vector) diquark versus the iso–vector vector (axial–vector) mesons.

The ladder approximation to the diquark BS equation is defined by

$$\begin{aligned} K_D^{EF;GH}(k, p; P) \left(S(k + \frac{1}{2}P) \Gamma_D(k; P) S^T(-k + \frac{1}{2}P) \right)^{GH} \\ \equiv g^2 D_{\mu\nu}(p - k) \left(\gamma_\mu \frac{\lambda^a}{2} S(k + \frac{1}{2}P) \Gamma_D(k; P) \left[\gamma_\nu \frac{\lambda^a}{2} S(-k + \frac{1}{2}P) \right]^T \right)^{EF} \end{aligned} \quad (287)$$

in eq. (285), which illustrates the application of eq. (286).

As discussed in the last chapter, in the chiral limit the rainbow–approximation DSE and the pseudoscalar–meson BS equation in ladder–approximation are equivalent when $P^2 = 0$; *i.e.*, one necessarily has a massless pseudoscalar bound state when chiral symmetry is dynamically broken [276]. Goldstone’s theorem is manifest. In any truncation, such an identity between the quark DSE and the BS equation in the iso–vector pseudoscalar meson channel is sufficient to ensure that this meson is a Goldstone boson [275].

For the purpose of illustration and clarity the simple model gluon propagator of ref. [254] is employed here,

$$g^2 D_{\mu\nu}(k^2) \equiv 16\pi^4 G \left(\delta_{\mu\nu} - \frac{k_\mu k_\nu}{k^2} \right) \delta^4(k) , \quad (288)$$

where $G = \eta^2/4$ with η a mass scale. This one–parameter model is appropriate in a study whose focus is confinement and DB χ S. It allows for an algebraic solution of the DSE and BS equations. The qualitative features of our results are not sensitive to this choice. In particular, for the extremely different special case, the constant momentum space interaction of the NJL model, the same conclusions have been verified to result from these features [372].

As the next level of truncation for the quark DSE the quark–gluon vertex function

$$\Gamma_\nu^g(k, p) = \gamma_\nu + \frac{1}{6} \int \frac{d^4 l}{(2\pi)^4} g^2 D_{\rho\sigma}(p - l) \gamma_\rho S(l + k - p) \gamma_\nu S(l) \gamma_\sigma \quad (289)$$

has been employed [371,372]. This is the first–order correction of the vertex by the dressed–gluon propagator and the dressed–quark propagator, which is obtained as the solution of this DSE. Here the explicit 3–gluon vertex that could contribute at this order is omitted. As a consequence one explores 3– and 4–body interactions only to the extent that they are incorporated via the non–perturbative dressing of the gluon propagator.

Using eqs. (289) and (288) in the quark DSE one obtains

$$S^{-1}(p) = i\gamma \cdot p + m_q + G \gamma_\mu S(p) \gamma_\mu + \frac{1}{8} G^2 \gamma_\mu S(p) \gamma_\nu S(p) \gamma_\mu S(p) \gamma_\nu . \quad (290)$$

Neglecting the $O(G^2)$ term yields the rainbow–approximation quark DSE of this algebraic model.

In extending the kernel of the BS equation one must preserve the Goldstone boson character of the pion. To this end one observes that the ladder–approximation kernel in the meson BS equation can be obtained from the expression for the quark self–energy in the rainbow–approximation quark DSE via the replacement

$$\gamma_\mu S(k) \gamma_\nu \rightarrow \gamma_\mu S(k + P/2) \Gamma_M(k, P) S(k - P/2) \gamma_\nu , \quad (291)$$

which is illustrated in the top diagram of Fig. 28.

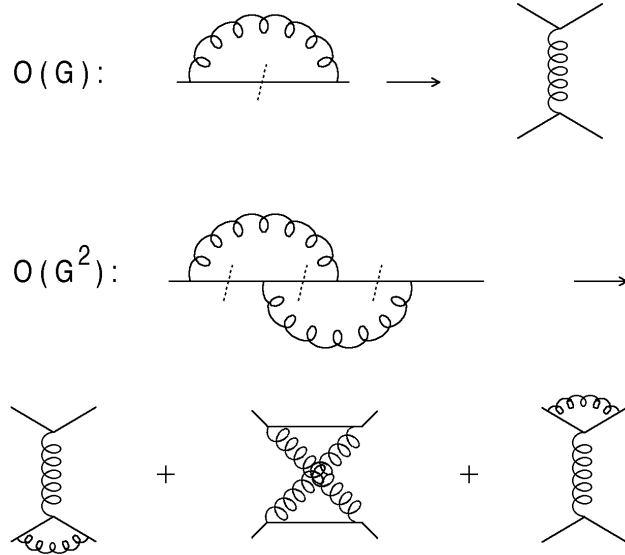


Fig. 28. Eq. (291) illustrated to $O(G^2)$, which provides the kernel of the meson and diquark BS equations. The internal solid lines represent dressed quark and gluon propagators. The internal quark lines of a given DSE contribution are cut sequentially to introduce the meson total-momentum; *e.g.*, the 3 diagrams in the last line are obtained by the sequential application of the cuts illustrated in the line above. (Adapted from ref. [371].)

In the iso-vector channel this procedure can be implemented at every order; *i.e.*, in every term of the quark DSE one may sequentially replace each internal (non-perturbative) quark propagator in this way. This generates all contributions of a given order to the kernel and ensures that Goldstone's theorem is preserved at that order, as will become clear below. This is in fact quite analogous to the Baym-Kadanoff procedure in many-body physics [373]. Its application to vacuum polarization insertions does not generate additional terms in the iso-vector kernel; a fact that very much simplifies the study of iso-vector systems, allowing one to employ a model gluon propagator and maintain Goldstone's theorem. These arguments are independent of the explicit form of the model gluon propagator.

The iso-scalar channel receives additional contributions from quark annihilation diagrams as discussed in sect. 6.2.2. In the systematic generation described above these diagrams are obtained from the quark DSE by applying eq. (291) to the dressed-quark loops in the gluon vacuum polarization, which is implicit in the dressed model gluon propagator.⁶¹ While for a given model gluon propagator the corresponding diagrams thus have to be added to the BS kernel at a specified truncation explicitly, there is no need to simultaneously modify the quark DSE in this case, since the iso-scalar meson channel is not protected by Goldstone's theorem.

The full $O(G^2)$ kernel for the iso-vector meson BS equation is illustrated in fig. 28. Using eq. (288), the BS equation for color singlet, iso-vector mesons is

$$\begin{aligned} \Gamma_M(p; P) = & -G \gamma_\mu \chi_M \gamma_\mu \\ & -\frac{1}{8} G^2 \gamma_\mu \left(S_+ \gamma_\nu S_+ \gamma_\mu \chi_M + \underline{S_+ \gamma_\nu \chi_M \gamma_\mu S_-} + \chi_M \gamma_\nu S_- \gamma_\mu S_- \right) \gamma_\nu \end{aligned} \quad (292)$$

⁶¹ Additional quark loops arise in vertex corrections at orders beyond those employed here.

Table 7

Weights of the different kernel contributions of fig. 28 corresponding to the meson and diquark BS equations, eqs. (292) and (293) respectively, for general $SU(N_c)$ (minus signs indicate attractive contributions).

kernel	$O(G)$ ladder	$O(G^2)$ vertex corr.	$O(G^2)$ crossed box
meson	$-\frac{3}{4} \frac{N_c^2 - 1}{2N_c}$	$-\left(\frac{3}{4}\right)^2 \frac{N_c^2 - 1}{4N_c^2}$	$\left(\frac{3}{4}\right)^2 \frac{N_c^2 - 1}{4N_c^2}$
diquark	$-\frac{3}{4} \frac{N_c + 1}{2N_c}$	$-\left(\frac{3}{4}\right)^2 \frac{N_c + 1}{4N_c^2}$	$\left(\frac{3}{4}\right)^2 \frac{N_c + 1}{4N_c^2} (N_c^2 - 1 - N_c)$

where $S_{\pm} \equiv S(p \pm P/2)$ and $\chi_M \equiv S_+ \Gamma_M(p; P) S_-$. Using Eq. (286) the BS equation for $(\bar{3})_c$, iso-vector diquarks can be written

$$\begin{aligned} \Gamma_{D^3}^C(p; P) = & -\frac{1}{2} G \gamma_\mu \chi_{D^3}^C \gamma_\mu - \frac{1}{16} G^2 \gamma_\mu \left(S_+ \gamma_\nu S_+ \gamma_\mu \chi_{D^3}^C \right. \\ & \left. + 5 \underline{S_+ \gamma_\nu \chi_{D^3}^C \gamma_\mu S_-} + \chi_{D^3}^C \gamma_\nu S_- \gamma_\mu S_- \right) \gamma_\nu , \end{aligned} \quad (293)$$

with $\Gamma_{D^3} \equiv \Gamma_{D^3}^C C$ and $\chi_{D^3}^C \equiv S_+ \Gamma_{D^3}^C(p; P) S_-$, where $C = \gamma_2 \gamma_4$ is the charge conjugation matrix. In these equations the underlined term is the “crossed box” contribution of fig. 28.

At $O(G)$ the only difference between Eqs. (292) and (293) is that the coupling is twice as strong in the meson equation. This follows from the algebra of the $SU(3)_c$ generators and entails [374] the existence of scalar and axialvector diquark bound-states with $m_{qq}^{0+} > m_{\bar{q}q}^{0-}$ and $m_{qq}^{1+} > m_{\bar{q}q}^{1-}$.

Only the underlined term in each of eqs. (292) and (293) is repulsive in the $0_{\bar{q}q}^-, 1_{\bar{q}q}^-, 0_{qq}^+, 1_{qq}^+$ channels. The numerical factors arise from the $SU(3)_c$ algebra. Relative to its companion this term is 5-times as large in the diquark equation, which provides for the possibility that it eliminates diquark bound-states. It might be interesting to see, how this result for the quite different weights of the repulsive to the attractive contributions in the $(1)_c$ mesonic versus the $(\bar{3})_c$ diquark channel generalizes for arbitrary numbers of colors N_c . In table 7 these weights are given for general $SU(N_c)$. Negative signs indicate attractive contributions. The crossed box contributions are the only repulsive ones at this order. One can see that for all numbers of colors $N_c > 2$ the diquark kernel is suppressed by a common overall factor $(N_c + 1)/(N_c^2 - 1)$ in all contributions. For $N_c = 2$ this factor is equal to unity and no such suppression occurs. The partial cancellation of the next order contributions in the meson channel is also found to be independent of N_c , as the repulsive crossed box term generally has the same strength as the vertex correction contributions to the kernel in this channel.

The relevant factor for removing the diquark poles of the ladder approximation from the spectrum is the factor $(N_c^2 - 1) - N_c$ which is unique to the repulsive crossed box term of the diquark channel. Again, for the $SU(2)$ gauge group this factor is unity and a complete degeneration between meson and diquark channels is obtained in this case. The color singlet diquarks for $N_c = 2$ can be interpreted as baryons which are degenerate with mesons in the gauge group $SU(2)$ due to the Pauli–Gürsey symmetry.

In the large N_c limit, on the other hand, the leading term, of $\mathcal{O}(N_c)$, in the meson BS equation is the ladder kernel. The higher orders are suppressed by $1/N_c$, and the ladder approximation for mesons thus gets better at larger N_c . In the diquark BSE this leading order $\mathcal{O}(N_c)$ is given by the repulsive term in the kernel. This is in agreement with the general large N_c argument that mesons are the only relevant effective degrees of freedom in this limit [248,301].

7.1.2 Disappearance of the Diquark Bound States

In order to study the bound-state spectrum one must solve the quark DSE. The $\mathcal{O}(G^2)$ corrections become noticeable for $p^2 < \eta^2/2$, which is important because it is the domain sampled in the BS equation. It is also important to note that one has dynamical chiral-symmetry breaking for any $G > 0$. Furthermore, the quark propagator possesses no pole on the real p^2 -axis. Therefore the quark propagator certainly has no Lehmann representation.

The model gluon propagator of eq. (288) entails that the bound-state constituents have zero relative momentum; *i.e.*, $p = 0$. In this case the most general form of the $0_{\bar{q}q}^-$ BS amplitude is

$$\Gamma_M^{0-}(P) = \left[\theta_1^{0-}(P^2) + i \frac{P}{\eta} \theta_2^{0-}(P^2) \right] \gamma_5. \quad (294)$$

Substituting Eq. (294) into Eq. (292), with $p = 0$, one obtains a 2×2 matrix eigenvalue problem of the form $H\Theta = \Theta$ where the elements of H depend on P^2 , and $\Theta^T = (\theta_1, \theta_2)$. The eigenvalue problem is solved for $\det\{H(P^2) - \mathbb{1}\} = 0$. The same procedure is applied to each of the other channels. The vector meson BS amplitude has the form

$$\Gamma_M^{1-}(P) = \gamma_\mu \epsilon_\mu^\lambda(P) \theta_1^{1-}(P^2) + \frac{i}{\eta} \sigma_{\mu\nu} \epsilon_\mu^\lambda(P) P_\nu \theta_2^{1-}(P^2), \quad (295)$$

where $\epsilon_\mu^\lambda(P)$, $\lambda = 0, \pm 1$, is the polarization vector: $\epsilon^\lambda \cdot P = 0$. $\Gamma_{D^3}^{0+}$ has the same form as the pseudoscalar meson amplitude in Eq. (294); and $\Gamma_{D^3}^{1+}$ the same form as the vector meson amplitude in eq. (295).

The chiral limit results are presented in table 8, the eigenvectors are:

	$\mathcal{O}(G): \mathcal{O}(G)$	$\mathcal{O}(G^2): \mathcal{O}(G^2)$
$(\theta_1^{0-}, \theta_2^{0-})$	(0.83, 0.55)	(0.87, 0.49)
$(\theta_1^{1-}, \theta_2^{1-})$	(1, 0)	(0.99, -0.12)

(296)

The Goldstone theorem is manifest when the quark DSE and pseudoscalar meson BS equation are truncated consistently; *i.e.*, at $\mathcal{O}(G):\mathcal{O}(G)$ and $\mathcal{O}(G^2):\mathcal{O}(G^2)$. This can be shown analytically via a straightforward generalization of the arguments of Ref. [276]. If the dressing is inconsistent, *e.g.*, $\mathcal{O}(G):\mathcal{O}(G^2)$, the pseudoscalar is half as massive as the vector meson. The $\mathcal{O}(G^2)$ corrections only provide for a small (10%) mass increase in the vector meson channel,

Table 8

Calculated meson and diquark masses (in GeV). The labels “ $O(G^n): O(G^m)$ ” mean that the solution of the $O(G^n)$ quark Dyson–Schwinger equation was used in the $O(G^m)$ Bethe–Salpeter equation. The mass scale $\eta = 1.06$ GeV ($G = \eta^2/4$) and the non-zero quark mass were chosen to reproduce the experimental ratio m_π/m_ρ at $O(G^2):O(G^2)$. “Unbound” means that there is no solution of the associated homogeneous Bethe–Salpeter equation for real P^2 . (Adapted from ref. [371].)

$m_q = 0$	$O(G): O(G)$	$O(G): O(G^2)$	$O(G^2): O(G^2)$
$m_{\bar{q}q}^{0-}$	0	0.30	0
$m_{\bar{q}q}^{0+}$	1.19	Unbound	Unbound
$m_{\bar{q}q}^{1-}$	0.750	0.745	0.823
$m_{\bar{q}q}^{1+}$	1.30	Unbound	Unbound
<hr/>			
$m_q = 0.012$			
$m_{\bar{q}q}^{0-}$	0.140	0.328	0.136
$m_{\bar{q}q}^{0+}$	1.21	Unbound	Unbound
$m_{\bar{q}q}^{1-}$	0.767	0.760	0.770
$m_{\bar{q}q}^{1+}$	1.32	Unbound	Unbound

as one would expect of a weak, net–repulsive interaction. It is weak because of the cancellation between the vertex correction and crossed box contributions, which is a necessary consequence of the preservation of Goldstone’s theorem.

In the diquark channel, however, where the coefficient of the repulsive term is larger and the cancellation incomplete, the $O(G^2)$ corrections have the significant effect of eliminating the (bound state) pole on the real P^2 –axis. This means that the $(\bar{3})_c$ 4–quark correlations do not have a spectral representation with asymptotic diquark state contribution.

The results for $m_q \neq 0$ are also presented in table 8. The Goldstone boson character of the pseudoscalar is clear; *i.e.*, at a consistent level of truncation its mass increases rapidly from zero as m_q is increased. For $m_q = 0.012$ GeV, $\det\{H(P^2) - \mathbb{1}\}$ is plotted in fig. 29. It illustrates the effect of the $O(G^2)$ repulsive term in the BS kernel, which shifts the zero in the meson channel very little but completely eliminates it in the diquark channel.

While the absence of a Lehmann representation for gluon and quark correlations suffices to ensure there are no gluons and quarks in the strong interaction spectrum, it neither entails nor precludes the existence of bound states, whether colored or not. The rainbow–ladder truncation is peculiar in the sense that it alone contains either purely attractive or purely repulsive terms in the BSE kernel in a given channel. In every truncation beyond this there are both attractive and repulsive terms. The systematic procedure for extending the rainbow–ladder kernel presented here ensures the preservation of Goldstone’s theorem at every step.

To illustrate these points the simple model gluon propagator, eq. (288), was employed. In a consistent truncation there is almost complete cancellation between the $O(G^2)$ attractive and repulsive terms in the meson channel. This is an indication of why the studies of meson spectroscopy and decays using a model gluon propagator in rainbow–ladder approximation

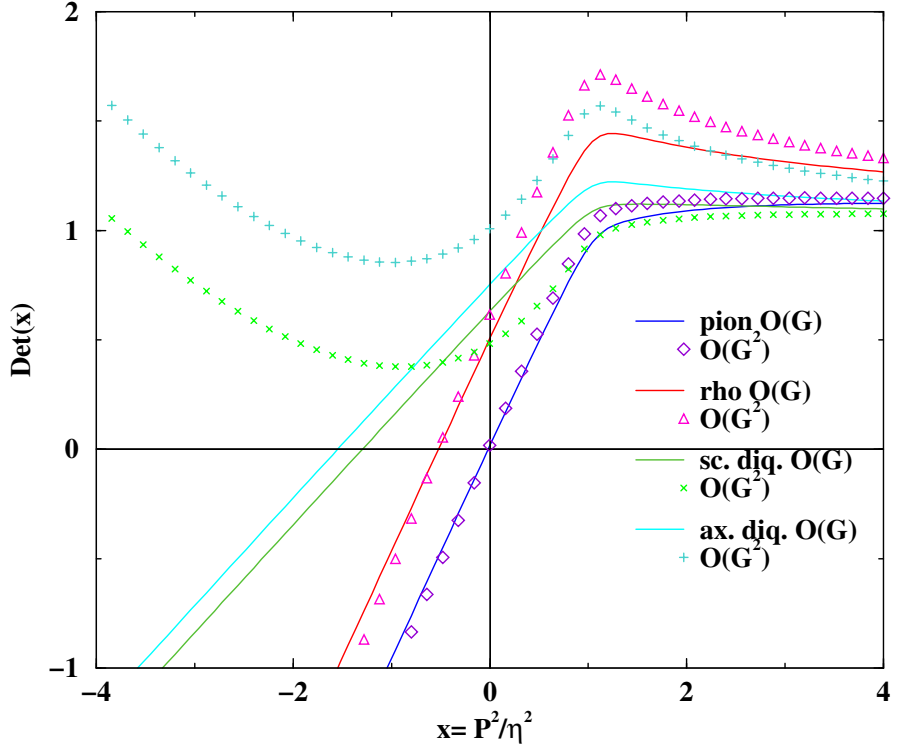


Fig. 29. $\det\{H(P^2) - 1\}$ plotted as a function of P^2 . This function vanishes at the square of the bound state mass in the channel under consideration. (Adapted from ref. [371].)

have been successful; *i.e.*, that the truncation scheme may converge rapidly in the meson channel. The situation is quite different in the diquark channel, however. The $SU(3)_c$ algebra ensures that the coefficient of the $O(G^2)$ repulsive term is considerably larger. This entails that the repulsive effect survives to ensure that there is no diquark bound state. This effect cannot reasonably be reproduced in rainbow-ladder approximation and indicates that this truncation is inadequate for the study of 4-quark correlations.

7.2 Modelling of Diquarks

In the simple algebraic gluon model employed in the last section, the diquark poles are actually moved into the complex P^2 -plane by the repulsive contributions to the quark interactions. This affects the analytic properties of the 4-quark Green's function, of course. As on the level of the elementary quark correlations in this model, the analytic structure of amplitudes is in general not what one might naively expect from a local quantum field theory. Nevertheless, complex poles in diquark correlations might in principle also serve to parameterize the relevant part of diquark correlations in baryons in a separable fashion. It is then, however, important to study the domain of holomorphy of these correlations in detail to verify the justification of a Euclidean formulation and its limitations. Standard analyticity arguments cannot be used anymore.

Another realization of diquark confinement might be due to a negative norm for the corresponding amplitudes. An analytic structure of 4-quark correlations in agreement with Lorentz

covariance and locality actually implies that singularities occur on the timelike P^2 -axis only, exactly as in color-singlet channels. The difference between physical, *e.g.*, meson states and unphysical diquark states would then have to be due to their respective norms. Very much like quarks and transverse gluons, a spectral function for the discontinuity (at the cut along the timelike total P^2 -axis) in diquark correlations which is not positive would imply that the corresponding states are in the unphysical part of the indefinite metric space of gauge theories. It is a peculiarity of indefinite metric spaces that possible components of such states in a properly defined positive subspace can always be removed by an equivalence transformation, *i.e.*, one which leaves physical matrix elements (in the positive subspace) unchanged [47]. Obviously, given the standard analyticity of correlation functions there is nothing to worry about the implementation of timelike (*e.g.*, bound state) momenta by analytically continuing the Euclidean formulation. The absence of anomalous thresholds, easily established fundamentally, is technically harder to realize in actual calculations, however.

Leaving the question aside here as to whether singularities in diquark correlations occur at complex or timelike P^2 (with negative norm), separable contributions due to isolated poles in the possibly complex total momentum of diquark correlations are in either case the ones of interest in the present description of baryons. The general model building presented in the following thus assumes separable pole contributions to parameterize diquark correlations. Quark correlations are parameterized in the simplest case by free constituent fermion propagators. Model correlations mimicing confinement by the absence of quark poles can technically be implemented straightforwardly with minor modifications, see refs. [364,365]. The notations used in this section resort to Minkowski space conventions with formal Wick rotations performed in the last step before numerical calculations. Given there are no subtleties by non-standard analyticity properties of the amplitudes, the procedure is completely equivalent to a complex Euclidean formulation from the beginning. It might seem more intuitive, though, to start the description of bound states in Minkowski space.

The 4-point quark Green's function,

$$G_{\alpha\beta\gamma\delta}(x_1, x_2, x_3, x_4) = \langle T(q_\gamma(x_3)q_\alpha(x_1)\bar{q}_\beta(x_2)\bar{q}_\delta(x_4)) \rangle. \quad (297)$$

is assumed to have a diquark pole in the total momentum P which gives rise to a contribution

$$\begin{aligned} G_{\alpha\gamma,\beta\delta}^{\text{pole}}(p, q, P) &:= e^{-iP\bar{Y}} \int d^4X d^4y d^4z e^{iqz} e^{-ipy} e^{iPX} G_{\alpha\beta\gamma\delta}^{\text{pole}}(x_1, x_2, x_3, x_4) \\ &= \frac{i}{P^2 - m_d^2 + i\epsilon} \chi_{\gamma\alpha}(p, P) \bar{\chi}_{\beta\delta}(q, P) , \end{aligned} \quad (298)$$

where the definitions $X = \eta_1 x_1 + \eta_3 x_3$, with $\eta_1 + \eta_3 = 1$, and $\bar{Y} = \eta_4 x_2 + \eta_2 x_4$, with $\eta_2 + \eta_4 = 1$; and $y = x_1 - x_3$, $z = x_2 - x_4$ have been used. m_d denotes the diquark mass. The BS wave functions $\chi(p, P)$ of the diquark bound state are defined by the matrix elements,

$$\chi_{\alpha\beta}(x, y; \vec{P}) := \langle q_\alpha(x)q_\beta(y) | P_+ \rangle \quad (299)$$

$$\bar{\chi}_{\alpha\beta}(x, y; \vec{P}) := \langle P_+ | \bar{q}_\alpha(x)\bar{q}_\beta(y) \rangle = \left(\gamma_0 \chi^\dagger(y, x; \vec{P}) \gamma_0 \right)_{\alpha\beta} \quad (300)$$

Note that there is no need for time ordering here in contrast to quark–antiquark bound states. The following normalization of the states is used,

$$\langle P'_\pm | P_\pm \rangle = 2\omega_P (2\pi)^3 \delta^3(\vec{P}' - \vec{P}) , \quad \omega_P^2 = \vec{P}^2 + m_d^2 , \quad (301)$$

and the charge conjugate bound state is defined as $|P_- \rangle = C|P_+ \rangle$. The contribution of the charge conjugate bound state is included in (298) for $P_0 = -\omega_P$. From invariance under space–time translations, the BS wave function has the the general form,

$$\chi_{\alpha\beta}(x, y; \vec{P}) = e^{-iP X} \int \frac{d^4 p}{(2\pi)^4} e^{-ip(x-y)} \chi_{\alpha\beta}(p, P) , \quad (302)$$

with $X = \eta_x x + \eta_y y$, $p := \eta_y p_\alpha - \eta_x p_\beta$, and $P = p_\alpha + p_\beta$, where p_α , p_β denote the momenta of the outgoing quarks in the Fourier transform $\chi_{\alpha\beta}(p_\alpha, p_\beta; \vec{P})$ of $\chi_{\alpha\beta}(x, y; \vec{P})$. One thus has the relation, $\chi_{\alpha\beta}(p, P) := \chi_{\alpha\beta}(p + \eta_x P, -p + \eta_y P; \vec{P})|_{P_0=\omega}$. In the definition of the conjugate amplitude, the convention

$$\bar{\chi}_{\alpha\beta}(x, y; \vec{P}) = e^{iP \bar{X}} \int \frac{d^4 p}{(2\pi)^4} e^{-ip(x-y)} \bar{\chi}_{\alpha\beta}(p, P) , \quad (303)$$

with $\bar{X} = \eta_x y + \eta_y x$, ensures that hermitian conjugation from eq. (300) yields,

$$\bar{\chi}_{\alpha\beta}(p, P) = (\gamma_0 \chi^\dagger(p, P) \gamma_0)_{\alpha\beta} . \quad (304)$$

In the conjugate amplitude $\bar{\chi}_{\alpha\beta}(p, P)$, the definition of relative and total momenta corresponds to $p = \eta_x p'_\alpha - \eta_y p'_\beta$ and $P = -p'_\alpha - p'_\beta$ for the outgoing quark momenta p'_α, p'_β in

$$\bar{\chi}_{\alpha\beta}(p'_\alpha, p'_\beta; \vec{P}) = (\gamma_0 \chi^\dagger(-p'_\beta, -p'_\alpha; \vec{P}) \gamma_0)_{\alpha\beta} . \quad (305)$$

Note here that hermitian conjugation implies for the momenta of the two respective quark legs, $p_\alpha \rightarrow p'_\alpha = -p_\beta$, and $p_\beta \rightarrow p'_\beta = -p_\alpha$, which is equivalent to $\eta_x \leftrightarrow \eta_y$ and $P \rightarrow -P$. Besides the hermitian conjugation of eq. (304), one has from the antisymmetry of the wave function, $\chi_{\alpha\beta}(x, y; \vec{P}) = -\chi_{\beta\alpha}(y, x; \vec{P})$. For the corresponding functions of the relative coordinates/momenta, this entails that η_x and η_y have to be interchanged in exchanging the quark fields,

$$\chi(x; \vec{P}) = -\chi^T(-x; \vec{P}) \Big|_{\eta_x \leftrightarrow \eta_y} , \quad \chi(p, P) = -\chi^T(-p, P) \Big|_{\eta_x \leftrightarrow \eta_y} . \quad (306)$$

This interchange of the momentum partitioning can be undone by a charge conjugation, from which the following identity is obtained,

$$\chi^T(p, P) = -C \bar{\chi}(-p, -P) C^{-1} . \quad (307)$$

This last identity will become useful to relate $\bar{\chi}$ to χ in Euclidean space, which is a highly non-trivial task. In particular, this avoids the somewhat ambiguous definition of the conjugation following from eq. (300) in Euclidean space with complex bound state momenta.

One last definition for diquark amplitudes concerns the truncation of the quark legs, defining the amputated amplitudes $\tilde{\chi}$, $\tilde{\bar{\chi}}$,

$$\chi_{\alpha\beta}(p, P) = \left(S(p_\alpha) \tilde{\chi}(p, P) S^T(p_\beta) \right)_{\alpha\beta} , \quad (308)$$

$$\bar{\chi}_{\alpha\beta}(p, P) = \left(S^T(-p'_\alpha) \tilde{\bar{\chi}}(p, P) S(-p'_\beta) \right)_{\alpha\beta} . \quad (309)$$

With the definitions above, the same relations hold for the amputated amplitudes, in particular,

$$\tilde{\bar{\chi}}(p, P)_{\alpha\beta} = \left(\gamma_0 \tilde{\chi}^\dagger(p, P) \gamma_0 \right)_{\alpha\beta} . \quad (310)$$

Once a gluonic interaction kernel between the quarks is specified, the diquark amplitudes could in principle be obtained from homogeneous BS equations very much like mesons are obtained in the quark-antiquark bound state problem. However, as we have seen that correlations beyond the ladder approximation are important, and because no symmetry-preserving way of including a non-trivial quark-gluon vertex function is known, as a first step towards this more complete calculation, parameterizations for scalar and axialvector diquark amplitudes are explored in the Bethe-Salpeter/Faddeev nucleon bound state equation. No quark-quark BS equation for the diquark amplitudes is solved but the general aspects anticipated for such solutions are studied in baryonic bound states. For a given parameterization the standard normalization integrals are calculated to fix the normalization of the amplitudes. These integrals are obtained from the inhomogeneous quark-quark BS equation under the usual assumption that the gluonic interaction kernel be independent on the total diquark momentum P . Given the exchange symmetry of the quark-quark BS equation such an assumption seems reasonable also for general kernels. For identical quarks with propagator $S(p)$ the resulting normalization condition reads:

$$1 = \frac{-i}{4m_d^2} \int \frac{d^4 p}{(2\pi)^4} \left\{ \text{tr} \left(S^T(p_\beta) \tilde{\bar{\chi}}(p, P) \left(P \frac{\partial}{\partial P} S(p_\alpha) \right) \tilde{\chi}(p, P) \right) + \left(\tilde{\bar{\chi}}(p, P) S(p_\alpha) \tilde{\chi}(p, P) \left(P \frac{\partial}{\partial P} S^T(p_\beta) \right) \right) \right\} , \quad (311)$$

with $p_\alpha = p + \eta_1 P$ and $p_\beta = -p + \eta_2 P$.

Contrary to the quark-antiquark and quark-quark case the kernel of the quark-diquark BS equation necessarily depends on the total bound state, *i.e.* baryon, momentum. To demonstrate this it is sufficient to consider only the leading Dirac covariant of the scalar isoscalar diquark,

$$\chi(p, P) = \gamma_5 C \frac{1}{N_s} \tilde{P}(p^2, pP) , \quad (312)$$

where C is the charge conjugation matrix. The normalization constant N_s is explicitly separated from the invariant function $\tilde{P}(p, P)$. This constant is then fixed from the normalization condition in eq. (311) for a given choice of \tilde{P} . For further simplicity, it might seem reasonable to neglect the dependence of this invariant function on the scalar pP in addition. This simplification, yielding the leading moment of an expansion of the angular dependence in terms of orthogonal polynomials, is known to give the dominant contribution to bound state amplitudes in many circumstances. However, in the present case the antisymmetry of the diquark wave function, *c.f.*, eqs. (306), for identical quarks, entails that

$$\tilde{P}(p^2, pP) = \tilde{P}(p^2, -pP) \Big|_{\eta_1 \leftrightarrow \eta_2} . \quad (313)$$

For general $\eta_1 = 1 - \eta_2 \neq 1/2$ and thus for $\bar{p} := p|_{\eta_1 \leftrightarrow \eta_2} \neq p$, it is therefore not possible to neglect the pP dependence in the amplitude completely without violating the quark-exchange symmetry. To correct this, one may assume instead that the amplitude depends on both scalars, p^2 and pP in a specific way as to guarantee this symmetry, namely via the scalar $x := p_\alpha p_\beta - \eta_1 \eta_2 m_d^2 = (\eta_2 - \eta_1)pP - p^2 = -(\eta_2 - \eta_1)\bar{p}P - \bar{p}^2$ with $\bar{p} = \eta_1 p_\alpha - \eta_2 p_\beta$, and with the definitions of $p_{\{\alpha, \beta\}}$ given above. For $\eta_1 = \eta_2 = 1/2$ this coincides with the usual relative momentum ($x = p^2$). Note further that $P^2 = m_d^2$ is not a free variable of the amplitude. For the two remaining scalars built out of the two momenta p and P the particular choice with definite exchange symmetry is given by the two independent combinations $p_\alpha p_\beta$, which is essentially the same x as above, and $p_\alpha^2 - p_\beta^2$. The latter has to appear in odd powers, *i.e.*, in higher moments. These are neglected thus setting,

$$\tilde{P}(p^2, pP) = P(x) = P((\eta_2 - \eta_1)pP - p^2) = P((\eta_1 - \eta_2)\bar{p}P - \bar{p}^2) . \quad (314)$$

The parameterizations of diquark amplitudes used in the baryon models of refs. [363–365] actually neglect possible sub-structure completely, corresponding to $P(p^2, pP) \equiv 1$. In this case, the normalization constant N_s is ill-defined. An additional free parameter is introduced as the strength of the diquark–quark coupling which in a more realistic description corresponds to exactly the normalization of the diquark amplitude as obtained from eq. (311). More recent studies [366,368] have improved on this model assumption and included a sub-structure of diquarks. As the quark–diquark coupling is then not at ones disposal, it is assessed this way whether in such a calculation the quark–diquark approximation can lead to a viable description of baryons for coupling strengths as obtained from BS diquark amplitudes rather than adjusted as free parameter.

The discussion of this section demonstrates some general aspects in such a parameterization, most importantly, due to the exchange symmetry of the amplitude. The precise shape of the function $P(x)$ can be conveniently fixed from the calculated electromagnetic form factor of the nucleon, see sect. 7.4 below. It will turn out that a dipole form $P_d(x) = \lambda^4/(x + \lambda^2)^2$ for the diquark amplitude will lead to good results for form factors. The respective width λ indirectly determines the coupling strengths to the quarks. These widths are adjusted in the calculation so as to yield the diquark normalization $1/N_s$ necessary from fixing the nucleon mass. From solutions to diquark BS equations in a next step, the question of the necessary diquark–quark coupling strengths to yield sufficiently strong binding to the 3rd quark in baryons by the mechanism described below will be shifted further to the strength of the gluonic quark–quark

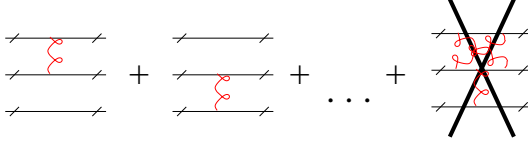


Fig. 30. Examples for admitted and excluded graphs in the 3-quark interaction kernel K . (Adapted from ref. [369].)

$$\boxed{t_1} = \sum_a \chi_1^a \otimes D_1^{(a)} \otimes \bar{\chi}_1^a$$

Fig. 31. The separable t -matrix. (Adapted from ref. [369].)

interaction kernel in the diquark channels. The finite width of the diquark correlations implies a further technical improvement. While some ultraviolet regularization is necessary with the point-like diquark–quark couplings of refs. [363–365], in a more realistic calculation sufficient ultraviolet convergence is naturally provided by the damping from the diquark amplitude.

7.3 Quark–Diquark Bethe–Salpeter Equations

7.3.1 General Structure of Bethe–Salpeter Amplitudes of Octet and Decuplet Baryons

Without a genuine 3–quark scattering kernel, see fig. 30, and assuming separability of the quark–quark t -matrix, see fig. 31, the Dyson series for the full 3–quark propagator reduces to a coupled set of Bethe–Salpeter/Faddeev equations for baryons as bound states of quark and diquark correlations, see, *e.g.*, ref. [354]. Hereby, neither for quark nor for diquark correlations a particle interpretation has to be assumed. In particular, the separability assumption for the quark–quark t -matrix may or may not be realized by a sum over particle pole contributions. To be concrete we will choose the following ansatz for the quark–quark scattering matrix (returning thereby to Euclidean notation)

$$t(k_\alpha, k_\beta; p_\alpha, p_\beta) \equiv t(k, p, P) = \chi_{\alpha\beta}^5(k, P) D(P) \bar{\chi}_{\gamma\delta}^5(p, P) + \chi_{\alpha\beta}^\mu(k, P) D^{\mu\nu}(P) \bar{\chi}_{\gamma\delta}^\nu(p, P) . \quad (315)$$

The relative momenta are defined as

$$k[p] = \sigma k_\alpha[p_\alpha] - (1 - \sigma) k_\beta[p_\beta], \quad \sigma \in [0, 1] . \quad (316)$$

The diquark propagators used in the scalar and the axialvector channel are taken to be

$$D(P) = -\frac{1}{P^2 + m_{sc}^2} C(P^2, m = m_{sc}) , \quad (317)$$

$$D^{\mu\nu}(P) = -\frac{1}{P^2 + m_{ax}^2} \left(\delta^{\mu\nu} + (1 - \xi) \frac{P^\mu P^\nu}{m_{ax}^2} \right) C(P^2, m = m_{ax}) . \quad (318)$$

With the choice $C(P^2, m) = 1$ and $\xi = 0$ they correspond to free propagators of a spin-0 and a spin-1 particle. This will be the form to be employed in this and the next section. Later on we will review investigations using nontrivial forms for C which remove the free-particle poles from the real axis and thus may mimic confinement.

Equipped with the separable form of the two-quark correlations, eq. (315), we will now derive the BS equation for the nucleon and the Delta baryon. The generalization to octet and decuplet baryons (using three flavours in the isospin limit) is given in ref. [365], and we will shortly comment on it at the end of this section. To complete the model definition, we have to specify the functional form of the quark propagator. We take it to be a free fermion propagator with a constituent mass m_q ,

$$S(p) = \frac{i\cancel{p} - m_q}{p^2 + m_q^2} i C(p^2, m = m_q) \quad \text{with } C(p^2, m = m_q) = 1. \quad (319)$$

Of course, when using modified diquark propagators, $C \neq 1$, the quark propagator will be altered accordingly.

The nucleon BS amplitudes (or wave functions) can be described by an effective multi-spinor characterizing the scalar and axialvector correlations,

$$\Psi(p, P) u(P, s) \equiv \begin{pmatrix} \Psi^5(p, P) \\ \Psi^\mu(p, P) \end{pmatrix} u(P, s). \quad (320)$$

$u(P, s)$ is a positive-energy Dirac spinor of spin s , p and P are the relative and total momenta of the quark-diquark pair, respectively. The vertex functions are defined by truncation of the legs,

$$\begin{pmatrix} \Phi^5 \\ \Phi^\mu \end{pmatrix} = S^{-1} \begin{pmatrix} D^{-1} & 0 \\ 0 & (D^{\mu\nu})^{-1} \end{pmatrix} \begin{pmatrix} \Psi^5 \\ \Psi^\nu \end{pmatrix}. \quad (321)$$

The diquark propagators D and $D^{\mu\nu}$ are defined in eqs. (317,318), and the quark propagator S in eq. (319). The coupled system of BS equations for the nucleon amplitudes or their vertex functions can be written in the following compact form,

$$\int \frac{d^4 p'}{(2\pi)^4} G^{-1}(p, p', P) \begin{pmatrix} \Psi^5 \\ \Psi^\mu \end{pmatrix}(p', P) = 0, \quad (322)$$

in which $G^{-1}(p, p', P)$ is the inverse of the full quark-diquark 4-point function. It is the sum of the disconnected part and the interaction kernel. The latter results from the reduction of the Faddeev equation for separable quark-quark correlations. It describes the exchange of the quark with one of those in the diquark which is necessary to implement Pauli's principle in the baryon, *i.e.* it describes the minimal dynamical coupling necessary to account for the full exchange symmetry in the quark-diquark model [350]. Due to the overall colour antisymmetry of the baryon (being a colour singlet) the other quantum numbers have to be symmetrized leading to Pauli attraction instead of Pauli repulsion familiar from most ordinary fermionic

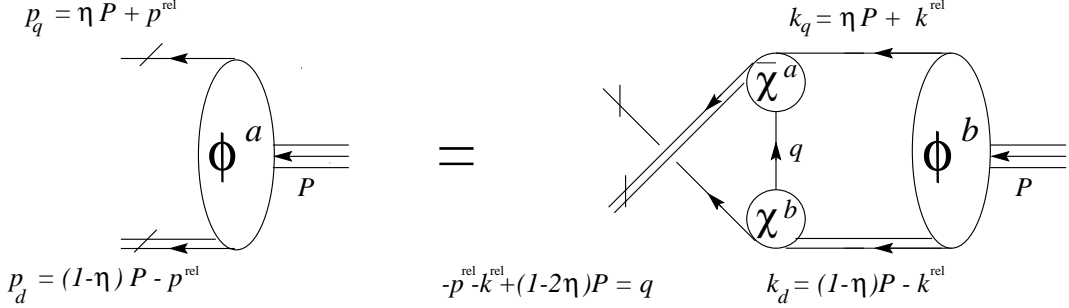


Fig. 32. The coupled set of BS equations for the vertex functions Φ . (Adapted from ref. [369].)

many-body systems. Taking into account the coupled channel nature of scalar and axialvector diquark contributions within the nucleon one obtains

$$G^{-1}(p, p', P) = (2\pi)^4 \delta^4(p - p') S^{-1}(p_q) \begin{pmatrix} D^{-1}(p_d) & 0 \\ 0 & (D^{\mu'\mu})^{-1}(p_d) \end{pmatrix} - \frac{1}{2} \begin{pmatrix} -\chi(p_2^2) S^T(q) \bar{\chi}(p_1^2) & \sqrt{3} \chi^{\mu'}(p_2^2) S^T(q) \bar{\chi}(p_1^2) \\ \sqrt{3} \chi(p_2^2) S^T(q) \bar{\chi}^{\mu}(p_1^2) & \chi^{\mu'}(p_2^2) S^T(q) \bar{\chi}^{\mu}(p_1^2) \end{pmatrix}. \quad (323)$$

The flavor and color factors have been taken into account explicitly, and χ , χ^μ stand for the Dirac structures of the diquark-quark vertices. The freedom to partition the total momentum between quark and diquark introduces the parameter $\eta \in [0, 1]$ with $p_q = \eta P + p$ and $p_d = (1 - \eta)P - p$ as usual. The momentum of the exchanged quark is then given by $q = -p - p' + (1 - 2\eta)P$. The relative momenta of the quarks in the diquark vertices χ and $\bar{\chi}$ are $p_2 = p + p'/2 - (1 - 3\eta)P/2$ and $p_1 = p/2 + p' - (1 - 3\eta)P/2$, respectively. Invariance under 4-dimensional translations implies that for every solution $\Phi(p, P; \eta_1)$ of the BS equation there exists a family of solutions of the form $\Phi(p + (\eta_2 - \eta_1)P, P; \eta_2)$. The corresponding BS equations are pictorially represented in fig. 32. The necessary presence of the total momentum P of the baryonic bound state in the exchange kernel for $\eta \neq 1/2$ was apparently not taken into account in the studies of refs. [363,364].

As stated in the last section the quark exchange kernel of the reduced Bethe-Salpeter/Faddeev problem for baryons, for $\eta \neq 1/2$, necessarily depends on the total momentum of the baryonic bound state P . Since this has important implications on the normalizations and charges of the bound state amplitudes, it is preferable to use the residual freedom in choosing the momentum partitionings in the relativistic bound state problem such as to keep the bound state momentum dependence of the exchange kernel to a necessary minimum. While the exchange quark momentum is found to be P -independent for $\eta = 1/2$, this choice, however, necessarily introduces P -dependence in the diquark amplitudes: The dominant momentum dependence of the diquark amplitudes are given by the scalars x_1 and x_2 ,

$$x_1 = -p_1^2 - (1 - 2\sigma)((1 - \eta)p_1 P - p_1 k), \quad (324)$$

$$x_2 = -p_2^2 + (1 - 2\sigma')((1 - \eta)p_2 P - p_2 p). \quad (325)$$

These coincide with $p_{1,2}^2$ only for symmetric quark momentum partitionings, *i.e.*, $\sigma = \sigma' = 1/2$, *c.f.*, the discussion at the end of the last section. These symmetrized arguments of the diquark

amplitudes $x_{1,2}$ are independent of the total nucleon momentum, only if $\sigma = \sigma' = \frac{1}{2}$ and thus $\eta = \frac{1}{3}$. This conclusion can be generalized [366]: The exchange symmetry of the diquark amplitudes suffices to show that these can generally be independent of P only if $\eta = 1/3$ and $\sigma = \sigma' = 1/2$. This is the only choice leading to diquark amplitudes independent of the total nucleon bound state momentum P , and this follows from the exchange symmetry alone and is *not* a result of the particular parameterizations employed in the model calculation.

In actual calculations the variable η is varied around the value $\eta = 1/3$ [368]. The diquark momentum partitionings are fixed to $\sigma = \sigma' = (1 - 2\eta)/(1 - \eta)$ for given η . While P -independent diquark amplitudes can be obtained only for the value $\eta = 1/3$ with this choice the exchange quark carries total momentum whenever $\eta \neq 1/2$. This entails that the exchange kernel of the reduced Bethe-Salpeter/Faddeev equation for baryons unavoidably depends on the total momentum of the baryonic bound state. This implies some considerable extensions to the calculations, *e.g.*, of electromagnetic form factors, which become necessary with the inclusion of diquark sub-structure [366,368].

Using the positive energy projector with nucleon bound-state mass M_n ,

$$\Lambda^+ = \frac{1}{2} \left(1 + \frac{P}{iM_n} \right), \quad (326)$$

the vertex functions can be decomposed into their most general Dirac structures,

$$\Phi^5(p, P) = (S_1 + \frac{i}{M_n} \not{p} S_2) \Lambda^+, \quad (327)$$

$$\begin{aligned} \Phi^\mu(p, P) = & \frac{P^\mu}{iM_n} (A_1 + \frac{i}{M_n} \not{p} A_2) \gamma_5 \Lambda^+ + \gamma^\mu (B_1 + \frac{i}{M_n} \not{p} B_2) \gamma_5 \Lambda^+ + \\ & \frac{p^\mu}{iM_n} (C_1 + \frac{i}{M_n} \not{p} C_2) \gamma_5 \Lambda^+. \end{aligned} \quad (328)$$

In the rest frame of the nucleon, $P = (\vec{0}, iM_n)$, the unknown scalar functions S_i and A_i are functions of $p^2 = p^\mu p^\mu$ and of $P \cdot p$. Certain linear combinations of these eight covariant components then lead to a full partial wave decomposition, see the next section.

The BS solutions are normalized by the canonical condition

$$M_n \Lambda^+ \stackrel{!}{=} - \int \frac{d^4 p}{(2\pi)^4} \int \frac{d^4 p'}{(2\pi)^4} \bar{\Psi}(p', P_n) \left[P^\mu \frac{\partial}{\partial P^\mu} G^{-1}(p', p, P) \right]_{P=P_n} \Psi(p, P_n). \quad (329)$$

The effective multi-spinor for the delta baryon representing the BS wave function can be characterized as $\Psi_\Delta^{\mu\nu}(p, P) u^\nu(P)$ where $u^\nu(P)$ is a Rarita-Schwinger spinor. The momenta are defined analogously to the nucleon case. As the delta state is flavor symmetric, only the axialvector diquark contributes and, accordingly, the corresponding BS equation reads,

$$\int \frac{d^4 p'}{(2\pi)^4} G_{\Delta}^{-1}(p, p', P) \Psi_{\Delta}^{\mu'\nu}(p', P) = 0, \quad (330)$$

where the inverse quark-diquark propagator G_{Δ}^{-1} in the Δ -channel is given by

$$G_{\Delta}^{-1}(p, p', P) = (2\pi)^4 \delta^4(p - p') S^{-1}(p_q) (D^{\mu\mu'})^{-1}(p_d) + \chi^{\mu'}(p_2^2) S^T(q) \bar{\chi}^{\mu}(p_1^2). \quad (331)$$

The general decomposition of the corresponding vertex function $\Phi_{\Delta}^{\mu\nu}$, obtained as in eq. (321) by truncating the quark and diquark legs of the BS wave function $\Psi_{\Delta}^{\mu\nu}$, reads

$$\begin{aligned} \Phi_{\Delta}^{\mu\nu}(p, P) = & (D_1 + \frac{i}{M_{\Delta}} \not{p} D_2) \Lambda^{\mu\nu} + \frac{P^{\mu}}{iM_{\Delta}} (E_1 + \frac{i}{M_{\Delta}} \not{p} E_2) \frac{p^{\lambda T}}{iM_{\Delta}} \Lambda^{\lambda\nu} + \\ & \gamma^{\mu} (E_3 + \frac{i}{M_{\Delta}} \not{p} E_4) \frac{p^{\lambda T}}{iM_{\Delta}} \Lambda^{\lambda\nu} + \frac{p^{\mu}}{iM_{\Delta}} (E_5 + \frac{i}{M_{\Delta}} \not{p} E_6) \frac{p^{\lambda T}}{iM_{\Delta}} \Lambda^{\lambda\nu}. \end{aligned} \quad (332)$$

Here, $\Lambda^{\mu\nu}$ is the Rarita-Schwinger projector,

$$\Lambda^{\mu\nu} = \Lambda^+ \left(\delta^{\mu\nu} - \frac{1}{3} \gamma^{\mu} \gamma^{\nu} + \frac{2}{3} \frac{P^{\mu} P^{\nu}}{M_{\Delta}^2} - \frac{i}{3} \frac{P^{\mu} \gamma^{\nu} - P^{\nu} \gamma^{\mu}}{M_{\Delta}} \right) \quad (333)$$

which obeys the constraints

$$P^{\mu} \Lambda^{\mu\nu} = \gamma^{\mu} \Lambda^{\mu\nu} = 0. \quad (334)$$

Therefore, the only non-zero components arise from the contraction with the transverse relative momentum $p^{\mu T} = p^{\mu} - P^{\mu}(p \cdot P)/P^2$. The invariant functions D_i and E_i in eq. (332) again depend on p^2 and $p \cdot P$. The partial wave decomposition in the rest frame is made explicit below.

Finally, we want to comment on an extension to three flavours. In the isospin limit the strange quark constituent mass is the only source of flavour symmetry breaking. The equations describing octet and decuplet baryons have been derived under the premises of flavour and spin conservation, *i.e.* only wave function components with same spin and flavour content couple [365]. The flavour structure of the eight equations describing $N, \Lambda, \Sigma, \Xi, \Delta, \Sigma^*, \Xi^*$ and Ω can be found in appendix A of ref. [365]. The Λ -hyperon is hereby of special interest. First, its measured polarisation asymmetry in the process $p\gamma \rightarrow K^+ \Lambda$ will provide a stringent test for the diquark-quark model for timelike momenta, see below. As discussed in [375], there are only scalar diquarks involved in this process. Secondly, broken $SU(3)$ -flavour symmetry induces a component of the total antisymmetric flavour singlet into wave and vertex function. In non-relativistic quark models with $SU(6)$ symmetry such a component is forbidden by the Pauli principle. As the flavour singlet is only composed of scalar diquarks and quarks, this generates two additional scalar amplitudes besides the usual two from the octet Λ state. The axialvector part of the vertex function remains unchanged in flavour space. In ref. [365] it has been found that the flavour singlet amplitudes are numerically small. Thus, one can safely regard the Λ -hyperon as an almost pure octet state in flavour space.

7.3.2 Partial wave decomposition

In a relativistic system only the total angular momentum, 1/2 for the nucleon and 3/2 for the Δ , is a good quantum number. Nevertheless it is instructive to decompose the BS amplitudes into partial waves in the rest frame. However, it has to be noted that these partial waves start to mix when the covariant amplitude is boosted.

In the rest frame the Pauli–Lubanski operator for an arbitrary multi–spinor ψ is given by

$$W^i = \frac{1}{2} \epsilon_{ijk} \mathcal{L}^{jk}. \quad (335)$$

Its eigenvalues are the total angular momentum

$$\mathbf{W}^2 \psi = J(J+1) \psi. \quad (336)$$

The tensor \mathcal{L}^{jk} is the sum of an orbital part, L^{jk} , and a spin part, S^{jk} . For a three–particle system they are given by

$$L^{jk} = \sum_{a=1}^3 (-i) \left(p_a^j \frac{\partial}{\partial p_a^k} - p_a^k \frac{\partial}{\partial p_a^j} \right), \quad (337)$$

$$2(S^{jk})_{\alpha\alpha',\beta\beta',\gamma\gamma'} = (\sigma^{jk})_{\alpha\alpha'} \otimes \delta_{\beta\beta'} \otimes \delta_{\gamma\gamma'} + \delta_{\alpha\alpha'} \otimes (\sigma^{jk})_{\beta\beta'} \otimes \delta_{\gamma\gamma'} + \delta_{\alpha\alpha'} \otimes \delta_{\beta\beta'} \otimes (\sigma^{jk})_{\gamma\gamma'}, \quad (338)$$

such that $\mathcal{L}^{jk} = L^{jk} + \frac{1}{2} S^{jk}$. The tensor L^{jk} is proportional to the unit matrix in Dirac space. The definition of $\sigma^{\mu\nu} := -\frac{i}{2}[\gamma^\mu, \gamma^\nu]$ differs by a minus sign from its Minkowski counterpart. The tensors L and S are written as a sum over the respective tensors for each of the three constituent quarks which are labeled $a = 1, 2, 3$ and with respective Dirac indices $\alpha\alpha', \beta\beta', \gamma\gamma'$.

Defining the spin matrix $\Sigma^i = \frac{1}{2} \epsilon_{ijk} \sigma^{jk}$ the Pauli–Lubanski operator can be written as

$$(W^i)_{\alpha\alpha',\beta\beta',\gamma\gamma'} = L^i \delta_{\alpha\alpha'} \otimes \delta_{\beta\beta'} \otimes \delta_{\gamma\gamma'} + (S^i)_{\alpha\alpha',\beta\beta',\gamma\gamma'}, \quad (339)$$

$$L^i = (-i) \epsilon_{ijk} \left[p^j \frac{\partial}{\partial p^k} + q^j \frac{\partial}{\partial q^k} \right], \quad (340)$$

$$(S^i)_{\alpha\alpha',\beta\beta',\gamma\gamma'} = \frac{1}{2} \left((\Sigma^i)_{\alpha\alpha'} \otimes \delta_{\beta\beta'} \otimes \delta_{\gamma\gamma'} + \delta_{\alpha\alpha'} \otimes (\Sigma^i)_{\beta\beta'} \otimes \delta_{\gamma\gamma'} + \delta_{\alpha\alpha'} \otimes \delta_{\beta\beta'} \otimes (\Sigma^i)_{\gamma\gamma'} \right). \quad (341)$$

Hereby the relative momentum p between quark and diquark and the relative momentum q within the diquark has been introduced via a canonical transformation:

$$P = p^1 + p^2 + p^3, \quad p = \eta(p^1 + p^2) - (1 - \eta)p^3, \quad q = \frac{1}{2}(p^1 - p^2). \quad (342)$$

Table 9

Components of the octet baryon wave function with their respective spin and orbital angular momentum. $(\gamma_5 C)$ corresponds to scalar and $(\gamma^\mu C)$, $\mu = 1 \dots 4$, to axialvector diquark correlations. Note that the partial waves in the first row possess a non-relativistic limit. (Adapted from ref. [376].)

“non-relat.” partial waves	$\begin{pmatrix} \chi \\ 0 \end{pmatrix}(\gamma_5 C)$	$\hat{P}^4 \begin{pmatrix} 0 \\ \chi \end{pmatrix}(\gamma^4 C)$	$\begin{pmatrix} i\sigma^i \chi \\ 0 \end{pmatrix}(\gamma^i C)$	$\begin{pmatrix} i\left(\hat{p}^i(\vec{\sigma}\vec{p}) - \frac{\sigma^i}{3}\right)\chi \\ 0 \end{pmatrix}(\gamma^i C)$
spin	1/2	1/2	1/2	3/2
orb.ang.mom.	<i>s</i>	<i>s</i>	<i>s</i>	<i>d</i>
“relat.” partial waves	$\begin{pmatrix} 0 \\ \vec{\sigma}\vec{p}\chi \end{pmatrix}(\gamma_5 C)$	$\hat{P}^4 \begin{pmatrix} (\vec{\sigma}\vec{p})\chi \\ 0 \end{pmatrix}(\gamma^4 C)$	$\begin{pmatrix} 0 \\ i\sigma^i(\vec{\sigma}\vec{p})\chi \end{pmatrix}(\gamma^i C)$	$\begin{pmatrix} 0 \\ i\left(p^i - \frac{\sigma^i(\vec{\sigma}\vec{p})}{3}\right)\chi \end{pmatrix}(\gamma^i C)$
spin	1/2	1/2	1/2	3/2
orb.ang.mom.	<i>p</i>	<i>p</i>	<i>p</i>	<i>p</i>

Taking into account only the leading Dirac covariant in the diquark amplitudes no orbital angular momentum is carried by the diquarks,

$$\mathbf{L}^2 \chi(q) = \mathbf{L}^2 \chi^\mu(q) = 0 . \quad (343)$$

The Pauli–Lubanski operator then simplifies and can be calculated by straightforward but tedious algebra [365,369].

In the nucleon (or generally in octet baryons) there is one *s*–wave associated with the scalar diquark and two *s*–waves associated with the axialvector diquark, one of them connected with its virtual time component, see table 9. In the non–relativistic limit only two *s*–waves out of the eight components would survive. It is remarkable that the relativistic description leads to accompanying four *p*–waves, the “lower components”, and a *d*–wave which are expected to give substantial contributions to the fraction of the nucleon spin carried by orbital angular momentum. At least, these *p*–waves would not be present in a non–relativistic model.

In the delta (or generally in decuplet baryons) only one *s*–wave described is found. Two *d*–waves that could in principle survive the non–relativistic limit are present and one *d*–wave can be attributed to the virtual time–component of the axialvector diquark. All even partial waves are accompanied by relativistic “lower” components that could be even more important as in the nucleon case.

The relativistic decomposition of nucleon and Δ quark–diquark wave functions yields a rich structure in terms of partial waves, for more details see refs. [365,369]. Well–known problems from certain non–relativistic quark model descriptions are avoided from the beginning in a relativistic treatment: First, photoinduced N – Δ –transitions that are impossible in spherically symmetric non–relativistic nucleon ground states will occur in this model through overlaps in the axialvector part of the respective wave functions. Additionally, photoinduced transitions from scalar to axialvector diquarks can take place, thus creating an overlap of the nucleon scalar diquark correlations with the Δ axialvector diquark correlations. Secondly, the total

baryon spin will be mainly made of the quark spin in the s -waves and the orbital angular momentum of the relativistic p waves (that are absent in a non-relativistic description). Which fraction of, *e.g.* the nucleon spin, is carried by the quark spins is related to the matrix element of the flavor singlet axial current and is subject of an on-going investigation.

7.3.3 Numerical Results for Ground State Baryons

The quark–diquark BS equations have been solved in the corresponding bound state rest frame using an expansion in Chebyshev moments, see refs. [363,365,369] for details. This method exploits the approximate $O(4)$ symmetry of the BS equation and proves to be very helpful in obtaining numerically accurate solutions of the full 4–dimensional equations. Actually, there is not much difference in the requirements for computational resources in solving the 4–dimensional equation this way or solving a reduced three–dimensional approximation. Given the non–covariance of the reduced equation (and the related shortcomings when calculating observables, see *e.g.* ref. [367]) further use of three–dimensional reductions seems questionable.

In ref. [368] the nucleon and delta amplitudes have been calculated using two different parameter sets. For one set a constituent quark mass of $m_q = 0.36$ GeV has been employed. Due to the free-particle poles in the quark and diquark propagators used in ref. [368] the axialvector diquark mass is below 0.72 GeV and the delta mass below 1.08 GeV. On the other hand, nucleon and delta masses are fitted by second set and accordingly the parameter space is constrained by these two masses. In particular, this implies $m_q > 0.41$ GeV. The first parameter set (in which the delta is much too light) results in much better nucleon properties, see below. Especially for the nucleon magnetic moments this is easily understood: For weak binding, *i.e.* close to the non–relativistic limit, the magnetic moment is roughly proportional to M_n/m_q . Thus a standard value for the constituent mass around 0.33 GeV would be highly desirable. However, one then faces the question how to describe confinement and thereby avoid unphysical thresholds.

In ref. [365] the quark and diquark propagators have been modified by choosing in eqs. (318,317,319)

$$C(P^2, m) = 1 - e^{-d(P^2 + m^2)}. \quad (344)$$

This cancels the pole of the propagators at the expense of introducing an essential singularity at time–like infinity. Such a form is sufficient to prevent any unphysical threshold in the BS equation. Furthermore, point–like diquarks have been used. The nucleon and the delta masses have been used as to fix the coupling strengths in the scalar and axialvector channel. The calculated hyperon masses are in good agreement with the experimental ones, see table 10. The wave functions for baryons with distinct strangeness content but same spin differ mostly due to flavour Clebsch–Gordan coefficients, the respective invariant functions being very similar.

Table 10

Octet and decuplet masses obtained with two different parameter sets. Set I represents a calculation with weakly confining propagators ($d = 10$ in eq. (344)), Set II with strongly confining propagators ($d = 1$ in eq. (344)). All masses are given in GeV. (Adapted from ref. [376].)

	m_u	m_s	M_Λ	M_Σ	M_Ξ	M_{Σ^*}	M_{Ξ^*}	M_Ω
Set I	0.5	0.65	1.123	1.134	1.307	1.373	1.545	1.692
Set II	0.5	0.63	1.133	1.140	1.319	1.380	1.516	1.665
Exp.			1.116	1.193	1.315	1.384	1.530	1.672

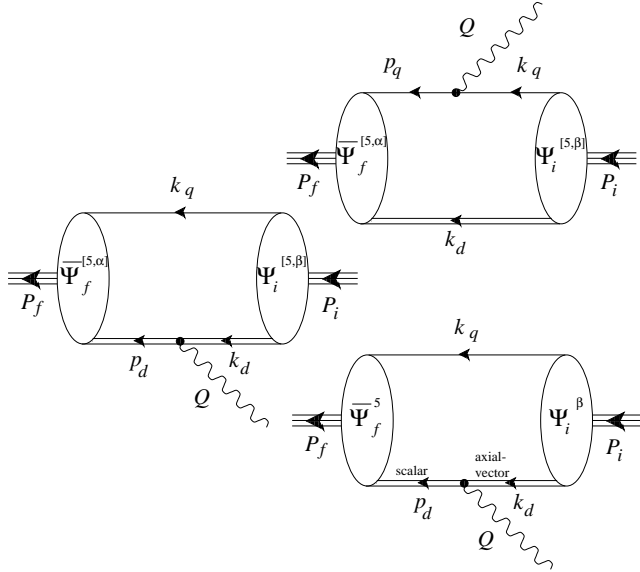


Fig. 33. Impulse approximate contributions to the electromagnetic current. (Adapted from ref. [368].)

7.4 Electromagnetic Form Factors

The Sachs form factors G_E and G_M can be extracted from the solutions of the BS equations using the relations

$$G_E = \frac{M_n}{2P^2} \operatorname{Tr} \langle J^\mu \rangle P^\mu, \quad G_M = \frac{iM_n^2}{Q^2} \operatorname{Tr} \langle J^\mu \rangle \gamma_T^\mu, \quad (345)$$

where $P = (P_i + P_f)/2$, $\gamma_T^\mu = \gamma^\mu - P^\mu P_f/P^2$, and the spin-summed matrix element $\langle J^\mu \rangle$ is given by

$$\begin{aligned} \langle J^\mu \rangle &\equiv \langle P_f, s_f | J^\mu | P_i, s_i \rangle \sum_{s_f, s_i} u(P_f, s_f) \bar{u}(P_i, s_i) \\ &= \int \frac{d^4 p_f}{(2\pi)^4} \int \frac{d^4 p_i}{(2\pi)^4} \bar{\Psi}(P_f, p_f) J^\mu \Psi(P_i, p_i). \end{aligned} \quad (346)$$

The current J^μ herein is obtained as in ref. [366,368], see, however, also refs. [364,361,362] where electromagnetic nucleon form factors have been calculated within a BS quark-diquark

model. This current represents a sum of all possible couplings of the photon to the inverse quark–diquark propagator G^{-1} given in eq. (323). This construction which ensures current conservation can be systematically derived from the general “gauging technique” employed in refs. [377,378].

The two contributions to the current that arise from coupling the photon to the disconnected part of G^{-1} , the first term in eq. (323), yield the couplings to the quark and the diquark in impulse approximation. They are graphically represented by the middle and the upper diagram in figure 33. The corresponding kernels, to be multiplied by the charge of the respective quark or diquark upon insertion into the r.h.s. of eq. (346), read,

$$J_q^\mu = (2\pi)^4 \delta^4(p_f - p_i - \eta Q) \Gamma_q^\mu \tilde{D}^{-1}(k_d), \quad (347)$$

$$J_{sc[ax]}^\mu = (2\pi)^4 \delta^4(p_f - p_i + (1 - \eta)Q) \Gamma_{sc[ax]}^{\mu[\alpha\beta]} S^{-1}(k_q). \quad (348)$$

Here, the inverse diquark propagator \tilde{D}^{-1} comprises both, scalar and axialvector components. The vertices in eqs. (347) and (348) are the ones for a free quark, a spin-0 and a spin-1 particle, respectively,

$$\Gamma_q^\mu = -i\gamma^\mu, \quad \Gamma_{sc}^\mu = -(p_d + k_d)^\mu, \quad \text{and} \quad (349)$$

$$\Gamma_{ax}^{\mu,\alpha\beta} = -(p_d + k_d)^\mu \delta^{\alpha\beta} + p_d^\alpha \delta^{\mu\beta} + k_d^\beta \delta^{\mu\alpha} + \kappa (Q^\beta \delta^{\mu\alpha} - Q^\alpha \delta^{\mu\beta}). \quad (350)$$

The Dirac indices α, β in (350) refer to the vector indices of the final and initial state wave function, respectively. The axialvector diquark can have an anomalous magnetic moment κ . In ref. [368] its value has been obtained from a calculation for vanishing momentum transfer in which the quark substructure of the diquarks is resolved. The corresponding contributions are represented by the upper and the right diagram in figure 34. It turns out that $\kappa = 1$ is a reasonable value independent of the parameters used. This is intuitively understandable: The magnetic moments of two quarks with charges q_1 and q_2 add up to $(q_1 + q_2)/m_q$, the magnetic moment of the axialvector diquark is $(1 + \kappa)(q_1 + q_2)/m_{ax}$, and if the axialvector diquark is weakly bound, $m_{ax} \approx 2m_q$, then $\kappa \approx 1$.

The vertices in eqs. (349) and (350) satisfy their respective Ward-Takahashi identities, *i.e.* those for free quark and diquark propagators (*c.f.*, eqs. (317,318) and (319)), and thus describe the minimal coupling of the photon to quark and diquark.

An important ingredient are the photon–induced transitions between scalar and axialvector diquarks as represented by the lower diagram in figure 33. These yield purely transverse currents and do thus not affect current conservation. The tensor structure of these contributions resembles that of the triangle anomaly. In particular, the structure of the vertex describing the transition from axialvector to scalar diquark is given by

$$\Gamma_{sa}^{\mu\beta} = -i \frac{\kappa_{sa}}{2M_n} \epsilon^{\mu\beta\rho\lambda} (p_d + k_d)^\rho Q^\lambda, \quad (351)$$

and the analogous expression for the reverse transition from an scalar to axialvector. The tensor structure of these anomalous diagrams is in the limit $Q \rightarrow 0$ determined by the quark

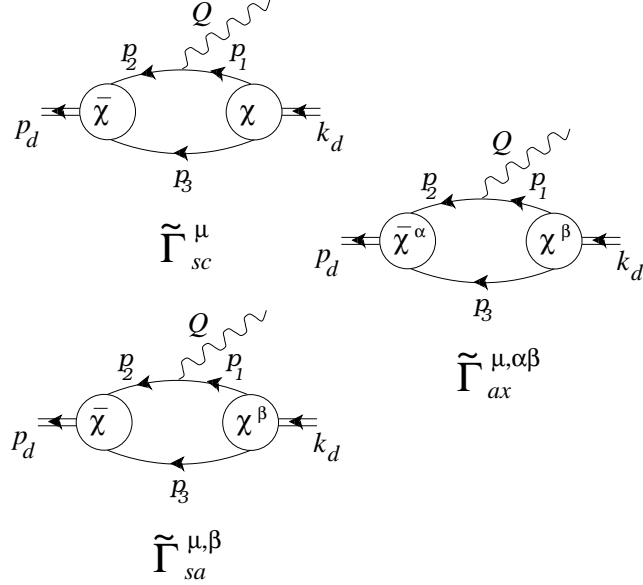


Fig. 34. Resolved vertices: photon-scalar diquark, photon-axialvector diquark and anomalous scalar-axialvector diquark transition. (Adopted from ref. [368].)

loop in a way as represented by the lower diagram in figure 34. The constant κ_{sa} turns out to be approximately 2 [368].

Upon performing the flavor algebra for the current matrix elements of the impulse approximation, one obtains the following explicit forms for proton and neutron,

$$\langle J^\mu \rangle_p^{\text{imp}} = \frac{2}{3} \langle J_q^\mu \rangle^{\text{sc-sc}} + \frac{1}{3} \langle J_{sc}^\mu \rangle^{\text{sc-sc}} + \langle J_{ax}^\mu \rangle^{\text{ax-ax}} + \frac{\sqrt{3}}{3} \left(\langle J_{sa}^\mu \rangle^{\text{sc-ax}} + \langle J_{as}^\mu \rangle^{\text{ax-sc}} \right), \quad (352)$$

$$\begin{aligned} \langle J^\mu \rangle_n^{\text{imp}} = & -\frac{1}{3} \left(\langle J_q^\mu \rangle^{\text{sc-sc}} - \langle J_q^\mu \rangle^{\text{ax-ax}} - \langle J_{sc}^\mu \rangle^{\text{sc-sc}} + \langle J_{ax}^\mu \rangle^{\text{ax-ax}} \right) - \\ & \frac{\sqrt{3}}{3} \left(\langle J_{sa}^\mu \rangle^{\text{sc-ax}} + \langle J_{as}^\mu \rangle^{\text{ax-sc}} \right). \end{aligned} \quad (353)$$

The superscript ‘sc-sc’ indicates that the current operator is to be sandwiched between scalar nucleon amplitudes for both the final and the initial state in eq. (346). Likewise ‘sc-ax’ denotes current operators that are sandwiched between scalar amplitudes in the final and axialvector amplitudes in the initial state, *etc.*. Note that the axialvector amplitudes contribute to the proton current only in combination with diquark current couplings.

Current conservation requires that the photon also has to be coupled to the interaction kernel in the BS equation, *i.e.*, to the second term in the inverse quark-diquark propagator G^{-1} of eq. (323). The corresponding contributions were derived in [366] and are represented by the diagrams in figure 35. In particular, in addition to the photon coupling with the exchange-quark (with vertex Γ_q^μ), irreducible “seagull” interactions of the photon with the diquark substructure have to be taken into account. These diquark–quark–photon vertices are constrained by Ward identities. The explicit construction of ref. [366] yields the following seagull couplings:

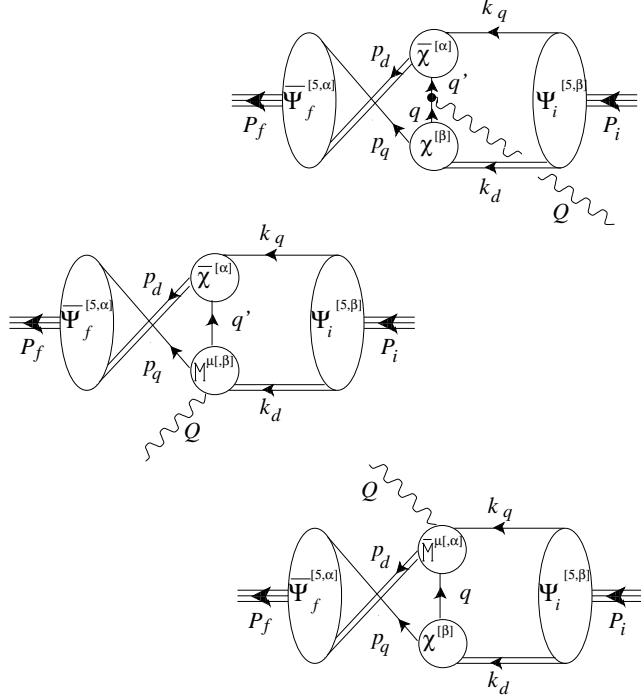


Fig. 35. Exchange quark and seagull diagrams. (Adopted from ref. [368].)

$$\begin{aligned}
M^{\mu[\beta]} = & q_q \frac{(4p_1 - Q)^\mu}{4p_1 \cdot Q - Q^2} \left[\chi^{[\beta]}(p_1 - Q/2) - \chi^{[\beta]}(p_1) \right] + \\
& q_{ex} \frac{(4p_1 + Q)^\mu}{4p_1 \cdot Q + Q^2} \left[\chi^{[\beta]}(p_1 + Q/2) - \chi^{[\beta]}(p_1) \right] . \tag{354}
\end{aligned}$$

Here, q_q denotes the charge of the quark with momentum p_q , q_{ex} the charge of the exchanged quark with momentum q' , and p_1 is the relative momentum of the two, $p_1 = (p_q - q')/2$ (see figure 35). The conjugate vertices $\bar{M}^{\mu[\alpha]}$ are obtained from the conjugation of the diquark amplitudes $\chi^{[\beta]}$ in eq. (354) together with the replacement $p_1 \rightarrow p_2 = (q - k_q)/2$.

The diagrams of figs. 33 and 35 have been evaluated in ref. [368] using the numerical solutions of the BS amplitudes. The continuation of these from the nucleon rest frame to the Breit frame is described in detail in refs. [364,366]. A warning is here, however, in order: For finite momentum transfer, care is needed in treating the singularities of the quark and diquark propagators that appear in the single terms of eq. (346). In ref. [366] it was shown that for some kinematical situations explicit residues have to be taken into account in the calculation of the impulse approximation diagrams.

The results of ref. [368] for the proton electric form factor are in excellent agreement with the phenomenological dipole behavior. Also the calculated neutron electric form factor agrees very well with data. The magnetic moments come out somewhat too small showing that stronger axialvector diquark correlations would be favorable for larger values of the magnetic moments.

Recent data from Jefferson Lab, see ref. [379], for the ratio $\mu_p G_E/G_M$ are compared to the results of ref. [368] in fig. 36. The ratio obtained from parameters with weak axialvector correlations lies above the experimental data, and that from parameters with strong axialvector correlations below. Thus, the experimental observation that this ratio decreases significantly

The Ratio $\mu_p G_E/G_M$

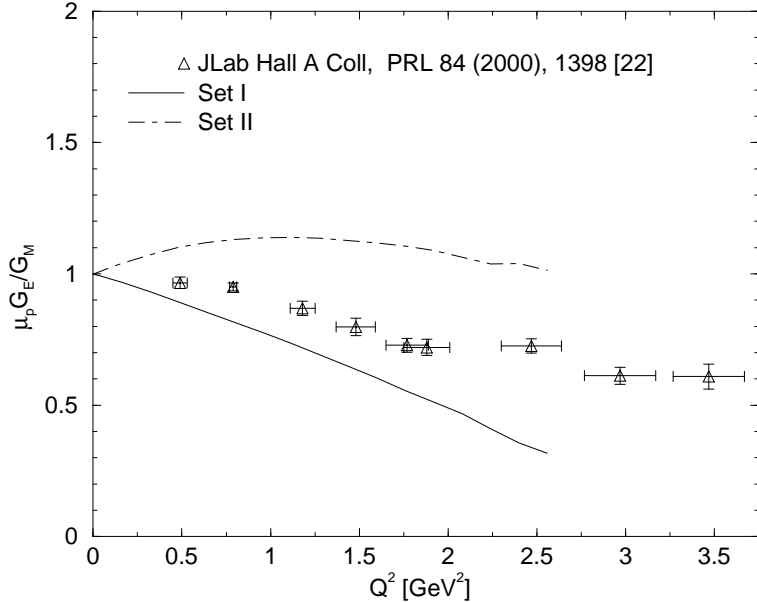


Fig. 36. The ratio $(\mu_p G_E)/G_M$ compared to the data from ref. [379].

with increasing Q^2 (about 40% from $Q^2 = 0$ to 3.5 GeV^2), can be well reproduced with axialvector diquark correlations of a certain strength included. The reason for this is the following: The impulse approximate photon–diquark couplings yield contributions that tend to fall off slower with increasing Q^2 than those of the quark. This is the case for both, the electric and the magnetic form factor. If no axialvector diquark correlations inside the nucleon are maintained, however, the only diquark contribution to the electromagnetic current arises from $\langle J_{sc}^\mu \rangle^{\text{sc-sc}}$, see eqs. (352,353). Although this term does provide for a substantial contribution to G_E , its respective contribution to G_M is of the order of 10^{-3} . This reflects the fact that an on-shell scalar diquark would have no magnetic moment at all, and the small contribution to G_M may be interpreted as an off-shell effect. Consequently, too large a ratio $\mu_p G_E/G_M$ results, if only scalar diquarks are maintained [366]. For parameters leading to weak axialvector correlations this effect is still visible, although the scalar-to-axialvector transitions already bend the ratio towards lower values at larger Q^2 . These transitions almost exclusively contribute to G_M , and it thus follows that the stronger axialvector correlations enhance this effect. The ratio $\mu_p G_E/G_M$ imposes an upper limit on the relative importance of the axialvector correlations of estimated 30% (to the BS norm of the nucleons).

The nucleon electromagnetic form factors have also been calculated in refs. [361,362] using a scalar diquark only. In these investigations a different approach has been taken: Not only the quark and diquark propagators have been modeled by entire functions but also the nucleon Faddeev amplitude (or more precisely, a BS-like quark–diquark amplitude) has been parameterized by a one-parameter entire function. The parameters of the quark propagator have been fixed by a fit to meson observables, the remaining three parameters (width of the nucleon amplitude, width of the diquark amplitude and diquark correlation length) have been determined by optimizing a fit to the proton electric form factor. The corresponding diagrams have been calculated in a generalized impulse approximation. This takes care of the internal

structure of the diquark. Due to the use of a dressed quark–photon vertex current conservation is explicit at the level of constituents. However, it has been questioned whether this approach is gauge invariant. In ref. [380] it was claimed that the calculations of refs. [361,362] suffer from an overcounting problem. This is substantiated by the fact that the impulse approximation of refs. [361,362] cannot be obtained from the general treatment of a relativistic three–body problem presented in ref. [377] in the limit of separable quark–quark correlations, however, this is possible in the approach of refs. [366,368]. As the disputable diagrams provide only small contributions to observables the results of refs. [361,362] are nevertheless interesting.

The neutron electric form factor obtained in ref. [361] is much larger than the experimental data at all (spacelike) momenta. This is very likely a defect due to neglecting the axialvector diquark as comparison with refs. [364,366] reveals: Also in these studies only the scalar diquarks have been taken into account and the neutron electric form factor has been overestimated. On the other hand, the result for the proton magnetic moment obtained in ref. [361] is close to its phenomenological value, the (absolute value of the) neutron magnetic moment is somewhat too small.

Summarizing this section: The electromagnetic properties of the nucleon can be described reasonably well within a Faddeev/BS equation approach. It would be interesting to see whether a more sophisticated study using “confined” quarks and diquarks, a calculated nucleon amplitude (from the quark–diquark BS equation), and a reasonable amount of axialvector diquark correlations could provide a more accurate description.

7.5 Strong and Weak Form Factors

In ref. [362] (using the ansätze of a ref. [361] and taking into account only a scalar diquark) the pseudoscalar, isoscalar– and isovector–vector, axial–vector and scalar nucleon form factors have been calculated. The pion–nucleon and the axial coupling based on a solution of the BS equation has been calculated with “confined” constituents and a scalar diquark only in ref. [364]. For “free” constituents and the axialvector diquark included corresponding results have been reported in ref. [368].

The coupling of the pion to the nucleon, described by a pseudoscalar operator, and the pseudovector currents of weak processes such as the neutron β -decay are connected to each other in the soft limit by the Goldberger-Treiman relation.

The matrix element of the pseudoscalar density J_5^a can be parameterized as

$$\langle J_5^a \rangle = \Lambda^+(P_f) \tau^a \gamma_5 g_{\pi NN}(Q^2) \Lambda^+(P_i) , \quad (355)$$

which yields

$$g_{\pi NN}(Q^2) = -\frac{2M_n^2}{Q^2} \text{Tr} \langle J_5^a \rangle \gamma_5 \frac{\tau^a}{2} . \quad (356)$$

As discussed in the last chapter the chiral Ward identity provides for the leading Dirac covariant of the pion–quark vertex

$$\Gamma_5^a(P, p) = \gamma_5 \frac{B(p^2)}{f_\pi} \tau^a, \quad (357)$$

where f_π is the pion decay constant and $B(p^2)$ is the scalar part of the quark self-energy in the chiral limit. The three additionally possible Dirac structures have been neglected in the calculations of refs. [362,368]. (Note that with free propagators as in ref. [368] one simply has $B(p^2) = m_q$.)

The matrix elements of the pseudovector current are parameterized by the form factor $g_A(Q^2)$ and the induced pseudoscalar form factor $g_P(Q^2)$,

$$\langle J_5^{a,\mu} \rangle = \Lambda^+(P_f) \frac{\tau^a}{2} \left[i\gamma^\mu \gamma_5 g_A(Q^2) + Q^\mu \gamma_5 g_P(Q^2) \right] \Lambda^+(P_i). \quad (358)$$

For $Q^2 \rightarrow 0$ the Goldberger-Treiman relation,

$$g_A(0) = f_\pi g_{\pi NN}(0)/M_n, \quad (359)$$

then follows from current conservation and the observation that only the induced pseudoscalar form factor $g_P(Q^2)$ has a pole on the pion mass-shell.

By definition, g_A describes the regular part of the pseudovector current and g_P the induced pseudoscalar form factor. They can be extracted from eq. (358) as follows:

$$g_A(Q^2) = -\frac{i}{4 \left(1 + \frac{Q^2}{4M_n^2}\right)} \text{Tr} \langle J_5^{a,\mu} \rangle \left(\gamma_5 \gamma^\mu - i\gamma_5 \frac{2M_n}{Q^2} Q^\mu \right) \tau^a, \quad (360)$$

$$g_P(Q^2) = \frac{2M_n}{Q^2} \left(g_A(Q^2) - \frac{M_n}{Q^2} \text{Tr} \langle J_5^{a,\mu} \rangle Q^\mu \gamma_5 \tau^a \right). \quad (361)$$

Chiral symmetry constraints may be used to construct the axialvector–quark vertex. In the chiral limit, the Ward-Takahashi identity for this vertex reads,

$$Q^\mu \Gamma_5^{\mu,a} = \frac{\tau^a}{2} \left(S^{-1}(k) \gamma_5 + \gamma_5 S^{-1}(p) \right), \quad (Q = k - p). \quad (362)$$

This constraint is satisfied by the form of the vertex proposed in ref. [276],

$$\Gamma_5^{\mu,a} = -i\gamma^\mu \gamma_5 \frac{\tau^a}{2} + \frac{Q^\mu}{Q^2} f_\pi \Gamma_5^a. \quad (363)$$

The second term which contains the massless pion pole does not contribute to g_A as can be seen from eq. (360). From these quark contributions to the pion coupling and the pseudovector current alone, eqs. (363) and (356) would thus yield,

$$\lim_{Q^2 \rightarrow 0} \frac{Q^2}{2M_n} g_P(Q^2) = \frac{f_\pi}{M_n} g_{\pi NN}(0). \quad (364)$$

Here, the Goldberger-Treiman relation follows if the pseudovector current was conserved or, off the chiral limit, from PCAC.

Current conservation is a non-trivial requirement in the relativistic bound state description of nucleons, however. First, we ignored the pion and pseudovector couplings to the diquarks in the simple argument above. For scalar diquarks alone which themselves do not couple to either of the two, as can be inferred from parity and covariance, pseudovector current conservation could in principle be maintained by including the couplings to the interaction kernel of the nucleon BS equation in much the same way as was done for the electromagnetic current.

Unfortunately, when axialvector diquarks are included, even this will not suffice to maintain current conservation. As observed recently in ref. [378], a doublet of axialvector *and* vector diquarks has to be introduced, in order to comply with chiral Ward identities in general. The reason essentially is that vector and axialvector diquarks mix under a chiral transformation whereas this is not the case for scalar and pseudoscalar diquarks. Since vector diquarks on the one hand introduce six additional components to the nucleon wave function, but are on the other hand not expected to influence the binding strongly, here vector diquark correlations have been neglected so far.

In ref. [368] the relevant couplings of the currents to the diquarks have been estimated from the quark loops at $Q^2 = 0$. In ref. [362] the impulse approximation discussed already in the last section has been employed.

In ref. [368] it was found that large contributions to $g_{\pi NN}(0)$ and $g_A(0)$ arise from the scalar–axialvector transitions, and both quantities are overestimated, $g_A(0) = 1.35 - 1.49$ instead of 1.27 and $g_{\pi NN}(0) = 16 - 17$ instead of ≈ 13.2 . As mentioned, the axialvector diquark contributions violate the Goldberger–Treiman relation. Some compensations occur between the small contributions from the axialvector diquark impulse–coupling and the comparatively large ones from scalar–axialvector transitions which provide for the dominant effect to yield $g_A(0) > 1$. Summing all contributions the Goldberger–Treiman relation is violated by 14 – 18%.

In ref. [362] $g_{\pi NN}(0)$ is slightly overestimated, too. On the other hand, $g_A(0)$ comes out consistently smaller than one. This may simply reflect the importance of scalar–axialvector transitions for this quantity. It is interesting to note that a non-vanishing $f_{\omega NN}$ has been obtained. As this quantity may be important for meson–exchange models of nuclear physics (where it has been neglected so far) this quantity certainly deserves to be studied further. The analysis of the σ –term in ref. [362] illustrates the only method known up to now that allows an unambiguous off-shell extrapolation in the estimation of meson–nucleon form factors. An important element in the calculation of the scalar form factor presented in ref. [362] is the dressed–quark

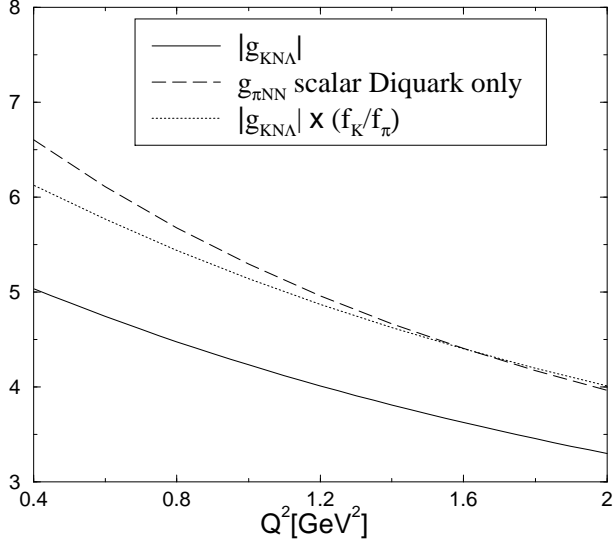


Fig. 37. Comparison of the $g_{K\Lambda}(Q^2)$ form factor with a “projected” $g_{\pi NN}(Q^2)$, only the scalar diquark component of the nucleon amplitude has been taken into account in the calculation. (Adopted from ref. [381].)

scalar vertex obtained from the solution of the inhomogeneous BS equation. As anticipated it possesses a pole at the scalar mass, and the residue of this pole provides the σ -meson nucleon coupling. The solution of the inhomogeneous BS equation allows to extract this coupling at every possible value of Q^2 , especially also at the soft point $Q^2 = 0$ where this coupling is directly related with the σ -term. In this way one obtains $\sigma = 14\text{MeV}$ whereas at the σ -meson pole a several times larger value would have been extracted.

As already stated, transitions from nucleons to the Λ -hyperon project out the scalar diquark component of the nucleon amplitude [375]. Therefore corresponding processes provide a test for the assumption of separable quark-quark t -matrix, *i.e.* the diquark hypothesis. A first and illustrative step in this direction is the $g_{K\Lambda}(Q^2)$ form factor. Its within this model calculated (absolute) value at all spacelike Q^2 is much smaller than $g_{\pi NN}(Q^2)$ [381]. Hereby the direct contribution to flavour symmetry breaking, $m_s > m_u$, is of minor importance. Some 20% are due to the larger kaon decay constant, $f_K > f_\pi$, but the most important effect is the projection onto the scalar diquark component of the nucleon amplitude, see fig. 37.

7.6 Hadronic Reactions

Production processes where the quark propagator is tested for time-like momenta are highly interesting with respect to employed parametrizations of confinement. On the other hand, such processes are quite complicated, and if numerous subprocesses, *i.e.* diagrams, are contributing the issue might be obscured. For this reason processes like kaon photoproduction with a Λ -hyperon in the final channel, $p\gamma \rightarrow K\Lambda$, is well suited for such an investigations. As stated already flavour algebra leads to the restriction of scalar diquarks. Furthermore, the kaon does not couple to the scalar diquark. Therefore, restricting to the impulse approximation leads to the justification of a spectator model.

It has to be emphasized that the investigations reported in this section have an exploratory character. They serve more or less to demonstrate the feasibility of such calculations.

7.6.1 Deep Inelastic Structure Functions

Before going to processes with strangeness in the final channel the results of the very first application of the diquark–quark BS solution will be briefly reviewed here. In ref. [363] the nucleon structure function $F_1(x)$ has been calculated. Hereby the nucleon was modeled as consisting of a valence quark and a scalar diquark of equal mass. The photon coupled only to the quark whereas the diquark was treated as a spectator. Despite the exploratory character of this first application of this kind of BS equation based diquark models it produced interesting results. The spin structure of the nucleon has been found to contribute non-trivially to the structure function $F_1(x)$: Its valence–quark contribution is governed by the “non–relativistic” components only in the case of very weak binding. The shape of the unpolarized valence–quark distribution has been found to be mainly determined by relativistic kinematics and does not depend on details of quark–diquark dynamics.

Furthermore, it is interesting to note that due to the full covariance of the model the structure function has the correct support ($x \in [0, 1]$) from the very beginning. No projection technique is needed. The valence–quark distribution shows a clear peak at approximately $x = 1 - m_{sc}/M$. Assuming that the scalar diquark mass m_{sc} is approximately $2/3$ of the nucleon bound state mass M , the empirically observed peak at $x \approx 1/3$ would be reproduced.

The investigations reported in ref. [363] are certainly a clear motivation to study all experimentally observable nucleon structure functions in a more sophisticated version of the diquark–quark BS model in the future.

7.6.2 Kaon Photoproduction off the Proton

As stated above a spectator picture emerges for the reaction $\gamma p \rightarrow K\Lambda$ in the impulse approximation, and this process is described within a diquark model by the diagrams shown in fig. 38. The model specific input that goes into the calculation of the cross section and the asym-

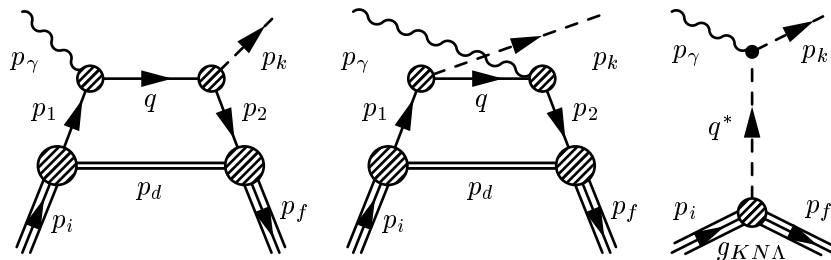


Fig. 38. Impulse approximation diagrams contributing to $\gamma p \rightarrow K\Lambda$.

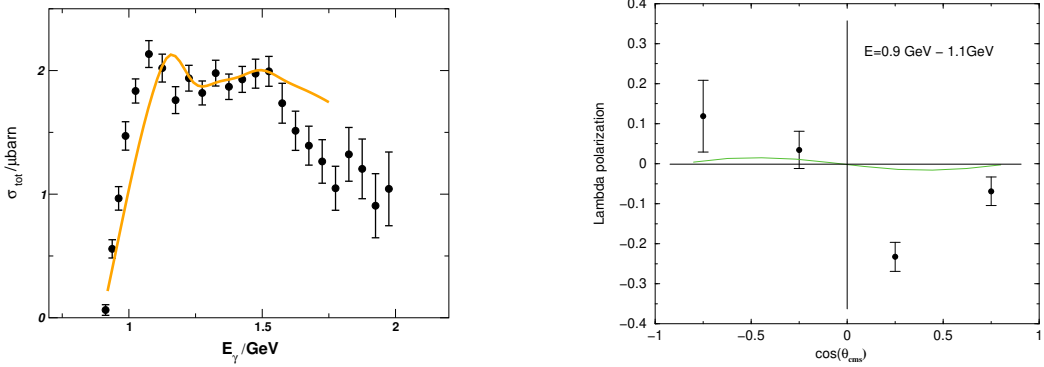


Fig. 39. Kaon photoproduction. The left panel shows the total cross section compared to the data of the SAPHIR collaboration, the right panel the asymmetry. (Adapted from ref. [376].)

metries for kaon photoproduction are the wave functions for the baryons (which are solutions of the BS equation) and the propagators of quarks and diquarks. Hereby it is important to note that the quark propagator in between the incoming photon and the outgoing kaon in the left diagram of fig. 38 is tested in a parabolic region of complex momenta q^2 such that the lowest real value of q^2 is given by $q_{\min}^2 = -(\eta_P M + E)^2$ where η_P is the momentum partitioning parameter, M is the nucleon mass, and E is the photon energy in the nucleon rest frame. Obviously, for large photon energies the quark propagator at time-like momenta becomes important.

The results of ref. [376] for $p\gamma \rightarrow K\Lambda$ using pointlike diquarks are shown in fig. 39. As anticipated it has been found that the total cross section strongly depends on the behaviour of the quark propagator in the time-like region. To obtain the results shown in fig. 39 the function $C(p^2, m)$ in eqs. (317,319) has been chosen to be $\exp(-0.25|1+p^2/m^2|)$. Using instead $C(p^2, m) = \exp(-(1+p^2/m^2))$ as done in previous calculations leads to enormously large cross sections. For the form chosen, however, the total cross section matches the data quite nicely and it even follows the peculiar structure of the measured data in the region above 1 GeV. This is due to interference with the kaon exchange diagram shown in fig. 38. The Λ polarization is shown in the right panel of fig. 39 and the comparison reveals that it falls short of the measured data by a substantial factor. However, the characteristic change of sign as required by the data is present.

7.6.3 Associated Strangeness Production in pp Collisions

The application of the diquark–quark BS model to the associated strangeness production $pp \rightarrow pK\Lambda$ [381] is based on the assumption that for intermediate reaction energies the interaction mechanism is dominated by the exchange of pseudoscalar mesons but that nevertheless the subhadronic quark structure is tested. The calculated total cross sections have been found significantly too small, however, this effect might be attributed to the strong initial and final state interactions. The form of the calculated differential cross sections agree, nevertheless, nicely with experiments.

Calculating the depolarization tensor, which is a measure of the relation between the spin of the incoming proton and the outgoing Λ –hyperon, and which is only marginally influenced by initial and final state interactions, one finds a pronounced dependence on the parametrizations

of the quark and diquark propagator. Hereby it is again the behaviour at large time-like momenta which, in this case, is amplified by the fact that one obtains even a different sign for the pion and kaon exchange diagrams in different models for the propagators. As mostly parallel spins of the proton and the Λ -hyperon contribute to the pion diagrams and antiparallel spins to the kaon diagrams a completely different interference pattern is obtained in the results for the depolarization tensor.

All the results mentioned for hadronic reactions are based on the assumption for point-like diquarks, and because a reasonable description of form factors requires extended diquarks, all these calculations can only be considered as exploratory. But they have nevertheless proven that a fully Lorentz covariant approach based on the substructure of hadrons can be applied even to quite complicated processes.

8 Concluding Remarks

In this review we have attempted to demonstrate the long way from the dynamics of confined quark and glue to a description of hadrons and their processes in one coherent approach. The results obtained so far encourage to pursue it. Of course, improvements are possible and highly desirable at practically every step. The hope is that future work will bridge more of the gaps remaining between them.

First of all, a consistent qualitative picture for all QCD propagators and vertex functions will hopefully emerge in the near future from lattice and Dyson–Schwinger calculations. These may then be employed in the rich meson phenomenology based on the Bethe–Salpeter equation. We have seen that many aspects of meson physics can be understood quite well on the basis of these investigations. Diquark correlations have also been studied from simple models of quark and gluon propagators. In a coherent calculation, these could of course be obtained as solutions to Bethe–Salpeter equations constructed from Dyson–Schwinger equations. Coupling the diquark correlations to a further quark propagator, the way to baryon wave functions from results of Dyson–Schwinger equations for quarks and gluons is straight ahead. The complications for physical observables such as form factors in a Bethe–Salpeter/Faddeev calculation of baryons from the results for the structure of diquark and quark correlations, are under control. The numerical machinery to calculate these observables in this extended diquark–quark approach is currently being developed.

The ideal calculations of this kind have the minimal parameter set of QCD. This allows to critically assess the necessary truncating assumptions on the infinite hierarchy of equations of motion for the QCD Green’s functions. No abundant parameters are present to tune, and thus to cover up possible insufficiencies of these calculations. The program so far yielded reliable results for the coupled system of equations for the gluon and ghost propagators in Landau gauge. In the momentum range overlapping with available lattice results good agreement is obtained. Confinement of gluons can be attributed to the violation of positivity found to be manifest in the solution. This feature is also seen in lattice results. The quenched solution to the quark Dyson–Schwinger equation from these results compare nicely to lattice results obtained more recently. The necessary non–perturbative mass scale is produced by the dynamics encoded in the Dyson–Schwinger equations of gluons, ghosts and quarks. The positivity and the analyticity properties of the quark propagator are interesting open questions. These can be addressed with the full unquenched solutions which became available very recently.

We hope to have demonstrated that this approach is worth to be further pursued, and that a coherent description of hadronic states and processes based on the dynamics of confined correlations of quark, glue and ghosts can be realized in the near future. Hereby the method based on the QCD Green’s functions has to be understood as being complementary to other techniques. Lattice calculations provide evidence that truncations of the infinite hierarchy of Dyson–Schwinger equations have been done reasonably. On the other hand, results of these truncated equations help to understand the lattice data. Solutions of Bethe–Salpeter equations provide explicit examples of different realization of symmetries in the meson and baryon spectrum. Meson and baryon properties as well as hadronic reactions may in the end serve as experimental tests of our understanding of confinement. And this connects to what might

be the most challenging goal in hadron physics: Not only to understand the mysterious phenomenon of confinement but also to find a way to verify it experimentally.

Acknowledgements

We have benefited from many discussions with colleagues and friends. Our warm thanks to all of them. A probably incomplete list of people we would like to mention in particular, includes F. Coester, A. Cucchieri, H. Gies, N. Ishii, O. Jahn, A. C. Kalloniatis, K. Langfeld, F. Lenz, P. Maris, S. Nedelko, J. Negele, K. Nishijima, M. Oettel, M. A. Pichowsky, M. Pennington, L. O'Raifeartaigh, H. Reinhardt, C. D. Roberts, M. Schaden, S. Schmidt, A. Schreiber, P. Tandy, M. Thies, K. Yazaki, P. Watson, H. Weigel and A. G. Williams.

We thank S. Ahlig for a critical reading of the manuscript and for providing Figs. 7 and 38.

This work has been supported in part by DFG (Al 279/3-3) and COSY (contract no. 41376610).

A Real vs. Complex Ghost Fields: Ghost-Antighost Symmetry and $SL(2, \mathbb{R})$

In this appendix we summarize the relation between real and complex ghost fields, *i.e.*, between the hermiticity assignments $c^\dagger(x) = c(x)$ and $(i\bar{c}(x))^\dagger = i\bar{c}(x)$ versus $c(x)^\dagger = \bar{c}(x)$ in the operator formalism. The latter assignment is used in Sec. 2. It has been stressed in the literature, see, *e.g.* Ref. [36], that the correct hermiticity assignment should be the former, however. This is true for the standard Faddeev-Popov gauges with $\xi \neq 0$. In Landau gauge ($\xi = 0$) we can make use of the additional ghost-antighost symmetry to establish the equivalence of both formulations, employing independent real or complex ghost fields (corresponding to the ghost and antighost degrees of freedom). The ghost-antighost symmetry and thus the complex formulation with $c(x)^\dagger = \bar{c}(x)$ can be maintained for $\xi \neq 0$ at the expense of quartic ghost interactions in (a special case of) the so-called Curci-Ferrari gauge(s) [382,383].

Let us first consider the hermiticity assignment $c^\dagger(x) = c(x)$ and $(i\bar{c}(x))^\dagger = i\bar{c}(x)$ corresponding to two independent and real Euclidean (Grassmann) ghost $c(x) \rightarrow u(x)$ and antighost fields $\bar{c}(x) \rightarrow iv(x)$. The gauge fixing part $\mathcal{L}_{\mathcal{GF}}$ of the effective Lagrangean \mathcal{L}_{eff} in Eq. (11) of Sec. 2 then reads,

$$\mathcal{L}_{\mathcal{GF}} = iB^a \partial_\mu A_\mu^a + \frac{\xi}{2} B^a B^a + iv^a \partial_\mu D_\mu^{ab} u^b , \quad (\text{A.1})$$

where we introduced the Nakanishi-Lautrup auxiliary field B as a real Euclidean field. Its integration yields the usual gauge fixing term $(\partial A)^2/2\xi$ introduced in Sec. 2. The last term in Eq. (A.1) specifies the ghost part $\mathcal{L}_{\text{ghost}}$, which is hermitean:

$$\mathcal{L}_{\text{ghost}} = \frac{1}{2}(\mathcal{L}_{\text{ghost}} + \mathcal{L}_{\text{ghost}}^\dagger) = -\frac{i}{2}(u, v) \begin{pmatrix} 0 & D\partial \\ -\partial D & 0 \end{pmatrix} \begin{pmatrix} u \\ v \end{pmatrix} . \quad (\text{A.2})$$

In Landau gauge we have $\partial_\mu D_\mu = D_\mu \partial_\mu$ and thus,⁶²

$$\mathcal{L}_{\text{ghost}}^{\xi=0} = -\frac{i}{2}(u, v) \partial D \varepsilon \begin{pmatrix} u \\ v \end{pmatrix} \quad \text{with} \quad \varepsilon = \begin{pmatrix} 0 & 1 \\ -1 & 0 \end{pmatrix} \quad (\text{A.3})$$

which is the metric in a 2-dimensional spinor space. Since

$$A^T \varepsilon A = \varepsilon \quad \text{for } 2 \times 2\text{-matrices } A \text{ with } \det A = 1, \text{ *i.e.*, } A \in SL(2, \mathbb{C}) , \quad (\text{A.4})$$

the ghost Lagrangean for $\xi = 0$ has a global $SL(2, \mathbb{R})$ symmetry, the subgroup of $SL(2, \mathbb{C})$

⁶² This holds *on-shell*, *i.e.*, after the constraint $\partial A = 0$ is implemented. On the level of the Lagrangean it is slightly inconsistent. To be precise, we would have to symmetrize the Faddeev-Popov operator first which can be achieved in the Landau gauge by shifting the B -field. We will do that anyway for the more general Curci-Ferrari gauges below. For the present argument we ignore this subtlety.

that preserves the above hermiticity assignment,

$$\begin{pmatrix} u \\ v \end{pmatrix} \mapsto A \begin{pmatrix} u \\ v \end{pmatrix}, \quad A \in SL(2, \mathbb{R}). \quad (\text{A.5})$$

Note that both, the ghost number symmetry and the Faddeev-Popov(FP) conjugation, are contained in this global symmetry. The former is generated by the (hermitean) ghost charge Q_c , *c.f.*, Sec. 3.4.2 in Ref. [36],

$$[iQ_c, u^a(x)] = u^a(x), \quad [iQ_c, v^a(x)] = -v^a(x), \quad (\text{A.6})$$

or, by exponentiation,

$$e^{iQ_c\theta} : \begin{pmatrix} u \\ v \end{pmatrix} \mapsto \begin{pmatrix} e^\theta & 0 \\ 0 & e^{-\theta} \end{pmatrix} \begin{pmatrix} u \\ v \end{pmatrix}. \quad (\text{A.7})$$

This corresponds to a (non-compact) Abelian subgroup of $SL(2, \mathbb{R})$. FP conjugation \mathcal{C}_{FP} , *i.e.*, the ghost-antighost symmetry of the Landau gauge, can be represented by

$$\mathcal{C}_{\text{FP}} : \begin{pmatrix} u \\ v \end{pmatrix} \mapsto \begin{pmatrix} 0 & 1 \\ -1 & 0 \end{pmatrix} \begin{pmatrix} u \\ v \end{pmatrix}, \quad (\text{A.8})$$

which corresponds to a rotation by $\pi/2$ along the compact direction in $SL(2, \mathbb{R})$.

For completeness, we give an explicit basis for the $sl(2, \mathbb{R})$ algebra as follows,

$$\sigma^0 = \begin{pmatrix} 1 & 0 \\ 0 & -1 \end{pmatrix}, \quad \sigma^+ = \begin{pmatrix} 0 & 1 \\ 0 & 0 \end{pmatrix}, \quad \sigma^- = \begin{pmatrix} 0 & 0 \\ 1 & 0 \end{pmatrix}, \quad (\text{A.9})$$

with $[\sigma^0, \sigma^\pm] = \pm 2\sigma^\pm$ and $[\sigma^+, \sigma^-] = \sigma_0$. The Noether charges generating the global $SL(2, \mathbb{R})$ with this Lie algebra can be identified with iQ_c , $iQ_{\bar{c}\bar{c}}/2$ and $-iQ_{cc}/2$ corresponding to σ^0 , σ^+ and σ^- , respectively. Their explicit forms are given in Secs. 3.4.2 and 3.5.1 of Ref. [36].

The connection with the complex formulation is now possible analogously to the Cayley map,

$$z \mapsto h(z) = \frac{z - i}{z + i}, \quad (\text{A.10})$$

which maps the upper half of the complex plane biholomorphically onto the unit disc. Just as $SL(2, \mathbb{R})$ is (locally) isomorphic to the automorphisms of the upper half-plane, with a

two-to-one homomorphism provided by

$$SL(2, \mathbb{R}) \ni A = \begin{pmatrix} \alpha & \beta \\ \gamma & \delta \end{pmatrix} \mapsto h_A(z) = \frac{\alpha z + \beta}{\gamma z + \delta}, \quad (\text{A.11})$$

so is $SU(1, 1)$ two-to-one with the automorphisms of the unit disk in the complex plane. We therefore introduce complex ghost fields $\eta^a(x)$ with $\bar{\eta} = \eta^\dagger$ by

$$\begin{pmatrix} \eta \\ \bar{\eta} \end{pmatrix} := S \begin{pmatrix} u \\ v \end{pmatrix}, \quad \text{with } S = \frac{1}{\sqrt{2}} \begin{pmatrix} 1 & -i \\ 1 & i \end{pmatrix}, \quad (\text{A.12})$$

with conventions such that the Cayley map $h(z) = h_{(\sqrt{-i}S)}(z)$. Since $\sqrt{-i}S \in SL(2, \mathbb{C})$, from (A.4) we then find immediately that the Landau gauge ghost Lagrangean of Eq. (A.3) reads,

$$\mathcal{L}_{\text{ghost}}^{\xi=0} = -\frac{1}{2} (\eta, \bar{\eta}) \partial D \begin{pmatrix} 0 & 1 \\ -1 & 0 \end{pmatrix} \begin{pmatrix} \eta \\ \bar{\eta} \end{pmatrix} = \bar{\eta}^a \partial_\mu D_\mu^{ab} \eta^b. \quad (\text{A.13})$$

The map S provides for an isomorphism $SL(2, \mathbb{R}) \simeq SU(1, 1)$,

$$SL(2, \mathbb{R}) \ni A \mapsto SAS^{-1} \in SU(1, 1) = \left\{ M := \begin{pmatrix} a & b \\ \bar{b} & \bar{a} \end{pmatrix} : a, b \in \mathbb{C}, \det B = 1 \right\}. \quad (\text{A.14})$$

Explicitly we have

$$M = SAS^{-1} = \frac{1}{2} \begin{pmatrix} \alpha + \delta + i(\beta - \gamma) & \alpha - \delta - i(\beta + \gamma) \\ \alpha - \delta + i(\beta + \gamma) & \alpha + \delta - i(\beta + \gamma) \end{pmatrix}, \quad (\text{A.15})$$

or $\alpha = \text{Re}(a + b)$, $\beta = \text{Im}(b - a)$, $\gamma = \text{Im}(a + b)$, $\delta = \text{Re}(a - b)$. The global symmetry of $\mathcal{L}_{\text{ghost}}^{\xi=0}$ in the complex formulation is now $SU(1, 1)$, the 3-parameter subgroup of $SL(2, \mathbb{C})$ that preserves the hermiticity assignement $\bar{\eta} = \eta^\dagger$ under

$$\begin{pmatrix} \eta \\ \bar{\eta} \end{pmatrix} \mapsto M \begin{pmatrix} \eta \\ \bar{\eta} \end{pmatrix}. \quad (\text{A.16})$$

One verifies furthermore that

$$M^\dagger \begin{pmatrix} 1 & 0 \\ 0 & -1 \end{pmatrix} M = \begin{pmatrix} 1 & 0 \\ 0 & -1 \end{pmatrix} \quad (\text{A.17})$$

and with $\det M = 1$ thus $M \in SU(1, 1)$. It is now simple to transcribe the action of the ghost number and FP conjugation symmetries under the map S :

$$e^{iQ_c\theta} : \eta \mapsto (\cosh \theta) \eta + (\sinh \theta) \bar{\eta} ; \quad \text{and} \quad \mathcal{C}_{\text{FP}} : \eta \mapsto i\eta . \quad (\text{A.18})$$

The original ghost number symmetry is no-longer diagonal,

$$[iQ_c, \eta^a(x)] = \bar{\eta}^a(x) , \quad [iQ_c, \bar{\eta}^a(x)] = \eta^a(x) . \quad (\text{A.19})$$

Now, in the complex basis, the FP conjugation is diagonal which arose from a rotation by $\lambda = \pi/2$ along the compact direction of $SL(2, \mathbb{R})$. This $U(1)$ -subgroup gives rise to a conserved global “ $U(1)$ ghost number” symmetry of the complex fields corresponding to $\eta \mapsto e^{i\lambda} \eta$.

Before we continue to discuss the BRS and anti-BRS symmetries, note that the full symmetry of the Landau gauge can be maintained for $\xi \neq 0$ in a slightly more general setting for the covariant gauge fixing [382,384,115,36]. As observed in Ref. [384], renormalizability, global gauge, BRS and Lorentz invariance allow, as the most general form in 4 dimensions, the addition of another independent term to $\mathcal{L}_{\mathcal{GF}}$ in Eq. (A.1) which can be expressed in terms of real or complex ghost fields as follows,

$$\frac{\zeta}{2}(B^a + gf^{abc}v^b u^c)^2 = \frac{\zeta}{2}\left(B^a + i\frac{g}{2}f^{abc}(\eta^b \eta^c - \bar{\eta}^b \bar{\eta}^c)\right)^2 , \quad (\text{A.20})$$

and which introduces a second gauge parameter ζ . This parameter controls the hermiticity of the Lagrangean. In particular, for $\zeta = 0$, in the standard Faddeev-Popov gauges with $\xi \neq 0$, the FP conjugation symmetry is broken and only the real formulation thus leads to a hermitean Lagrangean. The full global $SL(2, \mathbb{R}) \simeq SU(1, 1)$ which establishes the equivalence of both formulations on the other hand is maintained for $\zeta = \xi$. For $\xi \neq 0$, one can therefore introduce,

$$\begin{aligned} \mathcal{L}'_{\mathcal{GF}} &= iB^a \partial_\mu A_\mu^a + \frac{\xi}{4}\left(B^a B^a + (B^a + gf^{abc}v^b u^c)^2\right) + iv^a \partial_\mu D_\mu^{ab} u^b , \\ &= iB^a \partial_\mu A_\mu^a + \frac{\xi}{4}\left\{B^a B^a + \left(B^a + i\frac{g}{2}f^{abc}(\eta^b \eta^c - \bar{\eta}^b \bar{\eta}^c)\right)^2\right\} + \frac{1}{2}(\eta + \bar{\eta})^a \partial_\mu D_\mu^{ab} (\eta - \bar{\eta})^b , \end{aligned} \quad (\text{A.21})$$

to generalize the symmetry of the Landau gauge. The effect of this modification is most easily seen from shifting the B -field,

$$B' := B + \frac{g}{2}(v \times u) = B + i\frac{g}{4}(\eta \times \eta - \bar{\eta} \times \bar{\eta}) , \quad \text{with} \quad (v \times u)^a \equiv f^{abc}v^b u^c . \quad (\text{A.22})$$

In terms of the B' -field, it is straightforward to rewrite the gauge fixing Lagrangean $\mathcal{L}'_{\mathcal{GF}}$ of Eq. (A.21),

$$\mathcal{L}'_{\mathcal{GF}} = iB' \partial A + \frac{\xi}{2}B' B' + \frac{\xi}{2}\left(\frac{g}{2}(v \times u)\right)^2 + \frac{i}{2}v(\partial D + D\partial)u , \quad (\text{A.23})$$

$$= iB' \partial A + \frac{\xi}{2} B' B' - \frac{\xi}{2} \left(\frac{g}{2} (\bar{\eta} \times \eta) \right)^2 + \frac{1}{2} \bar{\eta} (\partial D + D \partial) \eta. \quad (\text{A.24})$$

For the quartic ghost-interaction in the complex version, the 2nd Eq. (A.24) above, we have made use of the Jacobi identity to rewrite $(\eta \times \eta - \bar{\eta} \times \bar{\eta})^2 = 4(\bar{\eta} \times \eta)^2$. At the expense of these quartic ghost self-interactions, the essential effect of the additional term in (A.21) is to “symmetrize” the Faddeev-Popov operator of the conventional covariant gauges, $\partial D \rightarrow (\partial D + D \partial)/2$. The $SL(2, \mathbb{R})$ or the $SU(1, 1)$ invariance of ghost self-interactions in the real or the complex version, respectively, is most easily seen from,

$$\begin{aligned} f^{abc}(\bar{\eta}^b \eta^c) f^{ade}(\bar{\eta}^d \eta^e) &= \frac{2}{N_c} (\bar{\eta}^a \eta^a)(\bar{\eta}^b \eta^b) + d^{abc}(\bar{\eta}^b \eta^c) d^{ade}(\bar{\eta}^d \eta^e) \\ &= \frac{1}{2N_c} \left((\eta^a, \bar{\eta}^a) \varepsilon \left(\frac{\eta^a}{\bar{\eta}^a} \right) \right)^2 + \frac{1}{4} \left(d^{abc}(\eta^b, \bar{\eta}^b) \varepsilon \left(\frac{\eta^c}{\bar{\eta}^c} \right) \right)^2. \end{aligned} \quad (\text{A.25})$$

One therefore verifies that $\mathcal{L}'_{\mathcal{G}\mathcal{F}}$ is invariant under the global $SL(2, \mathbb{R}) \simeq SU(1, 1)$ just as $\mathcal{L}_{\text{ghost}}^{\xi=0}$. In absence of the (anti-)BRS transformations discussed below, B' , A , and the quark fields q , could be taken to belong to the trivial (singlet) representation. Note, however, that this is not true for the original B field introduced in (A.1) which transforms non-trivially. Under FP conjugation for instance,

$$\mathcal{C}_{\text{FP}} : \quad B \mapsto B + g(v \times u), \quad \text{while } B' \mapsto B'. \quad (\text{A.26})$$

For $\xi = 0$ we recover the Landau gauge Lagrangean. Its symmetrized ghost part, when the $SL(2, \mathbb{R}) \simeq SU(1, 1)$ invariant B' field is employed as in Eqs. (A.23) or (A.24), is to replace $L_{\text{ghost}}^{\xi=0}$ for an *off-shell* extension of the discussion of the global ghost symmetries and the relation between the real and the complex formulation, *i.e.*, one which proceeds analogously to that leading from Eqs. (A.3) to (A.13) without need, however, to employ the constraint $\partial A = 0$.

Under the map S , we furthermore obtain from Eqs. (A.9) (a basis for $su(1, 1)$, of course),

$$\sigma_0 \mapsto \begin{pmatrix} 0 & 1 \\ 1 & 0 \end{pmatrix}, \quad \sigma^1 = \sigma^+ + \sigma^- \mapsto \begin{pmatrix} 0 & -i \\ i & 0 \end{pmatrix}, \quad \sigma^2 = \sigma^+ - \sigma^- \mapsto \begin{pmatrix} i & 0 \\ 0 & -i \end{pmatrix}. \quad (\text{A.27})$$

And the corresponding Noether currents, in terms of the complex ghost fields, are given by,

$$\begin{aligned} J_\mu^0 &= -\frac{1}{2} \left(\eta (\partial_\mu + D_\mu) \eta - \bar{\eta} (\partial_\mu + D_\mu) \bar{\eta} \right), & Q^0 &= \int d^3x J_0^0 = Q_c, \\ J_\mu^1 &= -\frac{i}{2} \left(\eta (\partial_\mu + D_\mu) \eta + \bar{\eta} (\partial_\mu + D_\mu) \bar{\eta} \right), & Q^1 &= \int d^3x J_0^1 = \frac{1}{2} (Q_{\bar{c}\bar{c}} - Q_{cc}), \\ J_\mu^2 &= \frac{i}{2} \left(\bar{\eta} (\partial_\mu + D_\mu) \eta + \eta (\partial_\mu + D_\mu) \bar{\eta} \right), & Q^2 &= \int d^3x J_0^2 = \frac{1}{2} (Q_{\bar{c}\bar{c}} + Q_{cc}). \end{aligned} \quad (\text{A.28})$$

We now introduce BRS variations $\delta\Phi \equiv \lambda\delta_{\mathbf{B}}\Phi$ of generic fields Φ with global Grassmann

parameter λ and the BRS charge Q_B such that in the operator formulation,

$$\delta_B \Phi = i\{Q_B, \Phi\} , \quad (\text{A.29})$$

where $\{, \}$ denotes the ghost-number graded commutator, *i.e.*, the anti-commutator if both operators have odd ghost number and the commutator otherwise. In presence of the full ghost-antighost symmetry one also has anti-BRS invariance, defined by

$$\bar{\delta}_B \Phi = i\{\bar{Q}_B, \Phi\} := \mathcal{C}_{\text{FP}} \delta_B \mathcal{C}_{\text{FP}}^{-1} . \quad (\text{A.30})$$

With the Euclidean conventions introduced in Sec. 2 for the real fields in Landau gauge we have (*c.f.*, Eqs. (A.8) and (A.26) for the action of \mathcal{C}_{FP}),

$$\begin{aligned} \delta_B A &= -Du & \bar{\delta}_B A &= -Dv \\ \delta_B u &= -\frac{g}{2}(u \times u) & \bar{\delta}_B u &= -B - g(v \times u) \\ \delta_B v &= B & \bar{\delta}_B v &= -\frac{g}{2}(v \times v) \\ \delta_B B &= 0 & \bar{\delta}_B B &= -g(v \times B) \\ \delta_B q &= ig(t^a u^a) q & \bar{\delta}_B q &= ig(t^a v^a) q . \end{aligned} \quad (\text{A.31})$$

As usual, one furthermore has $\delta_B \delta_B = \bar{\delta}_B \bar{\delta}_B = \delta_B \bar{\delta}_B + \bar{\delta}_B \delta_B = 0$.

For the complex formulation, employing the gauge fixing corresponding to $\mathcal{L}'_{\mathcal{GF}}$ of Eq. (A.24) which generalizes the Landau gauge in an $SU(1, 1)$ symmetric way, it is convenient to introduce *complex* BRS variations as follows,

$$\delta'_B := \frac{1}{\sqrt{2}}(\delta_B - i\bar{\delta}_B) \quad \bar{\delta}'_B := \frac{1}{\sqrt{2}}(\delta_B + i\bar{\delta}_B) . \quad (\text{A.32})$$

It is then straight forward to verify that for these, one obtains,

$$\begin{aligned} \delta'_B A &= -D\eta & \bar{\delta}'_B A &= -D\bar{\eta} \\ \delta'_B \eta &= -\frac{g}{2}(\eta \times \eta) & \bar{\delta}'_B \eta &= -iB' - \frac{g}{2}(\bar{\eta} \times \eta) \\ \delta'_B \bar{\eta} &= iB' - \frac{g}{2}(\bar{\eta} \times \eta) & \bar{\delta}'_B \bar{\eta} &= -\frac{g}{2}(\bar{\eta} \times \bar{\eta}) \\ \delta'_B B' &= -\frac{g}{2}(\eta \times B') - i\frac{g^2}{8}(\bar{\eta} \times (\eta \times \eta)) & \bar{\delta}'_B B' &= -\frac{g}{2}(\bar{\eta} \times B') + i\frac{g^2}{8}(\eta \times (\bar{\eta} \times \bar{\eta})) \\ \delta'_B q &= ig(t^a \eta^a) q & \bar{\delta}'_B q &= ig(t^a \bar{\eta}^a) q , \end{aligned} \quad (\text{A.33})$$

and again, of course, $\delta'_B \delta'_B = \bar{\delta}'_B \bar{\delta}'_B = \delta'_B \bar{\delta}'_B + \bar{\delta}'_B \delta'_B = 0$.

Clearly, originally real fields will in general no-longer remain real under the complex BRS transformations just as the real (anti-)BRS transformations lead to B', A and quark fields

that transform non-trivially under $SL(2, \mathbb{R})$. This is because the invariance of the symmetrically covariant gauge fixed theory is a *semi-direct* product of the global $SL(2, \mathbb{R}) \simeq SU(1, 1)$ with the BRS symmetry [382,383,115]. Though the former is an invariant subgroup, the latter is not and the transformations of both do not commute with each other.

For the complex BRS transformations given above one readily verifies that the gauge fixing Lagrangean in Eq. (A.24) can be represented by

$$\mathcal{L}'_{\mathcal{G}\mathcal{F}} = \delta'_{\mathbf{B}} \left[\bar{\eta} \left(\partial A - i \frac{\xi}{2} B' \right) \right]. \quad (\text{A.34})$$

The complex formulation can also be cast in a form which is less symmetric with respect to the complex BRS transformations which resembles the familiar real formulation, Eqs. (A.23) and (A.31), more closely, however. This is possible with a second shift of the B -field, *c.f.*, (A.22),

$$B'' := B' + i \frac{g}{2} (\bar{\eta} \times \eta) = B + i \frac{g}{4} \left(\eta \times \eta - \bar{\eta} \times \bar{\eta} + 2 \bar{\eta} \times \eta \right). \quad (\text{A.35})$$

The complex BRS transformations of Eqs. (A.33) can then be written,

$$\begin{aligned} \delta'_{\mathbf{B}} \bar{\eta} &= i B'' & \bar{\delta}'_{\mathbf{B}} \eta &= -i B'' - g (\bar{\eta} \times \eta) \\ \delta'_{\mathbf{B}} B'' &= 0 & \bar{\delta}_{\mathbf{B}} B'' &= -g (\bar{\eta} \times B'') \end{aligned} \quad (\text{A.36})$$

with the other transfromations in Eqs. (A.33) remaining unchanged. In terms of this field B'' , Eq. (A.24) yields,

$$\mathcal{L}'_{\mathcal{G}\mathcal{F}} = i B'' \left(\partial A - \xi \frac{g}{2} (\bar{\eta} \times \eta) \right) + \frac{\xi}{2} B'' B'' - \xi \left(\frac{g}{2} (\bar{\eta} \times \eta) \right)^2 + \bar{\eta} \partial D \eta, \quad (\text{A.37})$$

$$= \delta'_{\mathbf{B}} \left[\bar{\eta} \left(F(A) - i \frac{\xi}{2} \left(B'' + i \frac{g}{4} (\bar{\eta} \times \eta) \right) \right) \right], \quad \text{with} \quad F(A) = \partial A - \xi \frac{g}{2} (\bar{\eta} \times \eta), \quad (\text{A.38})$$

and with the constraint $F(A) = i \xi B''$ for the B'' -field in (A.37) being equivalent to $\partial A = i \xi B'$ from (A.24). The form for the gauge fixing Lagrangen given in Eq. (A.24) should be viewed as the correct extension beyond the Landau gauge of the complex formulation introduced in Sect. 2 in Eqs. (11) and (13) with the identification $\eta \rightarrow c$, $\lambda \delta'_{\mathbf{B}} \rightarrow \delta$ and the hermiticity assignement $\bar{c} = c^\dagger$. In particular, integrating the B' -field in Eq. (A.24) (or the B'' -field in (A.37) above), the (unique) result is,

$$\mathcal{L}'_{\mathcal{G}\mathcal{F}} = \frac{1}{2\xi} \left(\partial_\mu A_\mu^a \right)^2 - \frac{\xi}{2} \left(\frac{g}{2} f^{abc} \bar{c}^b c^c \right)^2 + \frac{1}{2} \bar{c}^a \left(\partial_\mu D_\mu^{ab} + D_\mu^{ab} \partial_\mu \right) c^b. \quad (\text{A.39})$$

And the *on-shell* BRS transformation for \bar{c} then reads,

$$\delta \bar{c}^a = \frac{1}{\xi} F^a(A) \lambda, \quad \text{with} \quad F^a(A) = \partial_\mu A_\mu^a - \xi \frac{g}{2} f^{abc} \bar{c}^b c^c. \quad (\text{A.40})$$

The Landau gauge limit $\xi \rightarrow 0$ is smooth for the $SL(2, \mathbb{R}) \simeq SU(1, 1)$ symmetric gauge fixing, the renormalizability is maintained [384], and the important observation that $\tilde{Z}_1 = 1$ in Landau gauge was also verified at one-loop level in Ref. [384].

The relation between the BRS-algebra and de Rahm cohomology is quite well established. Pedagogical accounts of this can be found in, *e.g.*, refs. [36,98,41]. The semi-direct product of the $SL(2, \mathbb{R})$ with the double BRS-algebra generated by the charges Q_B and \overline{Q}_B can be obtained by a Inonu-Wigner contraction of the simple $OSp(1, 2)$ superalgebra in which the Curci-Ferrari mass term [382,383] is sent to zero, see refs. [115,36]. For completeness we furthermore mention that a relation of the double BRS-algebra to the theory of double complexes (the Dolbeault cohomology for complex manifolds) was realized in refs. [385–388,115]. The $SL(2, \mathbb{R})$ ghost-antighost symmetry was combined with the Lorentz symmetry to arrive at a superspace formulation in refs. [389–391].

B Conventions for Fourier Transformations

In this appendix we summarize our conventions for Fourier transforming Green's functions from Euclidean space to the corresponding momentum space. For all propagators $D(x, y)$ which depend in a translationally invariant background only on $\xi = x - y$ we use

$$D(p) := \int d^4\xi e^{-ip\xi} D(x, y). \quad (\text{B.1})$$

For the fermion–photon, quark–gluon and gluon–ghost vertex functions we use notations adopted to having in– and out–going fermion (ghost) legs. The momentum of the photon is defined as outgoing whereas the two fermion momenta are chosen differently, one incoming and one outgoing:

$$\Gamma_\mu(k, q, p) = \int d^4x d^4y d^4z e^{ikx} e^{iqy} e^{-ipz} \Gamma_\mu^a(x; y, z). \quad (\text{B.2})$$

Momentum conservation allows to define a reduced vertex function:

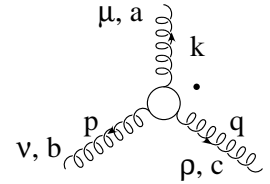
$$\Gamma_\mu(k, q, p) = -ie (2\pi)^4 \delta^4(k + q - p) \Gamma_\mu(q, p), \quad (\text{B.3})$$

The momentum dependence of the quark–gluon and the ghost–gluon vertex is defined completely analogous, see Sect. 3.3.

For the three-gluon vertex function, on the other hand, we choose a momentum dependence emphasizing its complete Bose symmetry:

$$\Gamma_{\mu\nu\rho}^{abc}(x, y, z) = \int \frac{d^4 p}{(2\pi)^4} \frac{d^4 q}{(2\pi)^4} \frac{d^4 k}{(2\pi)^4} e^{ipx} e^{iqy} e^{ikz} \Gamma_{\mu\nu\rho}^{abc}(p, q, k) . \quad (\text{B.4})$$

The corresponding reduced vertex is then defined as

$$\Gamma_{\mu\nu\rho}^{abc}(k, p, q) =: g f^{abc} (2\pi)^4 \delta^4(k + p + q) \Gamma_{\mu\nu\rho}(k, p, q) . \quad (\text{B.5})$$


Hereby the indices are given in counterclockwise order starting at the dot.

C Dyson–Schwinger Equation for the Gluon Propagator

In this appendix we will give the explicit form of the DSE for the gluon propagator. Using

$$\begin{aligned} -\frac{\delta^2 \Gamma_{\text{QCD}}}{\delta A_\mu^a(x) \delta A_\nu^b(y)} &= -Z_3 \left[\delta_{\mu\nu} \partial^2 - \left(1 - \frac{1}{Z_3 \xi} \right) \partial_\mu \partial_\nu \right] \delta^{ab} \delta(x - y) \\ &\quad + Z_1 g f^{ade} \int d^4 z \langle A_\nu^b(y) A_\rho^c(z) \rangle^{-1} \left\{ \langle A_\rho^c(z) A_\sigma^d(x) \partial_\mu A_\sigma^e(x) \rangle \right. \\ &\quad \left. - \langle A_\rho^c(z) A_\sigma^d(x) \partial_\sigma A_\mu^e(x) \rangle - \langle A_\rho^c(z) \partial_\sigma A_\sigma^d(x) A_\mu^e(x) \rangle \right\} \\ &\quad + Z_4 g^2 f^{afg} f^{gde} \left\{ \delta^{bf} \langle A_\mu^d(x) A_\nu^e(x) \rangle + \delta^{be} \langle A_\nu^f(x) A_\mu^d(x) \rangle \right. \\ &\quad \left. + \delta^{bd} \delta_{\mu\nu} \langle A_\rho^f(x) A_\rho^e(x) \rangle \right\} \delta(x - y) \\ &\quad + Z_4 g^2 f^{afg} f^{gde} \int d^4 z \langle A_\nu^b(y) A_\rho^c(z) \rangle^{-1} \langle A_\rho^c(z) A_\sigma^f(x) A_\mu^d(x) A_\sigma^e(x) \rangle_c \\ &\quad - Z_{1F} i g t^a \gamma_\mu \int d^4 z \langle A_\nu^b(y) A_\rho^c(z) \rangle^{-1} \langle A_\rho^c(z) \bar{\psi}(x) \psi(x) \rangle_c \\ &\quad + \tilde{Z}_1 g f^{ade} \int d^4 z \langle A_\nu^b(y) A_\rho^c(z) \rangle^{-1} \langle A_\rho^c(z) (\partial_\mu \bar{c}^d(x)) c^e(x) \rangle_c \end{aligned} \quad (\text{C.1})$$

where the functional identity

$$\begin{aligned} \frac{\delta}{\delta A_\mu^a(x)} &= \int d^4 z \frac{\delta J_\nu^b(z)}{\delta A_\mu^a(x)} \frac{\delta}{\delta J_\nu^b(z)} \\ &= - \int d^4 z \frac{\delta^2 \Gamma}{\delta A_\mu^a(x) \delta A_\nu^b(z)} \frac{\delta}{\delta J_\nu^b(z)} \end{aligned} \quad (\text{C.2})$$

has been used. The resulting gluon DSE then reads

$$\begin{aligned}
D^{-1}_{\mu\nu}^{ab}(x-y) = & Z_3 D_{(0)\mu\nu}^{-1ab}(x-y) \\
& + Z_1 \frac{1}{2} \int d^4x_1 d^4x_2 d^4y_1 d^4y_2 \\
& \quad \times \Gamma_{\mu\alpha\beta}^{(0)acd}(x, x_1, x_2) D_{\beta\gamma}^{de}(x_2 - y_1) D_{\alpha\delta}^{cf}(x_1 - y_2) \Gamma_{\nu\gamma\delta}^{bef}(y, y_1, y_2) \\
& + Z_4 \frac{1}{2} \int d^4x_1 d^4x_2 \Gamma_{\mu\nu\alpha\beta}^{(0)abcd}(x, y, x_1, x_2) D_{\alpha\beta}^{cd}(x_1 - x_2) \\
& + Z_4 \frac{1}{6} \int d^4x_1 d^4x_2 d^4x_3 d^4y_1 d^4y_2 d^4y_3 \Gamma_{\mu\alpha\beta\gamma}^{(0)acde}(x, x_1, x_2, x_3) \\
& \quad \times D_{\alpha\lambda}^{cm}(x_1 - y_3) D_{\beta\sigma}^{dl}(x_2 - y_2) D_{\gamma\rho}^{ek}(x_3 - y_1) \Gamma_{\nu\rho\sigma\lambda}^{bklm}(y, y_1, y_2, y_3) \\
& + Z_4 \frac{1}{2} \int d^4x_1 d^4x_2 d^4x_3 d^4y_1 d^4y_2 d^4y_3 d^4z_1 d^4z_2 \\
& \quad \times \Gamma_{\mu\alpha\beta\gamma}^{(0)acde}(x, x_1, x_2, x_3) D_{\alpha\rho}^{ck}(x_1 - y_1) D_{\beta\lambda}^{dm}(x_2 - y_3) D_{\gamma\delta}^{ep}(x_3 - z_1) \\
& \quad \times \Gamma_{\rho\sigma\lambda}^{klm}(y_1, y_2, y_3) D_{\sigma\kappa}^{lq}(y_2 - z_2) \Gamma_{\nu\delta\kappa}^{bpq}(y, z_1, z_2) \\
& + Z_{1F} \int d^4x_1 d^4x_2 d^4y_1 d^4y_2 \\
& \quad \times \Gamma_{\mu}^{(0)a}(x, x_1, x_2) S(x_2 - y_1) S(y_2 - x_1) \Gamma_{\nu}^b(y, y_1, y_2) \\
& + \tilde{Z}_1 \int d^4x_1 d^4x_2 d^4y_1 d^4y_2 \\
& \quad \times \Gamma_{\mu}^{(0)acd}(x, x_1, x_2) G^{de}(x_2 - y_1) G^{fc}(y_2 - x_1) \Gamma_{\nu}^{bef}(y, y_1, y_2)
\end{aligned} \tag{C.3}$$

Finally, after Fourier transforming into momentum space this equation becomes

$$\begin{aligned}
D^{-1}_{\mu\nu}^{ab}(p) = & Z_3 D_{(0)\mu\nu}^{-1ab}(p) \\
& + Z_1 \frac{1}{2} \int d^4q d^4k \Gamma_{\mu\alpha\beta}^{(0)acd}(p, -q, -k) D_{\beta\gamma}^{de}(k) D_{\alpha\delta}^{cf}(q) \Gamma_{\nu\gamma\delta}^{bef}(-p, k, q) \\
& + Z_4 \frac{1}{2} \int d^4q_1 d^4q_2 \Gamma_{\mu\nu\alpha\beta}^{(0)abcd}(p, -p, -q_1, q_2) D_{\alpha\beta}^{cd}(q_1) \\
& + Z_4 \frac{1}{6} \int d^4k_1 d^4k_2 d^4k_3 \Gamma_{\mu\alpha\beta\gamma}^{(0)acde}(p, -k_1, -k_2, -k_3) \\
& \quad \times D_{\alpha\lambda}^{cm}(k_1) D_{\beta\sigma}^{dl}(k_2) D_{\gamma\rho}^{ek}(k_3) \Gamma_{\nu\rho\sigma\lambda}^{bklm}(p, k_3, k_2, k_1) \\
& + Z_4 \frac{1}{2} \int d^4k_1 d^4k_2 d^4k_3 d^4k_4 \\
& \quad \times \Gamma_{\mu\alpha\beta\gamma}^{(0)acde}(p, -k_1, -k_2, -k_3) D_{\alpha\rho}^{ck}(k_1) D_{\beta\lambda}^{dm}(k_2) D_{\gamma\delta}^{ep}(k_3) \\
& \quad \times \Gamma_{\rho\sigma\lambda}^{klm}(k_1, -k_4, k_2) D_{\sigma\kappa}^{lq}(k_4) \Gamma_{\nu\delta\kappa}^{bpq}(-p, k_3, k_4) \\
& + Z_{1F} \int d^4q d^4k \Gamma_{\mu}^{(0)a}(p, q, k) S(-q) S(k) \Gamma_{\nu}^b(-p, k, q) \\
& + \tilde{Z}_1 \int d^4q d^4k \Gamma_{\mu}^{(0)acd}(p, q, k) G^{de}(-q) G^{fc}(k) \Gamma_{\nu}^{bef}(-p, k, q)
\end{aligned} \tag{C.5}$$

which is the Dyson-Schwinger equation for the (inverse) gluon propagator, derived in Refs. [168,392] and schematically depicted in Fig. C.1.

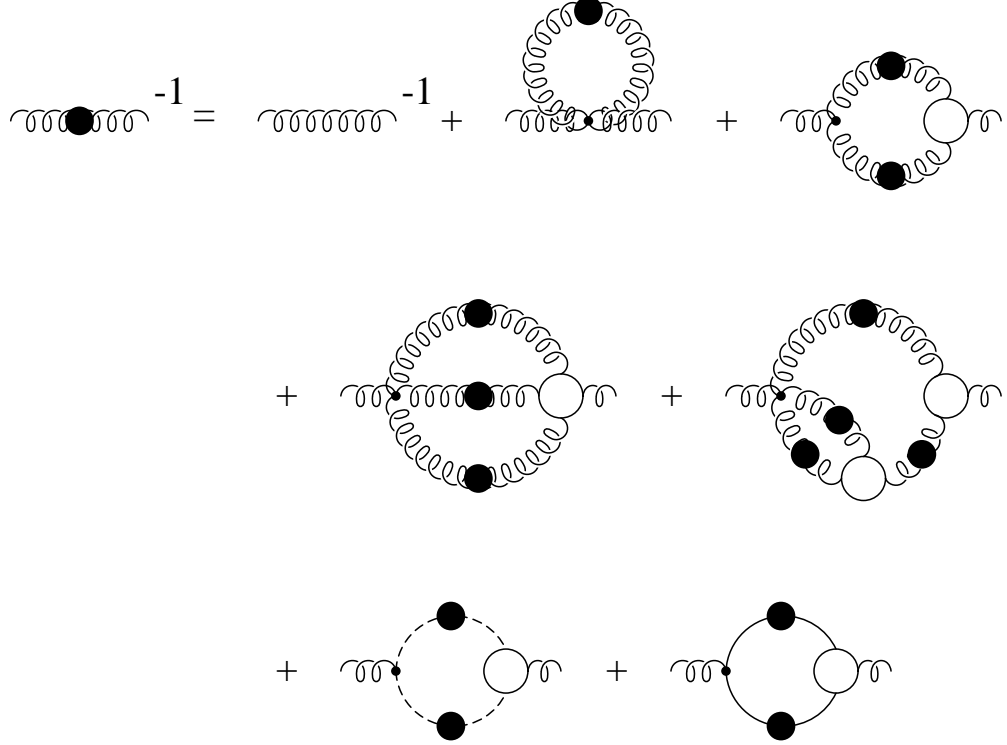


Fig. C.1. Pictorial representation of the gluon DSE.

In linear covariant gauges the gluon propagator has a general structure described by one scalar function $Z(k^2)$, see Eq. (97). On the other hand, in the axial gauge the gluon propagator involves in general two scalar functions g and f :⁶³

$$D_{\mu\nu}(p) = \Delta(p^2, (pt)^2) \left\{ \mathcal{M}_{\mu\nu}(p) g(p^2, (pt)^2) - t^2 \mathcal{P}_{\mu\nu}(t) f(p^2, (pt)^2) \right\} \quad (C.6)$$

$$\Delta(p^2, (pt)^2) = (g(p^2, (pt)^2) - t^2 f(p^2, (pt)^2))^{-1} (p^2 g(p^2, (pt)^2) - (pt)^2 f(p^2, (pt)^2))^{-1}.$$

Here, the transverse projector $\mathcal{P}_{\mu\nu}(t) = \delta_{\mu\nu} - t_\mu t_\nu / t^2$ appears in addition to the tensor

$$\mathcal{M}_{\mu\nu}(k) = \delta_{\mu\nu} - \frac{k_\mu t_\nu + k_\nu t_\mu}{kt} + t^2 \frac{k_\mu k_\nu}{(kt)^2}. \quad (C.7)$$

The tree-level propagator is obtained for $g = 1$ and $f = 0$. With the above parameterization of the gluon propagator (C.6), the vacuum polarization tensor follows to be of the form,

$$\Pi_{\mu\nu}(p) = p^2 \mathcal{P}_{\mu\nu}(p) g(p^2, (pt)^2) - (pt)^2 \mathcal{N}_{\mu\nu}(p) f(p^2, (pt)^2). \quad (C.8)$$

Due to the presence of f another tensor is involved,

$$\mathcal{N}_{\mu\nu}(k) = \delta_{\mu\nu} - \frac{k_\mu t_\nu + k_\nu t_\mu}{kt} + k^2 \frac{t_\mu t_\nu}{(kt)^2}, \quad (C.9)$$

⁶³ Colour indices are suppressed in the following formulas. As usual, we assume that the gluon propagator is color diagonal.

and one has,

$$D_{\mu\rho}(p) \Pi_{\rho\nu}(p) = \delta_{\mu\nu} - \frac{p_\mu t_\nu}{pt}, \quad \Pi_{\mu\rho}(p) D_{\rho\nu}(p) = \delta_{\mu\nu} - \frac{t_\mu p_\nu}{pt}. \quad (\text{C.10})$$

Thus, despite the fact the gluon propagator DSE contains in axial gauge one term less than in linear covariant gauges (the ghost loop) its explicit form is much more complicated.

D 3–Gluon Vertex in Axial Gauge

As mentioned in sect. 3.3 the Slavnov–Taylor identity for the 3–gluon vertex $\Gamma_{\mu\nu\rho}$ in axial gauge has the comparatively simple form,

$$ik_\rho \Gamma_{\mu\nu\rho}(p, q, k) = \Pi_{\mu\nu}(q) - \Pi_{\mu\nu}(p). \quad (\text{D.1})$$

Nevertheless allowing for the most general tensor structure, however, its solution becomes quite involved. With the additional requirement that it is free from kinematic singularities is implemented the solution has been obtained in Ref. [172], and can be cast in the form,

$$\begin{aligned} i\Gamma_{\mu\nu\rho}(p, q, k) &= (T_1(p, k)_{\mu\rho\nu} - T_1(q, k)_{\nu\rho\mu}) g(k^2, (kt)^2) \\ &+ (T_2(p, k)_{\mu\rho\nu} - T_2(q, k)_{\nu\rho\mu}) f(k^2, (kt)^2) + T_3(p, q)_{\mu\nu\rho} \frac{1}{2} (g(p^2, (qt)^2) - g(q^2, (pt)^2)) \\ &+ T_4(p, q)_{\mu\nu\rho} \frac{1}{2} (f(p^2, (qt)^2) - f(q^2, (pt)^2)) + \text{cycl. permutations}. \end{aligned} \quad (\text{D.2})$$

This compact form hides the complexity of this solution which, however, can be seen quite clearly from the explicit expressions for the tensors T_1, T_2, T_3 and T_4 :

$$\begin{aligned} T_1(p, q)_{\mu\nu\rho} &= \delta_{\mu\nu} q_\rho - \frac{1}{2} (\delta_{\mu\nu} p q - q_\mu p_\nu) \left(\frac{(p-q)_\rho}{p^2 - q^2} + \frac{t_\rho}{pt + qt} \right) \\ T_2(p, q)_{\mu\nu\rho} &= -\delta_{\mu\nu} t_\rho q t - t_\mu t_\nu q_\rho \\ &- \frac{1}{2} (\delta_{\mu\nu} p t q t - t_\mu p_\nu q t - t_\nu q_\mu p t + t_\mu t_\nu p q) \left(\frac{(p-q)_\rho}{p^2 - q^2} + \frac{t_\rho}{pt + qt} \right) \\ T_3(p, q)_{\mu\nu\rho} &= -(\delta_{\mu\nu} p q - q_\mu p_\nu) \left(\frac{(p-q)_\rho}{p^2 - q^2} - \frac{t_\rho}{pt + qt} \right) \\ T_4(p, q)_{\mu\nu\rho} &= (\delta_{\mu\nu} p t q t - t_\mu p_\nu q t - t_\nu q_\mu p t + t_\mu t_\nu p q) \left(\frac{(p-q)_\rho}{p^2 - q^2} - \frac{t_\rho}{pt + qt} \right). \end{aligned}$$

This solution for the 3–gluon vertex is not only free from singularities of the type $1/(p^2 - q^2)$ but also from the typical axial gauge singularities of the form $1/(pt)$ [172].

References

- [1] H. Lehmann, K. Symanzik, and W. Zimmermann, *Nuov. Cim.* **1** (1955) 205.
- [2] C. Itzykson and J.-B. Zuber, *Quantum Field Theory*, McGraw-Hill, 1980.
- [3] R. Haag, *Local Quantum Physics*, Springer Verlag, 2nd edition, 1996.
- [4] R. Haag, *Phys. Rev.* **112** (1958) 669.
- [5] K. Nishijima, *Phys. Rev.* **111** (1958) 995.
- [6] W. Zimmermann, *Nuov. Cim.* **10** (1958) 597.
- [7] T. Kinoshita, *J. Math. Phys.* **3** (1962) 650, T. D. Lee and M. Nauenberg, *Phys. Rev.* **133**, 6B (1964) 1549.
- [8] F. Bloch and A. Nordsieck, *Phys. Rev.* **52** (1937) 54.
- [9] W. Marciano and H. Pagels, *Phys. Rep.* **36** (1978) 137.
- [10] T. Kinoshita and A. Ukawa, *Phys. Rev.* **D13** (1976) 1573.
- [11] C. A. Nelson, *Nucl. Phys.* **B186** (1981) 187.
- [12] E. C. Poggio and H. R. Quinn, *Phys. Rev.* **D14** (1976) 578.
- [13] D. J. Gross and A. Neveu, *Phys. Rev.* **D10** (1974) 3235.
- [14] F. J. Dyson, *Phys. Rev.* **75** (1949) 1736.
- [15] J. S. Schwinger, *Proc. Nat. Acad. Sc.* **37** (1951) 452; *ibid.*, 455.
- [16] J. C. Taylor, *Nucl. Phys.* **B33** (1971) 436.
- [17] A. Slavnov, *Theor. Math. Phys.* **10** (1972) 99.
- [18] S. Mandelstam, *Phys. Rev.* **D20** (1979) 3223.
- [19] D. Atkinson, J. K. Dohrm, P. W. Johnson, and K. Stam, *J. Math. Phys.* **22** (1981) 2704.
- [20] N. Brown and M. R. Pennington, *Phys. Rev.* **D39** (1989) 2723.
- [21] A. Hauck, L. v. Smekal, and R. Alkofer, in *Quark Confinement and the Hadron Spectrum II*, edited by N. Brambilla and M. Prosperi, p. 258, World Scientific, 1997, preprint, ANL-PHY-8386-TH-96, UNITU-THEP-5/1996.
- [22] M. Baker, J. S. Ball, and F. Zachariasen, *Nucl. Phys.* **B186** (1981) 531 ; *ibid.*, 560.
- [23] M. Baker, J. S. Ball, and F. Zachariasen, *Nucl. Phys.* **B226** (1983) 4555.
- [24] A. Alekseev, B. A. Arbuzov, and V. A. Baikov, *Teor. Mat. Fiz.* **52** (1982) 187.
- [25] W. J. Schoenmaker, *Nucl. Phys.* **B194** (1982) 535.
- [26] J. R. Cudell and D. A. Ross, *Nucl. Phys.* **B358** (1991) 247.
- [27] K. Büttner and M. R. Pennington, *Phys. Rev.* **D52** (1995) 5220.

- [28] P. C. Tandy, *Prog. Part. Nucl. Phys.* **39** (1997) 117.
- [29] C. D. Roberts and A. G. Williams, *Prog. Part. Nucl. Phys.* **33** (1994) 477.
- [30] V. A. Miransky, *Dynamical Symmetry Breaking in Quantum Field Theories*, World Scientific, 1993, and references therein.
- [31] C. D. Roberts and S. M. Schmidt, *Prog. Part. Nucl. Phys.* **45** (2000).
- [32] S. N. Gupta, *Proc. Roy. Soc.* **A63** (1950) 681.
- [33] K. Bleuler, *Helv. Phys. Acta* **23** (1950) 567.
- [34] F. Strocchi, *Phys. Lett.* **B62** (1976) 60, see also, *Phys. Rev.* **D17** (1978) 2010.
- [35] I. Ojima, *Z. Phys.* **C5** (1980) 227.
- [36] N. Nakanishi and I. Ojima, *Covariant Operator Formalism of Gauge Theories and Quantum Gravity*, volume 27 of *Lecture Notes in Physics*, World Scientific, 1990.
- [37] C. Becchi, A. Rouet, and R. Stora, *Comm. Math. Phys.* **42** (1975) 127, *see also*: I. V. Tyutin, Lebedev preprint FIAN No. 39 (1975).
- [38] R. Fernández, J. Fröhlich, and A. D. Sokal, *Random Walks, Critical Phenomena, and Triviality in Quantum Field Theory*, Springer Verlag, 1991.
- [39] R. Oehme and W. Zimmermann, *Phys. Rev.* **D21** (1980) 471; *ibid.*, 1661.
- [40] R. Oehme, *Int. J. Mod. Phys.* **A10** (1995) 1995.
- [41] K. Nishijima, *Czech. J. Phys.* **46** (1996) 1.
- [42] L. D. Faddeev and V. N. Popov, *Phys. Lett.* **B25** (1967) 29.
- [43] P. van Baal, *Nucl. Phys.* **B369** (1992) 259.
- [44] P. van Baal, Global Issues in Gauge Fixing, in *Non-perturbative approaches to QCD*, edited by D. Diakonov, Trento, 1995, Procs. of the ECT* Workshop, hep-th/9511119.
- [45] O. W. Greenberg, *Phys. Lett.* **B416** (1998) 144.
- [46] R. Oehme, *Phys. Rev.* **D42** (1990) 4209, *Phys. Lett.* **B252** (1990) 641.
- [47] R. Oehme and W. Xu, *Phys. Lett.* **B333** (1994) 172.
- [48] L. von Smekal, A. Hauck, and R. Alkofer, *Phys. Rev. Lett.* **79** (1997) 3591.
- [49] L. von Smekal, A. Hauck, and R. Alkofer, *Ann. Phys.* **267** (1998) 1.
- [50] D. Leinweber, J. I. Skullerud, and A. G. Williams, *Phys. Rev.* **D58** (1998) 031501.
- [51] F. Bonnet, P. O. Bowman, D. B. Leinweber, and A. G. Williams, e-print (2000), hep-lat/0002020.
- [52] P. Maris, *Phys. Rev.* **D52** (1995) 6087.
- [53] A. Nakamura, H. Aiso, M. Fukuda, T. Iwamiya, T. Nakamura, and M. Yoshida, Gluon Propagators and Confinement, in *RCNP Confinement 1995*, pp. 90–95, 1995, e-print hep-lat/9506024.

- [54] J. C. Ward, Phys. Rev. **78** (1950) 1824.
- [55] Y. Takahasi, Nuov. Cim. **6** (1957) 370, *see also:* H. S. Green, Proc. Phys. Soc. **A66** (1953) 873.
- [56] C. H. Llewellyn-Smith, in *Quantum Flavour Dynamics, Quantum Chromodynamics and Unified Theories*, edited by K. T. Mahanthappa and J. Randa, New York, 1980, Plenum Press.
- [57] T. Kugo and I. Ojima, Prog. Theor. Phys. Suppl. **66** (1979) 1.
- [58] S. D. Joglekar and A. Misra, Int. J. Mod. Phys. **A10** (2000) 1453.
- [59] N. K. Nielsen, Nucl. Phys. **B101** (1975) 173.
- [60] P. Gambino and P. A. Grassi, e-print (1999), hep-ph/9907254.
- [61] J. Glimm and A. Jaffe, *Quantum Physics: A Functional Integral Point of View*, Springer Verlag, 1987.
- [62] L. V. Prokhorov, Phys. Uspekhi **42** (1999) 1099.
- [63] E. Bagan, M. Lavelle, and D. McMullan, Ann. Phys. **282** (2000) 471; *ibid.*, 503.
- [64] V. N. Gribov, Nucl. Phys. **B139** (1978) 1.
- [65] I. M. Singer, Comm. Math. Phys. **60** (1978) 7.
- [66] C. Nash, *Differential Topology and Quantum Field Theory*, Academic Press, 1991.
- [67] A. R. Zhitnitskii, Sov. J. Nucl. Phys. **46** (1987) 147; *ibid.*, 343.
- [68] B. Harrington and H. Shepard, Phys. Rev **D17** (1978) 2122.
- [69] P. Rossi, Nucl. Phys. **B149** (1979) 170.
- [70] D. J. Gross, R. D. Pisarski, and L. G. Yaffe, Rev. Mod. Phys. **53** (1981) 43.
- [71] H. Reinhardt, Nucl. Phys. **B503** (1997) 505.
- [72] O. Jahn and F. Lenz, Phys. Rev. **D58** (1998) 085006.
- [73] T. C. Kraan and P. van Baal, Nucl. Phys **B533** (1998) 627.
- [74] T. C. Kraan and P. van Baal, Nucl. Phys **A642** (1998) 299.
- [75] O. Jahn, J. Phys. **A33** (2000) 2997.
- [76] H. Reinhardt, K. Langfeld, and L. v. Smekal, Phys. Lett. **B300** (1993) 111.
- [77] M. Quandt and H. Reinhardt, Intern. J. Mod. Phys. **A13** (1998) 4049.
- [78] V. de Alfaro, S. Fubini, and G. Furlan, Phys. Lett. **B65** (1976) 163.
- [79] V. de Alfaro, S. Fubini, and G. Furlan, Phys. Lett. **B73** (1978) 463.
- [80] A. Actor, Rev. Mod. Phys. **51** (1979) 461.
- [81] T. T. Wu and C. N. Yang, in *Properties of Matter under Unusual Conditions*, edited by H. Mark and S. Fernbach, p. 349, Interscience Pub., J. Wiley & Sons, New York, 1969.
- [82] C. Callan, R. Dashen, and D. Gross, Phys. Lett. **B66** (1977) 375.

- [83] C. G. Callan, R. F. Dashen, and D. J. Gross, Phys. Rev. **D17** (1978) 2717.
- [84] J. V. Steele and J. W. Negele, e-print (2000), hep-lat/0007006.
- [85] G. Dell' Antonio and D. Zwanziger, Comm. Math. Phys. **138** (1991) 291.
- [86] R. J. Rivers, *Path integral methods in quantum field theory*, Cambridge University Press, 1987.
- [87] L. Baulieu and D. Zwanziger, e-print (1999), hep-th/9909006.
- [88] L. Baulieu, P. A. Grassi, and D. Zwanziger, e-print (2000), hep-th/0006036.
- [89] M. Mizutani and A. Nakamura, Nucl. Phys. B (Proc. Suppl.) **34** (1994) 253.
- [90] F. DiRenzo and L. Scorzato, in *LATTICE 99*, Nucl. Phys. B (Proc. Suppl.) **83-84** (2000) 822.
- [91] F. Shoji, T. Suzuki, H. Kodama, and A. Nakamura, Phys. Lett. **B476** (2000) 199.
- [92] D. Zwanziger, Nucl. Phys. **B378** (1992) 525.
- [93] D. Zwanziger, Nucl. Phys. **B412** (1994) 657.
- [94] C. Bernard, C. Parrinello, and A. Soni, Phys. Rev. **D49** (1994) 1585.
- [95] P. Marenzoni, G. Martinelli, and N. Stella, Nucl. Phys. **B455** (1995) 339.
- [96] H. Suman and K. Schilling, Phys. Lett. **B373** (1996) 314.
- [97] A. Cucchieri, Nucl. Phys. **B508** (1997) 353.
- [98] D. Birmingham, M. Blau, M. Rakowski, and G. Thompson, Phys. Rep. **209** (1991) 129.
- [99] K. Fujikawa, Prog. Theor. Phys. **61** (1979) 627.
- [100] P. Hirschfeld, Nucl. Phys. **B157** (1979) 37.
- [101] L. Baulieu and M. Schaden, Int. J. Mod. Phys. **A13** (1998) 985.
- [102] B. Sharpe, J. Math. Phys. **25** (1984) 3324.
- [103] L. Baulieu, A. Rozenberg, and M. Schaden, Phys. Rev. **D54** (1996) 7852.
- [104] M. Schaden and A. Rozenberg, Phys. Rev. **D57** (1998) 3670, see also, M. Schaden, *Quantization in the Presence of Gribov Copies*, in Procs. of 4th Workshop on Quantum Chromodynamics, Paris, France, 1-6 Jun 1998, hep-th/9810162.
- [105] M. Schaden, Phys. Rev. **D59** (1998) 014508.
- [106] M. Schaden, e-print (1999), hep-th/9909011.
- [107] M. Schaden, talk given at the 5th Workshop on QCD, Villefranche-sur-Mer, France, 3-7 Jan. 2000, e-print, hep-th/0003030.
- [108] G. B. West, Phys. Rev. **D27** (1983) 1878.
- [109] K. Nishijima, Int. J. Mod. Phys. **A9** (1994) 3799, *ibid.*, **A10** (1995) 3155.
- [110] K. Nishijima and N. Takase, Int. J. Mod. Phys. **A11** (1996) 2281.
- [111] K. Huang, *Quantum Field Theory, from Operators to Path Integrals*, John Wiley Inc., 1998.

[112] M. Göckeler, R. Horsley, V. Linke, P. Rakow, G. Schierholz, and H. Stüben, Phys. Rev. Lett. **80** (1998) 4119.

[113] L. v. Smekal, P. A. Amundsen, and R. Alkofer, Nucl. Phys. **A529** (1991) 633.

[114] W. J. Xu, *Asymptotic Limits and Sum Rules for Propagators in Quantum Chromodynamics*, PhD thesis, University of Chicago, 1996, hep-th/9607045; see also, R. Oehme and W. J. Xu, Phys. Lett. **B384** (1996) 269.

[115] J. Thierry-Mieg, Nucl. Phys. **B261** (1985) 55.

[116] N. Nakanishi, Prog. Theor. Phys. **62** (1979) 1396.

[117] I. Ojima, Nucl. Phys. **B143** (1978) 340.

[118] T. Kugo, at Int. Symp. on BRS Symmetry, Kyoto, 18-22 Sep. 1995, e-print, hep-th/9511033.

[119] R. Ferrari and L. E. Picasso, Nucl. Phys. **B31** (1971) 316.

[120] R. A. Brandt and W.-C. Ng, Phys. Rev. **D10** (1974) 4198.

[121] F. Lenz, H. W. L. Naus, K. Otha, and M. Thies, Ann. Phys. **233** (1994) 17; *ibid.*, 51.

[122] H. Hata, Prog. Theor. Phys. **67** (1982) 1607.

[123] S. Elitzur, Phys. Rev. **D12** (1975) 3978.

[124] E. Witten, Nucl. Phys. **B188** (1981) 513.

[125] J. Fröhlich, G. Morchio, and F. Strocchi, Nucl. Phys. **B190** (1981) 553.

[126] D. Stoll and M. Thies, e-print (1995), hep-th/9504068.

[127] L. F. Abbot, J. S. Kang, and H. J. Schnitzer, Phys. Rev. **D13** (1976) 2212.

[128] K. Langfeld, L. v. Smekal, and H. Reinhardt, Phys. Lett. **B308** (1993) 279.

[129] L. v. Smekal, K. Langfeld, H. Reinhardt, and R. F. Langbein, Phys. Rev. **D50** (1994) 6599.

[130] R. F. Langbein, K. Langfeld, H. Reinhardt, and L. v. Smekal, Mod. Phys. Lett. **A11** (1996) 631.

[131] K. Gawedzki and A. Kupiainen, Nucl. Phys. **B257** (1985) 474.

[132] K. Langfeld, L. v. Smekal, and H. Reinhardt, Phys. Lett. **B362** (1995) 128.

[133] E. Witten, Nucl. Phys. **B145** (1978) 110.

[134] J. C. Collins, A. Duncan, and S. D. Joglekar, Phys. Rev. **D16** (1977) 438.

[135] K. Langfeld, L. v. Smekal, and H. Reinhardt, Phys. Lett. **B311** (1993) 207.

[136] H. Nakajima and S. Furui, in *LATTICE 99*, Nucl. Phys. B (Proc. Suppl.) **83-84** (2000) 521.

[137] H. Nakajima and S. Furui, e-print (2000), hep-lat/0006002.

[138] H. Araki, K. Hepp, and D. Ruelle, Helv. Phys. Acta **35** (1962) 164.

[139] D. Ruelle, Helv. Phys. Acta **65** (1962) 147.

- [140] F. Strocchi, Phys. Rev. **D17** (1978) 2010.
- [141] U. Häbel, R. König, H.-G. Reusch, M. Stingl, and S. Wigard, Z. Phys. **A336** (1990) 423; *ibid.*, 435.
- [142] M. Stingl, Z. Phys. **A353** (1996) 423.
- [143] W. Dittrich and H. Gies, *Probing the Quantum Vacuum*, Springer Verlag, Berlin-Heidelberg, 2000.
- [144] G. V. Efimov and M. A. Ivanov, *The Quark Confinement Model of Hadrons*, IOP Publishing, London, 1993.
- [145] C. D. Roberts, Nucl. Phys. **A605** (1996) 475.
- [146] M. Buballa and S. Krewald, Phys. Lett. **B294** (1992) 19.
- [147] H. Haberzettl, Nucl. Phys. **A582** (1995) 603.
- [148] L. Driesen, J. Fromm, J. Kuhrs, and M. Stingl, Eur. Phys. J. **A4** (1999) 381.
- [149] L. Driesen and M. Stingl, Eur. Phys. J. **A4** (1999) 401.
- [150] J. Ahlbach, A. Streibl, and M. Schaden, Non-perturbative Solutions to the Dyson-Schwinger Equations of Pure QCD, in *Proceedings of the Workshop on QCD Vacuum Structure*, edited by B. Müller and H. Fried, Paris, 1992, World Scientific.
- [151] P. Emirdag, R. Easther, G. Guralnik, and S. Hahn, in *LATTICE 99*, Nucl. Phys. B (Proc. Suppl.) **83-84** (2000) 938; S.C. Hahn and G. S. Guralnik, e-print (1999) hep-th/9901019, talk given at the 4th Workshop on Quantum Chromodynamics, Paris, France, 1-6 June 1998.
- [152] S. Garcia, Z. Guralnik, and G. S. Guralnik, e-print (1996), hep-th/9612079.
- [153] H. M. Fried, *Functional Methods and Models in Quantum Field Theory*, MIT Press, Cambridge, 1972.
- [154] L. Baulieu and D. Zwanziger, Nucl. Phys. **B548** (1999) 527.
- [155] K. Geiger, Phys. Rev. **D60** (1999) 034012.
- [156] N. H. Christ and T. D. Lee, Phys. Rev. **D22** (1980) 939.
- [157] J. R. Finger and J. E. Mandula, Nucl. Phys. **B199** (1982) 168.
- [158] S. L. Adler and A. C. Davis, Nucl. Phys. **B244** (1984) 469.
- [159] A. LeYaouanc, L. Oliver, O. Pene, and J. C. Raynal, Phys. Rev. **D29** (1984) 1233.
- [160] A. Kocic, Phys. Rev. **D33** (1986) 1785.
- [161] R. Alkofer and P. A. Amundsen, Phys. Lett. **B187** (1987) 395.
- [162] R. Alkofer and P. A. Amundsen, Nucl. Phys. **B306** (1988) 305.
- [163] R. Alkofer, P. A. Amundsen, and K. Langfeld, Z. Phys. **C42** (1989) 199.
- [164] S. P. Klevansky and R. H. Lemmer, Phys. Rev. **D38** (1988) 3559.
- [165] T. Wilke and S. Klevansky, Ann. Phys. **258** (1997) 81.

- [166] U. Ellwanger, M. Hirsch, and A. Weber, *Z. Phys.* **C69** (1996) 687.
- [167] U. Ellwanger, M. Hirsch, and A. Weber, *Eur. Phys. J.* **C1** (1998) 563.
- [168] E. J. Eichten and F. L. Feinberg, *Phys. Rev.* **D10** (1974) 3254.
- [169] P. Boucaud, J. P. Leroy, J. Micheli, O. Pene, and C. Roiesnel, *JHEP* **12** (1998) 004, *JHEP* **10** (1998) 017.
- [170] U. Bar-Gadda, *Nucl. Phys.* **163** (1980) 312.
- [171] J. S. Ball and T. W. Chiu, *Phys. Rev.* **D22** (1980) 2542; *ibid.*, 2550.
- [172] S. K. Kim and M. Baker, *Nucl. Phys.* **B164** (1980) 152.
- [173] P. Maris and P. C. Tandy, *Phys. Rev.* **C61** (2000) 045202.
- [174] M. R. Frank, *Phys. Rev.* **C51** (1995) 987.
- [175] J. M. Cornwall and J. Papavassiliou, *Phys. Rev.* **D40** (1989) 3474.
- [176] J. M. Cornwall, *Phys. Rev.* **D26** (1982) 1453.
- [177] J. Papavassiliou, *Phys. Rev. Lett.* **84** (2000) 2782, e-print (1999), hep-ph/9912338.
- [178] N. J. Watson, *Nucl. Phys.* **B552** (1999) 461, e-print (1999), hep-ph/9912303, to appear in the proceedings of the International Workshop on Physical Variables in Gauge Theories, Dubna, Russia, 21 - 25 Sep 1999.
- [179] J. Schwinger, *Phys. Rev.* **128** (1962) 2425.
- [180] C. Adam, *Ann. Phys.* **259** (1997) 1.
- [181] C. Adam, *Czech. J. Phys.* **46** (1996) 893, (e-print hep-ph/9501273).
- [182] T. Radozycki, *Phys. Rev.* **D60** (1999) 105027.
- [183] M. N. Chernodub, M. I. Polikarpov, and V. I. Zakharov, *Phys. Lett.* **B457** (1999) 147.
- [184] A. Campbell-Smith and N. E. Mavromatos, *Acta Phys. Polon.* **B29** (1998) 3819, (e-print cond-mat/9810324).
- [185] S. B. Treiman, R. Jackiw, B. Zumino, and E. Witten, *Current Algebras and Anomalies*, Word Scientific, 1995.
- [186] A. M. Polyakov, *Gauge Fields and Strings*, Harwood Academic Publishers, 1987.
- [187] T. Matsumaya, H. Nagahiro, and S. Uchida, *Phys. Rev.* **D60** (1999) 105020, T. Matsumaya and H. Nagahiro, e-print (2000) hep-th/0004069.
- [188] Y. Hoshino and T. Matsumaya, *Phys. Lett.* **B222** (1989) 493.
- [189] Z. Dong, H. J. Munzcek, and C. D. Roberts, *Phys. Lett.* **B333** (1994) 536.
- [190] C. J. Burden and P. C. Tijiang, *Phys. Rev.* **D58** (1998) 085019.
- [191] A. Bashir, A. Kizilersü, and M. R. Pennigton, e-print (1999), hep-ph/9907418.
- [192] P. Maris, *Phys. Rev.* **D54** (1996) 4650.

- [193] N. Brown and M. R. Pennington, Phys. Rev. **D38** (1988) 2266.
- [194] A. W. Schreiber, T. Sizer, and A. G. Williams, Phys. Rev. **D58** (1998) 125014.
- [195] V. P. Gusynin, A. W. Schreiber, T. Sizer, and A. G. Williams, Phys. Rev. **D60** (1999) 065007.
- [196] A. Kizilersü, T. Sizer, and A. G. Williams, e-print (2000), hep-ph/0001147.
- [197] T. Appelquist, M. Bowick, D. Karabali, and L. Wijewardhana, Phys. Rev. **D33** (1986) 3704.
- [198] T. Appelquist, D. Nash, and L. Wijewardhana, Phys. Rev. Lett. **60** (1988) 2575.
- [199] V. P. Gusynin, V. A. Miransky, and A. V. Shpigin, Phys. Rev. **D58** (1998) 085023.
- [200] K. I. Kondo and P. Maris, Phys. Rev. Lett. **74** (1995) 18.
- [201] I. J. R. Aitchison, N. E. Mavromatos, and D. McNeill, Phys. Lett. **B402** (1997) 154.
- [202] S. Ahlig, R. Alkofer, P. Maris, and L. von Smekal, work in progress .
- [203] P. Maris, PhD thesis, University of Groningen, 1993.
- [204] E. Abdalla and R. Banerjee, Phys. Rev. Lett. **80** (1998) 238.
- [205] D. Dalmazi, A. de Souza Datra, and M. Hott, e-print (1999), hep-th/9912269.
- [206] J. C. R. Bloch and M. R. Pennington, Mod. Phys. Lett. **A10** (1995) 1225.
- [207] M. R. Pennington, in *Proceedings of the Workshop on Nonperturbative Methods in Quantum Field Theory*, edited by A. W. Schreiber, A. G. Williams, and A. W. Thomas, p. 49, Adelaide, 1998, World Scientific.
- [208] C. D. Roberts and R. T. Cahill, Aust. J. Phys. **40** (1987) 499.
- [209] R. T. Cahill and S. M. Gunner, Fizika **B7** (1998) 171.
- [210] R. Fukuda and T. Kugo, Nucl. Phys. **B117** (1976) 250.
- [211] J. Cornwall, R. Jackiw, and E. Tomboulis, Phys. Rev. **D10** (1974) 2428.
- [212] D. Atkinson and M. Fry, Nucl. Phys. **B156** (1979) 301.
- [213] D. C. Curtis and M. Pennington, Phys. Rev. **D42** (1990) 4165.
- [214] A. Kizilersü, M. Reenders, and M. R. Pennington, Phys. Rev. **D52** (1995) 1242.
- [215] D. C. Curtis and M. Pennington, Phys. Rev. **D48** (1993) 4933.
- [216] D. Atkinson, J. C. R. Bloch, V. P. Gusynin, M. R. Pennington, and M. Reenders, Phys. Lett. **B329** (1994) 117.
- [217] C. J. Burden and C. D. Roberts, Phys. Rev. **D47** (1993) 5581.
- [218] A. Bashir and M. R. Pennington, Phys. Rev. **D50** (1994) 7679.
- [219] A. Bashir, A. Kizilersü, and M. R. Pennington, Phys. Rev. **D57** (1998) 1242.
- [220] F. T. Hawes, A. G. Williams, and C. D. Roberts, Phys. Rev. **D54** (1996) 5361.
- [221] F. T. Hawes, T. Sizer, and A. G. Williams, Phys. Rev. **D55** (1997) 3866.

[222] K. Büttner, *Confinement and the Infrared Behaviour of the Gluon Propagator*, PhD thesis, University of Durham, 1996.

[223] S. Blaha, Phys. Rev. **D10** (1974) 4268.

[224] F. Gross and J. Milana, Phys. Rev. **D43** (1990) 2401.

[225] H. Pagels, Phys. Rev. **D15** (1977) 2991.

[226] G. B. West, Phys. Lett. **B115** (1982) 468.

[227] K. R. Natroshvili, A. A. Khelashvili, and V. Y. Khmaladze, Teor. Mat. Fiz. **65** (1985) 360.

[228] L. G. Vachnadze, K. R. Natroshvili, A. A. Khelashvili, and V. Y. Khmaladze, Teor. Mat. Fiz. **80** (1989) 264.

[229] L. G. Vachnadze, N. A. Kiknadze, K. S. Turashvili, and A. A. Khelashvili, Theor. Math. Phys. **100** (1994) 811.

[230] P. Gaigg, W. Kummer, and M. Schweda, editors, *Physical and Nonstandard Gauges*, volume 361 of *Lecture notes in physics*, Springer Verlag, 1990.

[231] Y. Nakawaki and G. McCartor, e-print (2000), hep-th/0004140.

[232] M. Lavelle and M. Schaden, Phys. Lett. **B217** (1989) 551.

[233] F. Lenz, H. W. L. Naus, and M. Thies, Ann. Phys. **233** (1994) 317.

[234] G. Frenkel and J. C. Taylor, Nucl. Phys. **B109** (1976) 439.

[235] N. Nakanishi, Phys. Lett. **B131** (1983) 381.

[236] A. Bassutto, Good and Bad News Concerning Axial Gauges, In Gaigg et al. [230].

[237] L. G. Vachnadze, N. A. Kiknadze, and A. A. Khelashvili, Theor. Math. Phys. **102** (1995) 34.

[238] P. Watson, PhD thesis, University of Durham, UK, 2000.

[239] A. Hauck, L. von Smekal, and R. Alkofer, Comput. Phys. Commun. **112** (1998) 149.

[240] A. Hauck, L. von Smekal, and R. Alkofer, Comput. Phys. Commun. **112** (1998) 166.

[241] N. Brown and N. Dorey, Mod. Phys. Lett. **A6** (1991) 317.

[242] S. Ahlig, L. v. Smekal, and R. Alkofer, work in progress .

[243] D. Atkinson and J. C. R. Bloch, Mod. Phys. Lett. **A13** (1998) 1055.

[244] D. Atkinson and J. C. R. Bloch, Phys. Rev. **D58** (1998) 094036.

[245] D. Zwanziger, Nucl. Phys. **B345** (1990) 461.

[246] H. Hata and I. Niigata, Nucl. Phys. **B389** (1993) 133.

[247] A. Cucchieri, private communication.

[248] G. t'Hooft, Nucl. Phys. **B72** (1974) 461.

[249] M. Schmelling, e-print (1997), hep-ex/9701002.

- [250] C. Caso et al., Eur. Phys. J. **C3** (1998) 1.
- [251] J. E. Mandula and M. Ogilvie, Phys. Lett. **B185** (1987) 127.
- [252] H. Aiso, J. Fromm, M. Fukuda, T. Iwamiya, A. Nakamura, T. Nakamura, M. Stingl, and M. Yoshida, Nucl. Phys. (Proc. Suppl.) **B53** (1997) 570.
- [253] J. E. Mandula, Phys. Rep. **315** (1999) 273.
- [254] H. J. Munczek and A. M. Nemirovsky, Phys. Rev. **D28** (1983) 181.
- [255] M. A. Ivanov, Y. L. Kalinovsky, and C. D. Roberts, Phys. Rev. **60** (1999) 034018, and references therein.
- [256] C. J. Burden, C. D. Roberts, and M. J. Thomson, Phys. Lett. **B371** (1996) 163.
- [257] M. Gell-Mann and F. E. Low, Phys. Rev. **84** (1951) 350.
- [258] J. I. Skullerud, Nucl. Phys. Proc. Suppl. **63** (1998) 242.
- [259] P. Maris and C. D. Roberts, Phys. Rev. **C56** (1997) 3369.
- [260] R. Alkofer, S. Ahlig, and L. von Smekal, in *Nuclear and Particle physics with CEBAF at Jefferson Lab*, Fizika **B8** (1999) 277; (e-print hep-ph/9901322).
- [261] R. Alkofer, S. Ahlig, and L. von Smekal, in *Understanding Deconfinement in QCD*, edited by D. Blaschke, F. Karsch, and C. D. Roberts, ECT* Trento, 1999, World Scientific, (e-print hep-ph/9905324).
- [262] J. Cudell, A. Donnachie, and P. Landshoff, Nucl. Phys. **B322** (1989) 55.
- [263] J. Schwinger, Phys. Rev. **125** (1962) 397.
- [264] F. T. Hawes, P. Maris, and C. D. Roberts, Phys. Lett. **B440** (1998) 353.
- [265] J. C. Vink and U.-J. Wiese, Phys. Lett. **B289** (1992) 122.
- [266] J. C. Vink, Phys. Rev. **D51** (1995) 1292.
- [267] C. Alexandrou, talk given at *Quark Confinement and the Hadron Spectrum IV*, Vienna, July 3-8, 2000 .
- [268] J. I. Skullerud and A. G. Williams, e-print (2000), hep-lat/0007028.
- [269] J. I. Skullerud and A. G. Williams, in *LATTICE 99*, Nucl. Phys. B (Proc. Suppl.) **83-84** (2000) 209.
- [270] J. R. Cudell, A. LeYaouanc, and C. Pittori, in *LATTICE 99*, Nucl. Phys. B (Proc. Suppl.) **83-84** (2000) 890.
- [271] D. Becirevic, V. Lubicz, G. Martinelli, and M. Testa, in *LATTICE 99*, Nucl. Phys. B (Proc. Suppl.) **83-84** (2000) 893.
- [272] B. Allés, D. Henty, H. Panagopoulos, C. Parinello, C. Pittori, and D. G. Richards, Nucl. Phys. **B502** (1997) 325.
- [273] M. Heß, F. Karsch, E. Laermann, and I. Wetzorke, Phys. Rev. **D58** (1998) 111502, F. Karsch, M. Heß, E. Laermann and I. Wetzorke, in *LATTICE98*, Nucl.Phys. (Proc.Suppl.) **73** (1999) 213.

- [274] E. E. Salpeter and H. A. Bethe, Phys. Rev. **84** (1951) 1232.
- [275] H. J. Munczek, Phys. Rev. **D52** (1995) 4736.
- [276] R. Delbourgo and M. D. Scadron, J. Phys. **G5** (1979) 1621.
- [277] A. Blumhofer and J. Manus, Nucl. Phys. **B515** (1998) 522.
- [278] V. Sauli, private communication.
- [279] K. Kusaka and A. G. Williams, Phys. Rev. **D51** (1995) 7026.
- [280] K. Kusaka, K. Simpson, and A. G. Williams, Phys. Rev. **D56** (1997) 5071.
- [281] N. Nakanishi, *Graph Theory and Feynman Integrals*, Gordon Breach, New York, 1971.
- [282] S. Ahlig and R. Alkofer, Ann. Phys. **275** (1999) 113.
- [283] G. C. Wick, Phys. Rev. **96** (1954) 1124.
- [284] R. E. Cutkosky, Phys. Rev. **96** (1954) 1135.
- [285] N. Nakanishi, Suppl. Prog. Theor. Phys. **43** (1969) 1.
- [286] W. B. Kaufmann, Phys. Rev. **187** (1969) 2951.
- [287] I. Fukui and N. Setô, Progr. Theor. Phys. **89** (1993) 205, *ibid.*, **95** (1996) 433.
- [288] L. Theussl and B. Desplanques, e-print (1999), nucl-th/9908007.
- [289] J. Bijtebier, Nucl. Phys. **A623** (1997) 498.
- [290] J. S. Goldstein, Phys. Rev. **91** (1953) 1516.
- [291] T. W. Allen and C. J. Burden, Phys. Rev. **D55** (1997) 4954.
- [292] T. W. Allen and C. J. Burden, Phys. Rev. **D53** (1996) 5842, erratum Phys. Rev. **D54** (1996) 6567.
- [293] R. Rosenfelder and A. W. Schreiber, Phys. Rev. **D53** (1996) 3337; *ibid.*, 3354.
- [294] C. H. Llewellyn-Smith, Ann. Phys. **53** (1969) 521.
- [295] P. Jain and H. J. Munczek, Phys. Rev. **D48** (1993) 5403, and references therein.
- [296] J. Govaerts, J. E. Mandula, and J. Weyers, Nucl. Phys. **B237** (1984) 59.
- [297] K. Langfeld, R. Alkofer, and P. A. Amundsen, Z. Phys. **C42** (1989) 159.
- [298] J. Kogut and L. Susskind, Phys. Rev. **D10** (1974) 3468.
- [299] A. Mecke, Diploma Thesis, University of Tübingen, 1997.
- [300] L. von Smekal, A. Mecke, and R. Alkofer, in *Intersections between Particle and Nuclear Physics, 6th Conference*, edited by T. W. Donelly, p. 746, World Scientific, 1997, e-print hep-ph/9707210.
- [301] E. Witten, Nucl. Phys. **B156** (1979) 269.
- [302] G. Veneziano, Nucl. Phys. **B159** (1979) 461, P. Di Vecchia and G. Veneziano, Nucl. Phys. **B171** (1980), 253.

- [303] R. Alkofer, M. Nowak, J. Verbaarschot, and I. Zahed, Phys. Lett. **B233** (1989) 205.
- [304] D. Kekez, D. Klabucar, and M. D. Scadron, e-print (2000), hep-ph/0003234.
- [305] M. Frank and T. Meissner, Phys. Rev. **C57** (1998) 345.
- [306] R. Alkofer, P. A. Amundsen, and H. Reinhardt, Phys. Lett. **B218** (1989) 75.
- [307] P. Maris and P. C. Tandy, Phys. Rev. **C60** (1999) 055214.
- [308] M. Alford and R. L. Jaffe, Nucl. Phys. **B578** (2000) 367.
- [309] N. A. Törnqvist, Eur. Phys. J. **C11** (1999) 359.
- [310] M. R. Pennington, e-print (1999), hep-ph/9905241, talk given at Workshop on Hadron Spectroscopy, Rome, Italy, 8-12 Mar 1999.
- [311] D. Black, A. H. Fariborz, and J. Schechter, Phys. Rev. **D61** (2000) 074001; *ibid.*, 074030.
- [312] G. Janssen, B. C. Pearce, K. Holinde, and J. Speth, Phys. Rev. **D52** (1995) 2690.
- [313] M. Neubert, Phys. Rep. **245** (1994) 259.
- [314] N. Isgur and M. Wise, Phys. Lett. **B232** (1989) 113, Phys. Lett. **B237** (1990) 527.
- [315] P. Maris and P. C. Tandy, e-print (2000), nucl-th/0005015.
- [316] H. O'Connell, B. Pearce, A. Thomas, and A. Williams, Prog. Part. Nucl. Phys. **39** (1995) 201.
- [317] F. T. Hawes and M. A. Pichowsky, Phys. Rev. **C59** (1999) 1743.
- [318] M. B. Hecht and B. H. J. McKellar, Phys. Rev. **C57** (1998) 2638.
- [319] K. L. Mitchell and P. C. Tandy, Phys. Rev. **C55** (1997) 1477.
- [320] K. L. Mitchell, P. C. Tandy, C. D. Roberts, and R. T. Cahill, Phys. Lett. **B335** (1994) 282.
- [321] M. A. Pichowsky and T.-S. Lee, Phys. Lett. **B379** (1996) 1.
- [322] P. Kroll and M. Raulfs, Phys. Lett. **B387** (1996) 848.
- [323] M. R. Frank, K. L. Mitchell, C. D. Roberts, and P. C. Tandy, Phys. Lett. **B359** (1995) 17.
- [324] P. Maris and C. D. Roberts, Phys. Rev. **C58** (1998) 3659.
- [325] D. Kekez and D. Klabucar, Phys. Lett. **B457** (1999) 359.
- [326] I. V. Anikin, A. E. Dorokhov, and L. Tomio, Phys. Lett. **B475** (2000) 361.
- [327] R. Alkofer and C. D. Roberts, Phys. Lett. **B369** (1996) 101.
- [328] B. Bistrovic and D. Klabucar, Phys. Rev. **D61** (2000) 033006.
- [329] B. Bistrovic and D. Klabucar, Phys. Lett. **B478** (2000) 127.
- [330] J. Praschifka, C. D. Roberts, and R. T. Cahill, Ann. Phys. **188** (1988) 20.
- [331] M. A. Pichowsky, S. Walawalkar, and S. Capstick, Phys. Rev. **D60** (1999) 054030.
- [332] D. Ebert and M. K. Volkov, Fort. Phys. **29** (1981) 35.

- [333] J. Gasser and H. Leutwyler, Ann. Phys. **158** (1983) 142.
- [334] R. Alkofer, A. Bender, and C. D. Roberts, Int. J. Mod. Phys. **A10** (1995) 3319.
- [335] J. Gasser and H. Leutwyler, Nucl. Phys. **B250** (1985) 465; *ibid.*, 517.
- [336] P. Hasenfratz and J. Kuti, Phys. Rep. **40** (1978) 75.
- [337] G. S. Adkins, C. R. Nappi, and E. Witten, Nucl. Phys. **B228** (1983) 552.
- [338] E. G. Holzwarth, *Baryons as Skyrme Solitons*, World Scientific, 1993.
- [339] H. Weigel, Int. J. Mod. Phys. **A11** (1996) 2419.
- [340] R. Alkofer and H. Reinhardt, *Chiral Quark Dynamics*, Springer Verlag, Berlin-Heidelberg, 1995, Lecture Notes in Physics, vol. m33.
- [341] R. Alkofer, H. Reinhardt, and H. Weigel, Phys. Rep. **265** (1996) 139.
- [342] C. V. Christov, A. Blotz, H. C. Kim, P. Pobylitsa, T. Watabe, T. Meissner, E. Ruiz-Arriola, and K. Goeke, Prog. Part. Nucl. Phys. **37** (1996) 91.
- [343] M. Gell-Mann, Phys. Rev. **8** (1964) 214.
- [344] G. Karl and E. Obryk, Nucl. Phys. **B8** (1968) 609.
- [345] D. Faiman and A. W. Hendry, Phys. Rev. **173** (1968) 1720.
- [346] R. P. Feynman, M. Kislinger, and F. Ravndal, Phys. Rev. **D3** (1971) 2706.
- [347] A. Chodos and C. Thorn, Phys. Rev. **D12** (1975) 2733.
- [348] M. Rho, Phys. Rep. **240** (1994) 1.
- [349] U. Zückert, R. Alkofer, H. Weigel, and H. Reinhardt, Phys. Rev. **C55** (1997) 2030.
- [350] H. Reinhardt, Phys. Lett. **B244** (1990) 316.
- [351] A. Buck, R. Alkofer, and H. Reinhardt, Phys. Lett. **B286** (1992) 29.
- [352] N. Ishii, W. Bentz, and K. Yazaki, Phys. Lett. **B301** (1993) 165.
- [353] N. Ishii, W. Bentz, and K. Yazaki, Phys. Lett. **B318** (1993) 26.
- [354] S. Huang and J. Tjon, Phys. Rev. **C49** (1994) 1702.
- [355] A. Buck and H. Reinhardt, Phys. Lett. **B356** (1995) 168.
- [356] N. Ishii, W. Bentz, and K. Yazaki, Nucl. Phys. **A587** (1995) 617.
- [357] H. Asami, N. Ishii, W. Bentz, and K. Yazaki, Phys. Rev. **C51** (1995) 3388.
- [358] H. Mineo, W. Bentz, and K. Yazaki, Phys. Rev. **C60** (1999) 065201.
- [359] C. J. Burden, R. T. Cahill, and J. Praschifka, Austral. J. Phys. **42** (1989) 147.
- [360] J. Praschifka, R. T. Cahill, and C. D. Roberts, Intern. J. Mod. Phys. **A4** (1989) 4929.
- [361] J. C. R. Bloch, C. D. Roberts, S. M. Schmidt, A. Bender, and M. R. Frank, Phys. Rev. **C60** (1999) 062201.

[362] J. C. R. Bloch, C. D. Roberts, and S. M. Schmidt, Phys. Rev. **C61** (2000) 065207.

[363] K. Kusaka, G. Piller, A. W. Thomas, and A. G. Williams, Phys. Rev. **D55** (1997) 5299.

[364] G. Hellstern, R. Alkofer, M. Oettel, and H. Reinhardt, Nucl. Phys. **A627** (1997) 679.

[365] M. Oettel, G. Hellstern, R. Alkofer, and H. Reinhardt, Phys. Rev. **C58** (1998) 2459.

[366] M. Oettel, M. A. Pichowsky, and L. von Smekal, Eur. Phys. J. **A8** (2000) 251.

[367] M. Oettel and R. Alkofer, Phys. Lett. **B484** (2000) 243.

[368] M. Oettel, R. Alkofer, and L. von Smekal, e-print (2000), nucl-th/0006082.

[369] M. Oettel, PhD thesis, University of Tübingen, 2000.

[370] L. Y. Glozman, Z. Papp, W. Plessas, K. Varga, and R. F. Wagenbrunn, Phys. Rev. **C57** (1998) 3406.

[371] A. Bender, C. D. Roberts, and L. v. Smekal, Phys. Lett. **B380** (1996) 7.

[372] G. Hellstern, R. Alkofer, and H. Reinhardt, Nucl. Phys. **A625** (1997) 697.

[373] L. P. Kadanoff and G. Baym, *Quantum Statistical Mechanics*, Benjamin Inc., New York, 1962.

[374] R. T. Cahill, C. D. Roberts, and J. Praschifka, Phys. Rev. **D36** (1989) 2804.

[375] P. Kroll, M. Schürmann, K. Passek, and W. Schweiger, Phys. Rev. **D55** (1997) 4315.

[376] R. Alkofer, S. Ahlig, C. Fischer, and M. Oettel, in *MENU 99, πN Newsletter* **15** (1999) 238; (e-print nucl-th/9911020).

[377] A. N. Kvinikhidze and B. Blankleider, Phys. Rev. **C60** (1999) 044003; *ibid.*, 044004.

[378] N. Ishii, e-print (2000), nucl-th/0004063.

[379] M. K. Jones et al., Phys. Rev. Lett. **84** (2000) 1398.

[380] B. Blankleider and A. N. Kvinikhidze, e-print (1999), nucl-th/9912003.

[381] C. Fischer, Diploma Thesis, University of Tübingen, 1999.

[382] G. Curci and R. Ferrari, Phys. Lett. **B63** (1976) 91.

[383] G. Curci and R. Ferrari, Nuovo Cim. **32A** (1976) 151.

[384] L. Baulieu and J. Thierry-Mieg, Nucl. Phys. **B197** (1982) 477.

[385] J. Thierry-Mieg and Y. Ne'eman, Ann. Phys. **123** (1979) 247.

[386] M. Quirós, F. J. de Urríes, J. Hoyos, M. L. Mazón, and E. Rodriguez, J. Math. Phys. **22** (1981) 1767.

[387] J. Hoyos, M. Quirós, J. Ramírez Mittelbrunn, and F. J. de Urríes, J. Math. Phys. **23** (1982) 1504.

[388] J. Hoyos, M. Quirós, J. Ramírez Mittelbrunn, and F. J. de Urríes, Nucl. Phys. **B218** (1983) 159.

[389] L. Bonora and M. Tonin, Phys. Lett. **B98** (1981) 48.

[390] A. C. Hirschfeld and H. Leschke, Phys. Lett. **B101** (1981) 48.

[391] R. Delbourgo and P. D. Jarvis, J. Phys. **A15** (1882) 611.

[392] M. Baker and C. Lee, Phys. Rev. **D15** (1977) 2201.

List of Figures

1	Sketch of the gauge-fixing hyperplane Γ , the Gribov and the fundamental modular region.	20
2	Pictorial representation of the photon DSE.	44
3	Pictorial representation of the ghost DSE.	46
4	Pictorial representation of the quark DSE.	47
5	Pictorial representation of the gluon DSE.	48
6	Feynman diagrams of the first few terms in a perturbative expansion of the kernel K .	55
7	The mass function $M(s)$ in QED.	66
8	Diagrammatic representation of the gluon, ghost and quark DSEs of QCD.	79
9	Diagrammatic representation of the gluon Dyson–Schwinger equation in Mandelstam’s approximation.	82
10	The gluon renormalization function for Mandelstam’s equation.	83
11	Diagrammatic representation of the gluon and ghost Dyson–Schwinger equations of QCD without quarks. In the gluon DSE terms with four-gluon vertices have been dismissed.	84
12	The renormalization functions $Z(x)$ and $G(x)$.	90
13	The running coupling $\alpha_S(\mu)$ for $t = 0$ and the corresponding β -function.	97
14	The running coupling α_S from the Dyson–Schwinger equations of pure QCD compared to the collection of the <i>world’s</i> experimental data.	98
15	The one-dimensional Fourier transform of the gluon propagator.	101
16	The renormalised dressed-quark mass function, $M(p^2)$, obtained by solving the quark DSE with the interaction (252. (Adapted from ref. [259].)	107
17	Quark mass functions $M(p^2)$ for various current masses from the quenched approximation (with $\bar{\beta}_0 = 11$).	108
18	The gluon renormalization function from Dyson–Schwinger equations compared to the corresponding lattice data from [50].	114
19	The ghost propagator from Dyson–Schwinger equations compared to lattice data.	115

20	Lattice results of the effective energy $\omega_{\text{eff}}(t, \mathbf{p})$.	116
21	<i>Left panel:</i> Lattice result for $Z_q(pa)$, where $a \simeq 2.0 \text{ GeV}^{-1}$ is the lattice spacing, calculated with $ma = 0.0603$. <i>Right panel:</i> Analogous plot for the mass function. (Adapted from ref. [268].)	117
22	Lattice results of the running coupling from the 3-gluon vertex.	118
23	Pictorial representation of the homogeneous Bethe–Salpeter equation in ladder approximation.	122
24	Plot of the complex p^2 plane. The interior of the parabola shows the subset of the complex plane where the BS equation 'probes' the propagators of the constituents. M is the mass of the bound state and η is the momentum partitioning parameter.	125
25	An illustration of the realisation of the axial–vector Ward–Takahashi identity for pion amplitudes in the chiral limit. (Adapted from ref. [259].)	130
26	The diamond diagram $\Pi(P^2)$. (A factor 2 arises from crossed gluon exchange.)	132
27	The pion charge form factor $F_\pi(Q^2)$ as obtained from different treatments of the quark–photon vertex. The inset shows the Q^2 region relevant for the charge radius. (Adapted from ref. [173].)	140
28	The kernel of the meson and diquark BS equations at next–to–leading order. (Adapted from ref. [371].)	151
29	$\det\{H(P^2) - \mathbb{1}\}$ plotted as a function of P^2 . This function vanishes at the square of the bound state mass in the channel under consideration. (Adapted from ref. [371].)	155
30	Examples for admitted and excluded graphs in the 3-quark interaction kernel K . (Adapted from ref. [369].)	160
31	The separable t –matrix. (Adapted from ref. [369].)	160
32	The coupled set of BS equations for the vertex functions Φ . (Adapted from ref. [369].)	162
33	Impulse approximate contributions to the electromagnetic current. (Adapted from ref. [368].)	168
34	Resolved vertices: photon-scalar diquark, photon-axialvector diquark and anomalous scalar-axialvector diquark transition. (Adapted from ref. [368].)	170
35	Exchange quark and seagull diagrams. (Adapted from ref. [368].)	171
36	The ratio $(\mu_p G_E)/G_M$ compared to the data from ref. [379].	172

37	Comparison of the $g_{K\Lambda}(Q^2)$ form factor with a “projected” $g_{\pi NN}(Q^2)$, only the scalar diquark component of the nucleon amplitude has been taken into account in the calculation. (Adopted from ref. [381].)	176
38	Impulse approximation diagrams contributing to $\gamma p \rightarrow K\Lambda$.	177
39	Kaon photoproduction. The left panel shows the total cross section compared to the data of the SAPHIR collaboration, the right panel the asymmetry. (Adapted from ref. [376].)	178
C.1	Pictorial representation of the gluon DSE.	192

List of Tables

1	Summary of the symmetries of the scalar BS equation in ladder approximation. (Adopted from ref. [282].)	127
2	Calculated values of the properties of light pseudoscalar mesons. (Adapted from ref. [307].)	134
3	Results for the vector mesons. (Adapted from ref. [307].)	134
4	The quantities used in χ^2 -fitting the model parameters of Ref. [255].	137
5	Calculated values of a range of observables not included in fitting the model's parameters. (Table adapted from ref. [255].)	137
6	Calculated charge radii compared with the experimental values. (Adapted from ref. [315].)	140
7	Weights of the different kernel contributions of fig. 28 corresponding to the meson and diquark BS equations.	152
8	Calculated meson and diquark masses. (Adapted from ref. [371].)	154
9	Components of the octet baryon wave function with their respective spin and orbital angular momentum. (Adapted from ref. [376].)	166
10	Octet and decuplet masses obtained with two different parameter sets. (Adapted from ref. [376].)	168